PILES IN SAND AND IN SAND OVERLYING CLAY

by

R.B. ROBINSON B.Sc.

Thesis presented in fulfilment of the requirement for the Degree of Doctor of Philosophy, Council for National Academic Awards, London.

Sponsoring Establishment

Department of Civil Engineering and Building,

The Polytechnic of Wales, U.K.

Collaborating Establishment

Building Research Establishment, Watford, U.K.

May 1989

CERTIFICATE OF RESEARCH

This is to certify that, except when specific reference to other investigations is made, the work described in this thesis is the result of the investigation of the candidate.

R.B. Robinson

R.B. Robinson

(Candidate)

July 1989

(Date)

G.O. Rowlands

Mr. G.O. Rowlands

(Director of Studies)

July 1989

(Date)

R. Delpak

Dr. R. Delpak

(Supervisor)

July 1989

(Date)

DECLARATION

This is to certify that neither this thesis, nor any part of it has been presented , in candidature form for any degree at any other Academic Institution.

R.B. Robinson.....

(candidate)

ACKNOWLEDGEMENTS

The author wishes to express his gratitude to Mr G. O. Rowlands, his director of studies, and Dr R. Delpak, his supervisor, at The Polytechnic of Wales, for their help and encouragement.

He wishes to thank Mr G. Price of the Building Research Establishment for his advice and suggestions.

He also wishes to express thanks to Dr S. N. Werschingand Dr G.C. Lake for their advice and helpful discussions.

The author acknowledges the help and guidance of Mr H. Davies and the technical staff at The Polytechnic of Wales. Particular thanks are extended to Mr B. Lloyd and Mr L. Whiteman for their assistance in the Geotechnics Laboratory.

Finally the author wishes to express gratitude to his wife Delyth for typing this thesis, and for the encouragement and understanding she has given throughout the duration of this study.

SUMMARY

PILES IN SAND AND IN SAND OVERLYING CLAY

by

R.B. ROBINSON

This thesis examines the behaviour of single 60mm and 114mm segmented tubular steel piles driven and placed into loose sand and loose sand overlying clay. The soil was placed and instrumented under controlled conditions in a 3.0m diameter by 3.0m deep concrete tank. The 60mm pile was dynamically driven using a pneumatically controlled driving rig, whilst the 114mm pile was driven at a constant rate of penetration via a hydraulic jack.

The static and dynamic axial load distributions were monitored for the 60mm pile. The variation in local shaft friction and radial effective stress were monitored along the pile shaft of the 114mm pile, together with the distribution of axial load within the pile.

The pore water pressure was continuously monitored at selected points in the clay from the placement of the overburden to the final stages of the experiment. The density of the sand was carefully controlled during placement and was subsequently measured at the relevant point in the experiment. Vertical and radial displacements were monitored within the sand. For the two soil profiles radial shear and vertical effective stresses were recorded at a defined level within the strata.

Data from both the pile and soil instrumentation was recorded throughout the pile installation and load testing programme by an Orion Data Logger which was interfaced with a Commodore PET micro computer.

The results show:

(i) During pile installation the major principal stress acting at depth within a soil profile, appears to emanate from the face of the active wedge driven ahead of the pile.

(ii) The boundary of the sand/clay interface has a considerable effect on the development of soil displacements and the effective vertical stress developed within the overlying sand.

(iii) The radial displacement during pile installation is directly related to the pile diameter. Within a sand profile the peak radial displacement can be predicted using an empirical compaction factor adjustment to a theoretical representation of radial soil movement.

(iv) In sand, the local unit shaft friction and the radial effective stress are practically constant along the pile shaft for a given pile embedment and increases at a diminishing rate with pile embedment.

(v) At full pile embedment and ultimate applied load, the local coefficient of earth pressure K_z, for a driven pile may approach or exceed the value of K_p near the top of the pile and tend to a lower limit of 0.6 near the pile base.

(vi) For a placed insitu pile at ultimate applied load, the local coefficient of earth pressure K_z may be less than K_p near the top of the pile and tend to K_a near the pile base.

(vii) Adjacent to the pile shaft the radial effective stress is the major stress.

(viii) The development of shaft friction is directly related to displacements within the surrounding sand and on the sand/clay interface.

(ix) The influence of the underlying clay layer affects the development of shaft friction to varying limits above and below the sand/clay interface.

(x) For shallow pile penetrations into the clay layer the drawdown of sand and sand plug driven ahead of the pile significantly reduces the pore water pressure generated at the soil/pile interface.

(xi) The development and radial distribution of pore water pressure within the clay can be represented be a logarithmic expression.

(xii) The maximum compressive strain due to pile installation in a sand profile radiates from below and around the pile base.

These results are compatible with and extend previous research work at the Polytechnic of Wales. They illustrate how soil behaviour and soil/pile interaction are influenced by the method of pile installation and the boundary effects of an incompatible underlying layer.

NOTATION

A_b = Pile Base Area

A_s = Pile Shaft Area

A_k, B_k = Bearing Capacity Factors (Berezantzev, 1961)

B = Pile Diameter

B_t = Diameter of Test Tank

C = Empirical Compaction Factor

C_{ui} = Initial Undrained Shear Strength

C_u = Undrained Shear Strength

D_b = Foundation Depth

D_c = Critical Depth

D_r = Relative Density

E = Elastic Modulus

E_u = Undrained Elastic Modulus

e = Voids Ratio

f_s = Average Unit Shaft Friction

f_{sf} = Average Unit Shaft Friction at Failure

f_z = Local Unit Shaft Friction

f_{zf} = Local Unit Shaft Friction at Failure

G = Shear Modulus

G_s = Specific Gravity

K_a = Active Earth Pressure Coefficient

K_o = At Rest Earth Pressure Coefficient

K_p = Passive Earth Pressure Coefficient

K_s = Average Lateral Earth Pressure Coefficient Acting on Pile Shaft at Failure

K_z = Local Lateral Earth Pressure Coefficient Acting on Pile Shaft at Failure

N_γ, N_q, N_c = Bearing Capacity Factors

N_q^* = Base Bearing Capacity Factor Incorporating Shape Factor

P,R = Pore Water Pressure Coefficients

P_s = Shear Load Applied To Active Face of the BOST

P_{sa} = Maximum Allowable Shear Load on the BOST

P_{sf} = Applied Shear Load Causing Failure of the BOST

P_n = Normal Load Applied to Active Face of the BOST

Q_a = Applied Load

Q_{af} = Applied Load at Failure

Q_{amax} = Maximum Applied Load

Q_{aw} = Applied Working Load

Q_b = Pile Base Resistance

Q_{bf} = Pile Base Resistance at Failure

Q_s = Pile Shaft Resistance

Q_{sf} = Pile Shaft Resistance at Failure

Q_t = Total Pile Resistance

Q_f = Bearing Capacity at Failure

q_{bf} = Unit Base Resistance at Failure

q_{sf} = Average Unit Shaft Resistance at Failure

R = Radial Displacement of the Soil

R_{max} = Surface Roughness Coefficient

r = Radius From the Pile Axis

Sr = Degree of Saturation

t = Web Thickness of the BOST

u = Pore Water Pressure

V = Vertical Displacement of the Soil

Z = Depth

$Z_{\hat{e}}$ = Depth at which the Ratio of Overburden Stress to Effective Radial Stress is Equal to Ks

$Z_{e'}$ = Shaft Bearing Capacity Factor

Z_i = Depth to Sand/Clay Interface

$Z_{i'}$ = Depth Below Sand/Clay Interface

α = Pile Shaft Adhesion Factor

α_T = Surcharge Reduction Factor (Berezantzev,1961)

γ = Unit Weight of Soil

γ_D = Unit Weight of Overburden (Berezantzev,1961)

Δ = Change in Any Defined Parameter

δ' = Effective Friction Angle Between Pile Shaft and Soil at Failure

ε_v = Volumetric Strain

ε_z = Elastic Vertical Strain

ε_r = Elastic Radial Strain

ε_θ = Elastic Circumferential Strain

ν = Poisson's Ratio

ζ_γ ζ_q = Shape Factors

ρ_d = Dry Density

σ_r = Radial Stress

σ'_r = Radial Effective Stress

σ'_{ri} = Radial Effective Stress Acting on the Sand/Clay Interface

σ'_z = Vertical Effective Stress

σ'_{zf} = Vertical Effective Stress Adjacent to Pile Shaft at Failure

σ'_{zi} = Vertical Effective Stress Acting on the Sand/Clay Interface

σ'_{θ} = Circumferential Effective Stress

σ'_1 = Major Principal Effective Stress

σ'_2 = Intermediate Principal Effective Stress

σ'_3 = Minor Principal Effective Stress

ϕ' = Angle of Effective Internal Friction

τ_f = Shear Strength of Sand at Failure

τ_i = Shear Stress Acting on the Sand/Clay Interface

ω = Moisture Content

ω_t = Pile Settlement

CONTENTS

LIST OF TABLES.

LIST OF FIGURES

CHAPTER 1

CHAPTER 3

CHAPTER 4

CHAPTER 5

CHAPTER 6

CHAPTER 7

LIST OF PLATES.

CHAPTER 3

CHAPTER 7

CHAPTER 1

INTRODUCTION AND OBJECTIVES

CHAPTER 1

INTRODUCTION AND OBJECTIVES

1.1 Introduction.

This study forms part of an ongoing investigation at the Polytechnic of Wales into the behaviour of single piles in sand and sand overlying clay. It also constitutes part of a special programme in large scale testing (Geotechnics) being developed by SERC (Science and Engineering Research Council).

Perren(1978) undertook a case study into the choice, construction and performance of bored piles in glacial tills. This material is common in the South Wales region and is generally granular in nature. In order to form a satisfactory pile he found that it was preferable to drive the temporary casing through the granular material and terminate it in the underlying cohesive strata. This effectively sealed off the pile base and prevented further ingress of water from the till, hence enabling a "dry condition" to be established for the formation of the concrete piles.

Kay(1980) used an instrumented 114mm segmented tubular steel pile to model the behaviour of a pile in a layered soil profile, within the confines of the laboratory. The underlying clay stratum was modelled by passing the pile base into a frictionless cylinder, which eliminated end bearing. The overlying granular material was represented by a sand which was placed around the pile in layers. This enabled the study into the development of shaft friction and showed that there was a linear increase in shaft friction at a

shallow depth, becoming constant at greater depths.

Wersching(1987) extended this work by jacking a 114mm pile into both sand and sand/clay profiles. He improved the axial load cells and incorporated contact stress transducers within the pile wall to directly measure the distribution of the shear and normal stresses acting along the pile shaft. Instrumentation was also developed to monitor the vertical movement of the soil and variation in the sand density. At the sand/clay interface various transducers were deployed to measure the development of effective vertical and radial shear stresses acting at the interface level during the test programme. This work showed that:

a) The local unit shaft friction and radial effective stress is practically constant along a pile shaft in sand for a given pile embedment and increases at a diminishing rate with pile embedment.

b) At full pile embedment and ultimate load the local coefficient of earth pressure, K_z, may greatly exceed K_p near the top of the pile and tend to a lower limit of 0.5 near the pile base.

c) The development of shaft friction is directly related to displacements within the sand and on the sand/clay interface.

d) Axial stresses within the sand around the pile shaft are reduced by the development of arching. Adjacent to the pile shaft the radial effective stress is the major axial stress.

Lake(1986) changed the method of pile installation from static to dynamic by using a pneumatic drop hammer system. For practical reasons the pile size was reduced to 60mm. Incorporated into this

pile were static axial core and dynamic load cells. This enabled the measurement of transient forces along the pile as well as the static load distribution. The soil profiles and instrumentation were similar to that employed by Wersching(1987). The work showed that:

a) The pile top impact force was dependent on ram impact velocity only.

b) The transient force at the pile tip could be less than, equal to or greater than the impact force depending on the nature of the bearing surface.

A theoretical method of predicting static bearing capacity using the dynamic equations of motion and dynamic measurements was also outlined. A good agreement was achieved between the experimental and theoretical results.

The work described in this thesis examines the development of shaft friction for the three methods of pile installation described by Kay(1980), Wersching (1987) and Lake(1986) respectively. Its aims were to compare the three methods and using as far as possible the same type of instrumentation. Additional instrumentation was developed by the author to include the monitoring of pore pressure in the clay and the radial movement of the sand.

In general the soil profiles were instrumented in a similar manner to that described by Wersching(1987). The properties of the soils used for the experiments are given in section 1.3.

The load testing schedule was extended to incorporate further maintained load tests to establish any significant effects on the pile/soil interaction due to the dissipation of pore water pressure

and cyclic loading.

1.2 Objectives of the Investigation.

A search of the available literature shows that investigations into pile behaviour within a layered soil profile, consisting of sand overlying clay, is extremely limited. The most relevant contributors outside the Polytechnic are Meyerhof and Tomlinson. The data reported from these authors was obtained with relatively limited instrumentation in both the pile and surrounding soil.

The purpose of the present research project was to perform six semi-full scale tests on piles driven or placed into a sand or sand overlying clay profile. From the data generated by these tests the research programme entailed three other principle aims:

1. An analysis of the data to establish useful relationships between relevant parameters.
2. A verification of the research work carried out by Kay, Wersching and Lake, using as far as possible standardised instrumentation in the course of the work.
3. To develop theoretical models to give further insight into the soil behaviour and soil/pile interaction. e.g. Dynamic formulae for pile installation and the Mohr-Coulomb yield criteria for pile loading.

However due to the volume of data generated, shortage of time and a general directive from the SERC steering group, the dynamic results recorded during the installation of the 60mm pile, have not been analysed or reported in this thesis.

1.3 Soil Properties.

1.3.1 Introduction.

The soils used in this investigation were a uniformily graded quartzitic Leighton Buzzard sand and a red-brown silty clay of low plasticity from the Mercia Mudstone (formerly Keuper Marl) geological formation. The properties of these soils were determined in accordance with BS1377 (1975) and are summarised in Table 1.1.

1.3.2 Leighton Buzzard Sand.

The particle size distribution curve determined from an average of ten samples is shown in Figure 1.1. It compares favourably to that given by Wersching(1987). The coefficients of uniformity ($C_u=D_{60}/D_{10}$) and curvature ($C_C=D_{30}^2/D_{60}D_{10}$) being 1.80 and 1.30 respectively.

The maximum and minimum density values determined by Wersching(1987) using methods described by Akroyd(1957) were 1439.1kg/m^3 and 1780.2kg/m^3 respectively. The placement density obtained during the experiments was generally in the region of 1520kg/m^3 .

A series of 38mm diameter drained triaxial tests was undertaken on a G.D.S. (Geotechnical Digital Systems) computer controlled triaxial system. For an average density of 1520kg/m^{3}a $\emptyset'$ of 36 degrees was established. Wersching(1987) established a relationship between the angle of internal friction and dry density, given in Figure 1.2. He obtained these values by performing a series of 102mm diameter drained triaxial tests on specimens of saturated sand.

1.3.3 Mercia Mudstone (Keuper Marl)

The general properties of the clay were determined by Wersching (1987). An average value of 2.78 was established for its specific gravity. The liquid and plastic limits were determined as 39.0% and 19.5% respectively.

To determine the clay's consolidation properties, four oedometer tests were performed on samples taken from the clay layer. The results gave an average coefficient of consolidation (C_v) of 0.641m^2/year and a coefficient of volume change (M_v) of $6.65 \times 10^{-4} m^2/kN$. From the e-log p graphs the remoulded clay indicated properties of a slightly over-consolidated clay. An average compressive index (C_c) value of 0.133 was established.

The effective angle of internal friction (ϕ') for the remoulded clay was established to be 26 degrees. This was determined from three 38mm diameter consolidated drained triaxial tests using the G.D.S. system.

Figures 1.3 and 1.4 (after Wersching(1987)) respectively illustrate variations in undrained shear strength and clay density with moisture content.

Leighton Buzzard Sand	
Specific Gravity, Gs	2.71
Coefficient Of Uniformity, C_u	1.80
Coefficient Of Curvature, C_c	1.40
Minimum Density	1439kg/m^3
Maximum Density	1780kg/m^3

Mercia Mudstone (Red Keuper Marl)	
Specific Gravity, Gs	2.78
Liquid Limit, Ll	39.0%
Plastic Limit, Pl	19.5%
Coefficient Of Volume Change, M_v	6.65x10^{4}m^2/kN
Coefficient Of Consolidation, C_c	0.641m^2/year

Table 1.1 Soil Properties.

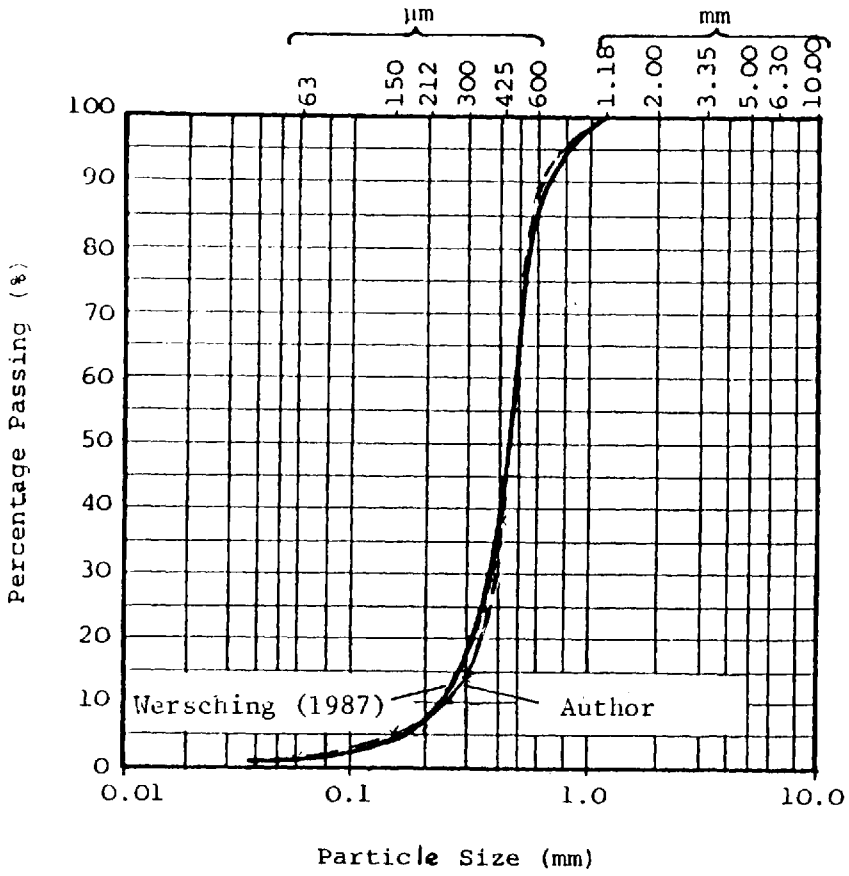

PARTICLE SIZE DISTRIBUTION FOR LEIGHTON BUZZARD SAND

FIGURE 1.1

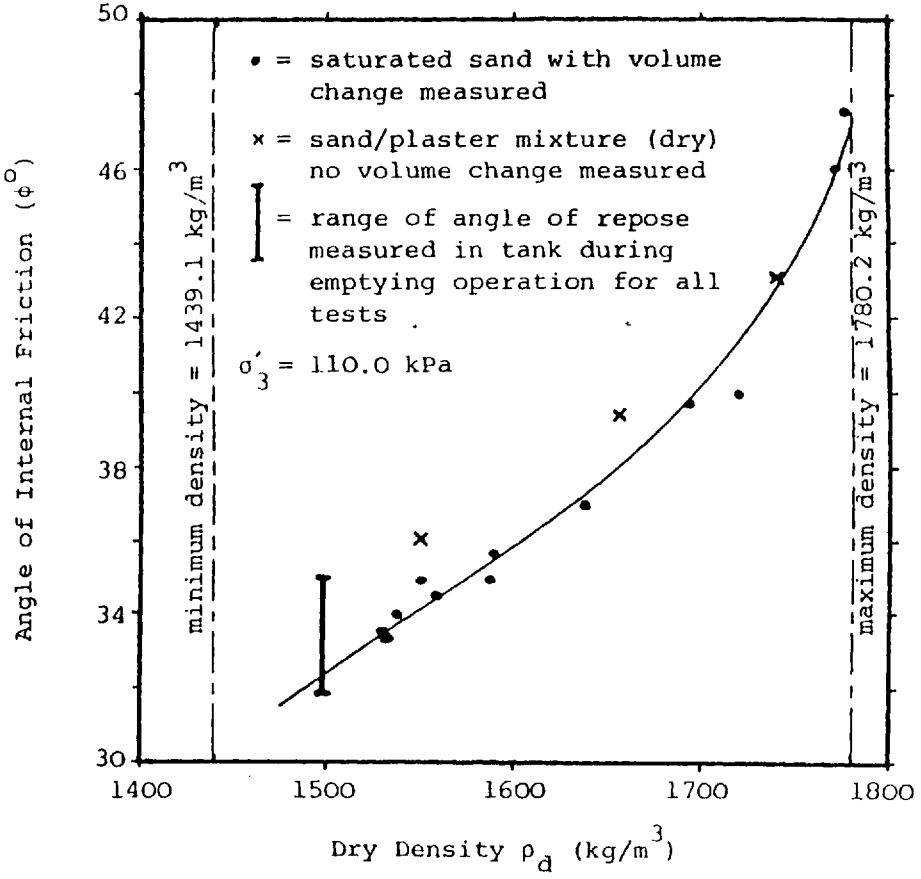

ANGLE OF INTERNAL FRICTION-DRY DENSITY RELATIONSHIP FOR LEIGHTON BUZZARD SAND FROM 102.0 MM DIAMETER DRAINED TRIAXIAL TESTS

FIGURE 1.2

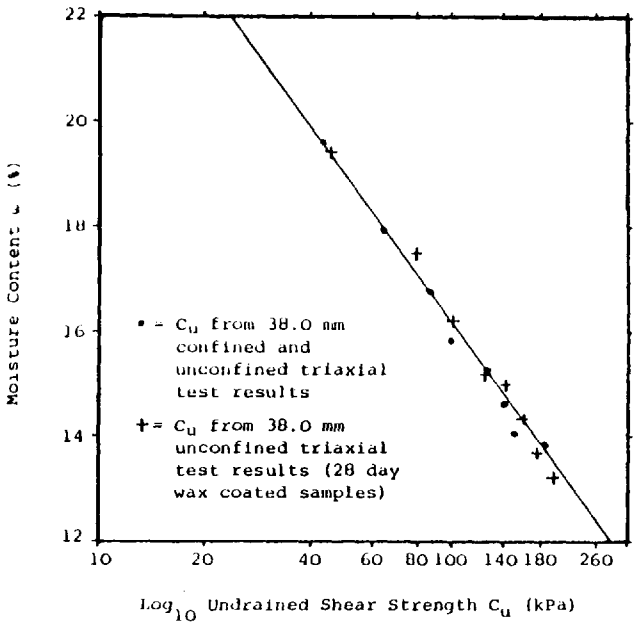

VARIATION IN UNDRAINED SHEAR STRENGTH OF CLAY WITH MOISTURE CONTENT

FIGURE 1.3

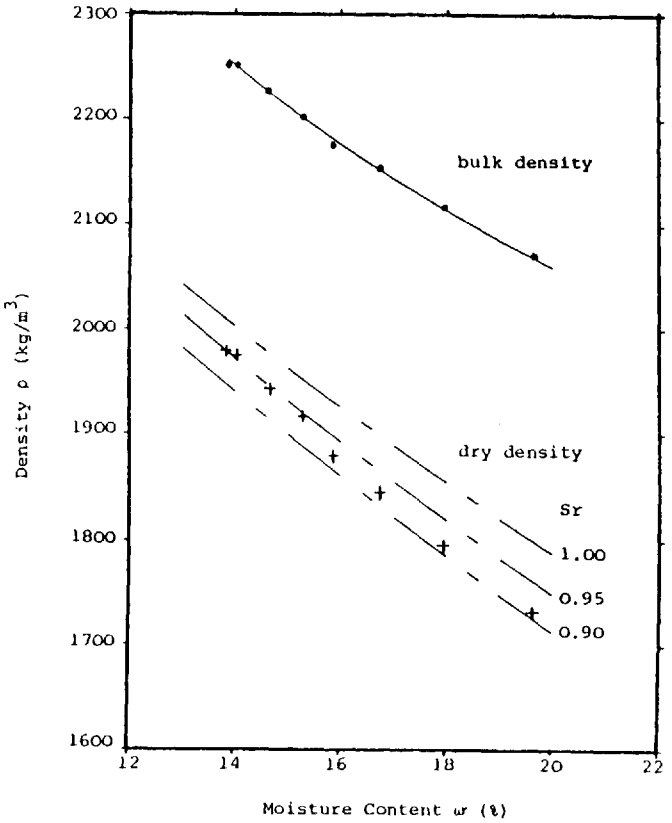

VARIATION IN BULK AND DRY DENSITY OF CLAY WITH MOISTURE CONTENT

FIGURE 1.4

CHAPTER 2

LITERATURE REVIEW

CHAPTER 2

LITERATURE REVIEW

2.1 Introduction

A comprehensive review of the relevant literature has been carried out by previous researchers at the Polytechnic and to avoid repetition, only the salient points are described here. A review of the research work carried out at the Polytechnic of Wales is also included. Where additional instruments have been installed a more detailed review has been undertaken in these particular areas as they have not been previously discussed.

2.2 Piles in Cohesionless Soils.

The generally accepted equation for calculating the resistance of piles in cohesionless materials is given by,

$$Q_t = N_q \gamma D_b A_b + 0.5 K_s \gamma D_b \tan \delta A_s \quad \text{.....equation 2.1}$$

where γ = unit weight of soil

D_b = pile embedment depth

A_b = area of the pile base

A_s = area of pile shaft in contact with the soil

K_s = coefficient of earth pressure

N_q = bearing capacity factor

δ = angle of friction between pile and soil

The first term in the equation relates to the contribution of the soil to end bearing resistance. It implies that Q_b increases linearily with pile embedment. In fact it has been shown by numerous authors that this is not the case, but reaches a limiting value at

some critical depth D_c.

Vesic(1964,1970) showed that for piles driven in medium dense to dense sand, the critical depth D_c was in the region of 20B-30B. In loose sand this value reduced to 10B. This implied that D_c was a function of the sand density. Vesic(1964) also carried out tests on buried, preplaced piles; the critical depths were 10B and 20B for piles in loose medium dense and dense sands respectively.

Kerisel(1964) carried out a series of large scale tests on jacked piles. His results show that below a critical depth the unit base resistance reached a quasi constant limiting value, the depth at which D_c was attained increased with B and the sand density.

Hanna and Tan (1973) reported a value of 30-40B for the onset of critical depth D_c from a series of tests on long slender preplaced piles in a medium dense sand.

From the work of Vesic(1964) it is stated that the base bearing capacity factor N_q was in agreement with values given by Berezantzev(1961) for both driven and buried piles, provided that driven piles were analysed by using an increased sand density equal to the mean density prior to and after pile installation. This infers that the relative increase in point bearing capacity of a driven pile of the same diameter as a placed pile, is due to the increase in sand density caused by pile driving.

Kishida(1967) suggests an effective increase in $\emptyset'$ for driven piles of:

$$\emptyset' = (\emptyset'+40)/2$$

this value of $\emptyset'$ was advocated by Poulos and Davis(1980) in the

determination of N_q for driven piles. For bored piles they suggest a reduction in the initial value of $\emptyset'$ by 3 degrees to account for possible loosening effects due to installation. These resultant changes in $\emptyset'$ alters the value of N_q which ultimately affects the point bearing capacity.

Vesic (1964) stated that at depth generally in excess of 15B the unit base resistance reached on asymtotic final value which was independent of the initial overburden stress and proved to be a function of the relative sand density only. This was explained by the development of arching within the sand above pile base level.

He further emphazised that a fundamental fallacy in the analysis of pile bearing capacity is the assumption that the stress condition at failure around the pile is the same as that prior to pile installation.

Meyerhof(1976) suggested that the effective vertical stress near the pile base at the onset of limiting unit base resistance, is practically independent of the effective overburden stress for a pile embedment of greater than the critical depth.

Hollaway et al (1978) stated that the overburden stress near the pile was affected by the load deformation condition throughout pile installation and subsequent load testing.

The second term in equation 2.1 relates to the contribution skin friction makes to the bearing capacity of the pile. Within this term the local unit friction at failure is given by:-

$$f_{zf} = K_z \sigma'_{zf} \tan \delta'$$

where K_z = local coefficient of earth pressure at failure

σ'_{zf} = vertical effective stress acting adjacent to the pile shaft at failure

δ' = effective friction angle between the pile shaft and the adjacent soil at failure

This equation implies a linear increase in f_z with depth along the pile with the assumption that K_z and δ' are constant along the pile shaft and σ'_{zi} equates to the initial effective overburden pressure.

However, Vesic(1964) reported that K_s varies according to sand density and method of installation. In a loose sand values given for K_s were 2.5 and 1.6 for driven and buried piles respectively. These values increased with sand density. He also suggested that the development in σ'_{zi} was only linear for shallow pile embedment and thereafter tended to a constant value; this condition being the result of the development of arching zones above pile base level.

Hanna and Tan (1973) reported on the distribution of f_{sf} for long, slender pile placed in a medium dense sand, and evaluated from axial load cells in the pile. From the results the value of f_{zf} increased rapidly at shallow depths, thereafter it increased at a reduced rate at a pile embedment of approximately 15.0B, and at 40.0B f_{zf} tended to a constant value.

Meyerhof(1976) reported that K_z may tend to K_p near the pile top and less than K_o near the pile base. Also he shows that K_s increases with ϕ' and is affected by pile installation in a similar manner to that reported by Vesic(1964)

Coyle and Castello(1981) analysed a number of well documented field

tests. They showed K_s to increase with $\emptyset'$ and decrease logarithmically with relative pile embedment (D_b/B). For a shallow pile embedment K_s tended to K_p whilst for deep piles K_s approached K_a

Chandhuri and Symons (1983) carried out tests on fully instrumented straight shafted model single piles, embedded in dense and medium sand, subjected to uplift loads. Their results showed that beyond critical depths of 30B and 11B for a smooth surfaced pile in dense and medium sand the average frictional resistance attained a constant value. They also report that the average value of K_s obtained from their experiments for piles in medium sand was between the limits of K_p and K_a.

An important consideration in the evaluation of pile shaft friction is the effective friction angle between the pile shaft and the adjacent soil. The most widely used values of δ' are those given by Broms(1966) based on work by Pontyondy (1961) and Broms and Silberman(1964).

Pile Material	Friction Angle δ'
Steel	20 degrees
Concrete	$(3/4)\emptyset'$
Wood	$(2/3)\emptyset'$

Various other authors have studied the behaviour of the frictional angle δ' between a sand/metal surface and these are as follows:

	Average $\emptyset'$	δ'
Coyle and Sulaiman(1967)	32 degrees	25 degrees
Hunter and Davisson(1969)	32 degrees	25 degrees
Holloway et al(1978)	32 degrees	26.5 degrees

Butterfield and Andrawes(1973) carried out direct shear tests on various materials in contact with dense or loose sand. Their work illustrated that the static friction angle was generally greater than the kinematic value by some 2 degrees.

2.3 Piles in a Layered Soil Profile

Other than research carried out at the Polytechnic of Wales, there is only a limited amount of published information on the behaviour of piles in a sand overlying clay stratum.

Tomlinson(1970) illustrated that by driving 168mm diameter pile through sand into clay there existed a drawdown zone of sand into the underlying clay. This region extended to approximately 3B into the clay.

Meyerhof and Sastry(1978b) performed a series of model tests on 76.0mm diameter piles driven through sand overlying clay. They identified that if piles penetrate this stratum that failure can occur by punching through the sand into the underlying clay. From their work they suggest that the depth to which piles can be safely driven through a layered soil system, without punching failure depends on the ratio of q_{1w}/q_{1s}, where q_{1w} and q_{1s} are the unit point resistances in the weaker and stronger layers respectively.

Meyerhof and Sastry(1978b) state that in order to avoid punching failure the critical distance between pile tip and the soil interface varied from 1.5B to 6B for q_{1w}/q_{1s} values of 0.67 to 0.02 respectively.

Meyerhof and Sastry(1978b) proposed the following equation for the maximum point resistance (q_p) in a strong layer overlying a weak one.

$$q_p = q_i + 4s_p K_{ps} p_o h' \tan \phi_s / B \leq q_{ls}$$

in which:

$$q_i = C_u N_{co} + \gamma (D_b + h') N_{qo} \leq q_{lw}$$

where q_p = maximum unit point resistance in strong layer

q_i = unit point resistance at the soil interface

C_u = undrained shear strength

K_{ps} = average punching coefficient for a strip footing

s_p = shape factor for punching

h' = maximum punching height

p_o = average overburden pressure at centre of h'

ϕ_s = angle of internal friction of strong soil

B = pile diameter

γ = unit weight of soil

D_b = depth of pile point

N_{co}, N_{qo} = surface bearing capacity factors for circular footing on weaker soil

Tomlinson (1981) reports on results of the piled foundation of a National Coal Board bulk handling plant. The soil profile consisted of variable thickness of dense sandy gravel between thick deposits of boulder clay. Into this stratum 508mm diameter piles were driven and cast in place. It was found that end bearing in the dense gravel was 3000kN. If the base of a pile came in close proximity to the gravel/clay interface the end bearing resistance would fall by some

67%. This reduced the factor of safety of the piles to 1.2. The piles had to be driven an extra 25% into the clay layer to gain additional skin friction to increase the factor of safety. This is broadly in line with the conclusions drawn by Meyerhof and Sastry.

2.4 Research Work at the Polytechnic of Wales.

Perren(1978) studied the behaviour of piled foundations for a series of viaducts along a portion of the M4 near Bridgend, Mid Glamorgan. The ground stratum consisted mainly of glacial till which was granular in nature, underlain by a clay strata. He found that during the use of bored and cast insitu piles it was preferable to form bored piles end bearing in the underlying cohesive soil. This ensured a sealed hole and prevented further ingress of water from the mainly granular glacial till, enabling a "dry condition" to be established for the formation of the concrete pile. However he found that additional information was required to predict the development of shaft friction for piles penetrating granular soils into clay.

Kay(1980) attempted to simulate the field conditions encountered by Perren(1978) within the laboratory. He placed instrumented 114mm diameter piles within a sand to represent the granular till and passed the pile base into a frictionless cylinder to model the underlying clay. His work showed the average skin friction increased linearily at shallow depth and tended to a constant value at greater depths. The point at which it became non-linear was dependent on sand density. He stated the value of K_s decreased as the sand density decreased and the embedment length of the pile increased. The values of K_s were 0.5 and 1.0 for loose and dense sand respectively and

became greater than unity for shallow depths.

Wersching(1987) extended this work by jacking a 114mm pile into both sand and sand/clay profiles. He improved the sensitivity of the axial core load cells, and incorporated contact stress transducers within the pile wall to directly measure the distribution of the shear and normal stresses acting on the pile shaft. The soil profile was also extensively instrumented.

His work principally showed;-

a) The local unit shaft friction and radial effective stress were practically constant along the pile shaft in sand for a given pile embedment and increased at a diminishing rate with pile embedment.

b) The development of shaft friction is directly related to displacements within the sand and on the sand/clay interface.

c) Axial stresses within the sand around the pile shaft are reduced by the development of arching. Adjacent to the pile shaft the radial effective stress is the major axial stress.

d) The critical depth was attained at a pile embedment of 10.5B.

e) At full pile embedment and ultimate load level the local coefficient of earth pressure K_z, may greatly exceed K_p near the top of the pile and tend to a lower limit of 0.5 near the pile base.

f) For a sand with a $\emptyset'$ value of 32 degrees the angle of shaft friction δ' was 23 degrees. Also the kinematic δ' was less than the static value.

During his research Wersching(1987) was critical of the use of axial load cells in the determination of skin friction. He argued that minor fluctuations in load cell readings could lead to inaccurate representation of the distribution of skin friction along the pile shaft.

It was clear from the work of Kay and Wersching that the method of forming a pile had a significant effect upon the development of shaft friction and end bearing resistance. It was, therefore, desirable to investigate the dynamic method of driving.

Lake(1986) changed the method of pile installation from static to dynamic by using a pneumatic drop hammer system. For practical reasons the pile size was reduced to 60mm. Incorporated in his work was a theoretical approach for predicting the static bearing capacity using the dynamic equations of motion and dynamic measurement. A good agreement was achieved between the experimental and theoretical results. His work also showed that:

a) The pile top impact force was dependent on ram impact velocity only.

b) The transient force at the pile tip could be less than, equal to or greater than the impact force, depending on the nature of the bearing surface.

c) K_s was marginally less than K_p at shallow depths and tended to K_a near the pile tip.

d) The stress transfer curves tended to a limiting value at shallow depth, and decreased at a reduced rate with depth.

2.5 Pore Water Pressure Developed in Clay During Pile Installation and Load Testing.

2.5.1 Introduction.

Very little information exists on the development of pore water pressure in the clay due to a driven pile in a layered soil system. The influence and effect of the overlying sand, the resultant influence of the drawdown area illustrated by Tomlinson(1970), and the sand plug at the pile base illustrated by Lake(1986) and Wersching(1987) are relatively unknown. To establish some relationship between relevant parameters for the generation of pore water pressure during pile installation in a clay soil, a review of the numerous papers published was carried out.

2.5.2 Pore Pressure Developed During the Installation of Displacement Piles in Clay.

Cooke and Price(1973) showed that when a displacement pile is installed there must be an equivalent volume of soil displaced. Some of this soil is shown in surface heave, but for large penetrations, the soil is predominantly displaced radially. It is this radial displacement which causes an increase in total stress levels in the soil close to the pile and the generation of excess pore water pressure. However this induced pore water pressure dissipates with time and consequently the local undrained shear strength and effective stress levels increase, which in turn increases the load capacity of the pile.

Lo and Stermac(1965) derived an expression to predict the maximum pore pressure generated near the surface of a driven pile. i.e.

$$\Delta u_m = ((1-K_o) + (\Delta u / p)_m)\sigma'_{zi} \quad \text{..... equation 2.2}$$

where Δu_m = maximum excess pore water pressure

K_o = insitu coefficient of earth presure at rest

$(\Delta u/p)_m$ = maximum pore pressure ratio

p = consolidation pressure

σ'_{zi} = initial effective vertical stress

By comparing the results of measured pore pressures obtained from a series of field tests they were able to reasonably predict the maximum induced pore pressure by a driven pile using equation 2.2. They also stated that the magnitude of the maximum induced pore pressure depended on the pore pressure ratio and the state of stress in the ground, but is independent of the dimensions or type of pile.

Poulos and Davis(1980) included a summary of measured pore water pressure from various field tests. It illustrates that the value of excess pore water pressure generated near driven piles is dependent on the sensitivity of the clay. It ranges from between 1.5 to 2.0 times the effective vertical stress near the pile, the higher values being obtained in the more sensitive clays.

As a means of estimating the excess pore water pressure distribution the following procedure is suggested by Poulos and Davis(1980)

1. Obtain the maximum pore water pressure Δu_m by using an adjusted form of Lo and Stermac's equation given by D'Appolonia and Lambe(1971):

$$\Delta u_m/\sigma'_{zi} = ((1-K_o)\ (2C_u/\sigma'_{zi}))A_f$$

2. Take this value to be acting at a distance R from the pile face. R varies from 1.5B to 2B for insensitive clays and up to 4B for sensitive clays.
3. Beyond the radial distance R the excess pore water

pressure is assumed to vary inversely as the square of the radial distance r' from the pile:

$$\Delta u = \Delta u_m/(r'/R)$$

This inverse relationship is predicted from elastic theory developed by Nishida(1963) and Ladanyi(1963). Beyond a radial distance of 8B the pore water pressures are negligible. It has been frequently shown that the pore pressures generated at the tip of an advancing pile are significantly higher than those acting on the pile shaft some distance above the tip.

Rigden et al(1979) have shown that for piles driven in glacial till, the pore water pressure developed at the tip was 6 times the undrained cohesive strength of the soil,and 4 times along the pile shaft.

Roy et al(1981) drove piles into soft sensitive clays. The excess pore water pressure at the tip was 7 times the undrained shear strength and reduced to 3.5Cu at a distance of approximately 7.5 pile diameters from the tip.

Holtz and Bomen(1974) studied the effect of drainage channels attached to piles during installation. To achieve this they attached paper plastic drains to wood piles. A total of 61 piles were driven, 48 had the drains attached. The results indicated at least a 50% relative reduction in excess pore water pressure where the drains were used.

Randolph et al(1979) considered the effects of pile permeability on the consolidation process after driving. They concluded that the rate of consolidation and hence the rate of gain of pile load carrying

capacity would be greater around permeable piles than impermeable ones.

2.5.3 Pore Pressures Developed During the Load Testing of Piles.

It has generally been observed that the generation of excess pore pressure is much less and more localised during loading of piles as compared to driving.

Lo and Strermac(1965) reported values of approximately $0.25C_u$ at a distance of 1.0B from the pile axis in a silty clay.

Clark and Meyerhof(1972) carried out tests on 75mm diameter steel piles driven in clay. They detected increases in pore water pressure of 0.2-0.6 times the undrained cohesion C_u, at a distance of 1.0B from the pile axis.

Massarsch et al (1975) measured changes in pore water pressure at the shaft face of 75-125mm piles in sensitive clay. They detected increases in pore water pressure of up to $1.25C_u$.

Roy et al(1981) performed load tests on 220mm diameter steel piles driven into soft sensitive Champlain Clay. The pore pressures recorded at the pile face varied between 0.6-1.5, the initial undrained compressive strength, C_{ui}. At a distance of 1.0B from the pile shaft no change in the pore pressure was recorded.

A study was undertaken by Briaud and Felio(1986) to study the response of piles subjected to cyclic loading. They concluded that the pore pressures at the soil/pile interface do not increase significantly during cyclic loading, in some cases a decrease in pore pressure was observed as the shear transfer degraded.

They also found that a cyclic threshold exists above which failure occurs by plunging or pull out of the pile. On average this threshold is 80% of the ultimate capacity of the pile. Cyclic loading below this threshold does not produce any significantly decrease in the ultimate static load capacity.

Prech (1982) performed cyclic load tests on 273mm diameter piles driven into silty sand and silty clay. After 1000 cycles he found that the pore water pressure at the soil/pile interface remained low at 4kPa

2.6 'Effective Stress Theory' in Pile Design.

Burland(1973) stated that there was little fundamantal justification for relating shaft adhesion to undrained shear strength because of the severe local disturbance during pile installation and local drainage of the soil adjacent to the pile shaft may be expected to be rapid. The skin friction may therefore be expressed in terms of effective stress:

$$q_s = 0.5\ K_s\ \sigma'_{zi}\ \tan\ \delta' = Bs\ \sigma'_{zi}$$

Bs is an empirical coefficient where the value of K_s depends on soil type, the method of pile installation and the stress history of the soil. The estimation of K_s and evaluation of δ are quite problematic. K_s in London Clay for example may be as high as 3 near the surface and decrease to less than 1 at depths below 30m. A lower bound value of Bs may be attained by assuming $\delta'=\emptyset'$ and $K_s=1-\sin\emptyset'$, where $\emptyset'$ is the remoulded drained angle of shear resistance. Tests on driven piles in London Clay showed values of Bs in the range 0.8 to 1.0.

Weltman(1978) calculated values of K_s from back analysis on results obtained from various pile installation and types in glacial till. The resultant valuesof B_s vary between 0.5 and 1.2. Parry (1980) shows that the first failure of the clay may occur on planes inclined to the pile axis and that the peak mobilisation of friction will in general be less than the effective angle of shearing resistance ϕ' for the clay.

2.7 Expansion of a Cavity in a Soil Media

The excess pore water pressure may be predicted using the theory of the expansion of a cavity in an infinite media. Ladanyi (1963) using a numerical integration technique, demonstrated that this theory applied to a saturated clay medium. It can be used for estimating approximately the excess pore water pressure distribution around a pile driven into a saturated clay during and immediately after driving.

Butterfield and Bannerjee(1970) modelled the installation of driven piles as the undrained plane strain expansion of a cylindrical cavity in the soil, from zero to a finite radius. The analysis predicted that the excess pore water pressure generated at the pile/soil interface would be of the order of 4.0 to 6.5 times the initial undrained shear strength of the clay. This compared favourably with field results presented by Lo and Stermac(1965) and Koizumi and Ito(1967)

Carter, Randolf and Wroth (1978) developed a technique which allowed the determination of pore pressure ans stress changes in a saturated clay due to cylindrical cavity expansion. Estimates of these changes

can be made at any time during the expansion as well as during the subsequent period of reconsolidation.

Martins(1983) stated that the predicted pore water pressure changes from the method given by Carter et al (1978) are in fair agreement with field measurements. Numerous authors e.g. Kirby and Esrig(1979), Randolph, Carter and Wroth (1979a) and Randolph and Wroth (1979) have attempted to model the effective and total stress changes during pile installation, the subsequent dissipation of excess pore pressure and axial loading of the pile to failure. These are complex problems to stimulate and have necessitated considerable use of simplifying assumptions in order to make any progress analytically.

Firstly pile installation has been modelled conceptually as the expansion of a cylindrical cavity, by purely radial soil movement, no real distinction being made between jacked or dynamically driven piles. Subsequent consolidation of the soil around the pile has been modelled assuming radial flow of pore water and radial soil movement, with no account taken of the free ground surface or the more complex conditions near the base of the pile

Steenfelt, Randolph and Wroth (1981) presented results of 19mm diamater pile tests, to validate cavity expansion theories. They concluded that the extent of radial soil movement and generation of excess pore water pressure were generally in good agreement with the cavity expansion model. The excess pore pressures at the pile shaft during installation were lower than predicted from the cavity expansion model; those generated in the body of the clay were in good agreement. The overall rate of dissipation of the excess pore pressures was also consistent with theoretical predictions for

normally and lightly over consolidated clay, but was more rapid than predicted for highly over consolidated clay.

2.8 Dissipation of Excess Pore Water Pressure

The excess pore water pressure generated during pile installation dissipates with time. Due to the increase in effective stress and loss in water content the clay adjacent to the pile has a higher undrained shear strength than the initial value. This increase in strength of the clay is reflected by the increased capacity of the pile. Numerous authors have modelled the rate of dissipation of excess pore water pressure and its consolidation effects.

Seed and Reese(1955) carried out tests on 150mm piles driven into organic silty clay to examine the effect of consolidation on the clay around the pile and the capacity of the pile. Their results showed that the undrained shear strength of the clay had increased in strength by 1.5 and 3 times the initial undisturbed and the initial disturbed values respectively. The capacity of the pile generally increased 5 fold during the dissipation period.

Soderburg (1962) produced a method of predicting the rate of dissipation of excess pore water pressure with time. It assumes that dissipation occurs radially only, the vertical dissipation that may occur near the top and bottom of the pile being ignored. The equation is:

$$\delta u/\delta t = C_h((\delta^2 u/\delta r^2)+(1/r)(\delta u/\delta r))$$

where C_h is the two dimensional coefficient of consolidation for horizontal drainage and u the excess pore water pressure.

Randolf and Wroth (1979) produced an analytical solution for the consolidation around a driven pile based on radial flow of pore water. The solution enabled them to deduce pore pressure and stress changes in the soil around an impermeable rigid pile. The initial excess pore water pressure distribution from pile installation is that presented by expansion of a cylindrical cavity from zero to the radius of the pile. The magnitude of this excess pore pressure distribution is approximately linear with the logarithm of the radius from the pile axis. Good correlation was shown between the predicted decay of pore pressure close to the pile and the increase in bearing capacity of driven piles.

Martins (1983) produced a one dimensional finite difference program enabling the rate of dissipation of excess pore water pressure around a driven pile to be predicted.

It is generally accepted that the nature of the pile material influences the dissipation rate of the pore pressure. Consolidation occurs faster around timber piles than it does around steel piles. Holtz and Bomen (1973) illustrated how drains attached to piles reduce the generation of pore pressure during installation.

For the two layered soil system of sand overlying clay, the dragdown of sand by a driven pile into the clay would have a similar effect. For a low L/B ratio into the clay this would have a considerable influence particularly when coupled with the effects of the sand plug driven ahead of the pile.

The above papers generally illustrate the limit of our understanding of piles in layered soils, consisting of sand overlying clay.

CHAPTER 3

SEMI-FULL SCALE EQUIPMENT, INSTRUMENTATION AND MONITORING SYSTEM

CHAPTER 3

SEMI-FULL SCALE EQUIPMENT, INSTRUMENTATION AND MONITORING SYSTEM.

3.1 Introduction.

The semi-full scale tests were carried out by utilising the extensive apparatus and equipment already available in the Geotechnics Laboratory. Only an outline description of the existing equipment is included in this thesis. A full description is given by; Kay(1980), Lake(1986) and Wersching (1987).

As a result of Wersching and Lake's work it was deemed necessary to develop and include monitoring systems for the measurement of horizontal movement within the sand strata and the monitoring of the pore water pressure in the clay.

The system for monitoring horizontal movement measures lateral soil displacements directly. By using these radial displacements in conjunction with the vertical displacements obtained from the inclinometers, a two dimensional soil displacement profile can be configured directly in relation to pile installation and load testing.

By monitoring the generation and dissipation of pore water pressure during driving and load testing of a pile the stress state within the clay can be examined. In particular, it was conceived that by monitoring this pressure it would be possible to examine the influence of the sand plug driven ahead of the pile on the pore water pressure dissipation.

Appropriate instrumentation was developed to achieve these additional measurements and a comprehensive description is included in this section.

The calibration, placement and location of all the instrumentation is described in Chapter 5.

3.2 Sand Tanks And Loading Frame.

The two 3m diameter times 3m deep sand tanks and loading frame used in the semi-full scale tests are illustrated in Figures 3.1 and 3.2. The tanks are connected by a Redlar conveyor system which enables sand to be transfered from one tank to another. Only one tank was used in the tests, the other was used for storage.

The influence of the boundary conditions set up by the confinement of the tank on the test results has been considered by previous researchers at the Polytechnic of Wales. The pile length to diameter ratios set up by the 60mm and 114mm piles were 34 and 16 respectively. They were specifically chosen by Wersching and Lake so that boundary zones previously prescribed by various authors were not encroached. Typical values given by Robinsky and Morrison (1964), Meyerhof (1959), and others are 8B radially from the pile and 5B below the pile base.

The loading frame is mounted on top of the testing tank as illustrated in Figure 3.2. This allows easy access to the test tank whilst providing a stiff crosshead for the Dartec Jack loading system. The datum frame on which the displacement transducers are mounted is located underneath, but independent of the loading frame.

A full description of this equipment is given by Kay (1980).

3.3 Secondary Clay Tank.

The secondary tank used to contain the clay was a sectional steel 'Braithwaite' tank. Constructed into this were wooden formers to give a cylindrical vessel of 1.10m in diameter by 1.13m deep. Again the influence of the boundary confinements on the test results were considered by Wersching and Lake. From literature reported by Clarke and Meyerhof (1972), Cooke et al (1979), Randolf et al (1979) and Poulos and Davis (1980), the influence zone around a driven pile in clay varies from 6B to 12B with a base clearance of typically 3B.

To examine and extract samples from the clay layer after testing, one side of the formwork had to be removed. Lake (1986) found that tension cracks were present within the clay. Whether these tension cracks developed during the load testing of the pile or the slumping action of the clay under its own self weight when the formwork was removed, was not fully established. It was therefore decided to divide the formwork into three horizontal sections. This allowed the clay to be removed in sections whilst the bulk of the clay was held in place hence preventing any slumping action.

3.4 Frictionless Cylinder.

To model the behaviour of a pile in sand overlying clay Kay(1980) simulated the underlying clay by passing the pile base into a frictionless cylinder. The shear stress developed along the pile shaft was determined from axial load cells within the pile. To make a comparison with the work of Kay using the pile developed by Wersching

(1987) into which Boundary Orthogonal Stress Transducers (B.O.S.T.s) (refer to Section 3.8.2) were incorporated, similar test conditions were used.

This was achieved by using the frictionless cylinder developed by Kay, illustrated in Figure 3.3. It consists of a steel cylinder which houses a configuration of two rubber seals and a phosphor-bronze bearing surface. The end of the pile passed into this cylinder and eliminated the end bearing.

3.5 Dartec Jack.

The load tests were carried out using a 50kN capacity Dartec jack mounted on the crosshead and loading frame. The jack was operated in either displacement or load control mode and was managed by a Dartec Jack control unit in conjunction with a Type Exact TY 336 MTFG function generator. The system was interfaced with a P.E.T. micro computer which enabled all the installation and loading operations to be synchronised and managed by the main control program.

3.6 Pile Guides.

3.6.1 Guide For 114mm Diameter Pile.

The 114mm diameter pile was kept vertical throughout installation and load testing by an arrangement of six roller bearings. These were arranged in two levels, with three bearings on each level set at 120 degrees to each other. This provided a frictionless guide which kept the pile vertical with a maximum deviation from the vertical plane of 1/175. This was well within the limit of 1/75 specified by B.S.8004 (1986). The pile could be locked in position between each

drive or load operation by three bolts located just below the upper level of bearings.

3.6.2 Guide For The 60mm Pile.

The pile was kept vertical by an arrangement of four 'V' shaped roller bearings. Two levels of bearings were employed with two bearings on each. The pile then sits tangential to the 'V' roller bearings restraining it from deviating from the vertical plane. The pile could be clamped between each driving increment through a clamping arrangement sited between the two levels of bearings.

3.7 The Installation And Load Testing Of The Semi-Full Scale Piles.

3.7.1 Dynamic Installation And Load Testing Of The 60mm Diameter Pile.

A pneumatically controlled pile driving system was designed by Lake (1986) to install the 60mm diameter pile, and is illustrated in Figure 3.4. This allows the pile to be driven in approximately 500mm increments at a constant blow rate whilst maintaining a constant drop height for the driving hammer. Once the pile is fully driven, the driving rig can be dismantled in preparation for the static load tests. (Refer to Chapter 5.4). These tests were carried out using the Dartec Jack system, Section 3.5, which was mounted co-axially over the pile on to the loading frame, refer to Figure 3.2. Full details are given by Lake(1986).

3.7.2 Static Installation And Load Testing Of The 114mm Diameter Pile.

The 114mm diameter pile was installed using a constant rate of penetration method. This was achieved by mounting the Dartec Jack co-axially over the pile. A routine was set up via the function generator for the Dartec Jack, which enabled the pile to be driven in 100mm increments at a rate of 10 mm/minute. When the pile was fully driven a series of load tests could then be carried out. (Refer to Chapter 5.4). Full details are given by Wersching (1987).

3.8 Semi-Full Scale Piles.

3.8.1. 60m.m. Diameter Steel Pile.

Lake(1986) designed this pile incorporating dynamic load cells as well as the static axial core load cells within its segmented elements.

There are five static axial core load cells and three dynamic force transducers (kistler piezoelectric load washers), the positions of which are illustrated in Figure 3.5a. Incorporated into the pile cap is an accelerometer to pick up the velocity, time and displacement history of the pile whilst it is dynamically driven. The full development and specification of this equipment is given by Lake (1986).

The Boundary Orthogonal Stress Transducer (B.O.S.T.) could not be incorporated within the 60mm pile because of its dimensional restrictions and the ambiguity of it operating satisfactorily and withstanding dynamic driving conditions.

3.8.2 114mm Diameter Steel Pile

This pile (refer to Figure 3.5b) was designed by Wersching (1987). It is fully instrumentated with four axial core load cells mounted within the pile. Incorporated into the wall of the pile at regular intervals are contact stress transducers which monitor the soil-pile interaction during the driving and the load testing. This boundary orthogonal stress transducer (B.O.S.T),is illustrated in Plates 3.1 and 3.2. It is based on the Cambridge stress contact transducer and was developed by Wersching (1987), full details are given in his thesis.

3.9 Existing Soil Instrumentation.

3.9.1. Electrolytic Levels. (Inclinometers).

The use of inclinometers to measure in-situ displacements around driven piles has been fully reported by Cooke, Price and Tarr (1979), Wersching (1987) and Lake (1986). They essentially consist of a tubular glass envelope half filled with electrolytic fluid which partially submerges three electrodes. The inclinometers are excited via a conditioning unit with a 3 volt alternating current. The output voltage is calibrated against the angle of rotation of the instrument. Using this relationship the vertical displacement can be deduced by an integration procedure developed by Wersching (1987).

From previous research work the electrolytic levels type 0714 placed nearest the pile proved to be slightly unreliable. There was some ambiguity over their exact orientation, particularly those at the sand/clay interface. These were replaced by type 0716 which gave more

reliable results, see Plate 3.3.

3.9.2 Sand Density Measurement.

Local sand densities were measured within the sand layer using a technique developed by Werscheing et al(1983). This involved locating small samples of an unhydrated sand/plaster mixture within the sand at predetermined positions and levels. These samples were hydrated with a water/detergent solution via a fine plastic tube, see Plate 3.4, after the completion of the testing programme. They were then retrieved from the sand and the in-situ dry density correlated from them.

3.9.3 Diaphragm Pressure Transducers. (D.P.T.s)

The Nottingham diaphragm pressure transducers (see Plate 3.5) which consists of a circular strain gauged diaphragm in a steel housing were used in the semi-full scale tests. The suitability of these instruments for use in the experiments with regard to soil type and load cell aspect ratio are fully discussed by Werscheing (1987).

3.9.4 Interface Shear Stress Transducers (I.S.S.T.s)

Shear stress transducers (see Plate 3.5) were used to monitor the movement of the sand at the sand/clay interface. These consist of a strain gauged, machined alloy unit housed within a steel box. The transducers were embedded within the clay leaving the active face exposed to the movement of the sand. Full details are given by Werscheing (1987).

3.9.5 Linear Voltage Displacement Transducers (L.V.D.T.s).

Three types of L.V.D.T.s were used namely the Sakae types, 15FLP, 20FLP and 30FLP. The 30 FLP and 20 FLP type L.V.D.T.s were mounted onto the datum frame located just below the loading gantry. They had two purposes:-

1. To measure the sand surface displacements due to pile installation and loading
2. To measure in-situ vertical displacements of the outermost electrolytic levels.

The 15FLP series transducer was used to monitor horizontal displacements within the sand layer. Initially several types of transducers were considered for this purpose, but the 15FLP series was deemed to be the most suitable.

Essentially the 15FLP series consists of a conductive plastic resistance element and a multi-fingered wiper contact contained in a high impact case. The conductive plastic element provides virtually infinite resolution and excellent linearity 0.005(0.5%)

The wiper contact is mounted on a spindle passing through both ends of the casing, giving double bearing surfaces for high stability. This was deemed an essential feature for the accuracy required from the transducer, particularly as the instrument would be mounted on the horizontal plane. The shaft is threaded at one end enabling the wire strand, connected to the terra plate, to be securely attached through a clamping device, see Plate 3.6. The spring return device on the spindle is incorporated within the plastic casing. This aided the placement technique of the terra plates in the sand.

3.10 Voltage Supply Units.

Four voltage supply units were used to energise the various types of instrumentation. Their stability was continually monitored during the testing programme and was found to be satisfactory.

3.11 Additional Soil Instrumentation

3.11.1 Horizontal Movement Within The Sand Layer.

3.11.1.1 Introduction.

A decision was made to incorporate a horizontal measuring system into the sand layer. This would monitor the horizontal radial movement of the sand particles during driving and loading of the test piles. Using these radial displacements in conjunction with the vertical displacements gathered from the inclinometers, a two dimensional soil displacement profile can be obtained.

The location and placement techniques of existing instrumentation developed by Wersching and Lake minimised any significant effect on the properties and behaviour of the soil. Particular care was taken in the influence zone around the pile. The additional instruments were located and placed within the soil in a similar manner to those developed by Wersching and Lake.

To date no reference has been established, to any author attempting to monitor directly the lateral movement in the sand layer during driving and loading operations of the test pile. Cooke(1978) states that at that time direct measurements of the soil displacements

around a driven pile were few, since the displacements can be small as to approach the limit of accuracy of the gauges used. However Clark and Meyerhof (1972) and Cooke and Price (1973) have monitored the lateral movement when piles have been driven into a clay media. Carr and Hanna (1971) monitored lateral movement in a sand media near anchor plates. Roscoe et al (1963) and Robinsky and Morrison(1964) monitored strains in soils by the use of an X-Ray method.

Clark and Meyerhof (1972) placed miniature linear voltage displacement transducers (L.V.D.T.) in the horizontal plane in a clay media and monitored their response during driving of a 75mm diameter steel pile.

Cooke and Price (1973) monitored the horizontal movement in a London clay whilst driving a 168mm diameter steel pile at a constant rate or penetration. The monitoring system consisted of horizontal probes, the movement of which was monitored by dial gauges.

Carr and Hanna (1971) monitored the horizontal movement in a sand, around circular anchor plates. The instruments consisted of small triangular plates connected to rods. These rods passed through the sand in cylindrical steel sleeves, and their movement was monitored by dial gauges.

Roscoe et al (1963) and Robinsky and Morrison (1964) used the X-Ray method to determine soil strains. This involved the monitoring of small metalic objects placed within the soil strata by the use of X-Rays. This is an expensive technique and only really applicable to smale scale tests.

Davidson et al (1981) monitored the deformations in sand around a

cone penetrometer tip using a pseudo stereo photographic technique. A computer program was then used to calculate volumetric strains and particle displacements at a number of points in the axial symmetry plane.

Kay (1980) initially considered the monitoring of horizontal movement in a sand. The main problem at the time was how the instrumentation would affect the properties of the sand.

The method selected by the author for monitoring this movement is similar to that employed by Kay (1980) for measuring the vertical movement in the sand. He used a series of 25mm square aluminium plates, " terra plates", which were connected to displacement transducers via strands of piano wire. It was proposed to translate this method into the horizontal plane within the sand layer.

3.11.1.2 Type Of Instrument.

The instrument consists of a linear voltage displacement transducer (L.V.D.T.) which is housed in a P.V.C box, see Plate 3.6. To the displacement transducer is attached a perspex plate via a length of piano wire. Any movement in the sand strata will be translated to the displacement transducer via this piano wire.

3.11.1.3 Optimum Size Of The 'Terra Plate'.

Kay used a 25mm square plate for the measurement of vertical displacement during his pile testing programme. During trial tests in placement techniques, it was found necessary to increase the size of the plate to 37.5mm. This was due to two main reasons:-

1. The larger plate aided the method of placement.

2. It gave greater stability against any creep effects.

The displacement transducer was spring loaded, and on release of the small tensile force the larger plates were held in equilibrium in the sand. After several days of monitoring in trial tests the transducer with the plate in position, showed no creep effects. Three sizes of square plates were monitored in this way, i.e. 25, 37.5, and 50mm. The optimum size was found to be 37.5mm as previously stated.

The method of placement of the instrument is discussed in Chapter 5.3.

The 'Sakae' 15FLP series displacement transducer was best suited for monitoring the displacement as discused in Section 3.9.5.

3.11.1.4 Construction Of The Horizontal Monitoring Device.

The displacement transducer was mounted onto a stiff perspex block and housed in a plastic box, see Plate 3.6. This was necessary for protection. They were located on the outer boundary of the sand layer, attached to the rigid framework around the wall of the concrete tank.

A length of piano wire was attached to each of the terra plates. This was achieved by passing the wire through a hole drilled in the centre of the plate and securing it with an epoxy resin glue. The other end of the piano wire was attached to the displacement transducer via a small connecting block. The piano wire leading from the transducer passed out of the box through a rubber grommet. This grommet was made of a flexible rubber membrane such that any sand grains trapped between the wire and the membrane would not impede the movement of

the monitoring device.

3.11.1.5 Tensile Test On The Piano Wire Strand.

Tensile tests were carried out on the steel wire strand to be used in the horizontal monitoring system, to establish the load / extension relationship. The tests were carried out on the Instron 1251. From the load extension graph the 0.5mm wire strand extended at a rate of 0.048mm per 1Kg of load.

The maximum tensile force due to the return spring in the transducer is 200grams. From this the maximum extension of the wire when initially setting up the terra plates , would be equal to 0.0096mm. Although this extension is in the elastic region of the steel strand and is recoverable, it is less than 0.05% for the displacement range of the transducer. It was therefore considered that it would have a negligible effect on the overall results.

3.11.2 Pore Water Pressure Monitoring System.

3.11.2.1 Introduction.

There have been numerous types of miniature pore pressure monitoring devices developed for various types of research work e.g. Hughes and Townsend (1966), Hight (1985), and Shuri, Driscoll and Garner (1985).

Hughes and Townsend (1966) developed a probe for measuring pore water pressure in varved clays. The probe was made from a modified Number 16 hyperdermic needle coupled to a fine bore plastic tube. This was then connected to a pressure transducer. The hyperdermic probe could be flushed with de-aired water and inserted into a triaxial sample.

This probe proved capable of picking up pore water pressure accurately and quickly, where the pressures developed ranged from 1-100p.s.i.

Hight (1985) developed a piezometer probe at Imperial College for the routine measurement of pore pressures in saturated clays tested in the triaxial apparatus. This type of piezometer probe has been used in triaxial testing since 1944 and has been intermittently used ever since. This particular type developed by Hight is a miniature silicon diaphragm pressure transducer with integral semiconductor strain gauge bridge and is similar in principle to the 'Druck' miniature pore pressure transducer. It is mounted and positioned with its porous ceramic face flush with the cylindrical surface at the sample mid-height. This combination leads to a minimum of interference between the piezometer and soil sample, and to a short response time for the piezometer soil system.

Shuri et al (1985) developed a stiff low volume, high air entry piezometer, which was used in controlled displacement - rate in-situ shear test with pore pressure measurement . The sensor consists of a high air entry ceramic disc 19mm in diameter and 6mm thick. This element is glued with an epoxy resin into a hollow brass cup. Two 3mm O.D copper tubes lead to an electronic pressure transducer and the whole system can be de-aired via a system of shut off valves. Again this system is very similar to that used at Imperial College in the testing of 100mm triaxial samples, where instead of a ceramic disc a small ceramic cup is used.

A miniature piezometer tip was developed similar to that used at Imperial College, London. After perfecting the manufacturing and

placement techniqes of the piezometer a series of tests were undertaken to monitor the response time. Initially the piezometer was incorporated into a 102mm clay sample placed within a triaxial cell. This was then used to monitor the pore water pressure developed in the clay (red marl) due to isotropic loading conditions.

Following the triaxial tests it was decided to perform a small pilot study using a 38mm diameter pile. (Refer to Chapter 4.2). It involved dynamically driving the pile into a two layered soil strata, i.e. sand overlying clay. Three miniature piezometer tips were placed in the clay layer to monitor changes in the pore water pressure.

After completion of the pilot study the pore pressure monitoring system was expanded and incorporated into the semi-full scale tests which were monitored by the Orion data logger, controlled by the P.E.T. micro-computer.

3.11.2.2 Factors Influencing The Choice Of The Piezometer System.

There were a number of factors which influenced the final decision on the type of pore pressure monitoring system which was developed.

1. The response time.
2. The reliability and durability of the instrument.
3. The robustness of the piezometer tip.
4. Size.
5. Method of placement.
6. Economics.

The first three points were obviously the most important to be considered, whereby the final points always carried an influencing factor in the final choice of piezometer.

The most readily available monitoring system to be considered was the 'Druck' miniature pore pressure transducer. It has been proven a reliable instrument and its size would have little influence on the properties of the soil considered. The main disadvantages are its possible lack of robustness over prolonged use in some possible adverse conditions. It is a self contained unit and any damage would result in a considerable replacement cost. Also there is no de-airing facilities when the transducer is placed in-situ. The facility for de-airing is considered necessary particularly when a series of loading tests over a period of time were being considered.

To satisfy the general requirement set out, it was decided to develop a piezometer system similar to that used by Imperial College and Shuri et al (1985). The ceramic element is a porous cup supplied by Soil Moisture Corporation, U.S.A. This element is glued with an epoxy resin into a brass cup. Two 2mm O.D. drawn annealled stainless steel tubes lead from the piezometer to an electronic pressure transducers and a system of valves which are used to de-air the system, refer to Figure 3.6.

3.11.2.3 Choice Of Ceramic Tip.

The bubbling pressure, or air entry value of a porous ceramic disc, is the pressure required to force air through the disc after it has been thoroughly soaked in de-aired water. The smaller the pores in the plate, the higher this pressure will be. Obviously the air entry value of the disc is an important consideration when involved with pore water pressure measurement in unsaturated soils. The clay which was used in the model pile tests is classed as saturated i.e.zero air

voids (Lake 1986). In this case the bubbling pressure is not as important as in unsaturated soils, particularly as the monitoring system adopted has the facility of de-airing the piezometer probe.

The response time of the probe is another important feature. Response times can be measured by monitoring the response of the transducer to the changes caused by instantaneous change in cell pressure. Implicit in this assessment are the assumptions that the true pore pressure response is instantaneous and is in no way restricted by the choice of porous tip and pressure transducer.

Initially due to availability two grades of ceramic cups were tested, the 5 bar standard tip and the 2 bar standard tip. The response times and equalisation period for the 2 bar and 5 bar were typically 1.5 and 14.5 minutes respectively, refer to Figure 3.7.

The increase in pore water pressure was initially expected to range from 10-20psi in the semi full scale tests. Working on this basis and taking into consideration the response time and the assumed saturation condition of the clay, the 2 bar porous ceramic tip was judged to be perfectly adequate for use in the pore water pressure monitoring system .

3.11.2.4. Manufacture Of The Piezometer Probe.

As previously mentioned the porous ceramic cup used for the probe is the 2 bar standard type supplied by Soil Moisture Corporation, U.S.A.

The other components required to manufacture the probe are Araldite grade CY/HY 1300/1301 epoxy resin and 2.0mm O.D.x0.23mm wall annealled stainless steel tube supplied by Cooper Needles,

Birmingham.

The first stage in the construction of the probe was to set in an epoxy resin two lengths of the 2.0m.m. O.D. stainless tubes, which leadfrom a pressure transducer, into a hollow brass cup. The ends of the tubes were staggered to ensure a good circulation of water when de-airing the system. Once the tubes were set in position the porous element was glued with an epoxy resin into the brass cup and then left to cure for 24 hours. All the epoxy resin used during the construction of the probe was de-aired using a vacuum desiccator.

3.11.2.5 Brass Housing For Ceramic Tip

Initially the housing was manufactured in a conical shape with a threaded portion, refer to Figure 3.8a. The shape provided a uniform body whereby the stainless steel tubes could be protected by sleeving them with a nylon tube coupled to the threaded sector. The overall design proved to be slightly cumbersome and was later replaced by a smaller brass unit and the nylon sleeving glued to it, refer to Figure 3.8b.

3.11.2.6 Pressure Transducer And Housing.

The pressure transducer used to monitor the change in water pressure was manufactured by C.E.C. Instruments, with a pressure range of 0-1.6bar. To incorporate this into the piezometer system a special housing unit was designed and manufactured, refer to Figure 3.9. It basically consists of a brass unit with two 2mm O.D. holes bored out at 90% to each other. The convergence point of these holes opens out into an orifice to accept the pressure transducer. Into one of these holes a length of 2mm O.D. stainless steel tube was inserted which

projects into the pressure transducer. The housing unit was designed in this way for several reasons, based on previous experience and prototype units.

1. With the ordinary 'T' housing unit it is virtually impossible to ensure that the pressure transducer is fully de-aired.
2. The 2mm O.D. stainless steel tube ensured that the circulation of water travelled right up into the transducer to remove any air bubbles which may have collected in it.

3.11.2.7 Piezometer Probe De-Airing System.

The de-aired water used for de-airing the piezometer tip and flushing the system was obtained from a Wykham and Farrance vacuum system. This system had to be set up and commissioned. It operates on the principle of spraying fine jets of water into a vacuum, this de-airs the water which is then left under a vacuum.

The piezometer probe was placed into a triaxial cell filled with de-aired water, which was specially adapted for the system. The cell was pressurised to 80p.s.i. and left for 24 hours. The probe was then flushed with de-aired water under a pressure of 10p.s.i. to evacuate any air accumulated in the system and out of the ceramic cup. This process was repeated three times to ensure that all the air is forced out of the system. A schematic representation of the system is shown in Figure 3.10.

3.11.2.8 Calibration.

The pressure transducers were calibrated using a G.D.S. controller

unit as described in Chapter 5.1.9.

3.11.2.9 Effects Of The Use Of Acetone.

During the initial stages of the investigation into response time curves one of the piezometer tips (5 bar) became slightly contaminated with grease. To remove the grease the ceramic was cleaned with acetone. Initially this improved the response time of the ceramic tip. This effect is reported by Fredland (1973) and is believed to be related to the vaporization of the acetone-water mixture, which is almost immediate when subject to changes in pressure. The result is a rapid build up of pressure. Hence the improvement in response time.

After the tip had been pressurised, and flushed several times, the response time slowly deteriorated, refer to Figure 3.11. This was probably due to the acetone being gradually flushed out of the ceramic and the effects of the grease contamination having not been fully eliminated by the use of the acetone. Because of the unpredictable results with the use of acetone any contaminated ceramic tips were replaced rather than any attempts made to clean them.

3.11.2.10 Response Curves.

Extensive tests were carried out on the two bar ceramic tip to determine the response time of the system chosen, to an instantaneous change in pressure. It was found that after the system had been pressurised and flushed three times in the manner described in section 3.11.2.7, any further de-airing cycles had little or no effect on the response time. The average time taken for the system to

respond to a change in the pressure of 10 psi was approximately 1.5 minutes. A typical response curve is illustrated in Figure 3.12.

In all cases the initial response was virtually linear except in earlier tests involving the five bar tip, which produced a slight 'S' curve. This particular trend was shown in Fredland's work, where the response curve for the five bar and fifteen bar ceramic discs used in his tests had an even more pronounced 'S' curve. The significance of this non linearity was thought not to be a totally essential factor in the eventual application of the piezometer probe, particularly as the two bar ceramic used for the piezometer probe, showed a very good total response time. This includes the stabilisation period at the end of each increment of pressure change, and the response was virtually linear up to this final equalisation period, where the system stabilises to the total pressure change.

3.11.2.11 Conclusion On Response Curves.

From the initial tests the two bar ceramic cup had proven to be an acceptable choice of ceramic to be used for the piezometer probe, for several reasons:-

1) Bubbling pressure.

2) Response time.

Obviously the tests carried out up to this period were in a water to water environment. The real test of the piezometer probe to changes in pore water pressure in a clay media, determined the final decision on the use of the system and is discussed in Chapter 4.

3.12 Semi-Full Scale Monitoring and Control System.

3.12.1 Introduction.

The equipment used to monitor the dynamic signals was that used by Lake (1986) and is fully described in his thesis. Only a brief description is included here.

Due to the additional monitoring equipment incorporated into the extended loading programme, the static monitoring and control systems were expanded. Again the full initial details are given by Lake (1986) and Wersching (1987), a summary of which is given here, covering the additional expanded format of the control program.

3.12.2 Dynamic Monitoring Equipment.

The four dynamic output signals generated during driving the 60mm diameter pile were all recorded on a Racal Store 4DS tape recorder via conditioning amplifier units, manufactured by Kistler and Bruel and Kjaer. The signals are analysed either directly as single shot or off the previously recorder tape using the narrow band spectrum analyser, in conjunction with an X-Y plotter. A schematic presentation of the dynamic equipment is given in Figure 4.4. Full specifications of the equipment is given in the available manufacturers' operational manuals and Lake (1986).

3.12.3 Static Monitoring Equipment.

The static axial load cells, inclinometers, pressure transducers, shear transducers and displacement transducers were all monitored by a Solatron Orion 3530A data logging system interfaced with and

controlled by a Commodore P.E.T. micro computer.

The Orion was expanded from a 100 to a 140 channel system to cater for the additional instrumentation. Consequently the control program enabling the P.E.T. to manage and recieve data from the Orion had to be modified.

The Commodore P.E.T. micro computer and disk drive system was updated from the 4000 to the 8000 series which expanded the data logging facility. This increased the number of data scans logged per disk from 90 to 300, reduced the use of the disk change routine and enabled the load testing programme to be more efficiently carried out.

The original control program written by Solatron and modified by Wersching and Lake to accommodate the specific needs of the two types of test procedure, operated from an option menu. This menu had to be modified to accommodate the extended load test program adopted for the semi-full scale tests. The option menu was as follows:

1.Initial Drive Increment.

2.Drive Increment.

3.C.R.P Test.

4.M.T.L. Test. / Cycle Load Test.

5.Initialisation / Initial Data.

6.Pull Out Test.

7.Disk Change Procedure.

The program was controlled by a displacement criteria governed by the movement of the pile cap. If this criteria defined by the option chosen from the menu was exceeded, the program went through a last data scan routine , stopped logging data, retracted the jack and

returned to the option menu.

All the data was stored on floppy disk with a partial output to a line printer giving readings of the load cells, pressure transducers, shear transducers and displacement transducers. The information from the inclinometers was processed at a later date.

Option 5 was used prior to testing and scaned all channels a total of 10 times, averaging and using them as zero values. This option was extended to re-run the program using the initial scan data. This simply read the initial scan data onto a new disk. This option was used after the first load test programme on each pile, where the scanning period to monitor the dissipation of pore water pressure was changed from one minute to one hour. It also proved helpful in a systems breakdown situation, where the program could be re-run without the loss of the original datum.

Options 1 and 2 were used to install the piles. For the 60mm pile the drive increments were 500mm +/- 50mm and 100mm +/- 10mm for the 114mm diameter pile. Options 3, 4 and 6 were used to carry out the load tests on the pile namely the constant rate of penetration test (1.5mm/minute), maintained load test, cyclic load test and pull out test, which are described in Chapter 5.4. For the constant rate of penetration and pull out tests the function generator controlling the Dartec jack was controlled directly by the P.E.T micro-computer. The maintained load and cyclic load tests were manually set up and operated via the function generator.

Option 7 was the floppy disk change routine. This either operated automatically when the data counter was exceeded in the control program or operated manually from the option menu.

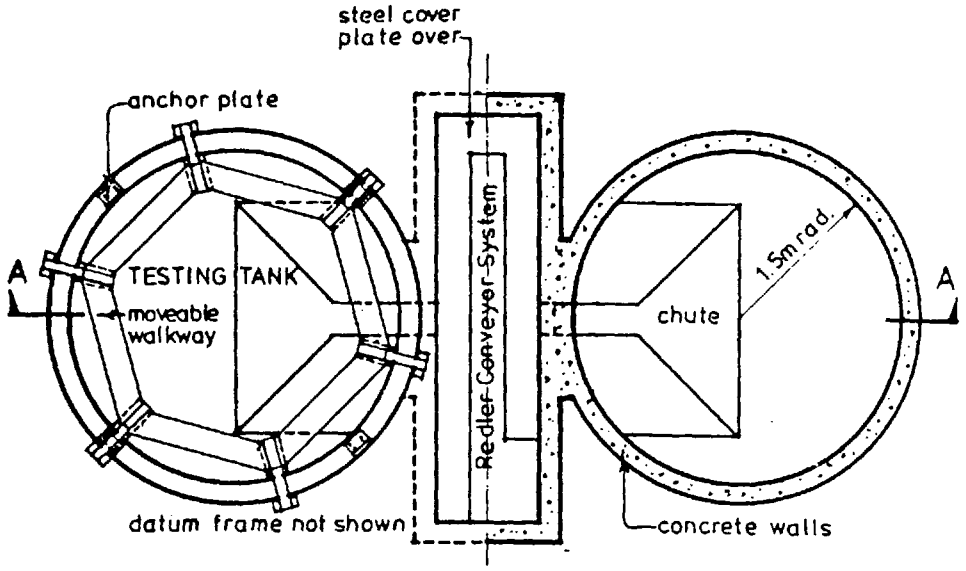

HALF PLANS

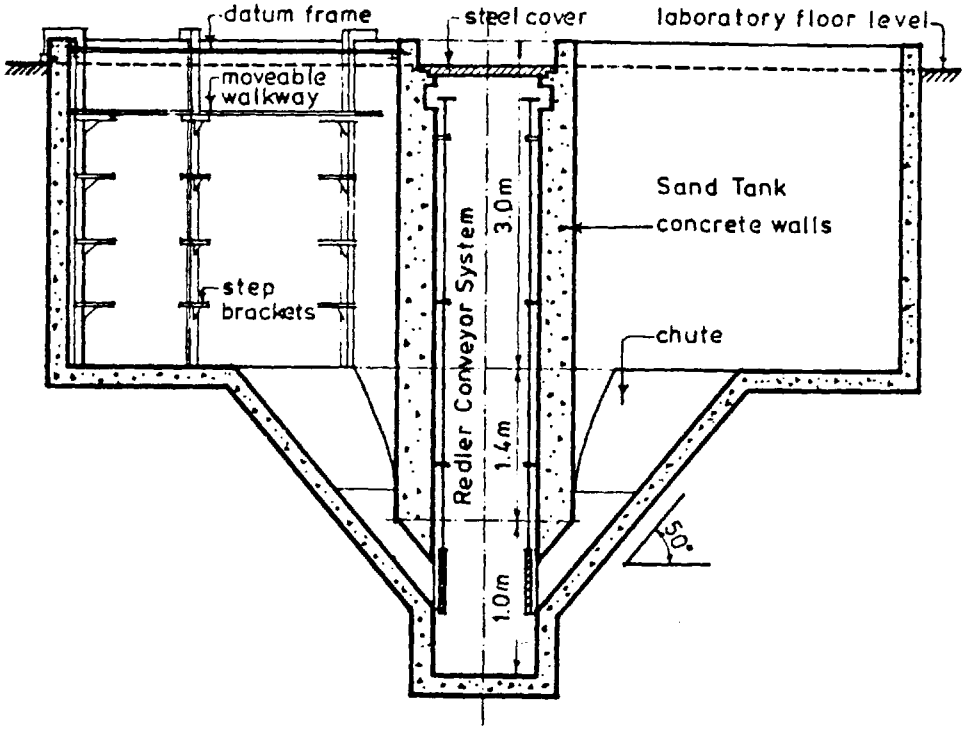

SECTION A-A

FIGURE 3.1

SAND TANKS AND REDLER CONVEYOR SYSTEM

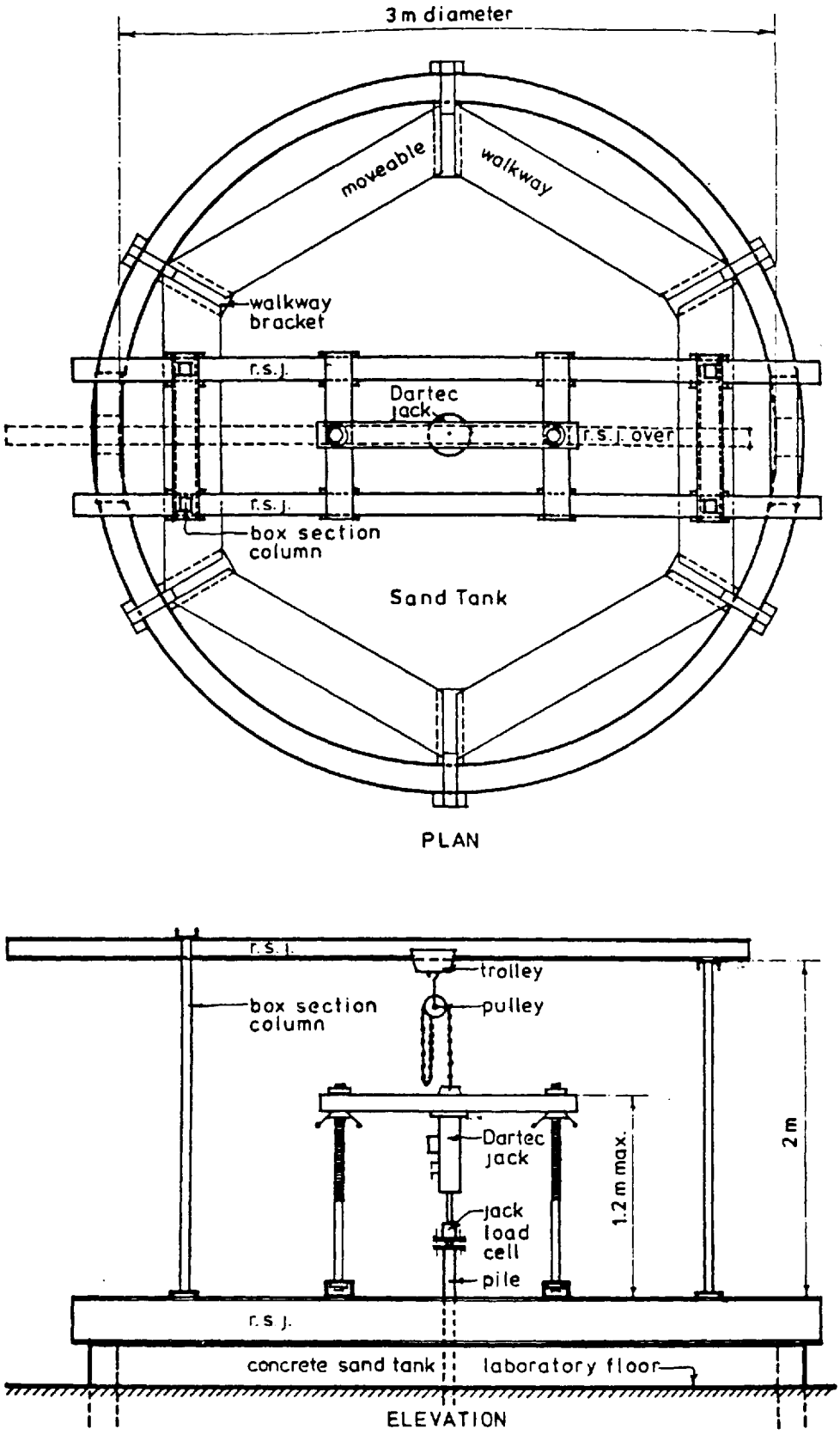

FIGURE 3.2

LOADING FRAME AND GANTRY

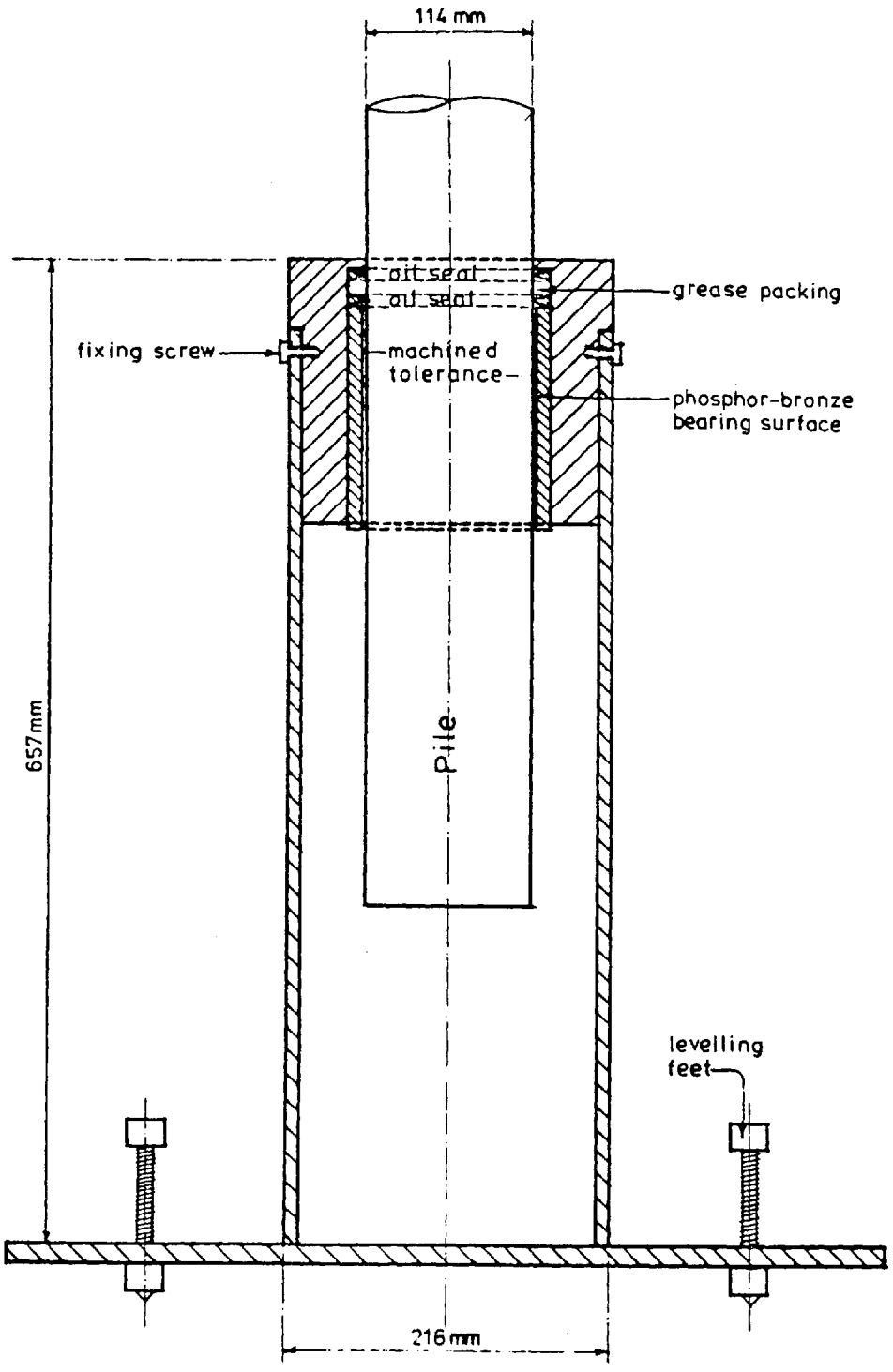

FIGURE 3.3

FRICTIONLESS CYLINDER

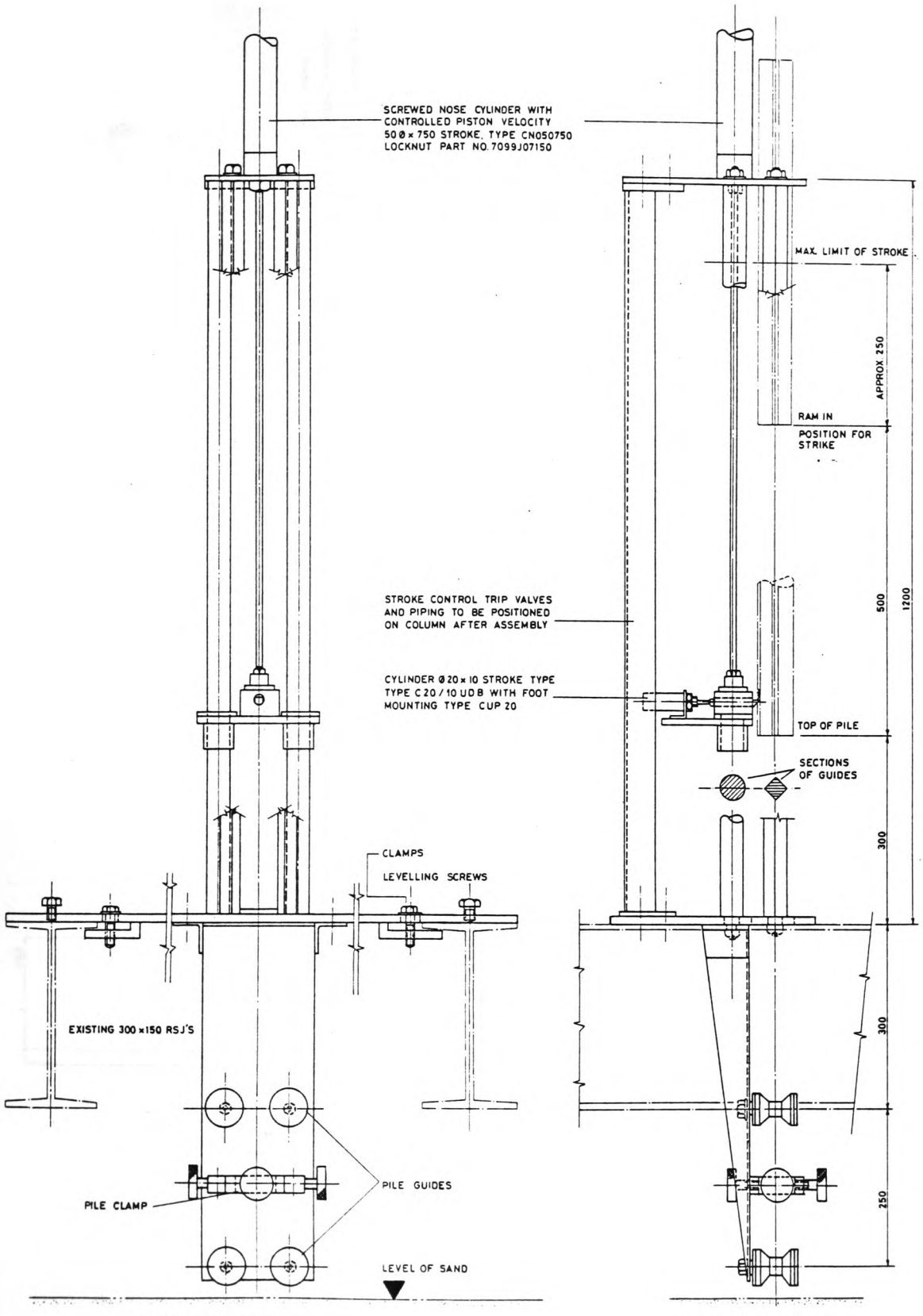

MODEL PILE DRIVING RIG

SCALE 1:4

NOTE ALL DIMENSIONS IN MILLIMETRES

Designed & Drawn by G.C.Lake

FIG. N°3.4

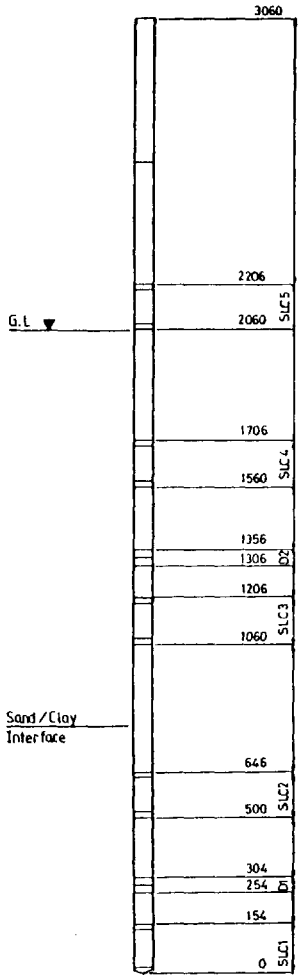

(a) 60mm. Ø COMPOSITE MODEL PILE

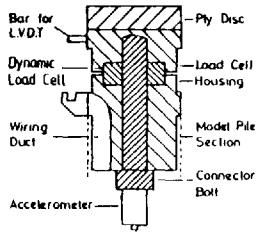

(i) 'Dynamic' Pile Cap

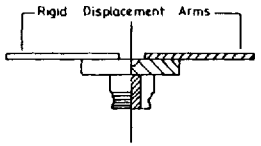

(ii) 'Static' Pile Cap

(b) 60mm. Ø MODEL PILE CAPS

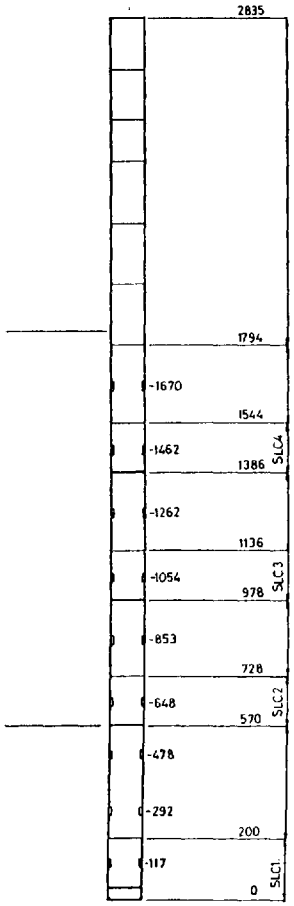

(c) 114mm Ø COMPOSITE MODEL PILE

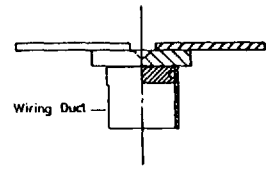

(i) Female Pile Cap

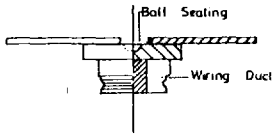

(ii) Male Pile Cap

(d) 114 mm Ø MODEL PILE CAPS

Key

SLC – Static Load Cell

D – Dynamic Load Cell

D – Boundary Orthogonal Stress Transducer (B.O.S.T.)

All Dimensions In Millimeters

FIGURE 3.5 GENERAL DETAILS OF THE SEMI-FULL SCALE PILES AND PILE CAPS

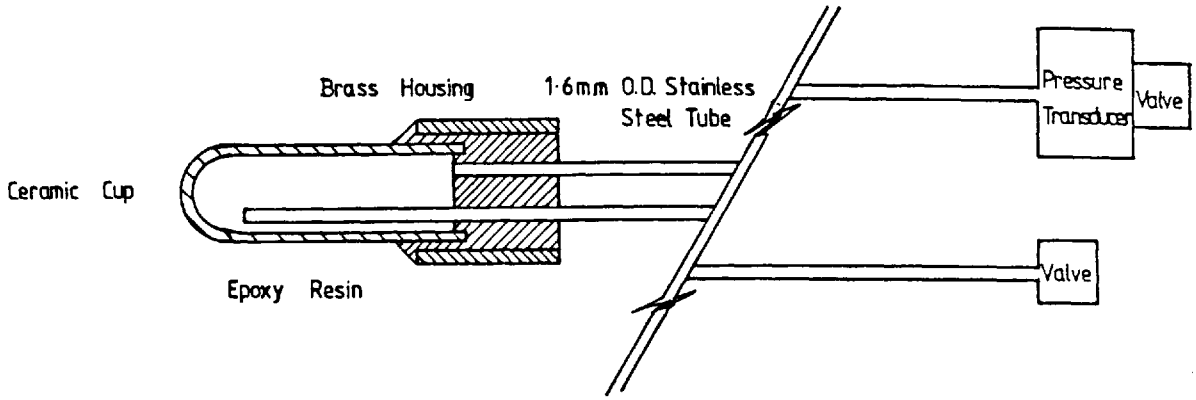

FIGURE N° 3.6 SECTION THROUGH PIEZOMETER TIP

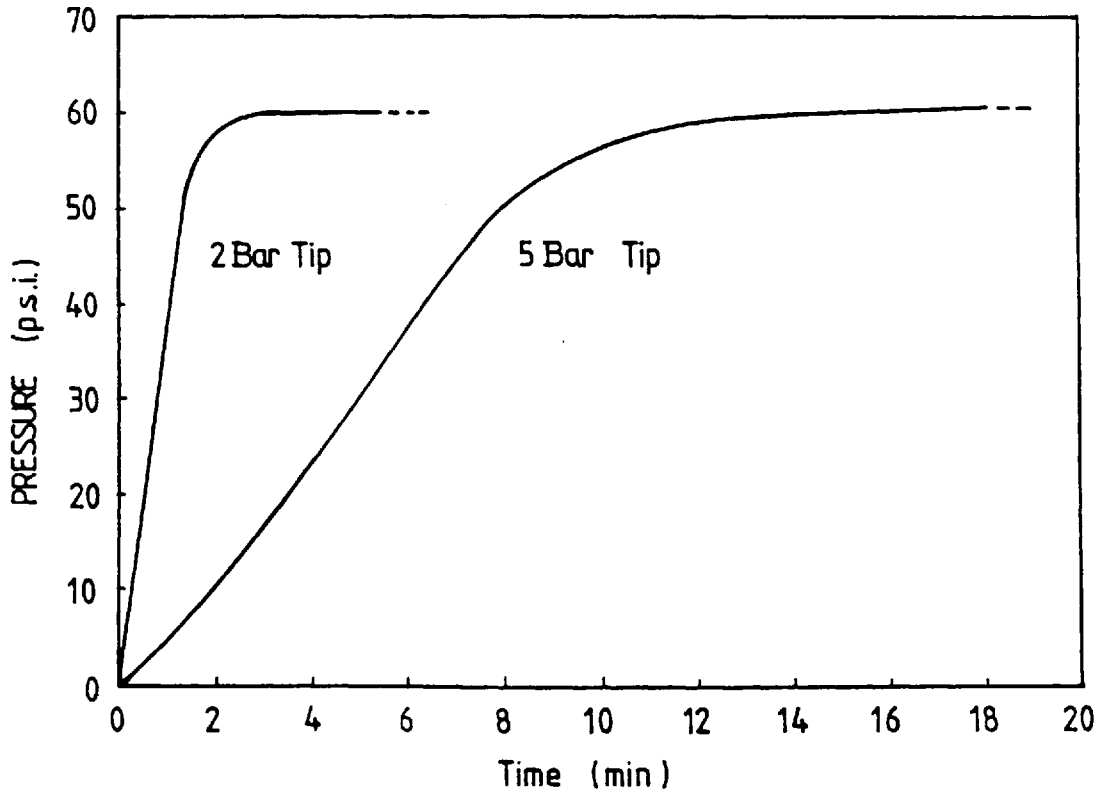

FIGURE N° 3.7 CERAMIC TIP - PRESSURE RESPONSE CURVES

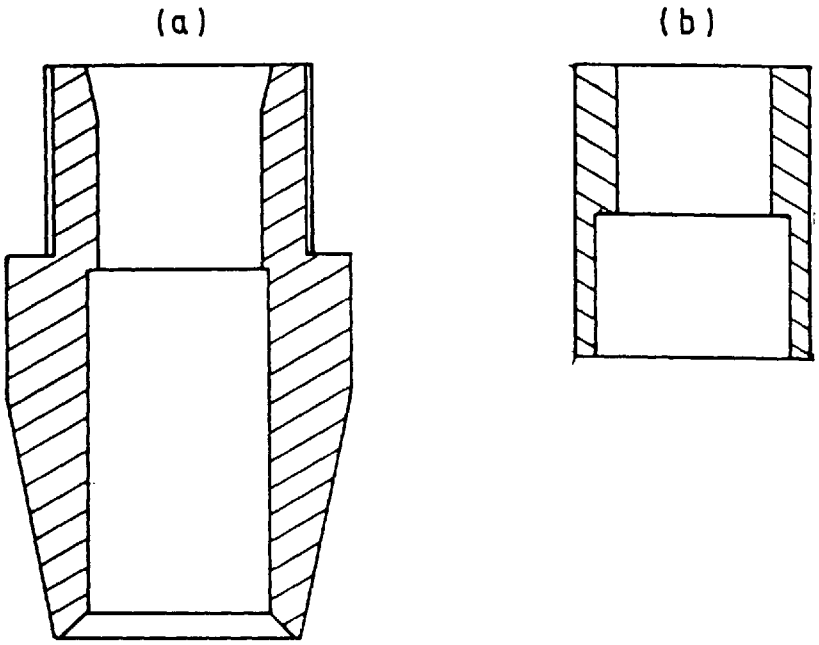

FIGURE N°3.8 BRASS HOUSINGS FOR CERAMIC CUPS

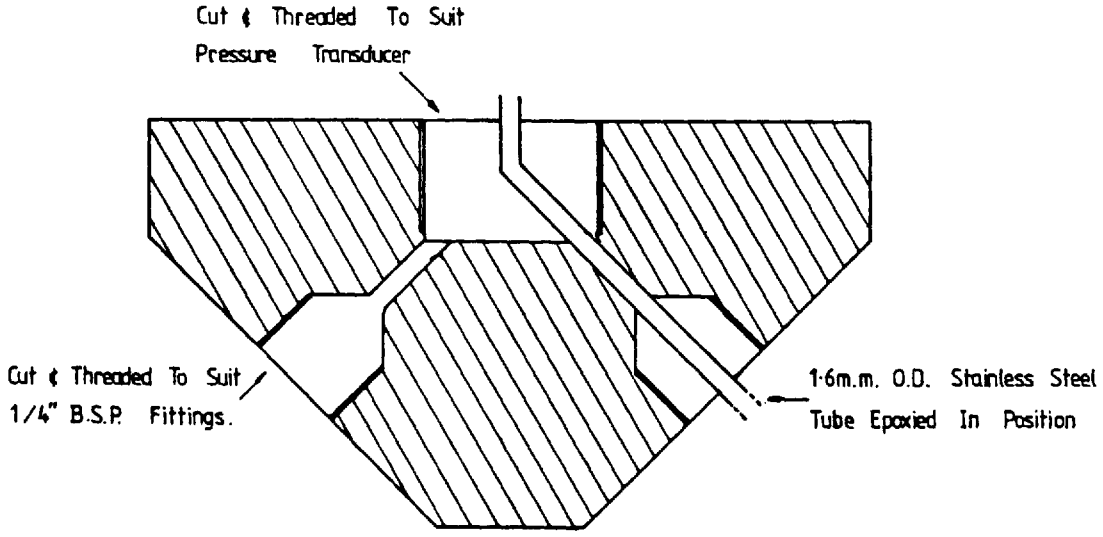

FIGURE N°3.9 BRASS HOUSING FOR PRESSURE TRANSDUCER

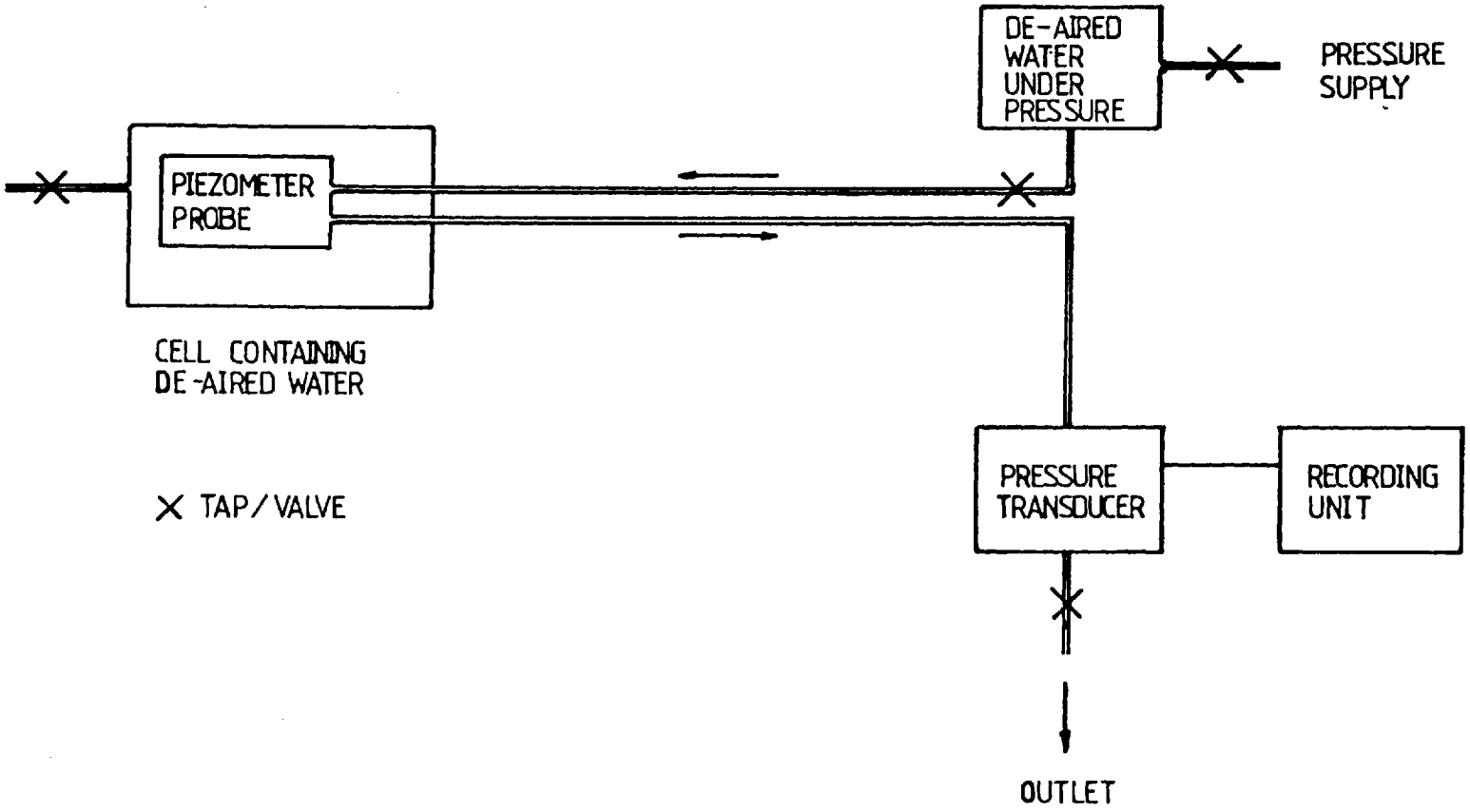

FIGURE N°3.10 SCEMATIC DIAGRAM OF DE-AIRING SYSTEM FOR PIEZOMETER TIP

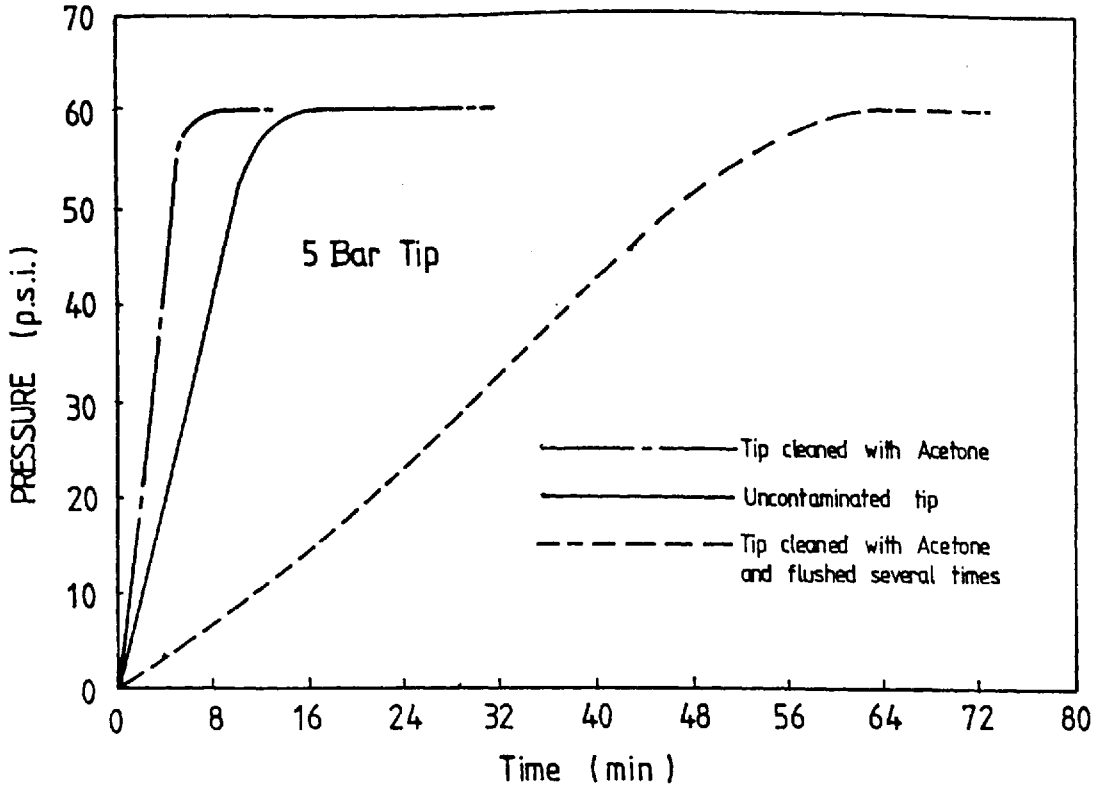

FIGURE N°3.11 EFFECT OF ACETONE ON PRESSURE RESPONSE CURVE

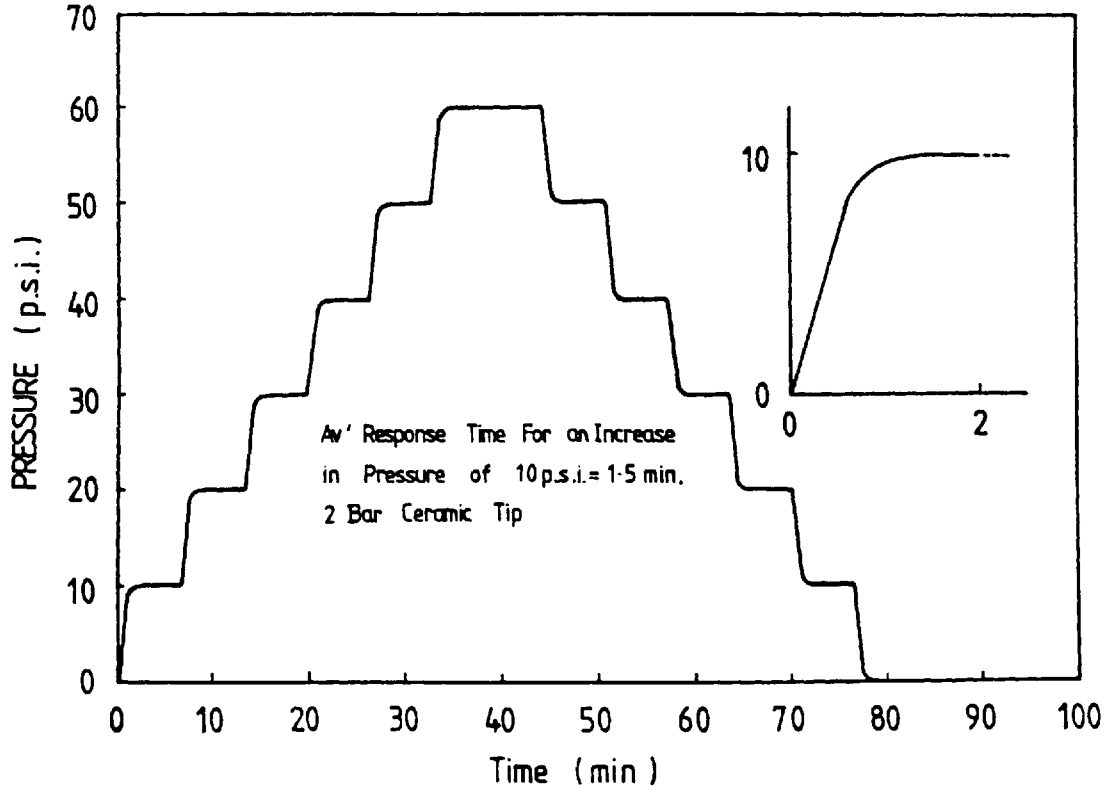

FIGURE N°3.12 PRESSURE INCREMENT - RESPONSE CURVE

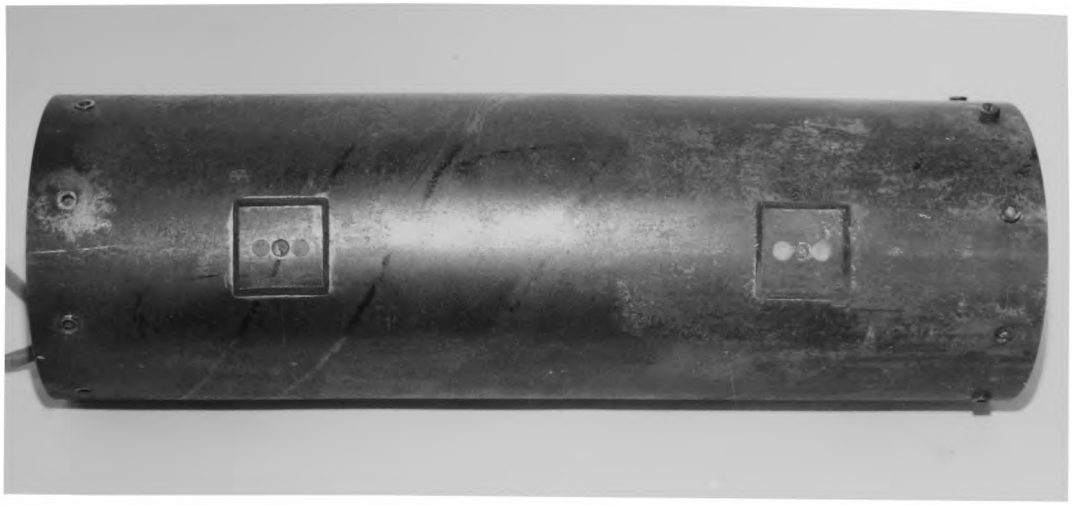

Plate 3.1 Boundary Orthogonal Stress Transducer in the Wall of the 114mm Pile

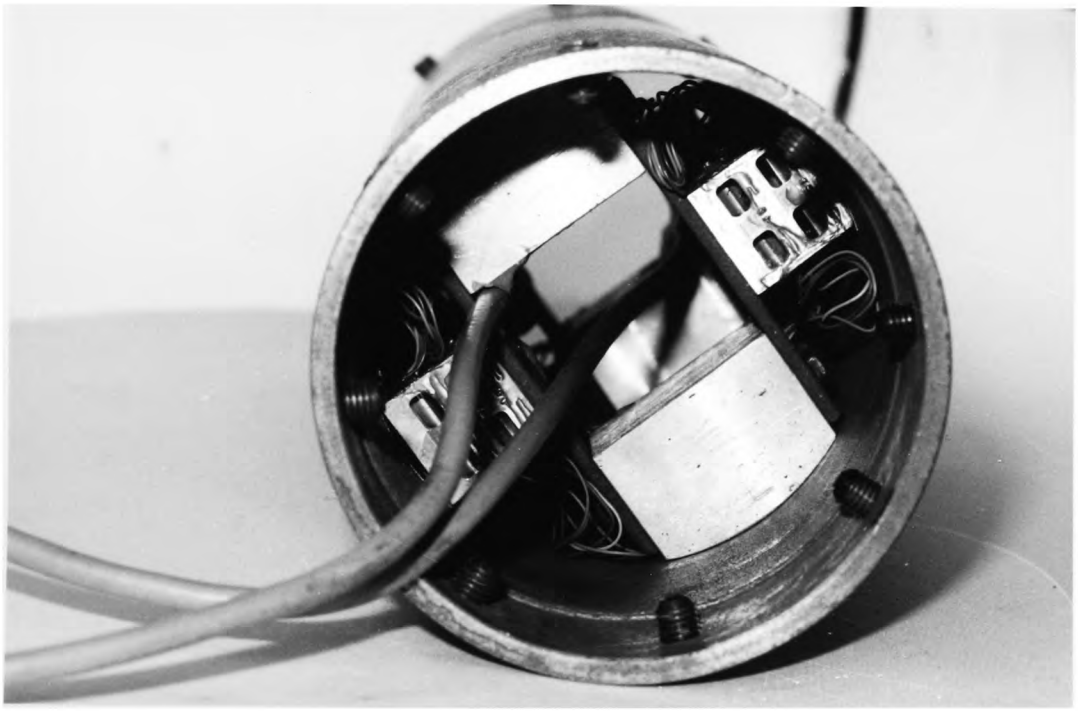

Plate 3.2 Internal View of the 114mm Pile Illustrating the Boundary Orthogonal Stress Transducer

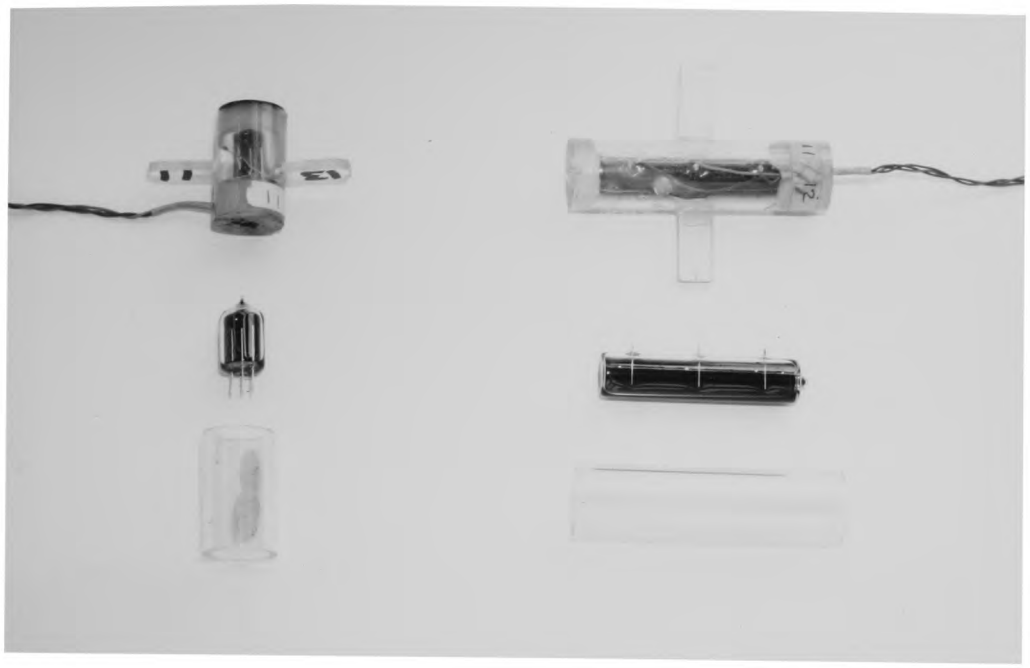

(a) Type 0714 (b) Type 0716

Plate 3.3 Electrolytic Levels (Inclinometers)

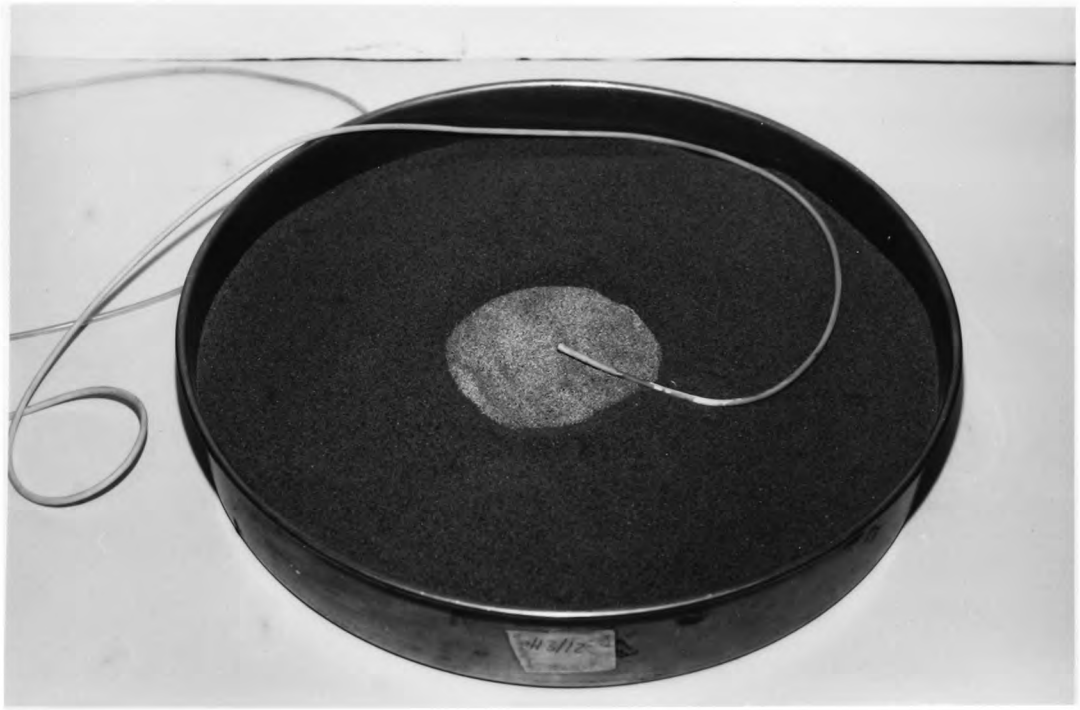

Plate 3.4 Sand Plaster Sample, Insitu Sand Density Measurement

(a) Diaphragm Pressure Transducer (c) Shear Stress Transducer

(b) Electrolytic Level

Plate 3.5 Instruments at the Sand/Clay Interface

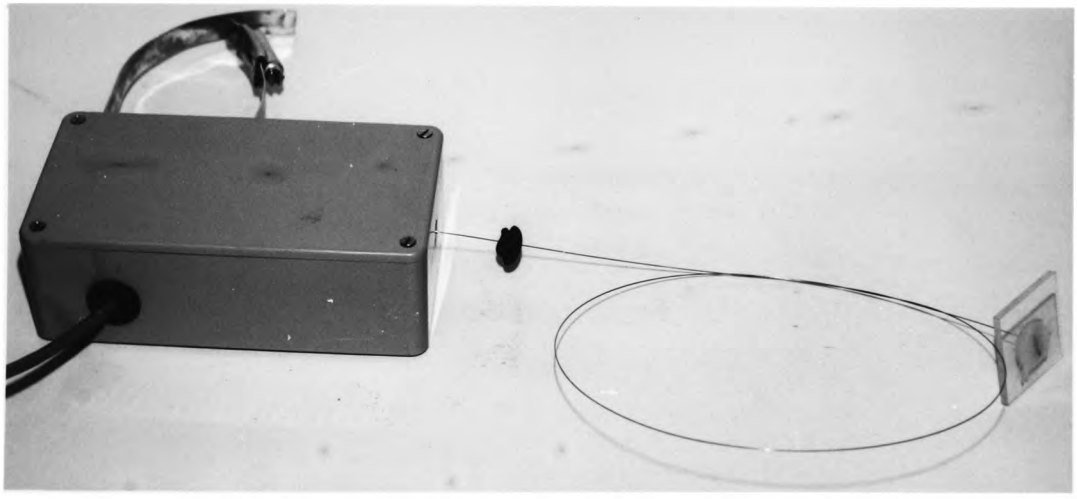

Plate 3.6 Linear Voltage Displacement Transducer and "Terra Plate" used to Monitor Horizontal Movement Within the Sand

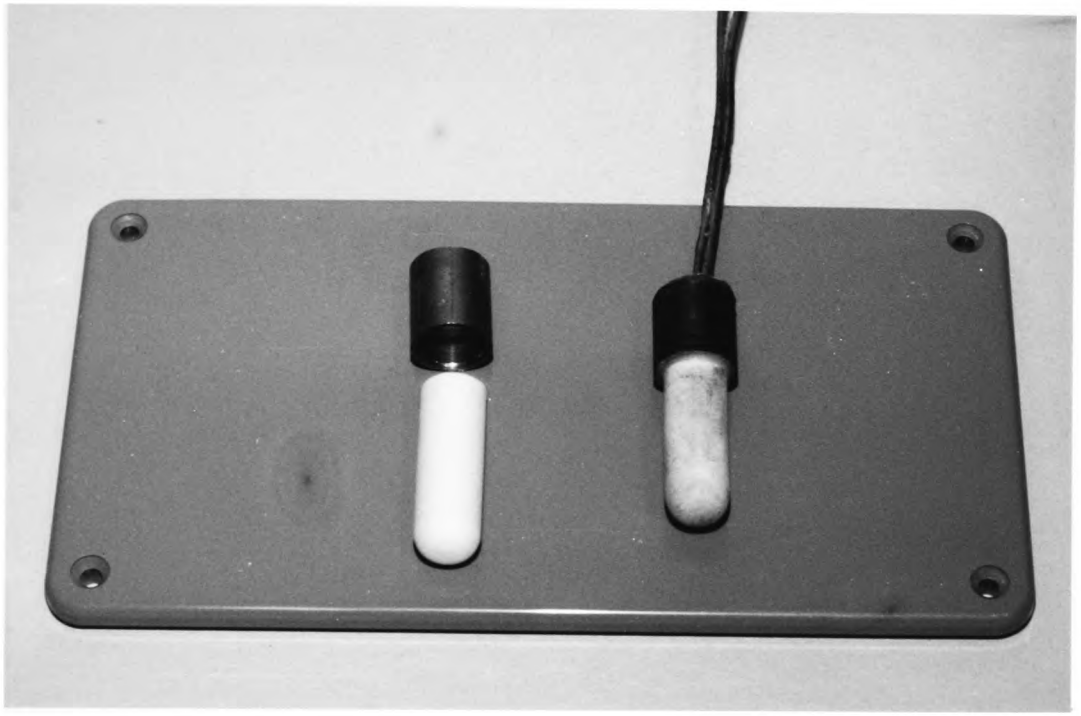

Plate 3.7 Piezometer Probe

CHAPTER 4

PILOT STUDIES

CHAPTER 4

PILOT STUDIES

4.0 Introduction

To develop the piezometer tip placement technique and monitor its response time a series of tests were carried out incorporating the piezometer system into a soil.

The first test involved using the piezometer in a 102m.m. diameter clay sample placed in a triaxial cell to monitor its response to isotropic pressure changes.

A series of small scale tests were then carried out using a 38m.m. diameter model pile. The pile was dynamically driven into a two layered soil stratum consisting of a sand overlying clay which was formed in a small tank. Into the clay layer were placed three piezometers which were located radially from the pile axis. The build up and dissipation of the pore water pressure within the clay due to the driven pile was then monitored by the piezometers.

4.1 Piezometer Probe In The Triaxial Test.

4.1.1 Introduction.

The piezometer probe was inserted into the mid height of a 102mm clay sample and monitored the change in pore water pressure due to isotropic changes in the confining pressure.

4.1.2 Equipment.

4.1.2.1 Introduction.

A standard 102mm triaxial cell was used for the experiment. This cell was modified to allow the piezometer probe to be placed inside. A voltmeter and chart recorder were used to monitor the piezometer's response to changes in pore water pressure.

4.1.2.2 Modification to Triaxial Cell.

The triaxial cell base plate was modified to allow the piezometer probe to be placed inside, see Figure 4.1. Also the triaxial cell was mounted on special steel spacers to prevent it crushing the stainless steel tubes leading from the piezometer probe, see Figure 4.1.

4.1.2.3 Modification To Rubber Membrane.

To allow the piezometer probe to be inserted into the 102mm diameter clay sample, a hole the diameter of the probe ceramic was made in the rubber membrane.

4.1.3. Clay Sample.

The soil used for the test was a red marl (Mercia Mudstone) with a moisture content of approximately 18.0%. This was the type used in the semi-full scale tests. The clay was then compacted using the dynamic compaction technique until as near zero voids was obtained, (Lake 1986). The soil sample was then placed in the triaxial cell in the usual manner as described by Head (1980).

4.1.4 Piezometer Probe.

The piezometer probe was manufactured, calibrated and de-aired in the manner described in Chapter 3.11.2. It was inserted into the clay sample and sealed to the rubber membrane which surrounded the sample, as illustrated in Figure 4.1.

4.1.5 Test Procedure.

The clay sample containing the piezometer probe was left to consolidate until it had stabilized. This could clearly be seen on both the chart recorder and voltmeter which were connected to the piezometer.

Once the piezometer probe had stabilised the soil sample was subjected to changes in isotropic loading conditions. For each change in cell pressure the sample and piezometer were allowed to consolidate and stabilise respectively, and a reading on the voltmeter was taken. This procedure was repeated with three separate soil samples and the results are given in Table 4.1.

4.1.6 Test Results.

The results from the three samples tested, clearly indicate that the piezometer system responded adequately to changes in pore water pressure. For a fully saturated soil the pore pressure parameter 'B' would approach the value of one. The results indicate a value slightly less than unity, this may have possibly been due to the clay having some voids present. This was a trial experiment to establish the response of the piezometer system in a clay soil which on average proved to be 10 minutes.

4.2. 38m.m. Model Pile Tests.

4.2.1 Introduction.

Two tests were carried out and were instigated for two main reasons:-

1. To develop and test the piezometer system and its suitability for use in pile driving tests.
2. To familiarise the author with the principles and procedures associated with the dynamic monitoring equipment.

4.2.2 Apparatus.

The experimental equipment developed by Lake (1986) was ideal for the purpose of these tests. Details and specifications of the apparatus are given fully by Lake (1986) and will only be briefly described here.

4.2.2.1 Model Pile.

The model pile used in these experiments was a 38mm diameter pile designed by Lake(1986) for his initial pilot study. The overall length of the model pile, including load cells and pile point, was 600mm. Within its construction were two dynamic load transducers, one housed in the toe of the pile and the other in the pile cap. Also located in the pile was an accelerometer to obtain the acceleration, velocity and displacement data during driving of the pile. A static axial load cell was mounted internally near the toe of the pile.

4.2.2.2 Model Pile Driving Rig.

The model pile driving rig was designed by Lake and fits onto a large 10kN triaxial loading frame, as illustrated in Figure 4.2. The driving rig is hand operated. It consists essentially of a cross member and guide system which allows the drop weight to fall freely but restrained in the vertical plane.

4.2.2.3 Force Transducers.

Two piezoelectric force transducers were used:-

1. A Bruel and Kjaer type 8201 with a maximum capacity of 10kN, which was located in the pile cap.
2. A Kistler type 9311A with a maximum capacity of 5kN, located in the pile toe.

4.2.2.4 Accelerometer.

The accelerometer used in the model pile was a D.J. Birchall Ltd accelerometer type A02/T

4.2.2.5 Static Load Cell.

An eight gauge full bridge circuit was used for the static load cell, which was located in the toe section of the pile. Full details are given by Lake (1986).

4.2.3 Piezometer Tips In The Clay Layer.

4.2.3.1 Manufacture of Piezometer Tips.

Three piezometric probes were used in the small scale test and were manufactured and de-aired as described in Chapter 3.11.2. The three

piezometers were inter-connected through a series of manifolds and valves. This was necessary to ease the process of de-airing the ceramic tips.

4.2.3.2 Location And Placement Of Piezometer Tips.

The piezometer probes were located in the clay layer at a depth of 120mm from the clay surface. This was the depth to which the pile was fully driven into the clay. They were placed radially at 120 degree centres at 1.25B, 2B, 2.5B from the proposed pile centre line as illustrated in Figure 4.2.

4.2.4 Dynamic Monitoring Equipment.

The specification and operational features of the monitoring equipment are readily available from the manufacturers, therefore only a brief description of the equipment is included here.

4.2.4.1 Conditioning Amplifiers.

Originally mini charge amplifiers, Fylde type 128CA, were proposed for use in this pilot study. Due to difficulty in obtaining the control boxes and then matching the output signals, they were replaced by Kistler type 5007 and Bruel and Kjaer type 2626 charge amplifiers. Also at this particular time, difficulty was experienced in obtaining the mini co-axial leads which connected the force transducers to the charge amplifiers. The Kistler and Bruel and Kjaer amplifiers were of the low noise type and feature precision conditioning networks.

4.2.4.2 Narrow Band Spectrum Analyser.

The narrow band spectrum analyser was a Bruel and Kjaer type 2031 instrument designed to analyse the narrow band frequency of continuous and transient data, coming from various signal sources. Its maximum frequency range was 20kHz. Amplitudes of the signal were displayed in decibels, which were converted into voltages and hence force. The analyser could be used with either a direct or pre-recorded signal.

4.2.4.3 Tape Recorder.

The tape recorder used to store the dynamic signals was a Racal Store 4DS which is capable of storing four signals simultaneously. Through the signal electronics, either direct or FM recording was available or a combination of both for standard intermediate or wideband. There were seven record or replay speeds, ranging from 15/16 to 60 inches per second.

4.2.4.4 X-Y Plotter.

A Bruel and Kjaer type X-Y plotter was used to obtain hard copy prints of the dynamic signals when connected to the real time analyser. A typical instrumentation set up for monitoring and recording dynamic signals is shown schematically in Figure 4.3.

4.2.5 Static Monitoring And Recording.

The monitoring of the static axial load cell, displacement transducer and the piezometer system, was achieved by the Orion 3530 data logger system interfaced with a Commodore P.E.T. micro-computer.

4.2.6 Preliminary Dynamic Tests.

The following preliminary dynamic tests were conducted on the 38mm diameter model pile to ensure that,-

1. The dynamic system was functioning correctly.
2. To verify repeatability with the results of Lake(1986).

4.2.6.1 Initial Voltage Check on Analyser.

One of the first tests to be carried out was a voltage check on the real time analyser. A known voltage source was relayed through an oscilloscope and then through the analyser. The decibel readings from the analyser were converted into volts and compared with the display on the osciloscope for authenticity.

4.2.6.2 Impact Tests.

Impact tests were carried out by dropping the 1.73kg drop weight on the model pile from a height of 20mm to compare with the results produced by Lake (1986). During the tests the pile tip was bearing on two types of surfaces;-

1. Thin layer of rubber overlying concrete.
2. Concrete.

4.2.6.3 Test Procedure.

The procedure used for the tests was as follows,-

1. The pile was impacted regularly with the drop weight until a consistent signal was obtained. (i.e. repeatability of test).
2. When step 1 had been achieved the next three to six

readings (depending on the repeatability of the signal) were recorded and a hard copy trace of the signals obtained.

Initially the tests were hand held just to familiarise the author with the equipment and to establish that it was functioning correctly. The hard copy traces were obtained when the pile was held in the triaxial frame.

4.2.6.4 Impact Test Results.

The initial preliminary impact tests results proved successful in their two main objectives. In particular the signals generated were identical to those produced by Lake (1986). Typical output signals are illustrated in Figure 4.4. A thorough and rigorous investigation into the performance of the pile and the force transducers is covered by Lake (1986). Duplication of these results was considered unnecessary.

4.2.7 38mm Diameter Pile Tests.

4.2.7.1 Red Marl Preparation.

The red marl (mercia mudstone) was prepared in the manner described by Lake (1986) where the clay was mixed to an optimum moisture content of 18.5%.

4.2.7.2 Red Marl Placement and Compaction.

The red marl was compacted into a pipe lined with polythene to prevent moisture migration. The method of placement again is described by Lake (1986) and was as follows:-

1. A known amount of marl (approx 10kg) was placed in the pipe and a Kango hammer used to compact the marl to as near zero air voids as possible as described in Chapter 5.2.2.
2. This was repeated until the pipe was full.
3. The surface was levelled off and a vinyl spray used to cover the surface of the clay with a membrane to prevent moisture migration. Sand was pressed into the surface of the clay before the vinyl coat dried out, to form a bond between the sand and the marl.
4. For test number two the polythene lining of the pipe was extended above the surface of the clay. This enabled a small head of water to be placed over the clay. The vinyl spray was not used in this test.
5. At this stage the piezometer tip was placed into the clay layer as described in section 4.1.2.1.
6. Sand was placed over the clay by pouring it carefully from a small scoop. Care was taken to ensure that the maximum drop height of the sand was less than 50mm. This was repeated until the tank was filled to the required height and then levelled off.
7. The prepared sample was left for a period of time to allow the piezometers to stabilise prior to a test being carried out.

4.2.7.3 Soil Tests.

The final moisture content profiles and soil properties, as determined from various standard laboratory tests are discussed in

sections 4.2.7.10 and 4.2.7.11 respectively.

The in-situ sand density samples for the dry sand (test number 1) were determined by a technique developed by Wersching et al (1983). These density samples were situated at the sand/clay interface. Due to the test conditions no sand density samples were taken during test number 2.

4.2.7.4 Trial Dynamic Test.

Prior to driving the pile a trial test was carried out by driving the pile into a container of sand. The test was necessary to set up optimum recording levels between the charge amplifiers and tape recorder. This gave continuity in pile driving which was essential in the assessment and monitoring of the pore water pressure during test conditions.

These levels were then set for the main test. Prior to fully driving the pile two blows were given to the pile, just to check that the signal output from the transducers was functioning correctly.

4.2.7.5 Model Pile Test Procedure.

The method employed in the tests is that given by Lake (1986) and will be given here.

1. The prepared sand marl specimen was mounted on the 10kN triaxial machine and the settlement in the sand layer noted.
2. The model pile was placed in the driving rig and allowed to settle in the sand under its own weight.
3. The drop weight was connected and the pile was again

allowed to settle. The settlement due to self weight and ram weight did not exceed 45mm.

4. The rest of the driving rig was carefully placed around the pile.
5. The model pile was pushed into the soil to a depth of 50mm.
6. The transducers and accelerometer were connected, the tape recorder switched on, tested, and the pile driven to the required depth.
7. Simultaneously at the start of the driving procedure the Orion data logger was started to scan the piezometer tips. This enabled the monitoring of the build up of pore water pressure and its subsequent dissipation.

4.2.7.6 Constant Rate Of Penetration Test.

This test was developed by Whitaker (1970) and is known as the constant rate of penetration test. (C.R.P. Test), (Code of practice 2004). A 1.0mm /minute rate of penetration was used in the tests. The ultimate bearing capacity was taken at 10% of the pile diameter. The results are discussed in section 4.2.7.12.

4.2.7.7 C.R.P. Test Procedure.

Two constant rate of penetration tests were carried out. The first test followed almost immediately after the dynamic driving of the pile, similar to Lake. The second test was carried out when the pore water pressure had dissipated to approximately 90% equalization. The ultimate bearing capacity from these tests were then compared.

Once the pile had been fully driven to a depth of 390mm the driving

assembly was carefully removed. The cross head of the triaxial apparatus was lowered and a proving ring fitted. Fixed to the proving ring was a linear displacement transducer, calibrated to convert change in voltage to load. The proving ring was then lowered onto the pile cap and a C.R.P. test carried out at the rate of 1.0mm per minute. The tank movement was monitored using a previously calibrated displacement transducer with a maximum stroke of 75mm. An adjustment was made at each deflection to allow for the compression of the proving ring.

Throughout the tests all the instrumentation was monitored by an Orion 3530 interfaced with a P.E.T. micro-computer. The program was originally written by Lake, and subsequently modified to scan the additional instrumentation, i.e. the piezometer system.

4.2.7.8 Sand Drag Down And Sand Plug In The Marl.

After completion of the final C.R.P. test in both experiments the sand was removed from the tank. The clay formwork was also removed, and the clay sliced vertically through the middle with a cheese wire . This enabled a close examination of the effects of driving the pile through the sand into the clay.

Figure 4.5 illustrates the drawdown of sand into the clay. The intensity of the sand dragged down diminishes with penetration. At a depth of approximately 60mm into the clay the sand dragged down was non existent. The extent of this dragdown (approximately 1.5 pile diameters) is reported by Lake (1986). Tomlinson suggests that the sand may be pulled down by as much as 3 pile diameters.

A sand plug driven ahead of the pile toe is also illustrated in

Figure 4.5. This is also reported by Werscheing (1987) and Lake (1986) and its effects on pile behaviour are not yet fully understood.

4.2.7.9 Effect Of The P.V.C. Membrane.

By comparing the rate of generation and dissipation of the excess pore water pressure illustrated in Figure 4.9 from the two experiments, there was a difference in the time history of these events. It was apparent, that the membrane had affected the drainage path conditions in the clay between the two experiments. The dissipation time between the two tests was effectively halved. This trend is significant but as discussed in section 4.2.6.12 the true value of the results in experiment two must be treated with some scepticism, although they were true recorded values.

4.2.7.10 Moisture Content Profiles.

The average moisture content values of the red marl before and after the two experiments are given in Table 4.2. For experiment one there does seem to be a reduction in this value. This was expected because there was some moisture present in the sand above the sand/clay interface. Other factors which contributed to this were the pile penetration through the P.V.C. membrane and the effect of the sand plug.

Considering these factors and the moisture content profile for experiment 1 shown in Figure 4.6, there was an apparent trend in the loss of moisture in the marl locally to these areas. The moisture content profile for experiment 2, refer to Figure 4.6, does not show any significant loss in moisture content in the regions mentioned above. This was a function of the test conditions of a head of water

applied to the sample, keeping the clay sample fully saturated. Unfortunately due to a puncture in the plastic lining of the mould containing the clay (probably caused by the Kango hammer when forming the clay sample) the true test conditions were not known. From Table 4.2 there was little significant difference in the moisture content before and after the experiment. There was a significant difference in the moisture content of the sand plug driven ahead of the pile. Again this was probably due to the difference in test conditions, one driven through dry sand and the other through a saturated sand.

4.2.7.11 Triaxial And Moisture Content Samples.

After the clay had been formed three 38mm core samples were taken. They were used to carry out immediate undrained triaxial tests at confining pressures of 276, 414 and 551kN/m^2. Three more 38mm core samples were taken after completion of the constant rate of penetration tests. These were tested in a similar manner to obtain the value of Cu. The results of these tests are given in Table 4.2.

During formation of the clay nine moisture content samples were taken. Samples were also taken from the initial triaxial tests and an average value for the initial moisture content was obtained.

The average value for the final moisture content was taken from the moisture profile (Figure 4.6) combined with samples taken from the final set of triaxial cores. The results are given in Table 4.2.

4.2.7.12 Ultimate Bearing Capacity.

As can been seen from Figure 4.7 the type of load - deflection curves produced are typical for the C.R.P. test. The C.R.P. test 1 was

carried out in a similar manner and time interval as Lake (1986), and the results obtained from these tests are very similar. Refer to Table 4.3.

C.R.P. test 2 was carried out after the excess pore water pressure had dissipated. A significant increase in the pile ultimate bearing capacity was observered in both experiments, refer to Figure 4.7. The value has almost doubled that achieved in C.R.P. test 1. Most notable was the shaft friction had increased by over four times the original value in C.R.P. test 1. These factors are obviously due to the dissipation of the excess pore water pressure which results in an increase in effective overburden pressure and an increase in skin friction.

A factor which may have contributed to such a large increase in bearing capacity over a relatively short period of time was the boundary conditions stipulated in Chapter 3.3. The testing conditions were on the verge of these limits particularly during C.R.P. test 2.

Vesic (1970) shows that bearing capacity increases with time when piles are driven into clay. From his results he found that 75% or more of the ultimate bearing capacity was achieved within 30 days of driving. In some cases only 20-30% of the ultimate bearing capacity was achieved just after driving, dependent on the type of pile and soil.

4.2.7.13 Dynamic Results.

The dynamic results are not included in this thesis.

4.2.7.14 Pile Penetration / Blow Number.

The graph of pile penetration against blow number is compared to the results given by Lake (1986) and are illustrated in Figure 4.8. For a pile penetration of approximately 200mm the blow counts are virtually identical for both experiments. As the pile approaches the sand/clay interface the blow count increased rapidly when compared to that given by Lake (1986). This may be attributed to several reasons;-

1. The time between forming the soil samples and testing in the two tests is significant. Lake on average allowed 18 hours between these operations. For experiment 1 the Orion data logging system broke down just before the testing procedure and delayed the test by more than a week. This allowed further conditioning and consolidation of the clay. For experiment 2 the period was less than a week but still greater than 18 hours. It must be noted that from the tests carried out before and after the experiment there were no significant effect in the strength of the clay for both experiments.
2. The pile may have been fouling on the driving rig or on the guide collar which would have increased the resistance to driving. Although no apparent fouling was observed during the driving operation. It was noted after completing the driving operation in experiment one, that the guide collar did appear to have moved on the crossmember, twisting slightly. This was not apparent in the second experiment.
3. During the pile driving operation there seemed to be a

significant amount of reverberation in the pile system. On inspection of the pile after the test no loose joints were evident.

4.2.7.15 Generation Of Excess Pore Water Pressure From Pile Driving.

From Figure 4.9 and 4.10 it can be seen that a significant generation of excess pore water pressure developed from driving the 38mm diameter pile. The piezometer nearest the pile in experiment 1 showed an increase in pore water pressure of over 9kPa while the other piezometers further out show an increase of around 8kPa. If these results are compared, to give some authenticity to their value, to those given by Poulos and Davis (1980), (published after Lo and Stermac and Bjerrum and Johannesson), they compare quite favourably, as illustrated in Figure 4.11, even though the soil strata was built up of sand and clay and of a relatively low pile penetration into the clay.

The pore water pressure results for experiment 2, refer to Figures 4.9 and 4.10, are actual values as measured during the test. Some ambiguity must be applied to them because the real test conditions regarding the head of water applied to the clay sample was not known. This was due to a leak in the plastic membrane lining the clay tank. If the axis of the graph is translated down to the -2kPa mark it is interesting to note that the pore water pressure in the piezometer nearest the pile would approximate to the same value as that in experiment one.

Observations made during experiment two regarding water migration were as follows:

1. The rate of water lost from the sample through the puncture in the membrane during the pile penetration into the clay, was noticeably greater due to the generation of higher pore water pressure.
2. At the sand surface around the location of the pile the sand became noticeably damper.

An important feature of the results was the sensitivity of the monitoring system. At the time one of the pressure transducers had a calibrated range of 0-700kPa which was latter replaced with a more sensitive unit. The resolution would obviously be affected by this, although it did seem to compare very favourably with the other transducers with a greater resolution.

4.2.7.16 Build Up And Dissipation Of Excess Pore Water Pressure.

The significant point in the build up of pore water pressure was the time lag from end of driving to the peak in excess pore water pressure. Although possibly the piezometer may be expected to have a quicker response in a saturated clay it may be attributed to the conductivity and the probable pseudo - saturated state of the clay.

Vesic and Tomlinson indicate along with the results from these tests that load tests carried out in this period of high pore water pressure under estimate the ultimate bearing capacity of the pile. More realistic values for piles driven in clay are given after the dissipation of pore water pressure as Tomlinson suggests. This is again illustrated in these test results, after approximately 95% of excess pore water pressure had occured, refer to Figure 4.9, the bearing capacity had greatly increased, refer to Figure 4.7.

4.2.7.17 Conclusions From Pilot Study.

The objectives of this pilot study have been successfully concluded by the following points:

1. The piezometer system has proven successful in the desired application of monitoring pore water pressure. The results obtained show significant relationships to published data, illustrating that the system is reliable and accurate.
2. Initially the time consumed in gathering the relevant dynamic equipment for the pilot experiment was prolonged, though experience was gained in the use of this equipment.
3. A piezometer system based on the one used in this pilot study was designed for use in the semi-full scale tests.

4.3 Assessment Of The Piezometer System And Response Times.

4.3.1 Assessment Of The Piezometer System.

As previously stated the piezometer system proved satisfactory in its response to changes to pore water pressure. In the triaxial experiment it responded to total changes in isotropic confining pressures, giving realistic values for the pore pressure parameter B. The generation of pore water pressure resulting from the 38mm pile tests are in good agreement with published data. From this practical assessment of the system it was deemed totally adequate for its designed purpose, for use in the semi full scale tests.

4.3.2 Response Times.

The response time of the piezometer is governed by the shape factor

F, of the piezometer tip, the volume factor V, of the measuring system, the coefficient of permeability K, and the coefficient of compressibility C , of the soil. For a partially saturated soil there is an interference effect. This affects the response time of the piezometer in registering a change in pore water pressure.

The theoretical value of the response time of the system in a clay (red marl) was approximately 2 minutes. In practice the total response for the system averaged 10 minutes, when monitored during the 'B' test. The difference in values is a probable reflection on the condition of the clay. Samples taken of the clay after experiment 1, in the 38mm pile test indicated on average a 97% degree of saturation. This would increase the response time. To substantiate this the response of the piezometers during experiment 2 was far quicker. For this test a head of water was applied over the clay, which allowed water to permeate into any possible air voids. The degree of saturation did approach 100% for this test. This did not affect the decision to use the system in the semi-full scale tests. On average it takes 15-20 minutes to set up and install a pile section in the semi-full scale tests. Generally a load increment during the maintained load tests was held a minimum of 10 minutes. It would seem acceptable on this basis to monitor the pore water pressure change at the end of each seperate installation or load operation. This would give a more accurate assessment of the pore water pressure, taking into account the response time of the piezometer.

Sample N°	Cell Pressure σ (kN/m²)	Pore Pressure u (kN/m²)	B - Value $\Delta u / \Delta \sigma$	Moisture Cont' %
1	0	0	–	18·13
"	275·6	256·14	0·93	"
"	413·4	376·86	0·91	"
"	551·2	478·79	0·87	"
2	0	0	–	18·01
"	137·8	129·67	0·94	"
"	275·6	260·44	0·95	"
"	413·4	384·46	0·93	"
3	0	0	–	17·96
"	137·8	133·67	0·97	"
"	275·6	270·09	0·98	"
"	413·4	405·13	0·98	"

TABLE N°4.1 EVALUATION OF THE PORE PRESSURE PARAMETER "B" USING THE MINIATURE PIEZOMETER PROBE

Test N°	Test Description	Av' Density of Sand (kg/m³)		Av' Density of Marl (kg/m³)	Av' Cu Value of Marl (kN/m²)		Ø Value	Av' Moisture Cont' of Marl (%)	
		Before Test	After Test		Before Test	After Test		Before Test	After Test
1	Sand over Marl 20 Blows/min	1505·7	1573·6	2137	42·33	45·55	0	19·51	19·15
2	Sand over Marl 20 Blows/min	–	–	2150	49·66	50·12	0	19·33	19·47

Table 4.2

Test N°	Constant Rate Of Penetration Test N°	Ultimate Bearing Capacity (N)	Shaft Friction (N)	Time Of C.R.P. Test After Pile Was Fully Driven
1	1	760	130	45 mins
1	2	1440	540	5 days
2	1	745	250	45 mins
2	2	1420	540	5 days
Lake '86	1	680	110	45 mins

Table 4.3

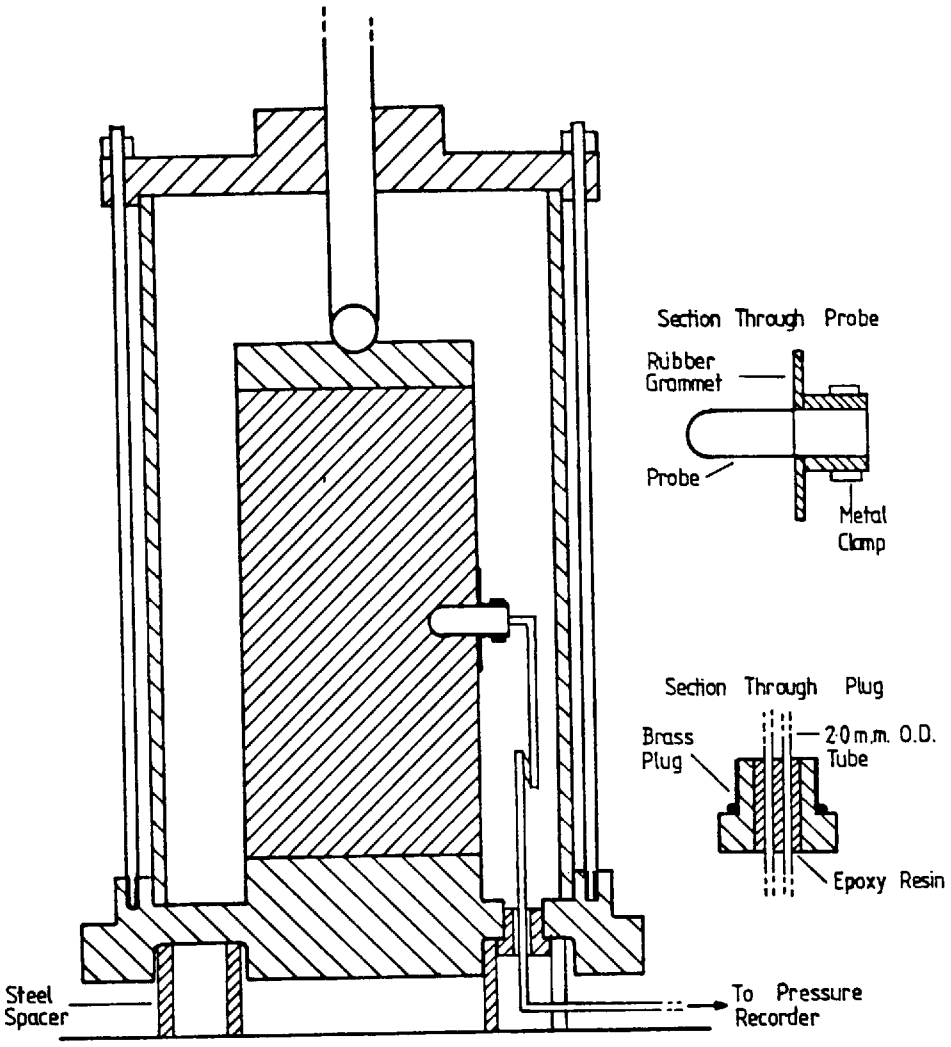

FIGURE N°4.1 PORE WATER PRESSURE MEASUREMENT USING THE TRIAXIAL APPARATUS

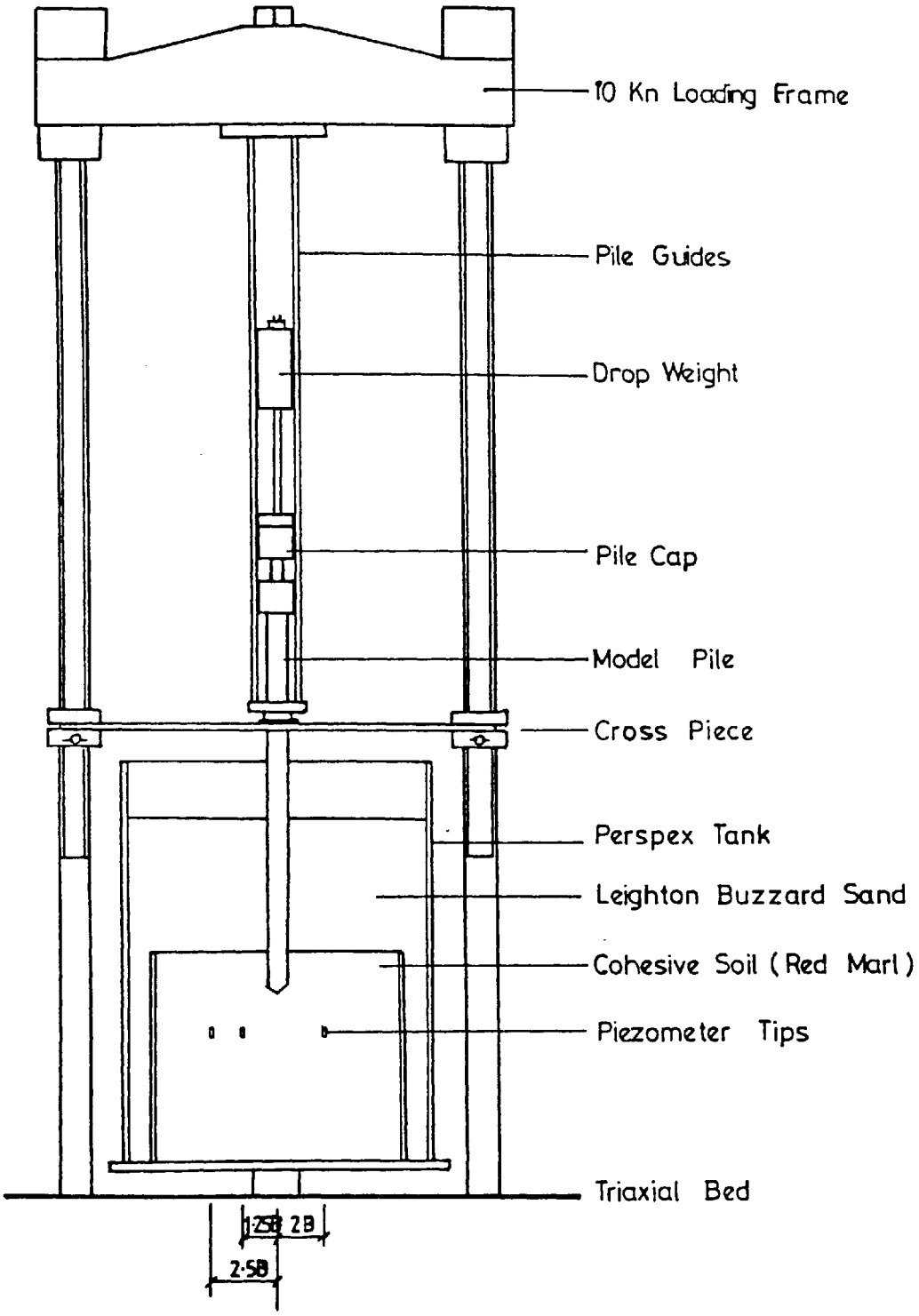

FIG 4.2 MODEL PILE DRIVING RIG

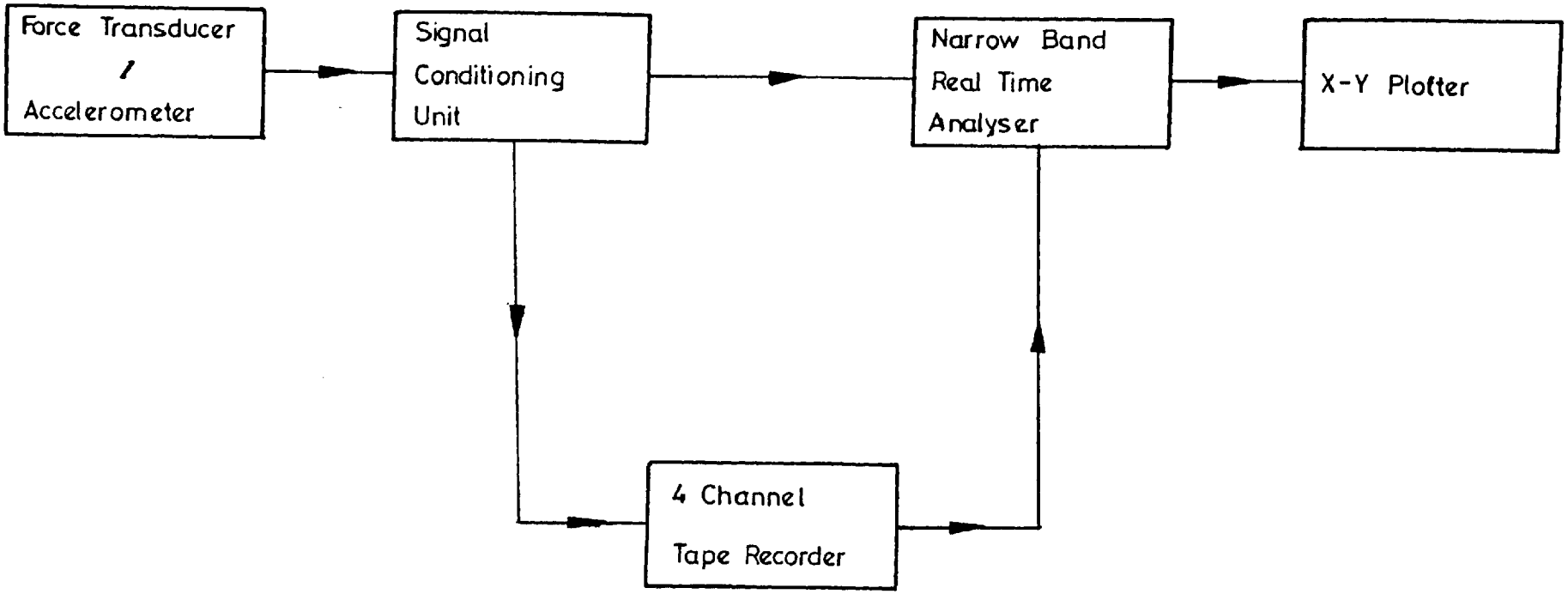

FIG 4.3 SCHEMATIC DIAGRAM OF A TYPICAL INSTRUMENT SET UP FOR DYNAMIC MEASUREMENTS

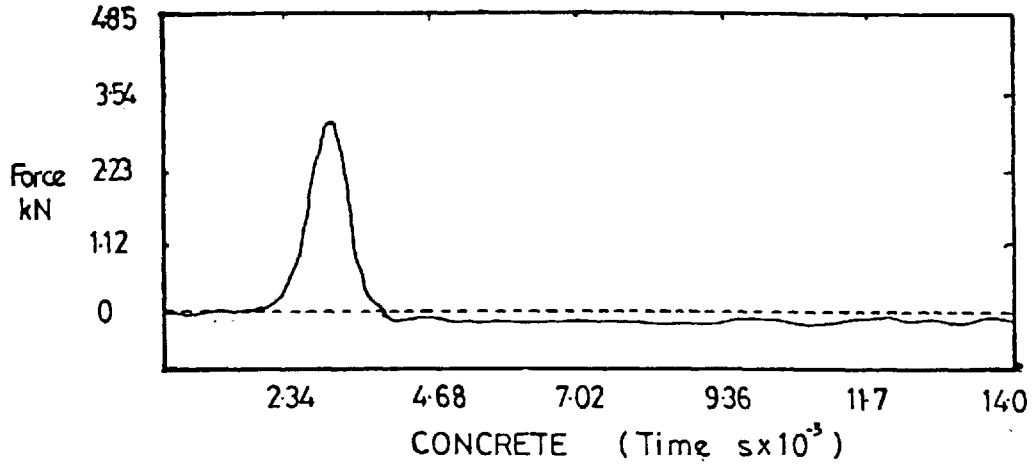

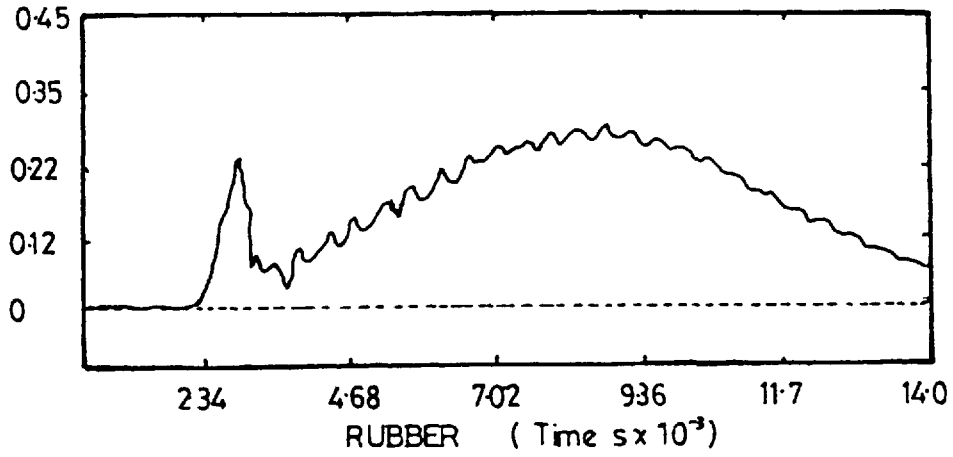

FIG N°4.4 SHOWING VARIATION IN OUTPUT SIGNALS FOR DIFFERENT BEARING SURFACES

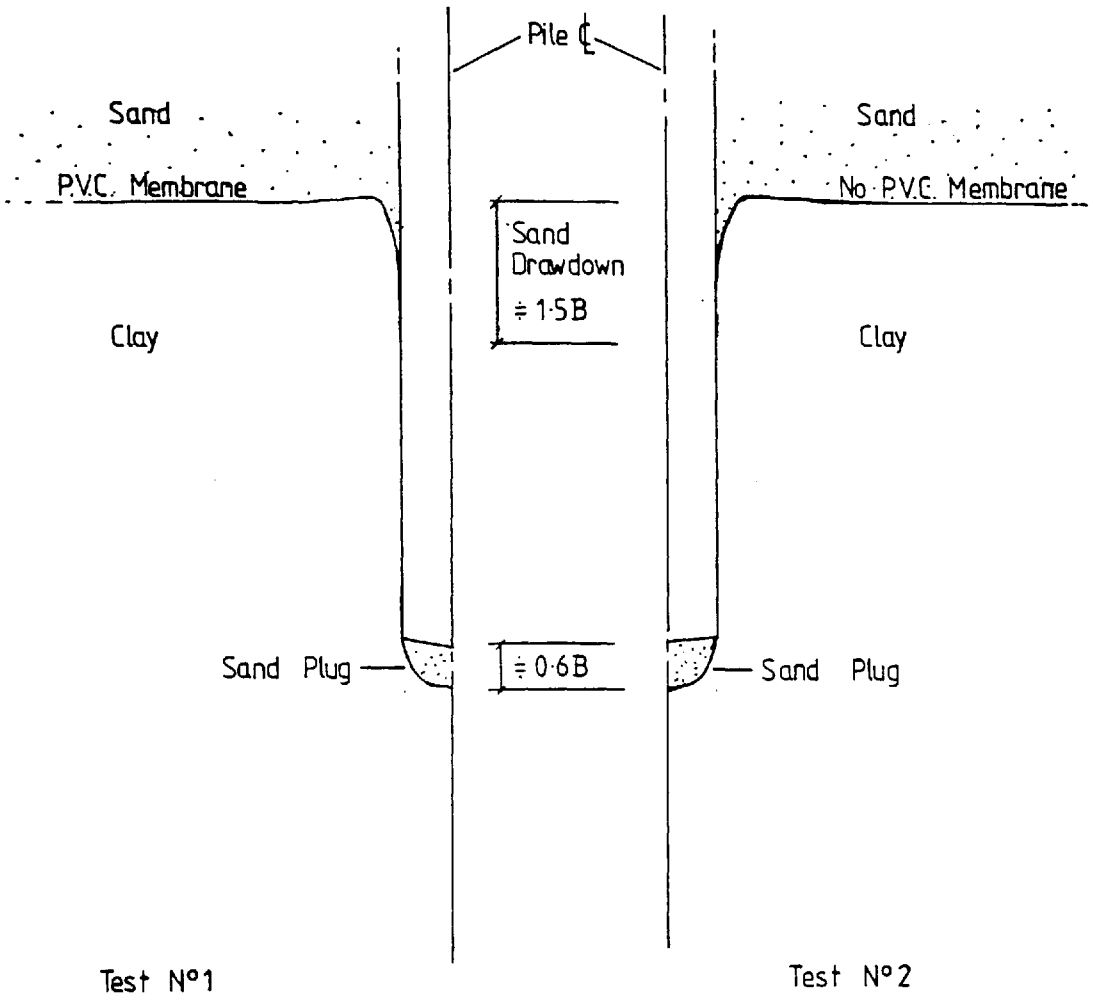

SAND DRAWDOWN AND SAND PLUG REGIONS WITHIN THE CLAY

FIGURE N° 4.5

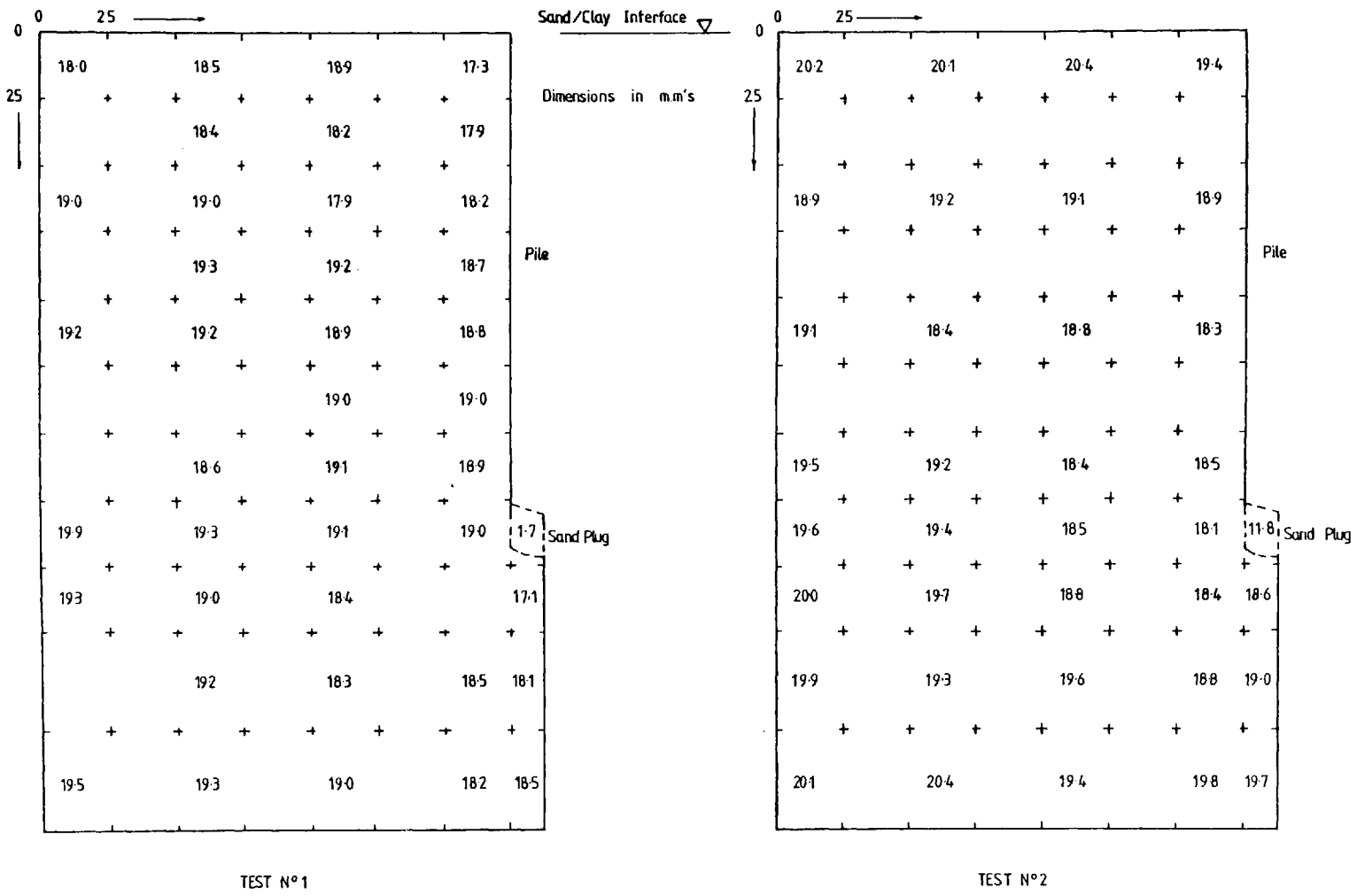

FIGURE N°4.6 CLAY MOISTURE CONTENT PROFILES (%) - 38m.m. Ø MODEL PILE TESTS

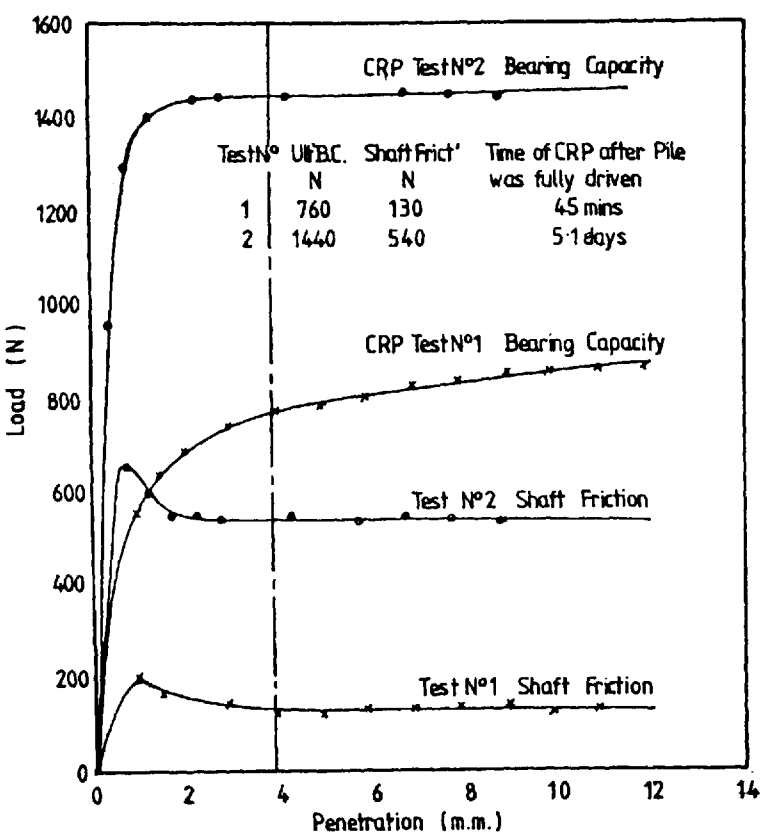

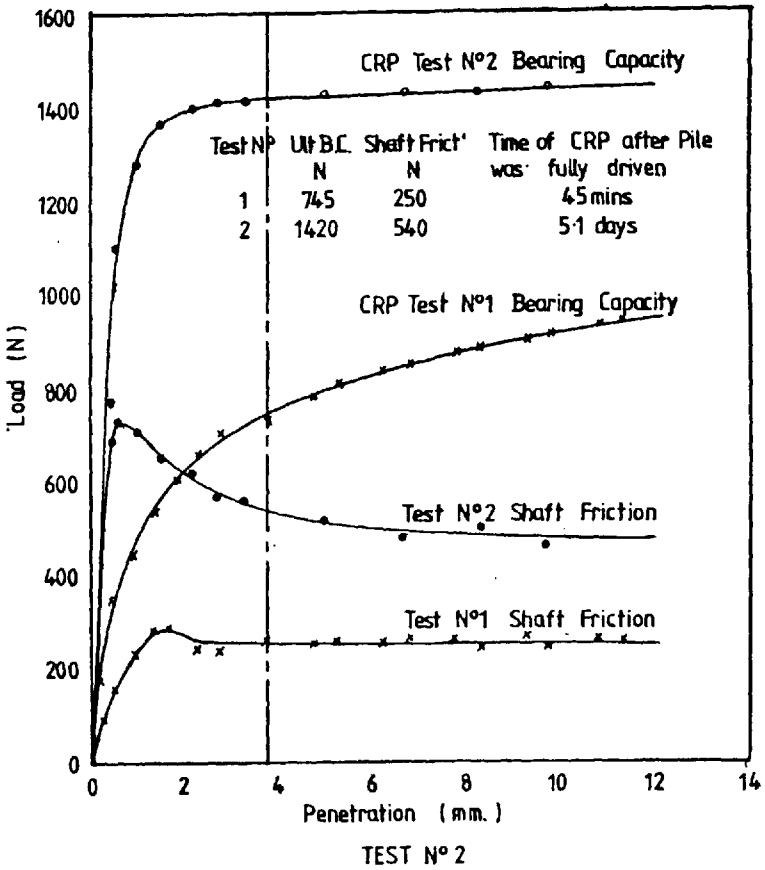

FIGURE N° 4.7 CONSTANT RATE OF PENETRATION TEST RESULTS - 38mm Ø MODEL PILE

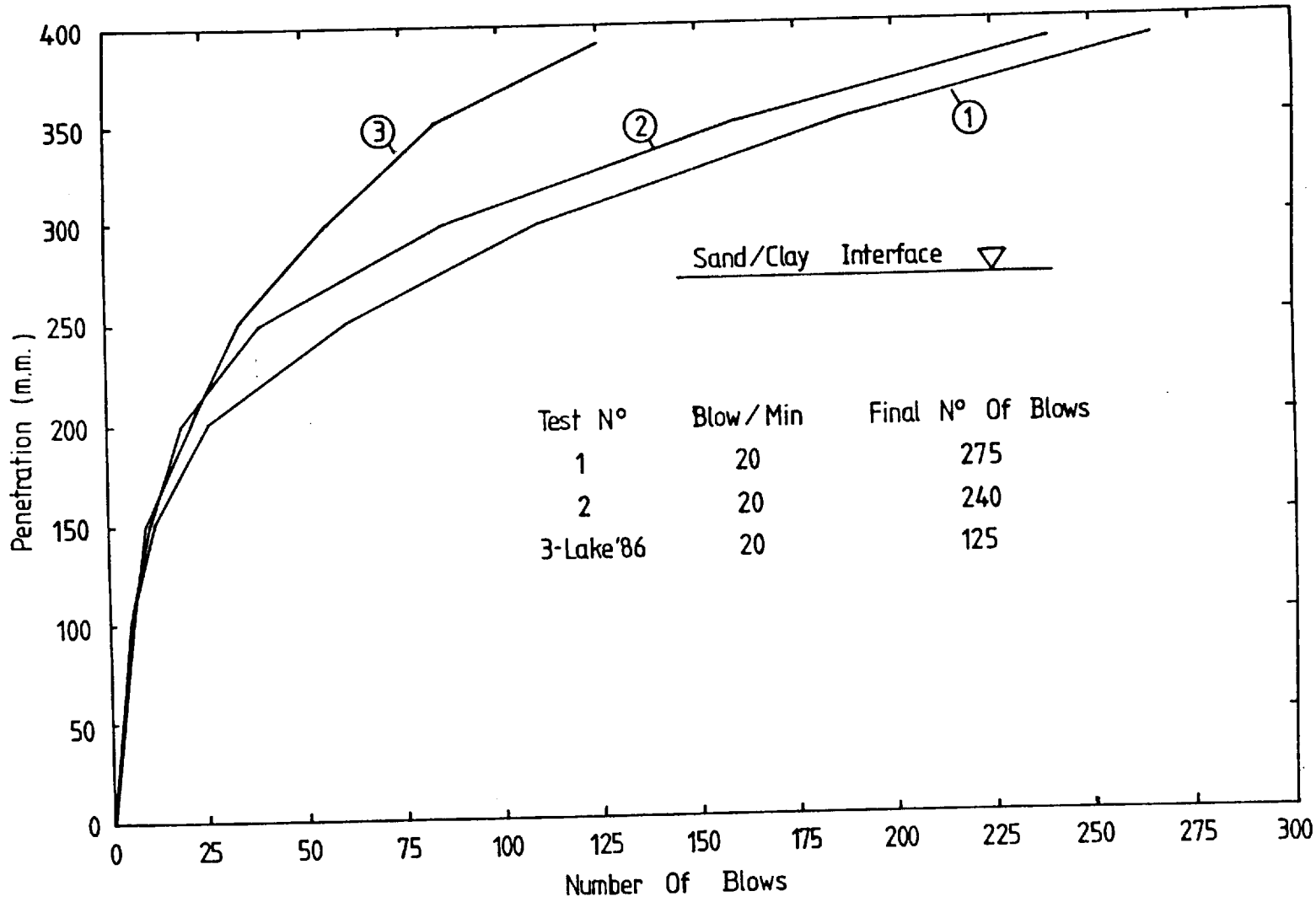

FIGURE N° 4.8 PENETRATION / BLOW NUMBER

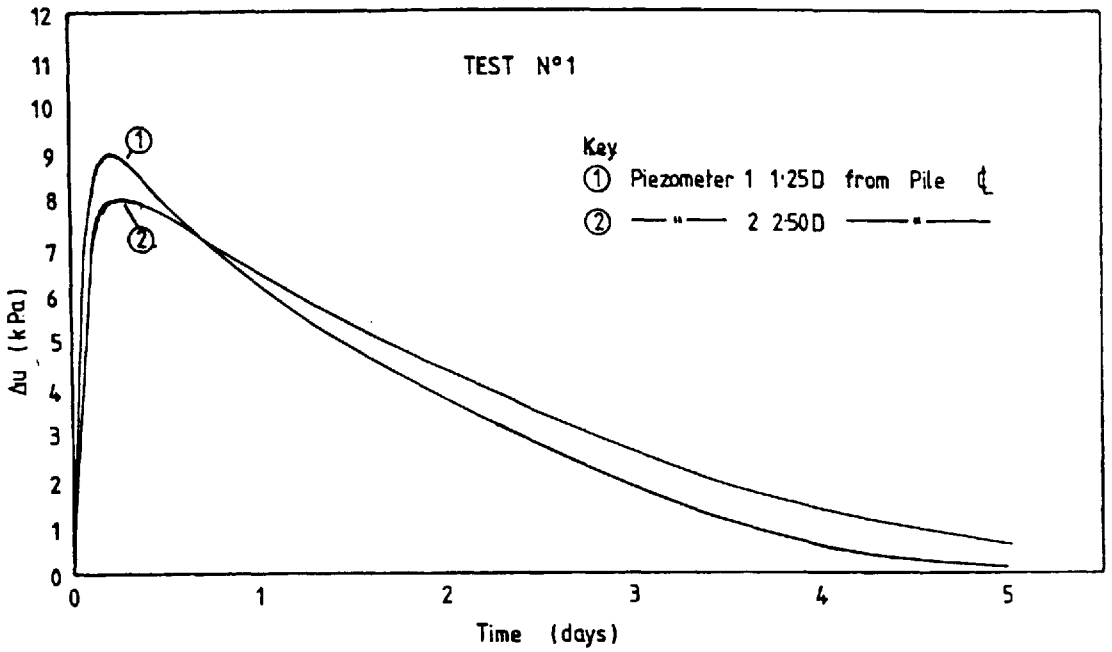

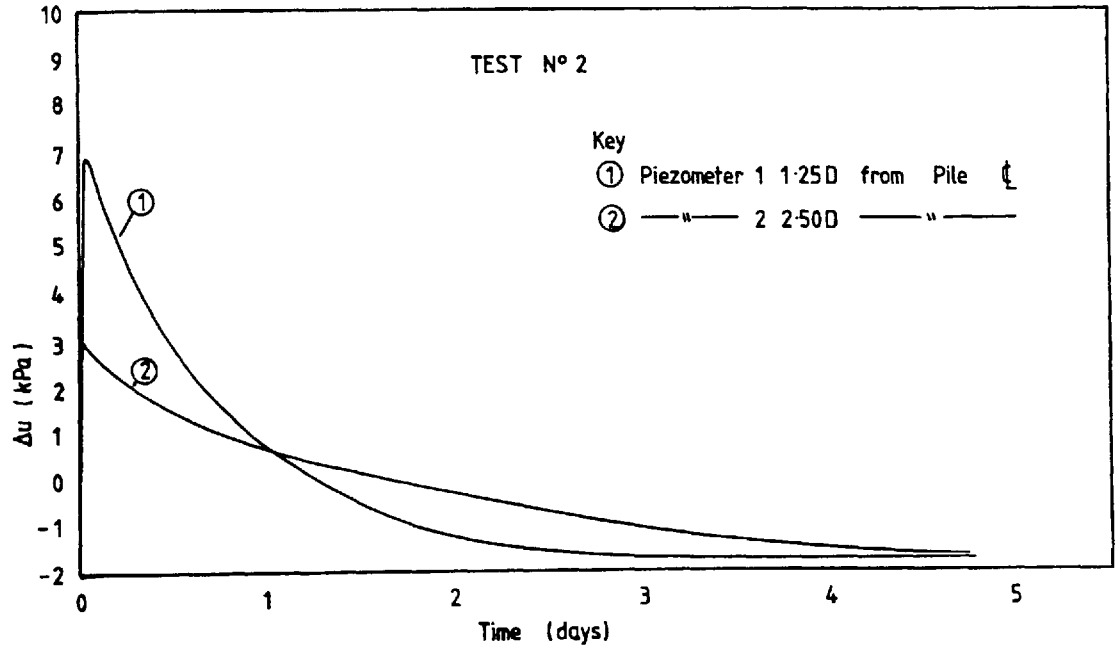

FIGURE N° 4.9 GENERATION AND DISSIPATION OF EXCESS P.W.P. DURING INSTALLATION OF A 38 m.m. DIAMETER MODEL PILE

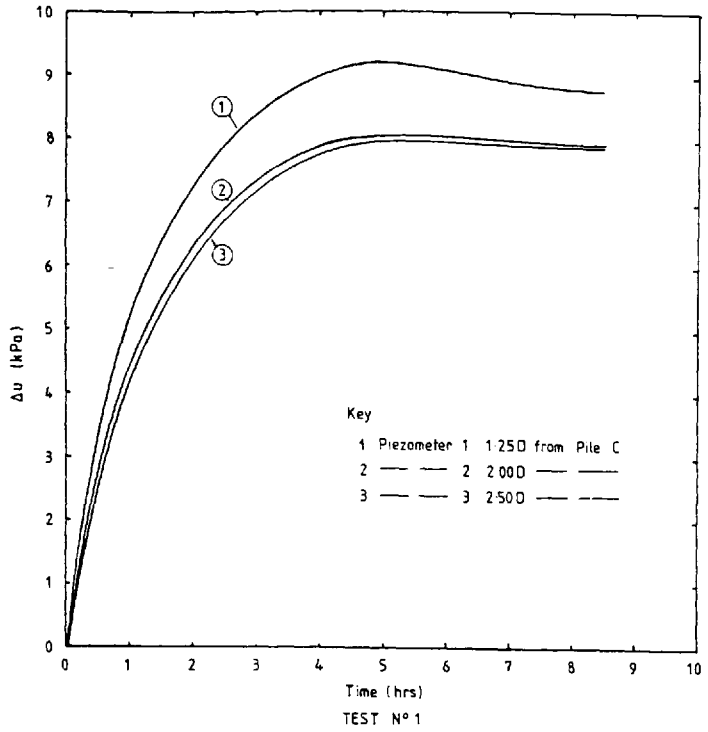

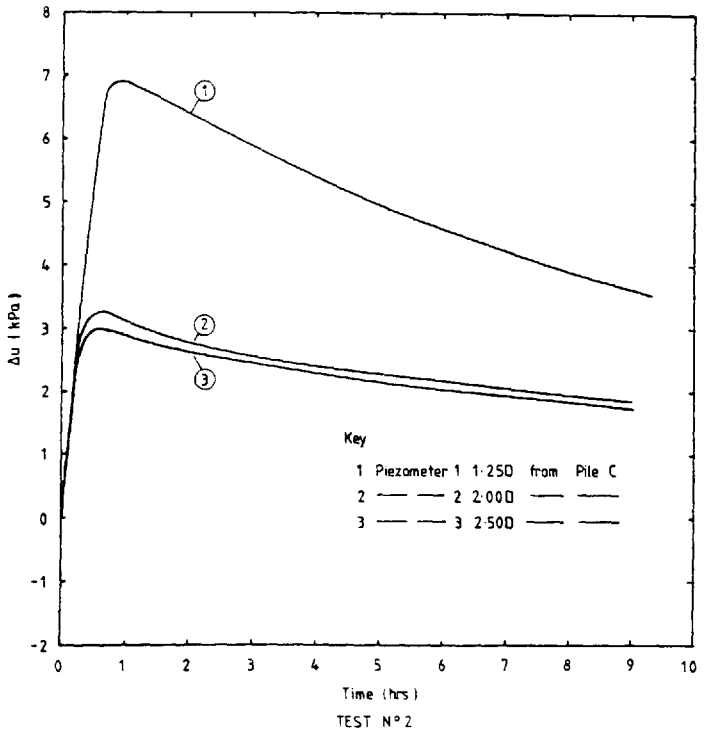

FIGURE 4.10 GENERATION AND DISSIPATION OF EXCESS P.W.P. DURING INSTALLATION OF A 38m.m. DIAMETER MODEL PILE

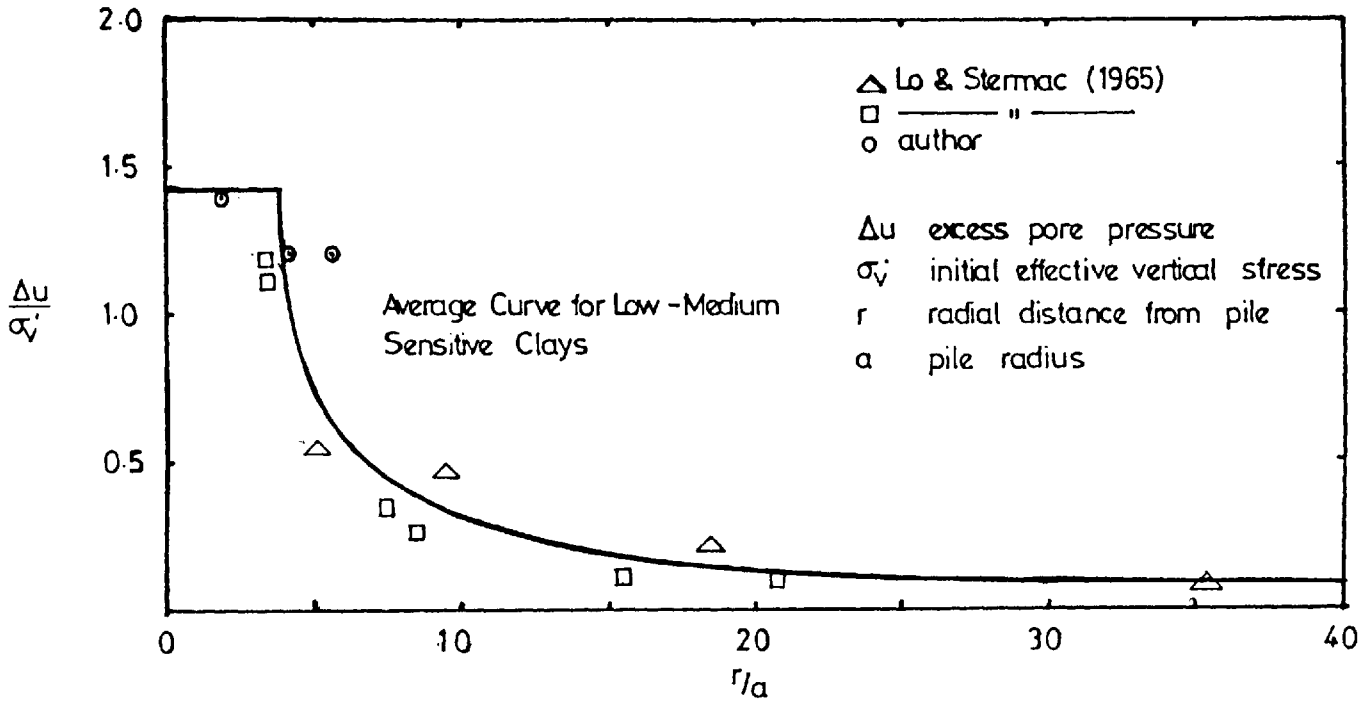

Fig4.11 Maximum Pore Pressures measured around driven piles (Poulos & Davis)

CHAPTER 5

CALIBRATION, PLACEMENT OF INSTRUMENTATION AND TEST PROCEDURE

CHAPTER 5

CALIBRATION, PLACEMENT OF INSTRUMENTATION AND TEST PROCEDURE

5.1 Calibration Of Instruments.

5.1.1 Introduction.

To calibrate the various types of instruments described in Chapter 3, the methods and techniques established by Wersching (1987) were used. Full details are given in his thesis. This involved the use of a set of calibration programs which are modified versions of the static monitoring programs, referred to in Chapter 3.12. These programs utilise the data scanning and logging facilities of the Orion data logger and P.E.T. microcomputer.

After each instrument was calibrated the data was run through a best fit polynomial (polyfit) program on the P.E.T. microcomputer to establish the calibration factors.

After completion of the semi-full scale tests a re-calibration programme was carried out. In general approximately half of the number of each type of instrument were re-calibrated and any others where there was doubt regarding their calibration. This gave a representative view on the maintained stability and accuracy of the instrumentation.

5.1.2 Static Axial Load Cell.

The static core type axial load cells used in both the 60mm and 114mm diameter piles were calibrated in a 200kN Instron 1251, universal materials testing machine. Special tube adaptors were

constructed to fit over each end of the load cells. This enabled the loading conditions encountered during the tests to be simulated during the calibration procedure.

Using appropriate end adaptors each load cell was calibrated in both compression and tension. The load cells in the 114mm pile were calibrated within the range of +50kN to -35kN except for the base load cell where more sensitive strain gauges were employed and limits of +/- 35kN were used. For the 60mm pile, calibration limits were +15kN in compression and -5kN in tension. Due to the method of construction of the toe load cell it could not be calibrated in tension.

5.1.2.1 Calibration Procedure.

The following procedure was adopted for both types of load cells. The loads applied to the 60mm pile load cells are shown in brackets.

1. Initially load and unload the cell 10 times to eliminate any possibility of locked in stresses due to construction and assembly.
2. Apply loads in increments of 5kN (3kN) up to a maximum of 50kN (15kN).
3. Release the final applied load in corresponding increments back down to zero.
4. Rotate the load cell through 90 degrees and repeat the load cycle.
5. This procedure was carried out for four load cycles, whereby the load cell is rotated through 360 degrees. This should minimize the effects of any unevenness in the bearing surfaces and eccentricity in the loading system.
6. The same procedure was carried out for the tensile tests,

where the increments of load were -5kN (-1.25kN) up to a maximum of -35kN (-5kN).

7. The resulting data was then processed using a 'polyfit' program to obtain the calibration constants.

5.1.2.2 Calibration Results.

The calibration graphs for the core load cells for both the 60mm and 114mm piles displayed excellent linearity, refer to Figure 5.1. The calibration factors were consistent both in compression and tension. For the 114mm pile the average accuracy at the 95% confidence limit was +/- 0.38kN with an average differance of 1.41% from the initial calibration factors. The accuracy of the load cells in the 60mm pile was +/- 0.12kN at the 95% confidence limit with an average differance of 1.49% from the original factors.

Over a period of 24 hours very little fluctuation or drift was observed in the load cells. Typically values were +/- 0.06kN. This time period was typical for any one series of load tests carried out in the semi-full scale experiments. For a 7 day period this value marginally increased to 0.075kN. This time period was typical of the sand/clay tests and the load cells did tend to drift more significantly. The effects of this is discussed in Chapter 6.

5.1.3 Boundary Orthogonal Stress Treansducer (B.O.S.T.).

The B.O.S.T. stress transducers used in the 114mm pile were calibrated using the direct method developed by Werscheing (1987). For calibration the individual pile sections were held horizontally in a loading frame. Dead loads were applied to the active faces of the transducers via a 'yoke' system mounted onto a 6BA bolt which

replaced the existing bolt in the centre of the transducer panel.

5.1.3.1 Calibration Procedure.

Once the pile section was set up the calibration procedure was as follows.

1. Calibration factors C1 and C2 in equations 5.1 and 5.2 i.e. factors relating to the shear stress were determined by subjecting the transducer to three cycles of shear whilst applying a constant radial stress equivalent to half the maximum radial calibration stress.
2. Calibration factors D1, D2, D3 and D4 relating to the radial stress component were determined by applying three cycles of radial stress in the absence of any applied shear stress.

$$Vc1 = C1Ps + D1Pn + D2 \quad \text{.... Equation 5.1}$$

$$Vc2 = C2Ps + D3Pn + D4 \quad \text{.... Equation 5.2}$$

The calibration limits as defined by Wersching (1987) were as follows

1. For transducers embedded in sand, limits of applied shear load of +/- 2.5Kg (maximum shear stress of 27.5KPa) and +2.5Kg normal load (maximum radial stress of 27.5KPa) were used.
2. For transducers embedded in clay, limits of applied shear load of +/- 16.0Kg (maximum radial stress of 174.4KPa) and +25kg normal load (maximum radial stress of 272.5kPa) were used.

5.1.3.2 Calibration Results.

The calibration curves remained reasonably stable for both the radial

and shear stresses. For the transducers embedded in clay the constants remained within +/- 10% of the original values. At the 95% confidence limit from the statistical analysis the values were accurate to +/- 3.57kPa and +/-1.21kPa for radial and shear stresses respectively.

The transducer constants for the sand only tests were within 8% of the original values and at the 95% confidence limit were within an accuracy of +/- 1.61kPa for the radial stress and +/- 0.5kPa for the shear stress.

Values at the 95% confidence limit are in good agreement with those given by Werscheing. The calibration constants on average varied by +/-10%. This may be attributed to possible variation in calibration technique. Other aspects as discussed by Werscheing (1987) which contribute to marginal variation in output from the B.O.S.T. are as follows;-

1. Possible local debonding of the silicone rubber around the B.O.S.T. active face.
2. Some degree of age harding of the silicone rubber.
3. Minor fluctuation in the energising voltage for the strain gauges.

A comparison between the results of the shear stress produced from the B.O.S.T. stress transducers and the load carried by skin friction deduced from the axial load cells is made in Chapter 6.

Some of the transducers did display marginal instability over a prolonged period of stress. The relative values remained constant but a drift from the origin was observed. This was particularly evident

in the sand/clay test and is discussed in Chapter 6. Typical values of instability over a 24 hour period are +/- 3.5kPa and +/- 0.4kPa and over a 7 day period +/- 5kPa +/- 0.4kPa for radial and shear stress respectively. These values still remain within the 95% confidence limits for the transducers.

5.1.4 Electrolytic Levels - Inclinometers.

The apparatus used for calibrating the inclinometers consists of a rigid beam upon which the inclinometer was placed, clamped in a pre-set groove. The beam is hinged at one end, so that its rotation is determined by a depth gauge, fitted with a special brass tip.

5.1.4.1 Calibration Procedure.

The calibration procedure was as follows;-

1. All the inclinometers had to be connected to the function supply box. This was necessary because the supply voltage was set for the total resistance of all the inclinometers connected.
2. Each inclinometer was mounted, in turn, onto the calibration rig with its electrode axis vertical and longitudinal axis in line with the beam axis.
3. The depth gauge was adjusted as necessary, until the bridge response indicated a null voltage. The inclinometer was then considered horizontal.
4. The beam was raised and lowered between the limits of +/-18mm in 2mm (0.21 rads) increments.

All the results were monitored using the P.E.T. - Orion control system. The data from the bridge output (V a.c.) against rotation

(rads) was then defined by a third order polynomial using the "polyfit" program.

5.1.4.2 Calibration Results.

The recalibration results again compared favourably with the initial values. At the 95% confidence limit the accuracy on average was +/- 1079 e-6 radians as compared to an original value of +/- 969.6 e-6 radians as deduced by Wersching (1987). Recalibration factors were within +/-2% of the original values. The effects of temperature and misalignment on the inclinometers has been rigorously investigated by Wersching (1987). In conclusion he showed that the effect of variation in temperature (+/-200.0 e-6 radians/ °C) was negligible. Due to the placement technique adopted a possible maximum misalignment of 0.050 rads of the inclinometers could occur. This placement error would have an insignificant effect on the calculated displacements.

5.1.5 Diaphragm Pressure Transducer (Nottingham Load Cells).

The diaphragm pressure transducers were calibrated in sand in a modified Rowe pressure cell. Full details of the technique is given by Wersching (1987). Negligible arching effects were encountered and subsequent calibration checks were carried out in the Rowe cell with water.

5.1.5.1 Calibration Procedure.

1. The pressure transducer was placed in an annular wooden former equal in depth to the transducer, the outer diameter of which being equal to the inner diameter of the

Rowe cell.

2. The wooden former and transducer were placed inside the Rowe cell. The cell was then sealed and filled with water.
3. The cell was pressurised a number of times to a pressure of 30 p.s.i. to ensure good contact between adjacent internal components within the cell chamber.
4. The transducers were then calibrated over three cycles. Each cycle consisting of pressure increments of 34.5kPa (5p.s.i.) up to 206.7kPa (30 p.s.i.) and released in 34.5kPa increments down to zero.

Again the data was stored on the P.E.T-Orion control system and processed through the polyfit program.

5.1.5.2 Calibration Results.

The recalibration factors compare to within +/- 3.8% of the original values used in the test programme. At the 95% confidence limit the accuracy was within +/- 2.81kPa. Over a 24 hour period the transducers drifted by typically +/- 1.5KPa. For a prolonged period of 7 days this value increased to typically +/- 5kPa.

5.1.6 Interface Shear Stress Transducers.

The radial shear stress at the sand/clay interface was monitored by four pairs of interface shear stress transducers, (I.S.S.T.s) The development of these transducers is given by Werscheing (1987). It is basically a modification of the B.O.S.T. transducer.

5.1.6.1 Calibration Procedure.

The calibration procedure is similar to that given in section 5.1.4.1

for the B.O.S.T. transducer with the exclusion of a normal applied stress and is as follows:-

1. The transducer was initially strain cycled.
2. The transducer was cycle loaded in 39.2kPa (3.0Kg) increments between the limits of +/- 196.2kPa (+/-15Kg).
3. This was repeated three times.

5.1.6.2 Calibration Results.

The recalibration factors fall within 4.5% of the original factors. At the 95% confidence limit the average accuracy was 2.40kPa, which compared very well with the average value of 1.96kPa stated by Wersching. Over 24 hours and 7 day monitoring periods the transducers drifted from the initial values by typically +/- 0.15kPa and +/- 0.25kPa respectively.

5.1.7 Linear Variable Displacement Transducers (L.V.D.T.).

All the L.V.D.T.'s used for measuring the vertical and horizontal displacements of sand movement in the semi full scale tests were calibrated in the same manner. This procedure was initially set out by Kay (1980) and employs the use of a standard micrometer.

5.1.7.1 Calibration Procedure.

The basic procedure was as follows.

1. The L.V.D.T. was set up in the modified micrometer rig.
2. The transducer position was adjusted until a zero reading was recorded.
3. The transducer arm was displaced in equal increments by the use of the micrometer, up to the maximum displacement

of the instrument being calibrated. The procedure was then repeated in the reverse direction.

4. The operation was repeated three times.

The results were processed through the 'polyfit' program and the calibration factors established.

5.1.7.2 Calibration Results.

At the 95% confidence limit on average the calibration factor had an accuracy of +/- 0.09mm. Over 24 hours and 7 day monitoring periods the transducers drifted by typically 0.01mm and 0.03mm respectively from the initial values.

5.1.8 Pressure Transducers.

The pressure transducers used to measure the change in pore water pressure were calibrated using a Geotechnical Digital System (G.D.S.) controller.

5.1.8.1 Calibration Procedure.

The procedure is as follows.

1. The pressure transducers were initially connected up to the G.D.S. controller system.
2. The transducers were then loaded and unloaded in 10kPa increments up to the maximum of 100kPa and correspondingly back to zero.

The results were again processed through the 'polyfit' program to establish the calibration constants.

5.1.8.2 Calibration Results.

The accuracy of the transducers was typically +/-0.4kPa at the 95% confidence limit. Temperature effects were considered to have a negligible effect since the temperature within the soil and inspection chamber where the pressure transducers were housed did not vary by more than +/-2 degrees centigrade.

For 24 hour and 7 day monitoring periods the transducers drifted by typically +/-0.45kPa and +/-0.55kPa respectively from the initial zero values.

5.2 Soil Placement.

The soil placement techniques used in the semi full scale test are those which have been well proven and established by various research work carried out at the Polytechnic Of Wales. They have been well documented elsewhere, but the general procedures are included here for information.

5.2.1 Sand Placement.

5.2.1.1 Introduction.

The sand placement involved the use of the Redlar conveyor system. This draws sand from the storage tank and deposits it through a flexible hose system into the test tank. The problem with this method is the amount of dust caused by the free falling sand. This was overcome by deploying the use of two 'Nilfisk' industrial vacuum cleaners. One was connected to the flexible hose system, which had an inner hose, and the other was held at the outlet during sand

placement. The sand was built up in layers to allow the instrumentation to be placed within the strata.

5.2.1.2 Sand Placement Method.

The following sand placement method was adopted and it follows that given by Lake (1986).

1. Sand was deposited in the tank using the flexible pipe previously mentioned. A sweeping motion was employed during pouring which distributed the sand evenly and ensured the secondary placement was kept to a minimum. This was necessary in order to limit the possibility of local density variations. During placement care was taken to ensure an even drop height of between 100 - 200mm was maintained. A bend was kept in the lower portion of the hose in order to retard the sand flow.
2. When a 250mm deep layer had been placed, the surface was smoothed over using level boards and the horizontal level corrected using a spirit level as a proprietary step to placing the instrumentation.
3. This process was repeated for each 250mm layer with the length of the flexible hose being adjusted to accommodate the decreased drop height. A total of 10, 250mm layers were placed in this way with care being taken not to pour sand directly onto any instrumentation in order to prevent disturbance.

This technique did produce some slight stratification in the sand. The influence of this on the behaviour of the pile is considered negligible relative to the size of the pile. Density checks were made

during sand installation and subsequent testing propgramme and are discussed in Chapter 7.

5.2.2 Placement of the Mercia Mudstone (Red Keuper Marl).

5.2.2.1 Introduction.

The red marl (Mercia Mudstone) used in the semi-full scale tests had previously been mixed. It was stored in sealed bins to prevent moisture loss and to maintain the clay at 18% moisture content. The moisture content of the clay in each bin was monitored during storage to ensure it remained in its prepared target condition of 18% moisture content and a shear strength of approximately 50kPa.

5.2.2.2 Red Marl Placement.

The red marl placement technique adopted was as follows.

1. The wooden former was graduated in increments of 150mm with sub increments of 50mm. It was lined with a polythene sheeting, the edges of which were sealed with 'sylglas' tape. This was to prevent moisture migration.
2. Sufficient marl was removed from the bins and placed in the wooden former, to such a depth that when compacted a 50mm layer would be formed.
3. Compaction was undertaken in accordance with the method described by Werscching(1987) and is given as follows:

i. 5 seconds compaction at each platten location. Further penetrations of the platten into the clay was minimal after this time.

ii. A 50% overlap of platten area at subsequent locations. This ensured a kneading action during compaction.

iii. Three complete passes over a given area of clay.

iv. The clay surface was "roughened" before placing the next layer to ensure good interlayer bonding.

4. Once a 150mm layer had been compacted, four 38mm diameter standard tube samples were taken at 90 degree intervals on a 300mm radius. After the cores were taken the resulting holes were refilled, and hand compacted using a hand rammer. The core locations were staggered on subsequent layers so as not to take cores from the same relative loations, in each layer.

5. The core samples were analysed to determine the unconfined compressive strength, moisture content, bulk density and degree of saturation.

6. The process was repeated until the wooden former was full.

7. Once all the clay had been compacted a vinyl membrane was sprayed on to the surface of the clay. This was only carried out for the first sand/clay Test No 2 which involved the dynamically driven 60mm pile. The process was as follows.

   The vinyl membrane was applied in two coats, the first allowed to partially dry before applying the second. Before this coat was dry sand was sprinkled over the surface, and the grains were partially embedded into the clay by applying a small pressure. A third coat of vinyl spray was then applied.

8. The specimen was left to cure for 24 hours.

The vinyl membrane technique was discontinued in subsequent tests for health and safety reasons. The moisture migration was not found to be

significant during the intial stages of Test 5. However it did affect the local properties of the soil with the passage of time which is discussed in Chapters 6 and 7.

5.3 Instrumentation - Location And Placement Details.

5.3.1 General Details.

The wall of the tank is graduated into 10 equal 250mm layers. The circumference of the tank is also marked off into 24 equal sectors. At each layer and on each sector location point is also marked the type and location of the instrumentation to be set out.

The central vertical axis was located by placing a dummy section of pile into the pile guides. A plumb bob was then lowered to the required level and fixed to cross wires attached to the pile section. From this central position the instrumentation was placed radially along two spiral arms, this was to avoid any local effects in the soil. The exact location of each instrument on each spiral arm was marked by aligning a pre-graduated measuring rod between the centre spot and radial sector marker. The position was marked with a cotton bud marker.

Exactly the same procedure was carried out for the instrumentation at the sand/clay interface.

The location of all the instrumentation is illustrated in Figures 5.2, 5.3 and 5.4.

The wiring / tubing leading from the instrumentation was placed radially and a slightly coiled from the central axis. This reduced

the possibility of creating a reinforced earth and allowed for any lateral movement in the soil respectively.

5.3.2 Electrolytic Levels (Inclinometers).

5.3.2.1 Inclinometers In Sand.

A function of the alternating current which energizes the inclinometers was that the output voltage was always positive. This was regardless of their orientation. In order to overcome this problem the inclinometers were initially installed tilted in the horizontal plane. The end adjacent to the pile being tilted upwards. The initial angle of installation tilt gave a reading of 0.8 volts. It was found by Wersching (1987) that this was sufficient to give the inclinometers enough displacement travel without going through the zero null voltage.

The installation was as follows;-

1. Having located the position of the inclinometers in the sand the Orion was set in manual control to scan the output voltage.
2. The longitudinal axis of the inclinometers were then set along the radial line from the centre spot to the sector marker on the wall of the tank.
3. The vertical axis was set by using a small plumb bob arrangement, aligning the bob line up with a slot cut in the vertical plane at the front of the inclinometer casing.
4. The inclinometers were carefully set at 0.8 V a.c. by use of the Orion data logger.

The outermost inclinometers were connected vertically to a displacement transducer mounted on the datum frame via a length of piano wire. Any movement from the inclinometers was detected even if there was no change in the horizontal attitude of the instrument. The inclusion of this movement into the integration program meant that gross displacements may be displayed as opposed to relative ones.

5.3.2.2 Inclinometers At The Sand/Clay Interface.

The setting out procedure at the sand/clay interface was similar to that of sand, except for the following points.

1. At the inclinometer location point a slot was cut into the surface of the clay equal to half the depth of the inclinometer.
2. The inclinometer was placed and set up in the previously mentioned manner and then sprayed with a coat of vinyl membrane to prevent moisture migration.

5.3.3 Sand Density Samples.

The sand/density samples were set according to the following procedure as stipulated by Wersching et al (1983).

1. At the predetermined location a paper former was positioned with a small identification tag placed within.
2. The sand/plaster mixture was poured into the former in an even manner, from a constant height to simulate the conditions to which the sand was placed.
3. Sand was placed around the former which was then carefully removed.
4. All the samples on a particular layer were formed before

hydration tubes were located in position. The tubes were laid radially outwards along the sand and up the test tank walls to which they were affixed.

The initial insitu density samples were hydrated 24hrs before pile installation and load testing commenced. Hydration of the remaining density samples was completed at the appropriate time in the testing programme and left for 24hrs before either the tank was emptied or another series of load tests carried out.

5.3.4 Horizontal Displacement "Terra Plates".

The procedure for setting out the terra plates was as follows;-

1. Having levelled off the sand the terra plate was held vertically over its designated position with the wire strand parallel to the sand surface and radially located from the centre point.
2. The L.V.D.T. was pulled out to the required displacement and locked in position with a small alluminium wedge.
3. Making sure the piano wire was taut, sand was back filled behind the plate and over the wire, taking particular care not to induce a sag in the piano wire.
4. The displacement arm on the transducer was unlocked by the removal of the wedge. Any possible slackness in the wire was pulled up by the small tensile force in the spring return mechanism inside the transducer.

5.3.5 Diaphragm Pressure Transducers.

The pressure transducers were located in position following the same procedure as the inclinometers except for the following points.

1. When located in position they were laid horizontally using a small bubble level.
2. When used at the sand/clay interface they were embedded to the total depth of the transducer unit.

5.3.6 Interface Shear Stress Transducers.

Again the "I.S.S.T.s" were placed in position following the same procedure as the inclinometers with the following exceptions;-

1. The shear plane was placed horizontal with the grooved surface perpendicular to the radial line from the pile axis.
2. When used at the sand/clay interface they were embedded the full depth of the transducer unit, so that the shear surface was part of the sand/clay interface.

5.3.7 Piezometer Probe.

The piezometer probes were placed in the following manner.

1. The radial positions of the piezometers were marked on the clay surface in the usual manner.
2. The clay was augered out to the pre-determined level using a specially manufactured auger bit. The auger being equal in diameter to the brass housing containing the ceramic tip.
3. The auger bit was then replaced by a smaller bit equal in diameter to the ceramic tip. Throughout the augering process the equipment was continually checked for verticality.
4. A small amount of clay slurry was placed at the bottom of

the bore hole. The piezometer tip was then removed from its water bath and the ceramic smeared with the marl slurry. This was to ensure a good contact when bedded into the clay.

5. The tip was carefully lowered to the bottom of the bore hole and gently "bedded in" by applying a small pressure behind the brass housing collar with a small brass rod.
6. The bore hole was back filled with marl; the piezometer tubes leading from the tip were buried radially in the surface of the clay.

5.4 Pile Installation And Test Procedure.

5.4.1 Introduction.

The experimental programme for the semi full scale tests involved the use of the 60mm and 114mm diameter piles. The methods adopted for the installation and the initial load testing programme were those established by Lake and Wersching respectively.

The extended load testing programme was a modification of the initial one with the inclusion of a cyclic load test. The cyclic loading test was only used on the 114mm diameter pile. (Refer to section 5.4.6).

5.4.2 Dynamic Installation - 60mm Pile.

The procedure adopted is that given by Lake (1986) and was as follows.

1. The model pile cap was positioned on the first pile section and secured in place. This section was then placed in position in the driving rig.

2. The model pile was pushed into the sand until the top of the cap reached a predetermined position on the driving rig. This was necessary so that any level irregularities in the sand surface would be compensated for, and the pile would be driven from the same position each time.
3. The L.V.D.T. was connected to the pile cap and the control program initialised.
4. After initialisation the driving option was selected from the control program, which scaned all the channels until a preset driving increment was reached.
5. Dynamic driving was started by activating the pneumatically controlled drop hammer system. The transient signals were stored and monitored as described in Chapter 4.2.4. A continual check on the operations of the dynamic transducers was kept by out putting one of the signals to the spectrum analyser.
6. The L.V.D.T. was also connected to a voltmeter so that the change in voltage due to each blow would be recorded to yield a complete driving record.
7. On the completion of each driving increment the model pile clamps were secured to prevent any movement in the already driven pile section when removing the pile cap and positioning the next section.
8. The pile cap was placed on the new section, the clamps released and the driving process was repeated.
9. This procedure was repeated until the pile was fully driven. The dynamic pile cap was removed and the driving rig dismantled down to the base plate. A dummy section

with the static pile cap was added to the pile in readiness for the static tests.

5.4.3 Constant Rate of Penetration Installation - 114mm Pile.

The procedure adopted is that given by Wersching (1987) and is as follows.

1. The initial sections of the pile were set up in the guide in readiness for the first drive increment and secured into position.
2. The appropriate pile cap was fixed to the pile section. The pile clamps were then released and the initial pile embedment in the sand was noted. The pile was again secured.
3. The Darteck jack was lowered onto the pile cap and the L.V.D.T.s were connected. At this stage the control program was initialised making sure all load cells were in an upright position.
4. The pile clamps were released and the first drive increment was selected on the control program. The pile was jacked at a constant rate of 10mm/minute until the first drive increment of approximately 100mm was completed.
5. On completion of each drive increment the pile was secured with the clamps, the Darteck jack removed and the next pile section secured into position.
6. The whole process was repeated until the pile was fully driven to approximately 1845mm.

The driving rate was selected by Wersching after consideration of the

rates reported by various authors; Koizumi (1971), Butterfield and Johnson (1973), Meyerhof and Valsangker (1977), Meyerhof and Sastry (1978a) and Cooke et al (1979).

5.4.4 Constant Rate Of Penetration Test.

The penetration rate of 1.524mm/minute chosen for this test was deduced from work carried out by Whitaker (1970). The pile was driven a total distance of 30mm during the test which is 0.5B and 0.26B of the 60mm and 114mm piles respectively. These values fall beyond the failure criteria set by Whitaker where he states that for end bearing piles, penetration may reach 25% of the base diameter, and for friction piles about 10% of the shaft diameter.

Throughout the six semi full scale tests, the deflection of the reaction frame under maximum working load never exceeded the limit of 2.5mm set by Whitaker.

The procedure for the test was exactly the same as a drive increment for the installation of the 114mm diameter pile.

5.4.5 Maintained Load Test.

The maintained load test was used to equate the settlement of the semi full scale piles to the applied loads. The failure load for the piles tested was taken as the load obtained from the C.R.P. test when penetration had reached 10% of the pile diameter. From this the working load was deduced by applying a factor of safety of 2.5.

During the maintained load test the pile was loaded in increments of 33.33% of the working load for the 60mm pile. For the 114mm pile the increments were reduced to 10% of the working load. This was as a

result of a discussion with Werscheing; it was thought advantageous to have small load increments. More data would be obtained this way from the B.O.S.T. stress transducers, in particular, near the failure load and unloading schedules.

The initial part of the loading programme, was to load the pile in increments up to the working load and release the load back to zero. Incremental loads were then reapplied until failure was reached, the load was then released in increments back to zero.

For each load increment cessation of movement was defined when the rate of penetration was less than 0.25mm per hour, provided the rate of settlement was reducing. This complied to B.S.8004 (1986). As a further check three consecutive reading were taken and each reading checked to be within 0.01mm of the preceding one.

Initially the minimum duration of any one load was 10 minutes. This was reduced to 5 minutes for the initial increments of load used on the 114mm pile, when the increments were 10% of the working load.

It was found during the earlier tests that the minimum holding time was not always necessary, particularly when the rate of settlement fell well within the criteria laid down by B.S. 8004 (1986). Lake (1986) also reported this, where he makes particular reference to the sand only tests, as there was no discernable consolidation stage, and protracted settlement periods are not manifest until failure is approached. Hence it was deemed justifiable to reduce the time duration, for the early increments, particularly when it was considered that the smaller increments effectively doubled the total time of the test. The testing was still carried out during one

working day, similar to Wersching and Lake.

Due to the updated micro-computer system, the extended loading test period did not restrict the data logging onto one floppy disk. The old system did restrict the time duration of the test.

To perform the maintained load test the following procedure was followed:-

1. The Dartec jack was brought under manual control by zeroing the load meter on the control unit, following the disconnection of the function generator.
2. The Dartec jack was then lowered onto the pile cap and the computer control program started.
3. The load tests were carried out by setting each load increment manually using the Dartec control box.

5.4.6 Cyclic Loading Test.

After completion of the initial C.R.P. and M.L. load tests a cyclic load test was carried out. This loading test was only used on the 114mm pile to investigate the effects on the soil/pile interaction and the response of the B.O.S.T. stress transducers under these conditions.

The frequency of loading was 0.1Hz which was applied in a positive sinusoidal form under load control, which gave one way cycling. (i.e. cyclic loading in compression only without reversal of load, Brown et al (1977). This value is typical of wave loading conditions where values generally range from 0.05 - 0.2Hz, as reported by Briaud and Felio (1986). The maximum load applied during the cycle was the working load deduced from the C.R.P. test.

The total number of cycles applied during the test was 1600. This was a reasonable number which enabled all the data scans to be stored onto one disk and subsequent load tests to be carried out in one day.

The introduction of this test expanded the loading programme into two days. On the first day installation, C.R.P. and maintained load tests were carried out. This was followed by cyclic loading and maintained load tests on the second day.

To perform the cyclic loading tests the following procedure was carried out.

1. The Dartec jack was brought under manual control by zeroing the load meter on the control unit, whilst maintaining the link up with the function generator.
2. The frequency and sinusoidal function were dialled into the function generator and the appropriate working load set on the Dartec control unit.
3. The Dartec jack was lowered onto the pile cap and the L.V.D.T. connected.
4. The control program was started and the "free run" cyclic load applied for 1600 cycles.

5.4.7 Constant Rate Of Uplift (Pull-Out) Test.

The procedure adopted for this test was essentially the same as the C.R.P. test and was as follows:

1. The Dartec jack was carefully lowered onto the pile cap. Bolts were placed up through the pile cap and secured into locating holes in the jack loading plate. This allowed tensile loads to be applied to the pile.

2. The pull out test was selected from the control program. The pile was then retracted a distance of 30mm at a rate of 1.524mm/minute.

The pull out test was not carried out on the 60mm pile sand/clay profile. It was deemed necessary to inspect the sand plug driven ahead of the pile without the influence of the induced suction action of the test.

5.4.8 Test Schedule.

In order to relate to and extend the existing work on pile load testing at the Polytechnic Of Wales a series of six semi-full scale tests were performed.

The first two tests involved the use of the 60mm pile whilst a 114mm pile was employed in the remaining four tests. The test schedule is given in Figure 5.5.

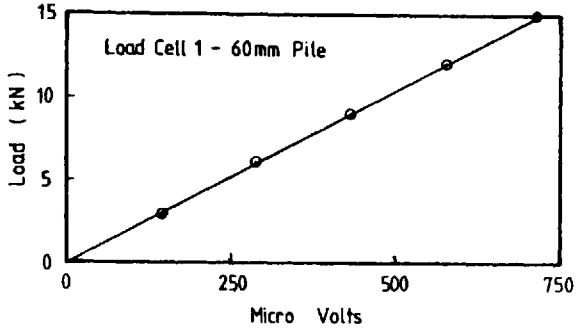

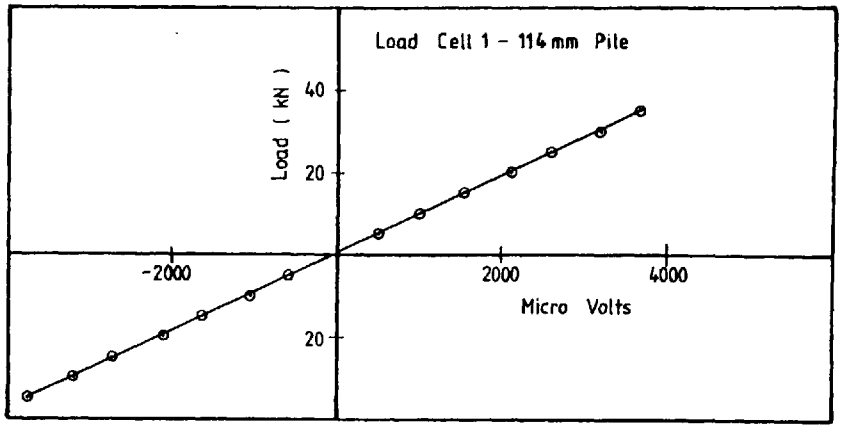

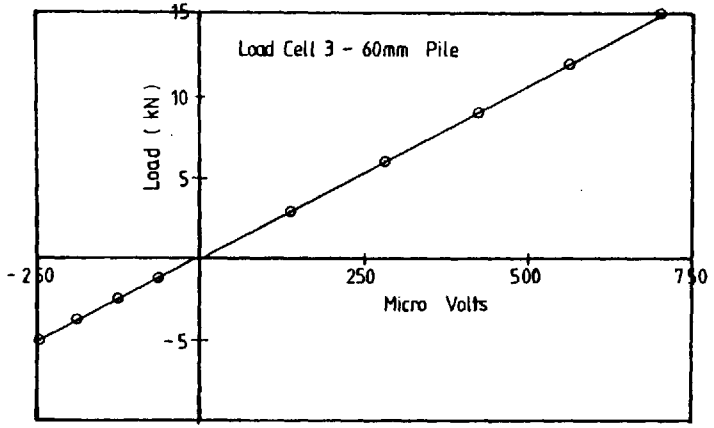

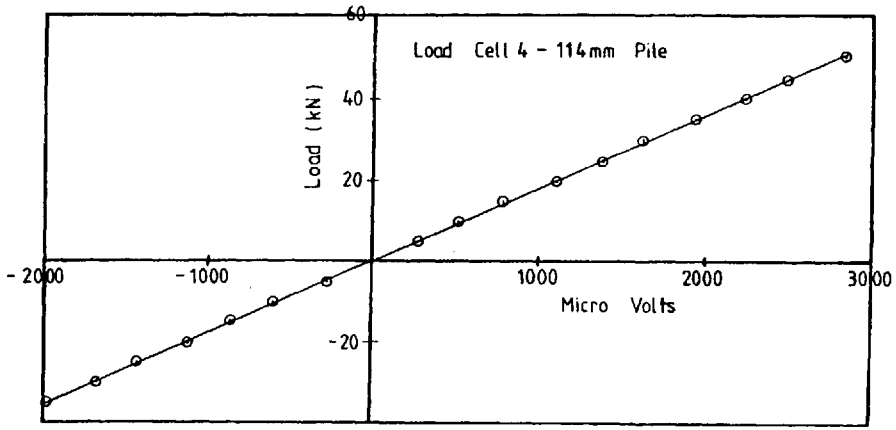

FIGURE N°5.1 TYPICAL CALIBRATION GRAPHS FOR THE STATIC AXIAL LOAD CELLS

KEY

A4I1 Fourth Inclinometer in the A Spiral on Vertical Level I1
B2D2 Second Density Sample in the B Spiral on Vertical Level D2
B1D3 Initial Density Sample " " " " " " " D3
DT Displacement Transducer Fixed to Datum Frame and Used to Monitor Suface Displacement
DTI " " " " " " " " " " Inclinometer "

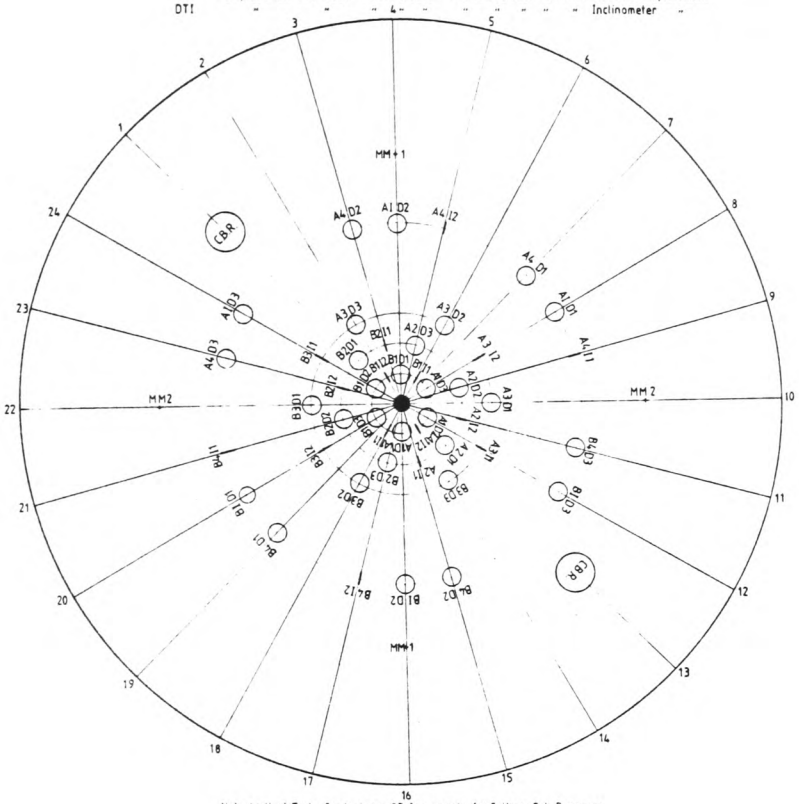

Note wall of Tank Graduated in 23 Increments for Setting Out Purposes

PLAN OF SAND TANK INDICATING POSITION OF INSTRUMENTATION ABOVE SAND/CLAY INTERFACE

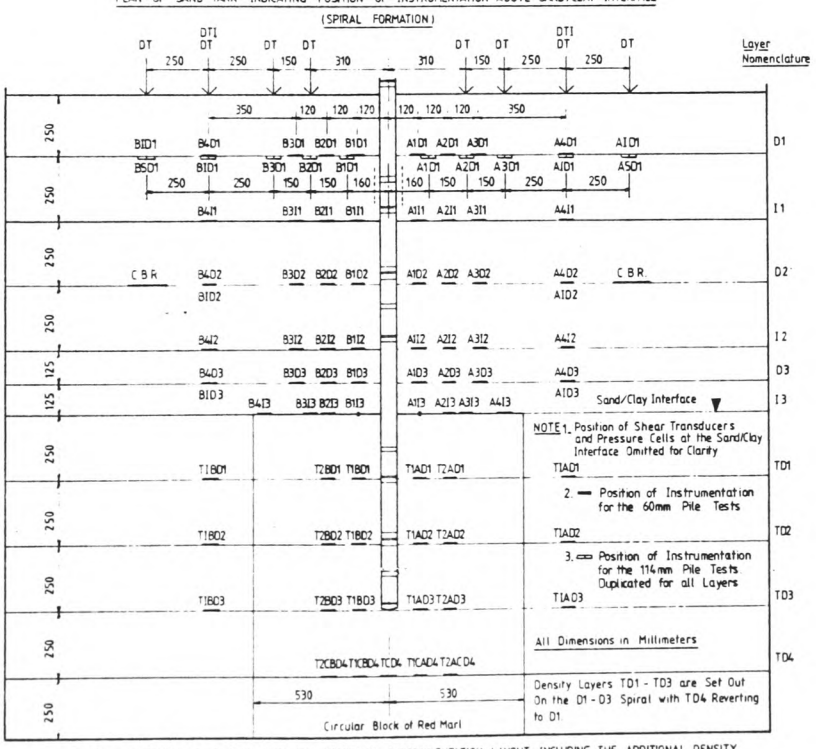

SECTION THROUGH SAND TANK SHOWING COMPLETE INSTRUMENTATION LAYOUT INCLUDING THE ADDITIONAL DENSITY LAYERS (TD1-TD4) USED IN THE SAND ONLY PROFILE TESTS

FIGURE N° 5.2 SHOWING GENERAL LAYOUT OF INSTRUMENTATION

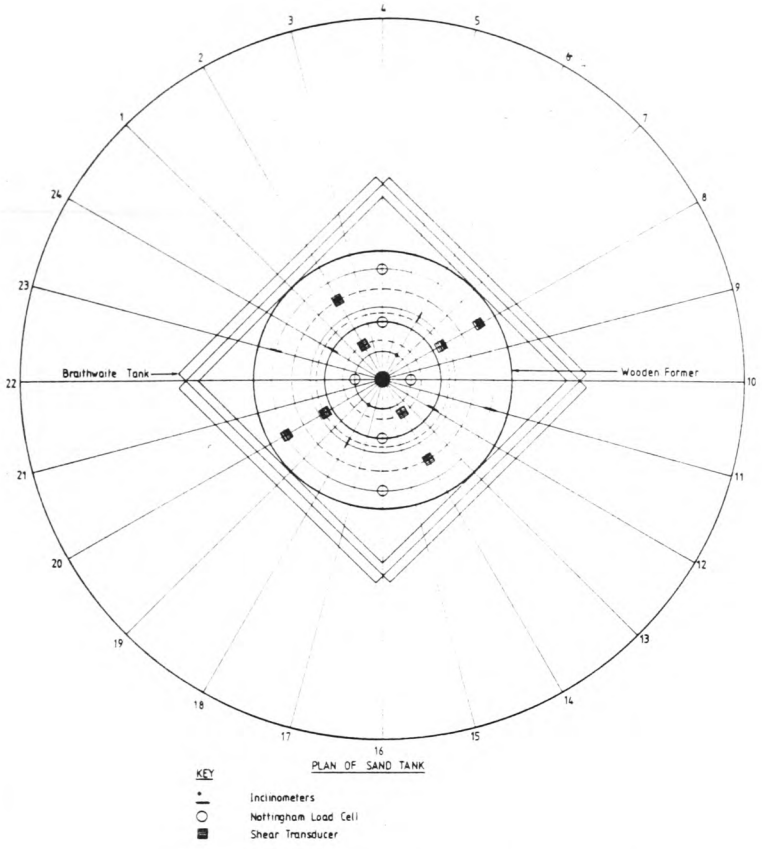

FIG 5.3 SHOWING THE INSTRUMENTATION LAYOUT AT THE SAND/CLAY INTERFACE

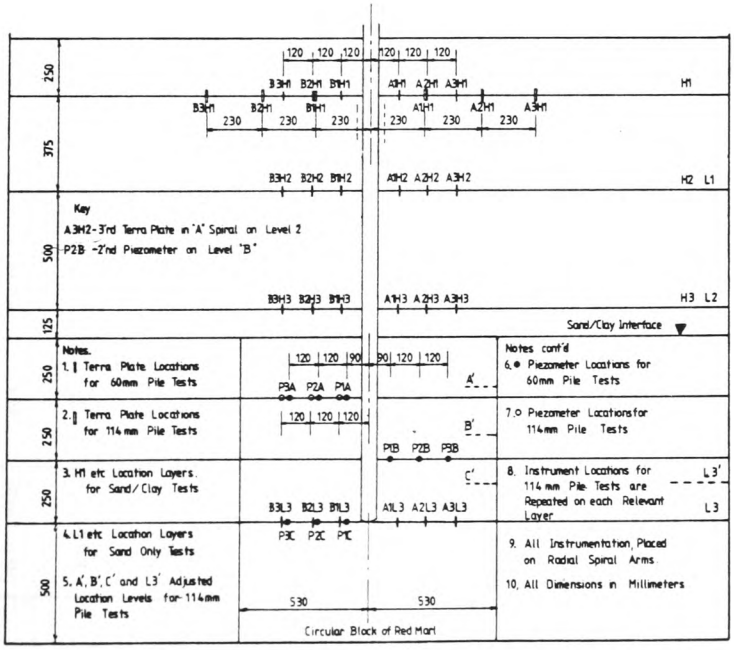

FIGURE Nº 5.4 SHOWING GENERAL LAYOUT OF ADDITIONAL INSTRUMENTATION

Load Schedule / Test N°	Pile Installation	C.R.P. Test	M.L. Test 1	Cyclic Load Test	P.W.P. Dissipation	M.L. Test 2	P.W.P. Dissipation	Cyclic Load Test	M.L. Test 3	P.W.P. Dissipation	C.R.U. Test
Test N° 1 (60DD -S)	Driven	√	√	–	–	–	–	–	–	–	√
Test N° 2 (60DD -S/C)	Driven	√	√	–	√	√	√	–	–	–	–
Test N° 3 (114DC -S)	Driven	√	√	√	–	√	–	–	–	–	√
Test N°4 (114IN -S)	Insitu	√	√	√	–	√	–	–	–	–	√
Test N°5 (114DC -S/C)	Driven	√	√	–	√	√	√	√	√	√	√
Test N°6 (114IE -S)	Insitu	√	√	√	–	√	–	–	–	–	√

Test N°1 (60DD -S) 60mm Pile Driven Dynamically into Sand

Test N°2 (60DD -S/C) ———— " ———— Sand Overlying Clay

Test N°3 (114DC -S) 114mm Pile Driven at a Constant Rate of Penetration into Sand

Test N°4 (114IN -S) 114mm Pile Placed "Insitu" with No End Bearing in Sand

Test N°5 (114DC -S/C) 114mm Pile Driven at a Constant Rate of Penetration into Sand Overlying Clay

Test N°6 (114IE -S) 114mm Pile Placed "Insitu" with End Bearing in Sand

C.R.P. - Constant Rate of Penetration Test

M.L. - Maintained Load Test

C.R.U. - Constant Rate of Uplift Test

P.W.P. - Pore Water Pressure Dissipation Period

FIGURE 5.5 TEST SCHEDULE

CHAPTER 6

PILE INSTALLATION AND LOAD TEST RESULTS

CHAPTER 6

INSTALLATION AND LOAD TEST RESULTS

6.1 Pile Installation and Load Tests

The stresses along the pile shaft are presented in the following sections. They were derived from the data obtained from the static axial core load cells of the 60mm and 114mm piles and the Boundary Orthogonal Stress Transducers located within the wall of the 114mm diameter pile. These results are presented separately with cross reference between them at relevant points in the analysis and discussions.

A direct comparison of results was made with the earlier work of Kay(1980), Lake(1986) and Werscheing(1987) for appropriate pile sizes and loading conditions as well as other comparable data reported in literature.

6.2 Pile Installation - Load Cell Results, Development of Total, Base and Shaft Resistance.

For the 114mm diameter pile the development of total pile load (Q_t), base resistance (Q_b) and shaft resistance (Q_s) with pile embedment is illustrated in Figures 6.1 and 6.2. These results were obtained from the data at the end of each 100mm jacking increment. As the 60mm diameter pile was dynamically driven only the residual values of Q_t , Q_b, and Q_s were obtained and these are not included here.

6.2.1 Homogeneous Sand Profile.

The development of total base load (Q_b) with pile embedment (D_b) is shown in Figure 6.1 It illustrates three phases in the development of the base load, which is also shown in terms of q_b the unit base resistance. During the initial phase of pile installation to a depth of 450mm (4.6B) there was a general non-linear increase in the base resistance. With further pile penetration the rate of increase in base resistance decreased. At a pile embedment depth of 1100mm the unit base resistance (q_b) reduced to a limiting value of 1250kPa. This value remained constant with further pile penetration. The pile embedment depth of 1100mm (9.65B) is considered to be the critical depth, D_c. Vesic (1963) reported that the initial development of q_b in a loose sand was linear to a depth of 4.0B for circular pre-placed piles. Thereafter q_b gradually reduced to a constant value for a D_b of approximately 10.0B for both preplaced and driven piles.

Meyerhof(1976) after De Beer(1971) presented the variation in D_c /B with Q_b. For $\emptyset'$=36 degrees D_c was equal to 11.0B.

Werscching(1987) reported that the limits of the three phases of development of q_b occured at 4.6B and 10.5B which corresponded to the critical depth D_c.

The development in q_b below D_c may suggest the possibility of a variation in sand density. The value of D_c coincides approximately with the depth at which the majority of the instrumentation had been placed within the sand. However the insitu sand density samples and the mini-Mackintosh probe results show that a fairly uniform density profile was established.

The total resistance against pile embedment (Q_t-D_b) profile was a reflection of the development in base resistance with the additional force due to shaft resistance. With pile embedment depths beyond the critical depth D_c, there was a marked divergence between the Q_t-D_b and the Q_b-D_b profiles due to the increase in shaft resistance and a reduction in the development of base resistance.

The development of the Q_s-D_b profile exhibited three phases although they were less distinctive than those shown in the development of Q_b and Q_t. The boundaries of the three phases in terms of pile penetration were 4.0B and 9.5B which are similar to those evaluated from the Q_b-D_b profile. The initial development in Q_s was non-linear but tended to a fairly linear relationship with D_b after a depth of 4.0B. At a pile penetration of D_b=10.0B a slight increase in the development of Q_s was observed. Thereafter a constant development in Q_s was maintained with further pile penetration. The average unit shaft friction (f_s) was evaluated from Q_s and is illustrated in Figure 6.2. During the initial part of pile installation corresponding to the first phase in the development of Q_b a scatter in f_s was observed. The range in magnitude of f_s was larger than that evaluated at steady state values for deeper pile penetration.

This local increase in f_s implies local high values of K_s which is in agreement with Lake(1986) and Werscher(1987). A fairly constant increase in f_s was observed for further pile penetrations below 4.0B. A marginal increase in its rate of development was observed at a depth of approximately 10.0B which was a reflection of the Q_s-D_b profile. This value was taken as the critical depth in the development of f_s although some sceptism exists since there was a

marginal increase in the value f_s beyond this point. The value of unit shaft friction towards the end of pile installation tended to 6.5kPa which compares closely to the value of 6.0kPa recorded by Wersching (1987).

Values of f_s reported by Kerisel(1964) and Vesic(1967) were 3.9kPa and 7.5kPa for driven and jacked piles in sand respectively.

The ratio of D_c(shaft) to D_c (base) was approximately unity which corresponds closely to the values for driven piles reported by Vesic(1967), Meyerhof(1976) and Wersching(1987).

6.2.2 Layered Soil Profile.

The development of Q_b and Q_t with pile installation for test 5 is shown in Figure 6.1. For a pile embedment depth of 650mm the development and magnitude of Q_b and Q_t were similar to those displayed during test 3. This indicated that the underlying clay did not adversely influence the development of Q_b for a pile penetration of 650mm (5.7B). However with further pile penetration there was a reduction in the rate of development of Q_b and hence Q_t. At a pile embedment depth of 1000mm, 250mm(2.2B) above the sand/clay interface a significant reduction in Q_b was observed. This correlated to a drop in the development of effective vertical stress at the sand/clay interface. It also indicated the influence of the weaker end bearing capacity of the underlying clay on the development of Q_b. A minimum value of 6.2kN for Q_b was reached when the pile base was 0.5B below the interface layer. With further pile penetration into the clay a constant limiting value of 6.7kN was attained.

Meyerhof and Sastry(1978b) state that the level to which piles can be

safely driven when a soft layer underlies the bearing stratum depends on the ratio of q_{1w}/q_{1s}, where q_{1w} and q_{1s} are the limiting unit point resistance in the weak and strong layers respectively. The critical distance between the pile tip and soil interface (h') in order to avoid punching failure increases with greater strength difference between the soil layers from a value of 1.5B for q_{1w}/q_{1s} = 0.67 to 6B when q_{1w}/q_{1s} = 0.02. The crtical distance (h') for test 5 appeared to be 250mm, i.e. 2.2B for a q_{1w}/q_{1s} of 0.56.

The critical depth D_c of the overlying bearing strata also appeared to have had a considerable influence on the development of q_b as suggested by Meyerhof and Valsangkar (1977) This is clearly indicated in the comparison between test 3 and test 5. The thickness of sand above the clay layer was not sufficient for full development of q_b below the critical depth without avoiding the influence of the weaker layer.

As the pile base penetrated through the sand/clay interface a significant increase in Q_t developed. This was accounted for by the greater cohesive properties of the clay which led to an appreciable increase in Q_s within the clay layer.

The development of Q_s with pile embedment within the sand was very similar to test 3. This was reflected in the average unit shaft friction (f_s) values where a limiting value of approximately 6kPa was reached within this region. In the region of the sand/clay interface there was a marginal increase in the f_s values, but not of the order of magnitude of f_z, the local unit shaft friction, indicated by the B.O.S.T. transducers, refer section 6.6.1.2

As the pile base entered the clay layer a significant increase in the development of Q_s was observed. The magnitude of f_s within the clay was calculated from Q_s, by assuming the value of Q_s within the overlying sand remained constant at the value recorded at a D_b value of 1250mm (sand/clay interface). This assumption was used by Meyerhof and Sastry(1978a) and Werscheing(1987). The development of f_s within the clay gradually increased with depth. At a pile penetration of approximately 1550mm an appreciable increase in f_s was observed. f_s tended towards a constant value of approximately 28kPa towards the end of pile installation. The depth of 1550mm, 2.6B below the sand/clay interface, approximated to the limit of the sand drag down zone (3.0B). This observation was also reported by Werscheing (1987).

6.2.3 Base Bearing Capacity Factors.

The variation in the base bearing capacity factors N_q and N_c for tests 3 and 5 are illustrated in Figure 6.3. For a pile penetration of 650mm (5.7B) the development in N_q was similar for both tests, where a peak N_q value occured at approximately 500mm into the sand. This corresponds to $0.45D_c$, a value which Werscheing (1987) observed from his results and data presented by Kerisel(1964). Kerisel(1961) also showed that N_q was not a unique function of $\emptyset'$ but was influenced by D_b/B.

With further penetration into the sand a deviation between the N_q values for test 3 and test 5 was observed. This is a reflection in the development of q_b for the respective tests and indicative of the development in Q_b. At a depth of 1250mm (the sand/clay interface) the N_q value for test 5 was approximately half of that developed during test 3. Towards the end of pile installation during test 3 a N_q value

of approximately 45 was recorded. This is comparable with a value of 50 recorded by Wersching(1987).

Wersching(1987) found that his values of N_q in a sand only profile compared favourably to values derived from a method suggested by Poulos and Davis (1980). This involved the use of an expression for q_b given by Berezantzev et al (1961)

$$q_{bf} = A_k \gamma B + B_k \alpha_t \gamma_d D_b$$

where:- q_{bf} = unit base resistance at failure

A_k and B_k = Bearing capacity factors dependant on $\emptyset'$

γ and γ_d = Unit weight of soil at base level and that forming the surcharge respectively.

B = Pile diameter

D_b = Foundation depth

A_k and B_k are evaluated by using a modified value of $\emptyset'$ given by Kishida (1967)

i.e. $\emptyset' = 1/2(\emptyset'+40)$

where $\emptyset'$ = modified value of angle of effective internal friction below pile base level

$\emptyset'$ = angle of effective internal friction prior to pile installation.

From back analysis a value of 7.5 was evaluated for N_c when the pile base was at an equivalent depth to the sand/clay interface. This indicated that the pile base to some extent was acting as a surface footing, which was influenced by the added overburden pressure of the sand. However if the cone of sand driven ahead of the pile was considered to be an extension of the pile, the value of N_c is equivalent to that given by Skempton (1951).

Towards the end of pile installation the value of N_c approximated to 9 conforming with the traditionally accepted N_c value for deep foundations in cohesive soils.

6.2.4 Shaft Bearing Capacity Factors.

The variation in shaft bearing capacity factors are illustrated in Figure 6.4.

$K_s \tan \delta'$ was evaluated through back analysis into the following equation,-

$$f_s = K_s \tan \delta'$$

This assumes a linear relationship between initial vertical effective stress and the effective radial stress prior to pile installation. The value of $\tan \delta'$ was considered to be constant at a value given by the results of the B.O.S.T. transducers, refer to section 6.6.1.3.

The resultant values of K_s illustrate that at shallow depth K_s was greater than K_p. As the pile base approached full embedment depth K_s tended to a value of 1. These results are in agreement with Wersching (1987).

The adhesion factor α varied from 0.42 near the surface of the clay to 0.55 at full pile embedment. The point at which α increased was indicative of the presence of the sand dragged down into the clay, which effectively reduced the adhesion to the pile shaft. This observation was similar to that reported by Wersching (1987).

6.3 Constant Rate of Penetration Tests.

During the constant rate of penetration tests the development of Q_t ,

Q_a, Q_b, and Q_s were evaluated. The results of the six tests are illustrated in Figure 6.5.

6.3.1 Homogeneous Sand Profile.

Generally for the four tests the attainment of Q_{sf} occured at penetrative depths which were less than that required to reach Q_{bf}. For test 1 Q_{sf} and Q_{bf} occured virtually simultaneously at a ω_t of 5.0mm. Once the shaft failure was reached, Q_s remained constant. A steady increase in Q_b was observed with the onset of Q_{sf}. These results are typical for the development of Q_s and Q_b.

The three different types of tests carried out on the 114mm diameter pile illustrate a variety of points. For the comparative tests 3, 4 and 6 Q_{sf} occured around a ω_t value of 3-4mm. Although the pile failure displacements were compatible along with the development pattern of Q_s, the magnitude of Q_s was considerably different. Q_s for tests 3 was approximatly twice that recorded for tests 4 and 6.

The base failure load Q_{bf} was reached around a ω_t value of 5-6mm. Thereafter a steady increase in Q_b was observed with increased ω_t values. The development of Q_b was more progressive during test 6 as compared to a more limiting value for test 3. At the end of the test, Q_b was equal to 12kN and 6kN for tests 3 and 6 respectively. This illustrates a considerable difference in the base resistance of a driven pile to that of a simulated bored or in-situ pile.

Vesic(1964) reported the variation of N_q and K_s for both driven and buried 100mm diameter piles. He stated that the bearing capacity factor N_q was in agreement with values given by Berezantzev (1961) for both driven and buried piles, provided that driven piles are

analysed by using an increased sand density equal to the mean density prior to and after pile driving. This infers that the point bearing capacity of a driven pile is higher than that of a bored pile of the same diameter due to the increase in sand density caused by pile driving.

Kishida(1967) suggests an effective increase in $\emptyset'$ for driven piles of,

$$\emptyset'_m = (\emptyset' + 40)/2$$

This value of $\emptyset'$ being advocated by Poulos and Davis (1980) in the determination of N_q for driven piles. For bored piles Poulos and Davis suggest a reduction in the initial $\emptyset'$ value by 3 degrees to allow for possible loosening effects due to installation. This resultant change in $\emptyset'$ alters the N_q value which ultimately affect the point bearing capacity.

Vesic(1964) reported that values of K_s varied according to sand density and method of installation. In a loose sand values of K_s were 2.5 and 1.6 for driven and buried piles respectively. These values increased with sand density. Hunter and Davisson(1969) also found that jetted piles had a 66% reduction in bearing capacity when compared to driven piles.

6.3.2 Layered Soil Profile.

The pile displacement ω_t which produced Q_{bf} and Q_{sf} for both tests 2 and 5 were similar to values given by their respective sand only tests. The significant difference between the two types of soil profiles was the expected variation in the ultimate values attained by Q_s and Q_b at the end of the test. The development of Q_b within the

clay was approximately half that developed during the sand only tests. The total shaft resistance encountered in the two layered soil system was generally twice that recorded in the sand only profile tests for driven piles.

6.4 Maintained Load Tests.

The load settlement results produced from the maintained load tasts are presented in Figures 6.6, 6.7, and 6.8. The ultimate load was taken as the load which produced increasing settlement without further additional load (C.P 2004:1972) This was upheld for most of the maintained load tests although an overcautious approach, to avoid excessive settlement, did prevail in some of the tests. However this deficiency was overcome by adopting the Terzaghi failure criteria where the failure load is that which causes a settlement of 10% of the pile diameter. If this failure load was not attained extrapolation of the load settlement curve allowed Q_S the ultimate capacity of the pile to be assessed with a reasonable degree of accuracy.

The initial maintained load tests included an incremental increase in load up to the working load (Q_{aw}), which was then released down to zero. This was followed by an incremental increase in load up to the failure load (Q_{amax}), whereby the load was decreased in increments to zero. For clarity the subsequent maintained load tests only includes the phase whereby the pile was loaded to failure.

6.4.1 Homogeneous Sand Profile (Driven Piles)

The load settlement curves for the driven piles are illustrated in

Figures 6.6a and 6.7a. From the load tests carried out after pile installation the failure loads were 4.85kN and 15.47kN for tests 1 and 3 respectively. These compare favourably with the results of Lake and Wersching.

The second maintained load test performed after the cyclic load test during test 3 produced a marginally greater failure load. This is discussed in more detail in the following sections.

6.4.2 Homogeneous Sand Profile (In-Situ Pile)

The results are illustrated in Figures 6.8a and b. During test 4 the 'slip/stick' phenomenon mentioned by Tan(1983) which was also evident in the work of Kay(1980), is clearly illustrated. That is for increments of applied load and relatively small successive increases in pile displacement is followed by a sudden increase in ω_t for a load increment. The load - displacement relationship then returns to its initial state until a further sudden increase in ω_t is observed. This process continues where the pile displacements become exaggerated towards pile failure. During both the maintained load tests carried out during this test, catastrophic failures occured, even with a very small increment of load. This rendered some of the results meaningless after load failure. The value of the failure load obtained from the second load test was assumed to be spurious. This is substantiated by the B.O.S.T. results, which did not signify that the cyclic load test had increased the shaft friction by any significant amount. The increased applied load may have been a result of the pile being misaligned by the cyclic load test. This would have caused additional frictional forces being set up at the base of the pile, which was evident in the load cell readings. Additional support

of this was reflected in the very small pile displacements observed during the test. An important feature in the first maintained load was that when the working load was released the displacement recovery was only marginal, although the total displacement values of ω_t were only small.

For test 6 the maintained load test carried out before and after the cyclic load test clearly indicated an improvement in bearing capacity for the latter test. The significant effects of this is discussed in section 6.5.

6.4.3 Sand/Clay Profile.

The load settlement relationship for test 2 and 5 are illustrated in Figures 6.6b and 6.7b. Both sets of results indicate an increased bearings capacity with time, and dissipation of pore water pressure. Increased Q_{sf} values of 9% and 10% were observed for test 2 and 5 over their respective dissipation periods. As a result of the second pore water pressure dissipation period and the cyclic load test the bearing capacity in test 5 had increased by approximately 25%. These results are discussed in section 6.5.

6.5 Stress Transfer Developed Along the Pile Shaft.

The distribution of load and shear stress developed during the maintained load tests are illustrated in Figures 6.9, 6.10 and 6.11. They were evaluated using the axial core load cells. The results for test 4 are not presented. This was due to the small variations in load transfer that developed and the detrimental effect of the build up in load at the toe of the pile. These effects made it virtually

impossible to define and separate the load distribution throughout the pile. However the B.O.S.T transducers which were independent of the load cells, produced a realistic stress distribution and are discussed later in section 6.6.

The average unit shaft friction (f_s) was derived from the load cell readings by taking the difference in the load registered at the top and bottom of a pile segment and dividing by the circumferential area of that segment. After strenuous attempts in "smoothing out" the load cell readings, their distribution was adjusted by using a linear "polyfit" method.

The fluctuation in the load cell readings, particularly in the 60mm pile, was such that this approach gave the best considered representation of stress transfer for the whole series of tests. Gregersen et al(1973) and Lake(1986) adopted the "smoothed" values of load distribution in calculating the skin friction along the pile shaft. Unfortunately the linear method does not give a truly accurate representation of the shear stress acting on the pile wall, and therefore may be viewed with some scepticism. However the derived average values of skin friction correspond reasonably well with the values of local unit shaft recorded by the B.O.S.T, refer to section 6.6.

6.5.1 Residual Loads.

The residual load distribution prior to the initial maintained load test are illustrated in Figures 6.9, 6.10 &6.11.To avoid confusion and for clarity the distributions for the subsequent load tests have been omitted but may be calculated from back analysis of the load

distribution curves derived from the applied loads.

6.5.1.1 Homogeneous Sand Profile.

The residual load distribution for test 1 shows a slightly negative value at the top of the pile base. Lake's(1986) results show a similar distribution. The negative value at the top of the pile was probably a result of the combined effect of differential elastic recovery within the soil and the limitation in accuracy of the load cells over low working loads. The higher positive value recorded at the pile base illustrates elastic recovery of the sand beneath the base after pile installation.

The residual load distribution for test 3 gave a linear distribution varying from zero load at the pile top to a positive value at the pile base. This gives a negative or reverse shear stress distribution along the pile shaft and reflects the variation in elastic soil recovery beneath and around the pile.

A similar distribution in the residual load was also evident in test 6 and was a result of the stresses set up by the C.R.P. test carried out prior to the maintained load test. The positive residual load at the base of the pile was small and within the accuracy of the load cells. However it is a reflection of the reduced bearing capacity of the insitu pile.

6.5.1.2 Sand/Clay Profile.

The residual load distribution for test 2 is similar in profile to results produced by Lake(1986). Negative loads were recorded within the sand which peaked 300mm above the sand/clay interface. The

residual load then increased to a positive value at the pile base. This effect may possibly be a result of differential soil recovery. This load pattern was not reflected in test 5 where the distribution was similar to test 3.

6.5.2 Applied Load and Average Unit Shaft Friction.

The applied load distribution throughout the pile is presented here in two forms i.e. with and without the inclusion of the residual load distribution.

6.5.2.1 Homogeneous Sand Profile.

Test 1 results are shown in Figure 6.9a. It illustrates that low applied loads are insufficient to overcome the residual load distribution. With the progressive increase in applied load the average shear stress tended to 4kPa. Without the inclusion of residual load this value was approximately 6kPa. This illustrates the importance of residual stresses set up within the pile during installation. The pile cannot therefore be considered as a stress free element. This point has been made by many authors, such as Hunter and Davisson (1969), Hanna and Tan (1973), Gregersen et al (1973) and Chan and Hanna (1979). Some sceptism is felt with regard to the distribution of the residual load in test 1; a point which Lake(1986) stresses during the analysis of similar test results in his work.

Test 3 results are illustrated in Figure 6.9a. They again emphasise the importance in the inclusion of residual loads. At the maximum failure load (Q_{amax}) the average unit shaft friction tended to values of 6kPa and 8kPa for the inclusion and exclusion of the residual

loads respectively. Cyclic loading had an apparently insignificant effect on the shaft friction. The subsequent maintained load test gave a similar failure load to the first test.

The initial residual loads in the pile for test 6 were small and were a consequence of sand placement and the C.R.P. test. The net result of this load distribution only had a marginal effect on the average shaft friction. The residual load within the pile after the cyclic load test decreased slightly. This effect has been reported in data by Gregerson et al (1973), and Chan and Hanna (1979). However the reduction was small and on the limits of accuracy of the load cells. The cyclic loading had a noticeable effect on the shaft friction by increasing the average value of f_s by approximately 1kPa, (15%). End bearing also increased by 13%.

From all the tests it was evident that shaft friction was mobilised along the full length of the pile at the onset of an applied load. The load cell at the base of the pile recorded positive readings for each increment of load. This illustrates the simultaneous development of end bearing with shaft friction. Similar findings have been reported by Lake(1986).

The linear approach to illustrate the distribution of load throughout the pile results in a vertical distribution of shear stress. This does not give any regional changes in f_s along the pile shaft as displayed by the B.O.S.T. which are discussed in section 6.6.

6.5.2.2 Sand/Clay Profile.

A comparison between tests 2 and 5 showed that within the sand layer at Q_{amax}, the average shaft friction (f_s) tended to a value of 8kPa

for all the maintained load tests. The location of the load cells in the 60mm pile led to some spurious results in the region of the sand/clay interface. Therefore only an approximate solution of the shaft friction could be deduced within this area.

A better representation of the shear stress distribution along the pile shaft in a two layered soil system is illustrated in Figure 6.10, deduced from the test 5 results. The variation is similar to the results produced by the B.O.S.T. illustrated in Figure 6.19.

An important point in the evaluation of f_s from load cell readings over a period of time is the assessment of zero drift and its effect on the evaluation of residual stress values. The maintained load test carried out after the cyclic load test illustrates this point. It gives erroneous values of f_s within the clay when the residual stresses are included. If the residual stress is excluded, which effectively eliminates the influence of drift, although more realistic shear stress values may be exhibited they do not necessarily represent the true state of stress within the pile.

6.6 Boundary Orthogonal Stress Transducer (B.O.S.T.).

6.6.1 Pile Installation.

Throughout pile installation the local unit shaft friction f_z, was taken as the mean value of each pair of B.O.S.T.s, distributed throughout the pile length. The radial stress, σ'_r within the sand is not presented in this section because it was directly related to f_z by $1/\tan \delta'$. This relationship was practically constant throughout pile installation.

6.6.1.1 Homogeneous Sand Profile.

Figure 6.12 illustrates that at each location along the pile shaft regardless of pile embedment, f_z tended to a unique function of D_b. Along this function the value of f_z for a given D_b was reasonably constant and increased at a reduced rate with greater pile embedment.

Extrapolation of the average function between f_z and D_b gave a peak value in f_z of 8kPa for a pile embedment depth of 2.5m. Wersching (1987) reported a peak value of 7.9kPa at a D_b value of 2.85m. Although these values are in agreement the maximum values of f_z recorded by the respective functions at full pile embedment were 6.4kPa and 7.70kPa, giving some 20% difference. This variation was probably a result of the difference in the initial ϕ' values recorded between the two sets of experiments, thus marginally altering the development of f_z with D_b.

Feda (1963,1976) reported that f_z is related to the effects of soil dilatancy on the pile shaft contact stresses. For a highly dilatant soil a depth of 2-4m was necessary before f_z would tend to a constant value. Conversely for a low dilatant soil f_z may be constant from ground level.

The development of f_z during each increment of driving was similar to the pattern shown during the C.R.P. test carried out on test 4. The observed initial peak in f_z was followed by a marginal reduction, and then increased with further pile embedment.

At the end of each jacking increment and at any depth (D_b) the residual or reversed skin friction f_z was in general 25% of the value

generated during pile installation.

6.6.1.2 Layered Soil Profile.

To a pile embedment depth of 1050mm the development and magnitude in f_z was similar to that shown in test 3 and is illustrated in Figure 6.12.

With further pile penetration and in a region of 200mm(2B) above the sand/clay interface there was a significant increase in f_z . Typical peak values of 12kPa were recorded at a pile embedment equivalent to the sand/clay interface which was twice that recorded at the same depth in Test 3.

Similar observations were reported by Wersching (1987). Meyerhof and Sastry (1978a&b) suggested that this local increase in f_z was caused by the wedging action of the soil trapped between the rigid pile shaft and the deformable soil interface.

For D_b value down to a depth of 650mm the variation in residual f_z was similar to that recorded during test 3. As the pile base approached the sand/clay interface it increased in value to approximately twice that recorded during the sand only tests. This was probably a result of the greater pile recovery caused by the underlying clay layer.

Once the pile base had penetrated below the sand/clay interface the rate of increase of f_z increased rapidly. At a depth of 250mm below the interface (which approximately coincided with the limits of the sand drawdown zone) the development in f_z subsided.

Towards the end of pile installation the value of f_z was 55kPa

approximately $1.0C_{ui}$. The transducers located further up the pile and within the clay displayed a similar development in f_z. The value of f_z recorded at z'=107mm was 22.5kPa($0.5C_{ui}$).

Towards the end of pile installation the residual values of f_z within the clay were positive. This indicated that the pile recovery within the clay was insufficient to induce reverse shear stress at the soil/pile interface. Werscheing (1987) expressed some doubt as to the validity of these results, and suggested that this may reflect the lack of stiffness of the B.O.S.T. relative to that of the clay. However with the passage of time and dissipation of pore water pressure within the clay, there was a reduction in the residual stress levels. This effectively reduced the δ' angle generated during the subsequent maintained load tests.

6.6.1.3 Friction Angle Between the Pile and the Soil.

A comprehensive study of the friction angle δ' (Tan f_z/σ_r') for steel piles in sand has been carried out by Werscheing (1987) which included the following summary

Reference	ϕ'	δ'
Coyle & Sulaiman(1967)	(28-36)32 degrees	25 degrees
Hunter & Davisson(1969)	(31-35)32 degrees	25 degrees
Holloway et al(1978)	(31-35)32 degrees	23-30 degrees
Werscheing(1987)	32 degrees	(23.2)&(24.3)degrees
Author(1989)	36 degrees	(25.7)&(26.7)degrees

The stresses acting on the pile shaft below the sand/clay interface were considered effective, which is substantiated by evidence in Chapter 7, sections 7.1 and 7.2. Butterfield & Johnston (1973) used contact stress transducers in 100mm piles jacked 3.3m into a

stratified profile of various clay types which contained small fissures at shallow depth. They concluded that σ_r' was an effective stress across the pile/clay interface.

During Test 5 the B.O.S.T. transducers located close to the pile base recorded a maximum σ_r' of 92.5kPa ($1.85C_{ui}$) and a δ' value of 31degrees at a D_b=1785mm. With further pile penetration there was a reduction in σ_r' but f_z stayed fairly constant. At full pile embedment δ' was approximately 37 degrees. σ_r' at the end of pile installation was approximately $1.5C_{ui}$. This is in agreement with Clark & Meyerhof(1972) who reported that σ_r' acting on the pile clay was $1.6C_{ui}$ which was based on field and laboratory results. During the maintained load test σ_r' did reduce to an average value of $1.3C_{ui}$

The greater δ' value recorded in the clay seemed to be a reflection on the high residual value of f_z. After a period of time this residual value subsided and the effective δ' deduced during the second maintained load test approximated to 26 degrees which was equivalent to $\emptyset'$ of the clay.

The value of f_z recorded in the upper section of the clay and within the sand drag down zone was approximately 22.5kPa. A proportional increase in σ_r' was observed which gave an average δ' value of 26 degrees. This reasonably corresponds to the δ' produced within the sand only profile.

6.6.1.4 Variation in the Local Coefficient of Earth Pressure with Depth and Pile Embedment.

From the unique function for the variation in f_z with D_b, σ_r' could be evaluated at any point along the pile shaft within the sand. The

vertical effective stress σ'_z; at any level adjacent to the pile shaft was assumed to be equal to the effective overburden pressure prior to pile installation and that tan δ' was constant at 0.481 (25.7 degrees)

Wersching (1987) found a linear relationship existed between the variation of K_z with depth for a given D_b /B when plotted on a logarithmic scale. This was true for the test 3 results which within the limits of the test produced a virtually identical relationship for K_z to that evaluated by Wersching, as defined by the following equation.

$$K_z = (B/z)(D_b/B)^{0.8} \quad \ldots\ldots \text{ equation 6.1}$$

This is presented in Figure 6.13 along with values of K_z deduced from actual σ'_r values during pile installation.

K_z was evaluated by integrating equation 6.1 between the limit of 1 and D_b/B and is given by the following equation.

$$K_s = \frac{(D_b/B)^{0.8} \log_e(D_b/B)}{(D_b/B) - 1} \quad \ldots\ldots\ldots\ldots 6.2$$

Using these relationships the depth Z_e at which the ratio of effective overburden stress to σ'_r was equal to K_s can be evaluated. This is defined by the following equation.

$$Z_e/B = \frac{(D_b/B) - 1}{\log_e(D_b/B)} \quad \ldots\ldots\ldots\ldots\ldots 6.3$$

These relationships are shown in Figure 6.14. It illustrates that for a D_b value of greater than 10, K_s tends to 1.73 and Z_e/B follows a near linear relationship.

Using these values Wersching (1987) suggested that Q_{sf} can be calculated using the following relationship:-

$$Q_{sf} = \pi B^2 D_b \gamma z_e K_s \tan \delta' \quad \ldots\ldots\ldots\ldots\ldots 6.4$$

and for D_b/B values greater than 10

$$Q_{sf} = \pi B^2 \gamma D_b K_e \tan \delta' \quad \ldots\ldots\ldots\ldots\ldots 6.5$$

where $K_e' = 0.425\ (6 + D_b/B)$

The variation in K_e' with D_b/B is also shown in Figure 6.14 along with values of K_e' produced by Werscching from data given by Vesic (1967).

6.6.2 Maintained Load Tests.

The reported results of f_z and σ_r' from the first series of maintained load tests were the actual values recorded by the B.O.S.T.s . Unfortunately, there was evidence of "drift" in the σ_r' readings. This was particularly prominent during test 5 where there was a significant interval of time between each maintained load test. It must be noted that although drift was present it was only prevalent in the normal stress plane and that the re-calibration constants evaluated after the last series of tests remained within the tolerable accuracy of the transducer. To compensate for this drift the δ' value had to be modified. From the results of test 3 it was clear that most of the f_z/σ_r' values evaluated during the second load test showed insignificant margins of drift. If there was any evidence of drift at this stage it was discarded and the average δ' evaluated from the considered true values. The resultant δ' value increased marginally due to the cyclic load test. Where applicable this δ' value was applied to any initially discarded values.For such cases the evaluted angle of δ' was drawn tangential to the f_z / σ_r' values, the intercept on the normal stress axis was the margin of drift.

6.2.2.1 Homogeneous Sand Profile

6.2.2.1.a Test 3, 114mm Diameter Pile Driven at a Constant Rate of Penetration.

Two maintained load tests were carried out during this test immediately after pile installation and post cyclic load test. The distribution of f_z and σ'_r during these tests are illustrated in Figure 6.15a and b. The following discussion on the variation in f_z was consistent with the results discussed by Wersching (1987) for load tests on driven piles in sand.

The post compressive residual stress f_z, was negative and fairly linear throughout the depth of the pile. Its value on average was -2kPa. The applied load Q_a which neutralised the residual stress over the upper two thirds of the pile was 3.00kN. (48% Q_{aw} & 19% Q_{amax}) A positive linear increase in f_z with depth to a maximum of 2kPa was exhibited over the lower third of the pile. At Q_{aw} there was a fairly linear increase in f_z which increased with depth. Values in f_z ranged from 1kPa near the surface to 4kPa close to pile base level.

On release of Q_{aw} back to zero, f_z returned to its original residual values. When increments of load were reapplied back up to Q_{aw}, f_z increased by typically 10% for an equivalent load on the first load cycle. This was associated with a reduction in the base load Q_b, a feature which was again apparent after the cyclic load test.

With further application of increments in applied load f_z increased linearily with depth. For Q_a above 12.57kN ($200Q_{aw}$) the distribution in f_z became progressively "D" shaped. The increase in f_z was less

near the sand surface and the pile base level. At Q_{amax} f_z over the lower 550mm(5B) of the pile had reduced significantly below the values obtained at 200%Q_{aw}, indicating failure along the shaft in this region. Also associated with these loads was the progressive relative increase in the pile displacement ω_t.

Touma and Reese (1974) suggested a mechanism which accounted for this reduction in f_z over the lower portion of the pile shaft. They considered that the soil below the base was compressed due to the action of high stresses, which was sufficient to cause arching around the pile base. Two distinct zones were considered to develop around and above the pile base due to displacement incompatibility between the sand above and below pile base level, namely flow and arching zones. A reduction in stress levels adjacent to the pile shaft occurred within the flow zone, whilst increased stress levels were produced with the arching zone which surrounded the flow zone. The size of the zone was influenced by the sand density and the amount of base settlement, with dense sand generating the worst condition.

The release of the applied load from Q_{amax} gave a significant reduction in f_z. At Q_{aw} (6.2kN) the distribution and magnitude of f_z was similar to that produced by $0.5Q_{aw}$ (3.0kN) on the upward cycle of loading. This gave a net reduction of f_z varying from 2-3kPa with the greater values being exhibited with depth. On complete release of Q_a the residual values of f_z resumed back to virtually the same initial values prior to the start of the maintained load test.

Only marginal changes in the magnitude of σ_r' were evident up to the applied working load. Thereafter a steady increase in their values was evident with each increment of load. At an applied load of 9.33kN

($1.5Q_{aw}$) the development of σ_r' was proportional to f_z. i.e. f_z / σ_r' = tan δ'. The recorded reduction in f_z around the lower section of the pile shaft due to the flow zone discussed earlier was accompanied by a reduction in σ_r'. These values were still proportional to each other and remained on the δ' line.

When the load was reduced from Q_{amax}, σ_r' reduced in value. At Q_{aw} the distribution and magnitude of σ_r' was equivalent to $1.5Q_{aw}$ (9.33kN) on the upward load cycle. Over the lower and upper section of the pile σ_r' had reduced to a considerable lower value. The reduced values around the base of the pile were probably a result of the loosening effect of the flow zone developed during loading. When Q_a was completely removed the σ_r' distribution over the upper section of the pile was similar to the pre-maintained load test values, however σ_r' around the pile base reduced to below the initial values.

The second maintained load test was carried out to study any effect of a continuous cyclic load, equivalent to Q_{aw}, had on the shaft and end bearing capacity of the pile. The general distribution of f_z and σ_r' along the pile shaft during this load test was very similar to the first test. There was however a marginal difference in the magnitude of these values.

The residual value of f_z after the cyclic load test increased marginal to an average -2.5kPa and was fairly constant at this value along the embedded length of the pile. For each increase in load the magnitude in the increase in f_z was marginally greater than that displayed in the earlier load test. There was also a corresponding increase in the σ_r' values. At Q_{amax}, which was the same for both tests the values of f_z had increased by 1kPa, when compared to those

given by maintained load test 1. Inspection of the load cell results revealed that although shaft friction had marginally increased there was a slight reduction in the base load cell of 0.4kN.

The increase in shear may be a direct result of the cyclic load, but it is most probably a result of increase in f_z due to a continued re-application of load. This phenomenon was consistently evident during all the maintained load tests.

6.6.2.1b. Test 4, 114mm Diameter Pile with No End Bearing.

The maintained load tests carried out during this test followed the same format as test 3.

Prior to any load tests the development of residual stress along the pile shaft was monitored during sand placement around the pile, see Figure 6.16. Because of the nature of the experiment the pile had to be suspended from the top during the sand filling operation. This effectively fully restrained any vertical movement of the pile. Therefore the relative sand displacements along the pile shaft were due to progressive compressive straining of the sand caused by the incremental increase in overburden pressure. This resulted in a build up in negative shear stress along the pile shaft, similar to that shown by Hanna & Tan(1973)

Around the base of the pile there was a drop in the build up of the radial stress which reflected in a reduction of f_z . The probable cause of this may have been the result of some effect of the shoulder of the frictionless cylinder locally restraining the development of f_z and σ'_r.

After completion of the sand placement the pile was released and a C.R.P. test carried out to determine the Q_{sf} value. The resultant post compressive residual stress was positive and is shown in Figure 6.17. The distribution of this stress was fairly linear varying from approximately 0.5kPa near the sand surface to 1.0kPa close to the pile base. This equated to within 2.5% of the pile self weight.

The first cycle of load up to Q_{aw} is not shown in Figure 6.17. Its effects were similar to that described in test 3 and were emitted for clarity.

For loads up to Q_{aw} there was a fairly linear increase in f_z along the length of the pile shaft. There was evidence at this stage of some development of base load recorded in the base load cell.

With further increase in the applied load f_z along the middle third of pile shaft increased at a marginally greater rate. This corresponded to the zone in the sand where a number of instruments were installed in the sand. This may have caused a slight variation in the density of the sand, although this effect was not particularly evident during the second load test. It may also have been a product of an anomaly of the arching mechanism set up during loading.

As the load approached Q_{amax} there was a slight drop in the development of f_z near the top of the pile, similar in effect to test 3. However around the base of the pile the development of f_z and σ'_r was still progressive and increased at a similar rate to f_z along the lower regions of the pile shaft. This justifies the theory postulated by Touma & Reese (1974) that in the absence of end bearing the flow region could not develop through any incompatible soil displacement

and reduce the local values of f_z and σ'_r.

It was expected that the confining effects of the sand at pile base level would have locally increased f_z and σ'_r similar to the results at the sand/clay interface.

It must be noted that at this stage of the test the lowest B.O.S.T. transducer was approximately 1.75B from the effective pile base level and may have been outside the region of local effect around the base.

Clements and Brumund (1975) carried out large scale model tests on drilled piers in sand, the end of which passed through a rigid steel plate. They observed an increase in f_z around the lower portion of the pier, to a height of 1.0B above base level. This was attributed to the confining effects of the plate, which increased the horizontal pressure on the pier and resulted in an increase in side friction.

A sudden complete pile failure occured when applying an increment of load above 1.87kN which was taken as Q_{amax}. At this point the applied load was released to avoid any damage to the test rig and therefore no unloading cycle of results were obtained. The residual value after the release of Q_{amax} returned to approximately their initial post compressive values.

For an applied load equivalent to Q_{aw} there was only a marginal but significant change in the distribution of σ'_r along the pile shaft. Over the upper half of the pile there was a reduction in σ'_r from the initial post compressive residual value. Over the lower portion of the shaft σ'_r increased by on average 0.5kPa. On closer inspection of the variation in f_z at the point at which σ'_r reduced in value (z=800mm(7B)) f_z varied by typically 0.5kPa over the two halves of

the pile. In the theory proposed by Wersching (1987) for the development of these stresses, this variation in the f_z- σ'_r relation is possible.

With further application of Qa there was a progressive increase in σ'_r.At an applied load of 1.29kN, $1.75Q_{aw}$, the development in σ'_r was proportional to f_z where f_z/σ'_r equalled tan δ'. As the pile approached Q_{amax} there was a reduction in the development of σ'_r near the pile top and as stated earlier there was still a progressive increase in σ'_r near the pile base.

During the second maintained load test the development in f_z was reasonably linear and did not display any local increases in shaft friction shown in the earlier test. However around the pile base level there were signs of a local increase in shaft resistance. During this test the B.O.S.T. transducers were within 1.3B of the effective pile base. At Q_{amax} f_z varied from 1.5kPa to 5.3kPa near the pile top and base respectively. For an increase in applied load over 2.55kN sudden pile failure occured. The total load was again released back to zero. The variation in distribution of σ'_r was similar to that displayed in the first maintained load test and was proportional to f_z for applied loads in excess of 1.81kN.

As stated earlier the values of Q_a during this second load test must be treated with some sceptism due to the development of load at the pile base. However although the distribution of f_z was marginally different between the load tests, the magnitude of Q_{sf} derived from the average f_z values were virtually identical and were approximately equal to 2.1kN.

6.6.2.1.c Test 6, 114mm Diameter Pile In-Situ With End Bearing.

During the sand placement around the pile the development in the residual stresses were monitored along the pile shaft. In this case the pile was "free standing" on the underlying sand. This permitted the pile to settle as the sand compressed underneath the pile base. Unfortunately the dial gauge monitoring the settlement was dislodged during the initial stages of sand placement and therefore the total pile displacements are not presented here. However the build up in f_z and σ'_r along the pile shaft are illustrated in Figure 6.16b.

The progressive variation in the build up of f_z supports the findings of Hanna & Tan (1973). They conducted a similar exercise during sand displacement around 25.4mm diameter piles. The shape of the residual stress distribution was due to the relative displacements between the pile and sand. When the pile displaced a greater amount than the sand a positive shear stress is formed. If the sand moved down relative to the pile a negative shear stress is formed.

Hanna & Tan(1973) state that as a pile is embedded in sand the relative displacements between the sand and pile creates a system of these negative and positive shear stresses along the embedded length of the pile and a compressive load at the toe of the pile. A neutral point occurs when there is no relative displacement between the pile and sand and is signified by an absolute change in the gradient of the shear stress profile. Below the neutral point the sand being confined by the overburden pressure will compress very slightly but the pile being loaded by the force generated above the neutral point will be pushed into the sand thus mobilising positive shear stresses. Above the neutral point negative shear stresses develop. On

completion of sand placement and at any intermediate stage the pile was in equilibrium under the internal force system. This describes the distribution of f_z along the pile shaft during pile embedment of this test. At full pile embedment the depth of the neutral point was 10.5B below ground level. From data presented by Hanna and Tan(1973) for an equivalent L/B ratio the depth of the neutral axis was 9.7B.

There was a progressive increase in σ_r' throughout sand placement. At full pile embedment K_z tended to the neutral point. Below the neutral point K_z was approximately equal to 0.75.

A constant rate of penetration test was carried out to determine Q_{aw}. The post compressive residual values of f_z and σ_r' are show in Figure 6.18.

The residual values of f_z have remained negative but their magnitude was considerably reduced. Allowing for irregularities the distribution was fairly linear and is synonimous to trends shown in the test 3 results. A load of $0.5Q_{aw}$ approximately neutralised the residual f_z value to zero along the pile shaft.

Further increase in applied load gave an increase in f_z which gradually became more "D" shaped. As stated previously this was due to a reduction in the rate of increase in f_z over the upper and lower portion of the pile shaft. The reduction in f_z over the lower part follows the mechanism described by Touma & Reese (1974). As the applied load approached Q_{amax} there was a marginal reduction in the development of f_z along the whole length of the pile. This suggests that the pile was in a state of plunging failure which was only restrained by end bearing resistance. When Q_{amax} was released the

values of fz were again less than those produced on the upward load cycle for an equivalent applied load. At Q_a =zero the residual f_z approximated to the initial post compressive stress values.

For an applied load of Q_{aw} there was only a small increase in σ'_r along the length of the pile. At Q_a=4.6kN, $1.5Q_{aw}$ the development in σ'_r became proportional to f_z, i.e. $f_z/\sigma'_r=\tan \delta'$. As stated for test 3 the reduction in f_z over the lower section of the pile for increased pile loads also lead to a reduction in σ'_r over this region, but the values remained proportional to each other.

The cyclic load applied to the pile had the effect of increasing the pile bearing capacity by 15%. This is shown in the shaft friction and end bearing results. The increased end bearing was probably due to compaction of the sand below the pile base caused by the cyclic action of Q_{aw}. The development and distribution of f_z and σ'_r were very similar to the first load test but displayed a progressive increase in value with greater applied load. As stated earlier this trend in f_z is more probably related to the re-application of load, than a function of the cyclic load.

From tests 3 and 4 it was apparent that the cyclic load did not significantly increase the skin friction of the pile. Although the δ' angle during test 3 increased slightly which may have possibly been a result of the adjustments, allowing for drift in the σ'_r value. It could be reasonably assumed that comparable values in f_z would be obtained from tests 4 and 6. In fact ignoring end effects the skin friction developed during test 6 was approximately 100% greater than test 4. It would seem apparent that the restraining effect of end bearing significantly helps the development of the arching mechanism

set up around the pile shaft.

This is related to ω_t the pile displacement. The second load test during test 6 gave a smaller pile displacement per unit applied load when approaching Q_{amax} than test 1. This maintained the development of arching mechanism around the pile. Once end bearing failure occured the development in the arching stresses collapsed and punching failure occured.

6.2.2.2 Layered Soil Profile.

The action of applying the initial load cycle upto Q_{aw} increased the f_z values by typically 0.2kPa,(10%) which was also evident during test 3. This load cycle was recorded for the first maintained, but for subsequent load tests it has been omitted for clarity.

The post compressive residual f_z within the sand was marginally greater than test 3 which was due to a slightly greater elastic recovery generated by the soil profile. The residual f_z close to the interface was greater than that within the body of the sand. This was a result of the increased stresses generated in the area of the sand/clay interface.

The application of increments in load gave a similar progressive increase in f_z along the pile shaft within the sand to that displayed during test 3. There was a local increase in f_z near to the sand/clay as displayed during the pile installation. At Q_{amax} the value of f_z within the sand was less than that recorded at Q_{amax} in test 3, Q_{amax} for test 3 was 8% greater. Interpolation of the results at the sand/clay interface gave a local increase in f_z to 15kPa. Unloading the pile to Q_{aw} resulted in a reduction in f_z along the upper section

of the pile shaft which was greater than that recorded during test 3. This was a result of greater elastic recovery of the pile base within the clay. Local to the sand/clay interface the value of f_z was greater than that given in test 3. This was a result of the local increase in the stress level and a lower relative displacement between the pile shaft and the adjacent sand due to the elastic recovery of the clay surface during unloading. The residual f_z values returned to their post compressive state on complete removal of Q_a . The development of σ'_r within the sand was comparable to that displayed during test 3.

Within the clay layer there was a significant variation in the distribution of the post compressive residual f_z. Below the sand/clay interface and within the sand drag down zone the value was similar to that displayed just above the interface layer. In the body of clay there was a high positive residual value of f_z,this was equivalent to an average value of $0.3C_{ui}$. The relative elastic recovery between the pile and soil was insufficient to overcome the high value of skin friction generated due to pile installation.

As the pile was loaded there was a progressive increase in f_z.At Q_{amax} f_z varied from $0.55C_{ui}$ within the sand drag down zone, to $1.0C_{ui}$ near the pile base. The applied load was released in increments down to Q_{aw}. The values of f_z varied from $0.3C_{ui}$ to $0.77C_{ui}$ near the sand/clay interface and pile base respectively. These values were greater than those recorded on the upward load cycle. On complete removal of Q_a, f_z returned to the initial residual distribution.

The post compressive residual variation in σ'_r varied from $0.80C_{ui}$ to $0.92C_{ui}$ close to the sand/clay interface and pile base respectively.

There was a small progressive increase in σ_r' with the application of Q_a and at Q_{amax} it was typically $1.2C_{ui}$. This gives a $\Delta\sigma_r'/\Delta f_z$ ratio of 42.5% as compared to a typical value of 135% produced during test 3 at the equivalent depth. Wersching (1987) gave respective values of 35.6% and 125% for comparable tests. Other authors such as Reese and Seed(1955) and Esrig and Kirby(1979) reported that loading had little permanent effect on σ_r'. From a finite element study carried out by the latter authors, they deduced that the total normal stress acting on a pile shaft during loading was generally less than $0.1f_z$.

On completion of the first load test the experiment was left for a period of 5.75 days to allow for the dissipation of the pore water pressure. After this period a second load test was performed to evaluate any increase in bearing capacity.

Over the dissipation period there was settlement within the soil profile as a result of consolidation effects in the clay layer. This resulted in marginally increasing the negative residual f_z within the sand. The residual f_z values in the clay were significantly reduced by approximately $0.3C_{ui}$, see Figure 6.20.

On application of Q_a the distribution of f_z along the pile in the sand layer was similar to that displayed by earlier maintained load tests. At Q_{amax} which was 12% greater to that recorded during the earlier load test, there was on average a 20% increase in f_z along the pile/sand interface. The distribution in σ_r' was again similar with a proportional increase in magnitude corresponding to $f_z/\sigma_r' = \tan\delta'$

The drop in the residual stress at the pile/clay interface

effectively translated the development in f_z with applied load by $0.5C_{ui}$. Although the change in shear stress Δfz at Q_{amax} was $0.7C_{ui}$, which was similar to the first load test.

There was a marginal change in the distribution of σ_r' within the clay, particularly near the sand/clay interface. The build up in σ_r' with the application of load was variable. Close to the pile base and sand/clay interface there was an increase in σ_r' equivalent to an average value of $0.33C_{ui}$, at Q_{amax}. This was similar to the initial load test. At a depth of 350mm into the clay the change in σ_r' was $0.65C_{ui}$.

The distribution and magnitude of f_z and σ_r' produced from the maintained load after cyclic loading are illustrated in Figure 6.21.

There was an increase in f_z within the sand layer of a further 12% at Q_{amax} which is a characteristic of the re-application of Q_a. A corresponding increase in σ_r' was also evident.

Within the clay layer there was a significant increase in the magnitude of f_z and σ_r' to a depth of 350mm in the clay, which corresponded to the depth of the sand drag down zone. At the end of the experiment the undrained cohesive strength of the clay within this area had increased by 50%.

6.6.3 The Mobilization of Load Unit Shaft friction, Radial Stress and Friction Angle With Pile Displacement.

6.6.3.1 Homogeneous Sand Profile.

The mobilization of f_z, σ_r', and with ω_t for tests 3, 4 and 6 are presented in Figures 6.22 to 6.27. Data is presented from alternate

sets of B.O.S.T.s and represents the application of Q_a from zero to Q_{amax} for each respective maintained load test.

Test 3 results are shown in Figures 6.22a & b. For both tests all the residual f_z values finally neutralised at an applied load of $0.5Q_{aw}$. The development of σ_r' up to $0.5Q_{aw}$ stayed at a fairly constant value. f_z then developed at a linear rate up to an applied load of $2.0Q_{aw}$. The second load test results showed a slightly greater rate of increase in f_z/ω_t and generally the values of f_z were greater along the length of the pile.

After the f_z values were neutralised σ_r' gradually increased in magnitude. At an applied load of $1.5Q_{aw}$ it became proportional to f_z by Tan δ'.

For an applied load of $2.0Q_{aw}$ there was a peak in the development of f_z, this approximated to a pile displacement of 2.5mm and correlated to a value of 2.2mm given by Wersching (1987). Prior to reaching this applied load there was a noticeable drop in the development of f_z along the lower section of the pile. This occurred at an applied load of $1.5Q_{aw}$ and an average pile displacement of 1.5mm for the two load tests. The mobilization in tan δ' is effectively described by the development in f_z and σ_r'. These values became proportional to tanδ at $1.5Q_{aw}$ for both tests. Average maximum values of δ' were 26.75 degrees and 27.24 degrees at ω_t = 1.35mm and 1.65mm for maintained load tests 1 and 2 respectively.

This corresponds to a value of 24.3 degrees at a pile displacement of 1.20mm obtained by Wersching (1987). The difference in the values of δ may be attributed to the variation in ϕ' values which resulted from

a slightly higher average placement density. Wersching (1987) used a ϕ' value of 32 degrees this compares to a ϕ' on average of 36 degrees.

From the theoretical stress path produced by Wersching it can be shown that $\delta' = 0.74\phi'$. This would give a theoretical δ' equal to 23.68 degrees and 26.64 degrees for Wersching's and the author's results respectively. The theoretical value will change marginally with variations in poissons ratio, ν, for varying sand densities.

Test 6 results are presented in Figure 6.23a & b. The distribution of f_z and σ_r' and δ' given for the two maintained load tests were again similar, with the marginally greater values of f_z and σ_r' being displayed during the second maintained load test. The development of f_z was more curvi-linear during this test and reached a maximum value at pile displacements of 3.66mm and 3.00mm at applied loads of 7.68kN and 7.96kN for load tests 1 and 2 respectively. A comparison between tests 3 and 6 reveals that the rate of development per unit pile displacement was approximately 50% less during test 6. Vesic (1967) suggests that the development of f_z is a function of the confining pressure around the pile and therefore is governed by the method of installation.

Another noteable difference between the tests was the development of f_z around the pile base. It would seem the flow and arching mechanism discused by Touma & Reese 1974 reduces the development in f_z . The lack of initial confining pressure around the base has allowed the flow zone to develop which in turn has reduced the relative pile/soil displacement and reduced the development in f_z. The angle measured

within this area never attained the value of 26.5 degrees due to this mechanism and tended to a value of approximately 12 degrees.

Along the pile shaft tan δ' remained approximately the same for both tests. Vesic(1967) suggests that the action of pile driving loosens the sand in the immediate vicinity of the pile and approximately restoring the density of the sand to its insitu condition, although the sand outside this zone is and remained densified. This action increases the lateral pressure on the pile which increases the development of f_z. For a buried pile the $\emptyset'$ value remains the same around the pile but lacks the additional lateral pressure caused by driving and hence the development of skin friction is significantly reduced.

Test 4 results are illustrated in Figure 6.24 and show an initial rapid increase in f_z for a pile displacement ω_t of approximately 0.2mm and an applied load of $1.75Q_{aw}$. This was true for both the maintained load tests although as stated earlier the magnitude of the applied load readings from the second load tests are regarded as spurious with respect to the values of f_z. The development in f_z reduced with further applied load, but the distribution along the pile shaft remained fairly linear. With this reduction in the development in f_z there was a relatively large increase in ω_t. At pile displacements of 1.92mm and 2.34mm for maintained load tests 1 and 2 respectively there was a sudden complete pile failure. These values of ω_t are similar to those given for tests 3 and 6 for peak development in f_z, although the magnitude of f_z varies considerably.

It could reasonably be expected that the magnitude of f_z produced during tests 4 and 6 would be the same. However this is not the case.

For a depth of approximately 5B the values of f_z were similar, for greater depths there was a significant difference in the development of f_z. This suggests a link between the development of f_z and the continual progressive mobilization of arching stresses due to the restraining development on ω_t by the base resistance.

The magnitude of σ_r' was again a reflection in the f_z values. At a pile displacement of 0.2mm σ_r' became proportional to f_z obeying the $f_z/\sigma_r' = \tan \delta'$ relationship, where δ' was on average 26.22 and 26.75 degrees for maintained load tests 1 and 2 respectively.

6.6.3.2 Layered Soil Profiles.

The mobilisation of f_z, σ_r' and δ' for the three load tests carried out during test 5 are presented in Figures 6.25 to 6.27. For each load test the development of the stresses have been separated for the two soil types. There was a lower relative pile/sand displacement per unit applied load. Within the sand there was a fairly linear rate of development in f_z. This rate generally increased with depth and was marginally less than that produced during test 3. A decrease in the development of f_z was observed at an average ω_t value of 2.5mm. During each load test it reached a peak of approximately 3.5mm.

As the load tests were systematically carried out the peak values in f_z along the pile shaft in sand progressively increased, along with the relative load per unit pile displacement.

The associated development in σ_r' values was similar to the sand only test. The angle δ' within the sand was similar to that reported for test 3.

Within the sand layer the rate of mobilisation of f_z per unit pile displacement was similar throughout the depth of clay. The initial residual distributon of f_z affected the ultimate values attained. This is reflected throughout the three maintained load tests.

At a depth of 110mm into the clay the pile was still in continuous contact with sand. The rate of development of f_z at this location was greatly increased due to a higher confining pressure within the clay.

The associated development in σ_r' was similar to the sand only test. This gave a resultant δ' angle of 26.75 degrees.

The initial mobilisation of f_z within the clay was linear to a pile displacement of 2.0mm. Thereafter it reduced to a constant rate.

The magnitude of the development in σ_r' was less significant in the clay although peak values were generally achieved with those attained by f_z.

Over the period of the three load tests there was as earlier stated a significant change in the δ' value within the clay layer. It varied from an initial value of 42 degrees to 26 degrees after the high positive initial residual stresses had reduced. This angle of 26 degrees was equivalent to ϕ' of the red marl.

6.6.4 Constant Rate of Uplift Test.

6.6.4.1 Homogeneous Sand Profile.

6.6.4.1a Test 1 (60DD-S)

The constant rate of uplift results are illustrated in Figures 6.28. The maximum pull out load of -0.75kN was attained at a pile

displacement of 6.52mm (0.1B). A tensile load of approximately 0.11kN was recorded at pile base level. This suggests that the base load cell had drifted beyond the initial zero datum taken at the beginning of the test.

The values of Q_{sf} and ω_t compare favourably with respective average values of 0.72kN and 6mm reported by Lake(1986).

6.6.4.1b Test 3 (114DC-S)

Test 3 results are illustrated in Figure 6.28 and 6.29a. The initial residual value of f_z along the pile shaft was fairly constant at an average value of -2kPa. On application of the pullout load there was a rapid negative increase in f_z along the full length of the pile. This tended to a constant average value of -4.0kPa.

During the early phase of the pull out test the B.O.S.T.s located near the base of the pile displayed a large change in f_z which was accompanied by a significant increase in σ'_r. This cannot be readily explained; however, towards the end of the test there was a sharp reduction in both values which can be explained with sand flow into the void formed beneath the base of the pile by the extraction process.

A maximum pull out load of -2.86kN was attained at a pile displacement of -6.22mm. This compares favourably to values of -2.68kN and -6.58mm produced by Werscheing(1987).

The distribution of f_z varied significantly to that reported by Werscheing(1987). His f_z values varied from -2.2kPa near the pile top to -6kPa near the pile base. The distribution can be explained to be

due to a build up of flow and arching zones around pile base level, similar to the effect suggested by Touma & Reese (1974) as discussed earlier. In comparing these results it is important to note the initial variation and difference in the residual stress conditions.

The variation ane distribution in σ_r' was again a reflection in the build up of f_z. Because Q_{sf} was quickly achieved, σ_r' only fluctuated marginally from the associated Q_{sf} value. This early development in Q_{sf} gave $f_z / \sigma_r' = -\tan \delta'$.

6.6.4.1c. Test 4 (114IN-S)

The post maintained load test residual stress distribution of f_z was positive and varied linearly from 0.5kPa to 2.0kPa from top to bottom of the pile as shown in Figure 6.30a. This distribution had a significant bearing on the resultant f_z and σ_r' values. As with test 3 there was a virtual instantaneous development from $Qa = 0$ to Q_{sf}. The resultant distribution in f_z was again linear and varied from -0.5kPa to 1.5kPa.

The greater development in f_z along the lower pile section can be explained by refering to the vertical displacements. Compressive straining developed within this region which would reflect in a greater relative movement between the pile and sand and hence a greater development in f_z.

There was no evidence of any arching stress development from the σ_r' results. σ_r' reduced in value over the lower section of the pile. This is a direct reflection on the initial distribution of f_z and σ_r' as stated earlier. By inspection of the f_z results, the values generated by Q_{sf} can be reasonably said to be generally a diminished mirrored

reflection about the zero vertical axis of the residual f_z distribution. The resultant f_z/σ_r' relationship was proportional to -tan δ'. To maintain this relationship there had to be a reduction in the values of σ_r'.

6.6.4.1d. Test 6 (114IE-S).

The pre-tensile residual distribution of f_z which varied linearly from -0.75kPa near the top of the pile to -0.1kPa close to the pile base as illustrated in Figure 6.30b. With the application of the tensile load Q_{sf} was again quickly achieved. The maximum value of Q_{sf} was 1.60kN for a ω_t value of 5.38mm, refer to Figure 6.28 This compares to values obtained during test 4 of 1.65kN and 6.09mm. As the applied load approached Q_{sf} there was a general increase of -1kPa in negative shear stress values. At a depth of 85mm there was however a drop in f_z below the residual value. This was a probable result of extensive straining being developed within the sand during this period of the test.

With increased pile displacement there was a progressive reduction in the applied load, Q_a . For a ω_t value of 3.26mm there was evidence in the development of a sand flow region into the void formed beneath the pile base. This reduced the local f_z and σ_r' values within this region.

Due to this sand flow region there was evidence of the development of an arching mechanism around the pile base. This may be associated with the flow and arching zone concept set up during compressive loading as suggested by Touma & Reese (1974). The development of σ_r' was again directly related to f_z and was proportionally by -tan δ'.

6.6.4.2 Layered Soil Profile.

6.6.4.2a Test 5 (114DC-S/C).

The compressive residual f_z within the sand layer was linear in form and had an average value of -2kPa throughout the layer, refer to Figure 6.29b. The residual f_z profile within the clay varied from a 30kPa at mid pile embedment to -6kPa close to pile base level. Such a variable residual stress profile cannot be readily explained but at this stage in the experiment there was a significant change in the properties of the clay.

On application of the uplift load there was a fairly insignificant change in the f_z values down to a depth of 650mm (5.7B) in the sand. As stated earlier in previous tests the residual stress levels had mobilised f_z and σ_r' close to maximum tensile levels. For greater depth down to the sand/clay interface there was a progressive increase in f_z and σ_r'. These values at Q_{sf} were similar in magnitude but opposite in sign to those developed during the compressive test.

This localised increase in f_z was a result of upward displacement at the sand/clay interface which increased the stress levels in the sand.

Q_{sf} was attained at a displacement of -12.44mm and the relationship of f_z/σ_r' equal to -tan δ' was maintained during the test.

Within the underlying clay there was a significant change in f_z until Q_{sf} was reached. After the applied load had reached Q_{sf} , f_z within the pile/clay contact region remained fairly constant. Within the sand drawdown region there was a fluctuation in f_z before and after Q_{sf}

was attained. This may be related to an increase and release in compressive vertical movement similar to that exhibited above the sand/clay interface.

The variation in σ'_r within the underlying clay was again a reflection of the f_z values.

6.6.5 Mobilization of the local Coefficient of Earth Pressure with Applied Load.

The distribution of K_z mobilized throughout pile loading for tests 3 to 6 are illustrated in Figure 6.22 to 6.27. The values at Q_{aw}, Q_{amax} and Q_{sf} are summarised in Table 6.1.

The variation in K_z for driven piles was similar to those produced by Wersching (1987). At Q_{aw}, K_z tended to values of 0.5 over the lower half of the pile to 1.5 near the pile top. At Q_{amax}, K_z varied from 0.6 near the pile base to 5 near the surface which is greater than K_p

Lake (1986) obtained values of K_s for driven piles which varied between K_p near the surface to K_a close to the pile tip.

For the buried piles there was a considerable reduction in the magnitude of K_z. At Q_{amax}, K_z varied from 1.5 near the pile top to 0.3 around the pile base level.

Vesic(1967) compared derived values of K_s for driven and buried circular pile and showed that for the latter there was a reduction in K_s.

In the tensile load condition there was a comparable reduction in K_z

for the two type of pile installations. For a driven pile K_z varied between values close to but not exceeding K_p near the surface to 0.4 near the pile base which approximates to K_o.

The distribution of K_z at Q_{sf} for buried piles range from 1.0 at a $D_b/B=2$ and 0.2 which was marginally lower than K_a near the pile base.

Chaundhuri & Symons (1983) summarised results of model scale tests on piles in compression and tension. They show that for a loose sand K_s varies between K_a and K_p and in a dense sand it can increase above K_p

6.6.6 Stresses Developed on the Pile Shaft During Compressive and Tensile Loading.

Werscheing (1987) proposed a theoretical stress history for sand adjacent to the pile shaft under both compressive and tensile loading. He based this theory on results produced from load tests carried out on driven piles. To make a comparison with his work the variations in f_z with σ'_r from tests 3-6 (driven & buried piles) were plotted in a similar manner to those given by Werscheing (1987) and are illustrated in Figures 6.31 to 6.39. They illustrate various points made between f_z and σ'_r in the previous sections and conform with the following theory proposed by Werscheing (1987).

6.6.6.1 The State of Three Dimensional Stress Developed Within the Sand Adjacent to the Pile Shaft Throughout Pile Loading as Proposed by Werscheing (1987)

The idealised f_z-σ'_r history acting on a typical prismatic element of sand adjacent to the pile shaft remote from end effects is

illustrated in Figure 6.40a.

Several tentative assumptions were made as to the behaviour of the pile shaft/sand interface and the magnitude of the cylindrical stresses acting on a prismatic element of sand adjacent to this boundary and are as follows:

1. The mode of failure developed along the pile shaft was based on work by Yoshimi & Kishida(1981). This implied that shear failure occurs within the sand in conjunction with slip at the pile shaft/soil interface. Their work shows that the shear zones begin to develop once f_z/σ_r' had exceeded 0.7-0.8 tan δ.
2. For the condition f_z equal to zero the magnitude of σ_r' adjacent to the pile shaft will be less than that at failure and therefore less than the initial effective overburden pressure. Also as f_z tends to zero, ε_v may be taken as zero for a first order approximation. These assumptions were based on work by Hanna & Tan (1973), Vesic(1963) and the results of the D.P.T.s located within the sand.
3. The circumferential strain (ε_θ) was assumed to be zero throughout loading. This was deduced from Robinsky and Morrison's(1964) test data and neglecting the insignificant diametric expansion of the pile shaft under load.

Thus when $f_z=0$ and $\varepsilon_z=\varepsilon_\theta=0$;-

$$\sigma_z' = \sigma_\theta' = (\nu/(1-\nu))\sigma_r' = K_o\sigma_r'$$

This stress condition is indicated in Figure 6.40b

Throughout loading $\sigma_\theta' = \sigma_2'$

Where $\sigma_2' = \nu(\sigma_1' + \sigma_3')$ and $\nu = 0.3$

With the application of Q_a , the principal stresses rotate in a clockwise direction until the f_z-σ_r' profile is tangential to the δ' envelop, refer to Figure 6.40c. At this point slip occurs at the pile/sand interface and shear develops in the sand. With further increase in Q_a to Q_{amax} the magnitude of the f_z-σ_r' profile increases but remains on the δ' envelop and no additional rotation of the principal stress planes occur.

Figure 6.41 illustrates the normalised effective stresses acting on a prismatic element of sand adjacent to the pile shaft at Q_{sf} for the driven and placed piles. The magnitude of these stresses were derived from the conditions proposed by Wersching (1987).

Upon unloading of the pile the stress intensity within the sand adjacent to the pile shaft reduces to a level less than that necessary to sustain a state of shear failure. This occurs in conjunction with an anti-clockwise rotation of the principal stress.

During unloading a condition is eventually reached where the shear stress developed along the pile shaft is insufficient to resist the elastic displacement recovery of the sand which was induced during loading. This results in a upward displacement of the sand relative to the pile shaft and the development of slip along the pile shaft/sand boundary and shear failure within the sand adjacent to the pile shaft. It is possible therefore for the sand adjacent to the pile shaft to be in a state of shear failure in conjunction with a positive f_z as the pile is unloaded, refer to Figure 6.40d. Beyond this point the f_z-σ_r' profile traverses the δ_u' line.

As the applied load approaches zero the f_z-σ_r' relationship remains on the δ_u' line and a state of shear failure in the sand adjacent to the pile is maintained. This results in the development of a negative f_z since the pile shaft recovery was greater than that of the surrounding sand due to the elastic displacement recovery of the pile and the highly compressed sand below its base. At zero applied load the sand adjacent to the pile shaft was at a state of shear failure under the system of post compressive residual stresses indicated on Figure 6.40f.

On application of a tensile load the post compressive stress system is maintained. The shear failure within the sand adjacent to the shaft remains, the stress intensity increases resulting in a further anti-clockwise rotation of the principal stress plane. This continues until the f_z-σ_r' relationship attains a limiting value and follow the $-\delta'$ envelope. Beyond this point of initial tangency with the δ' envelope the stresses continue to increase without further rotation of the principal stresses.

Figure 6.42 illustrates the normalised effective stresses acting on a prismatic element of sand adjacent to the pile shaft at Q_{sf} in tensile loading for the driven and placed piles. The magnitude of the stresses were derived from the conditions given by Wersching(1987).

On release of the tensile load there is a collapse in the stress system, which is unable to maintain a state of shear in the sand adjacent to the pile. This would continue until the relative displacements between the pile shaft and sand was such to result in shear failure and follow the $-\delta_u'$ line in a similar manner to the load and unload stress cycle.

$\frac{D_b}{B}$	VALUES OF K_z							
	TEST 3 (114DC-S)		TEST 4 (114IN-S)		TEST 5 (114DC-S/C)		TEST 6 (114IE-S)	
	Q_{aw}	Q_{amax}	Q_{aw}	Q_{amax}	Q_{aw}	Q_{amax}	Q_{aw}	Q_{amax}
2	0·85	4·35	0·90	1·50	1·00	3·50	0·73	1·15
7·5	0·40	1·70	0·35	0·48	0·37	1·37	0·25	0·70
15	0·60	0·75	0·16	0·28	–	–	0·15	0·37

VARIATION IN THE LOCAL COEFFICIENT OF EARTH PRESSURE ALONG THE PILE SHAFT WITH APPLIED LOAD

TABLE 6.1

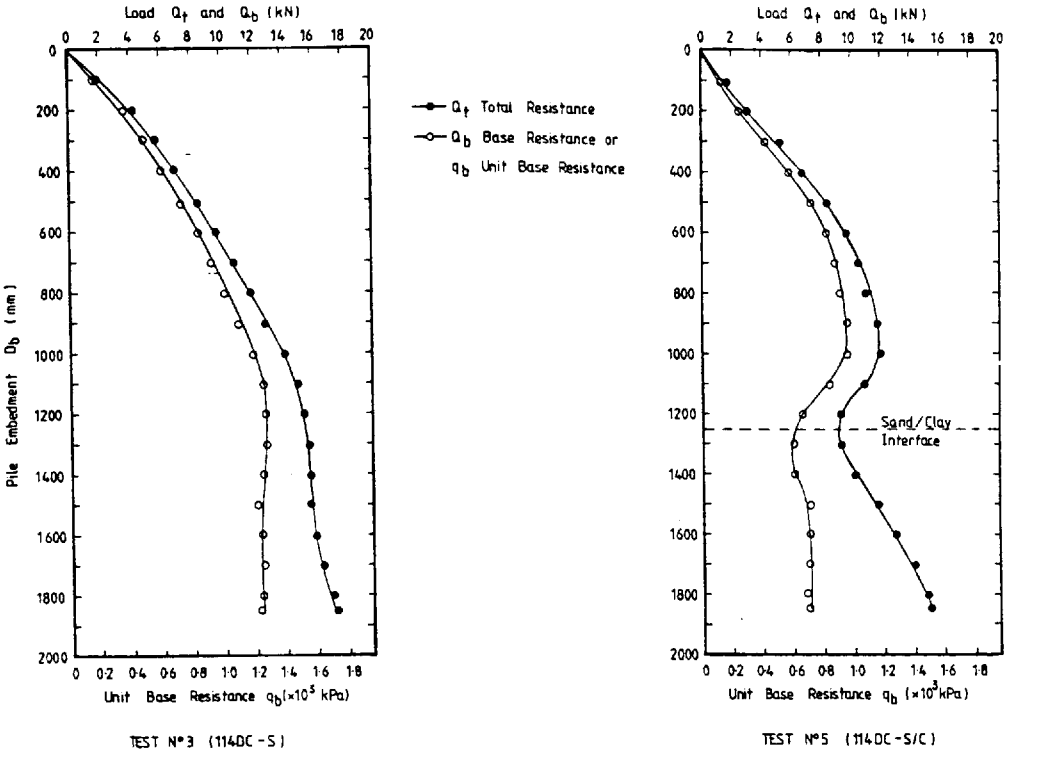

DEVELOPMENT OF TOTAL AND BASE RESISTANCE DURING PILE INSTALLATION

FIGURE 6.1

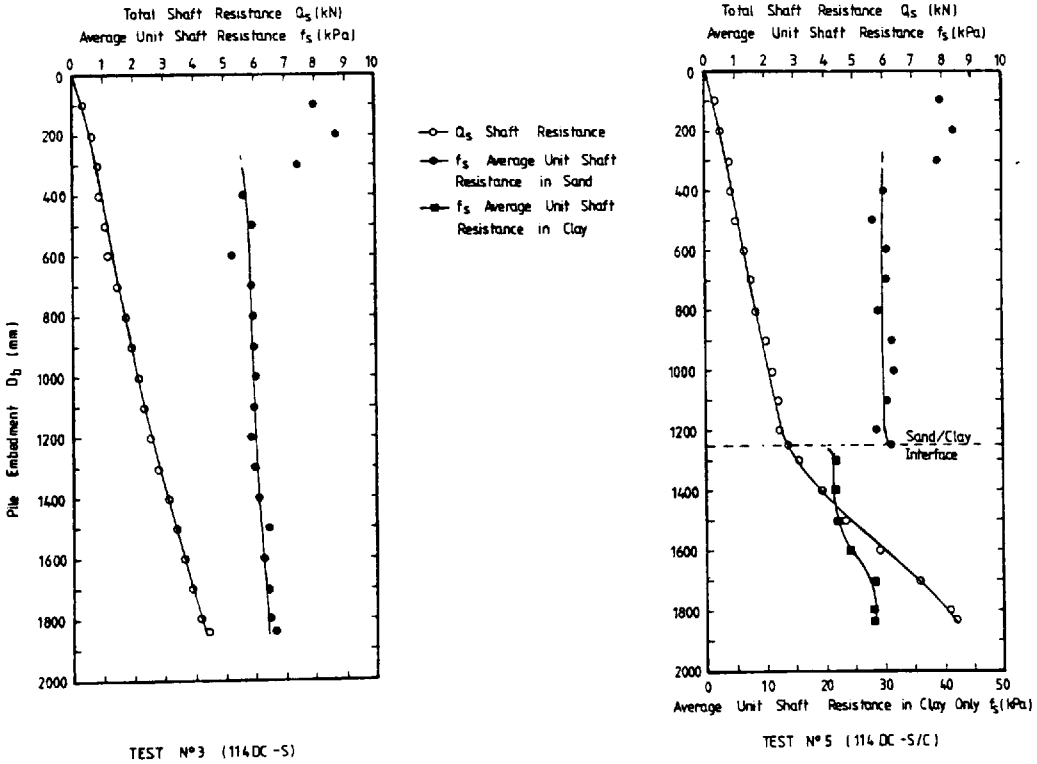

DEVELOPMENT OF TOTAL SHAFT AND UNIT SHAFT RESISTANCE DURING PILE INSTALLATION

FIGURE 6.2

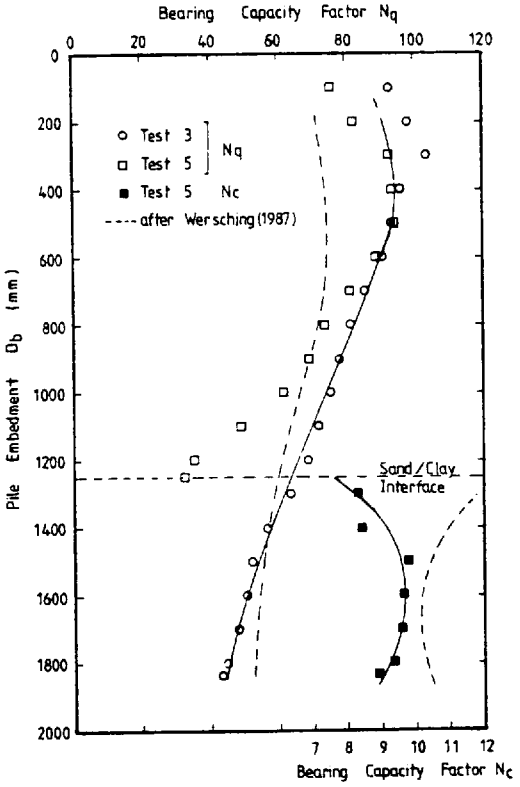

VARIATION IN BASE BEARING CAPACITY FACTORS WITH PILE EMBEDMENT DURING INSTALLATION

FIGURE 6.3

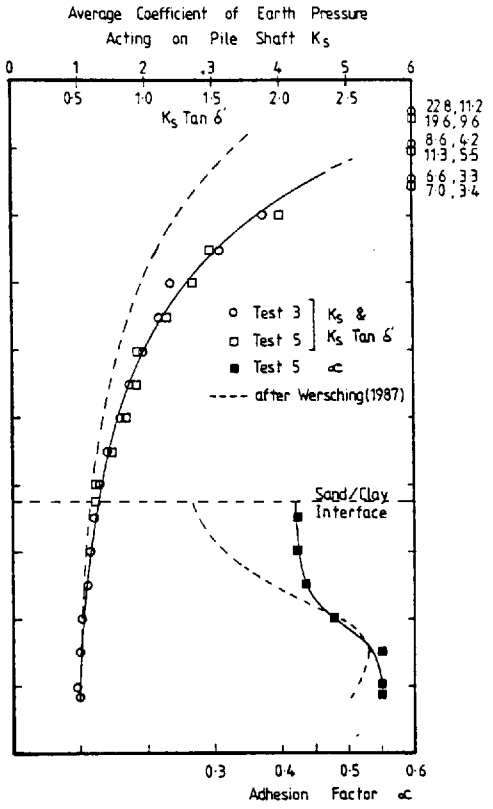

VARIATION IN AVERAGE SHAFT BEARING CAPACITY FACTORS WITH PILE EMBEDMENT DURING INSTALLATION

FIGURE 6.4

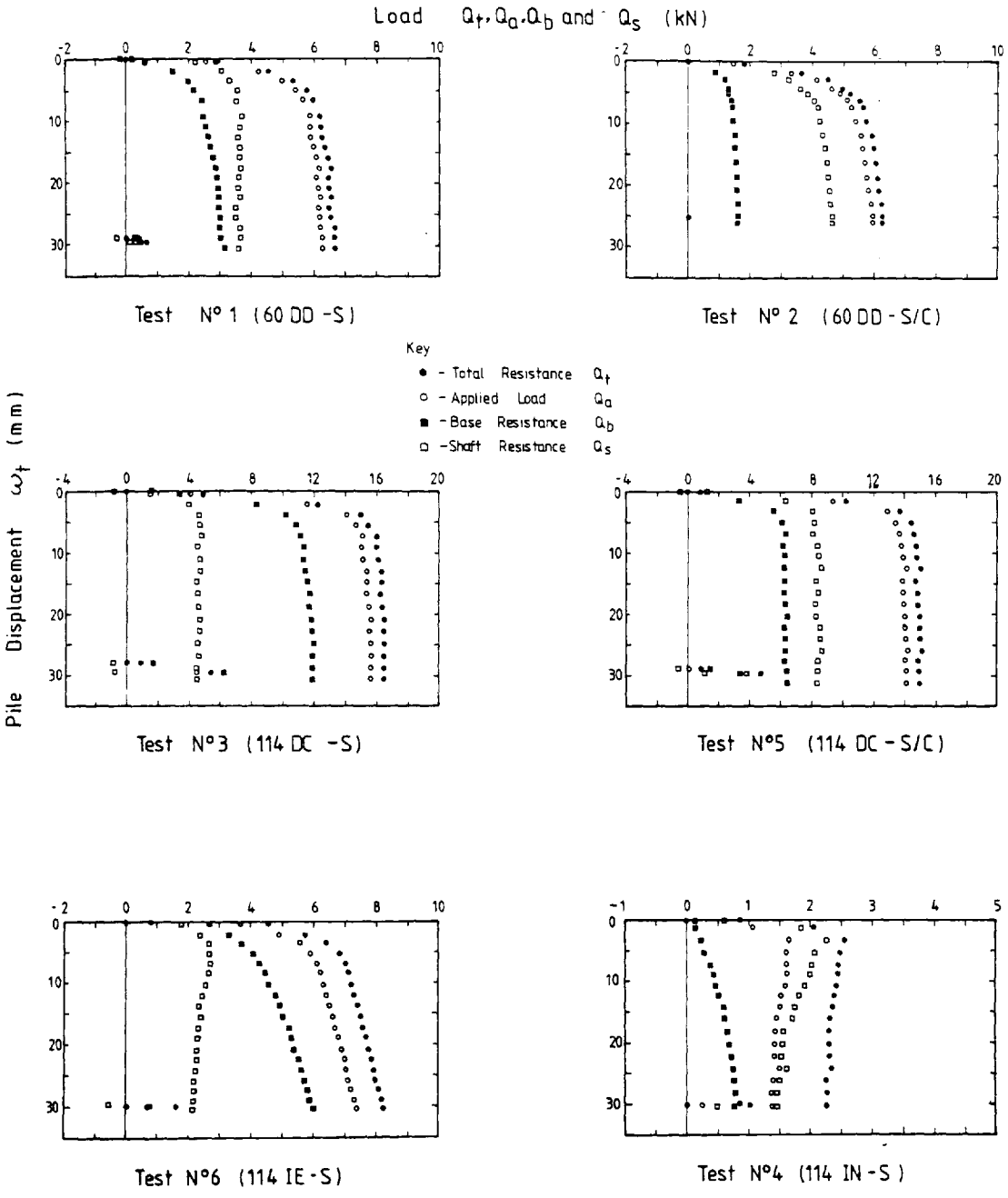

FIGURE N° 6,5 CONSTANT RATE OF PENETRATION TEST
(Rate = 1·524mm / minute)

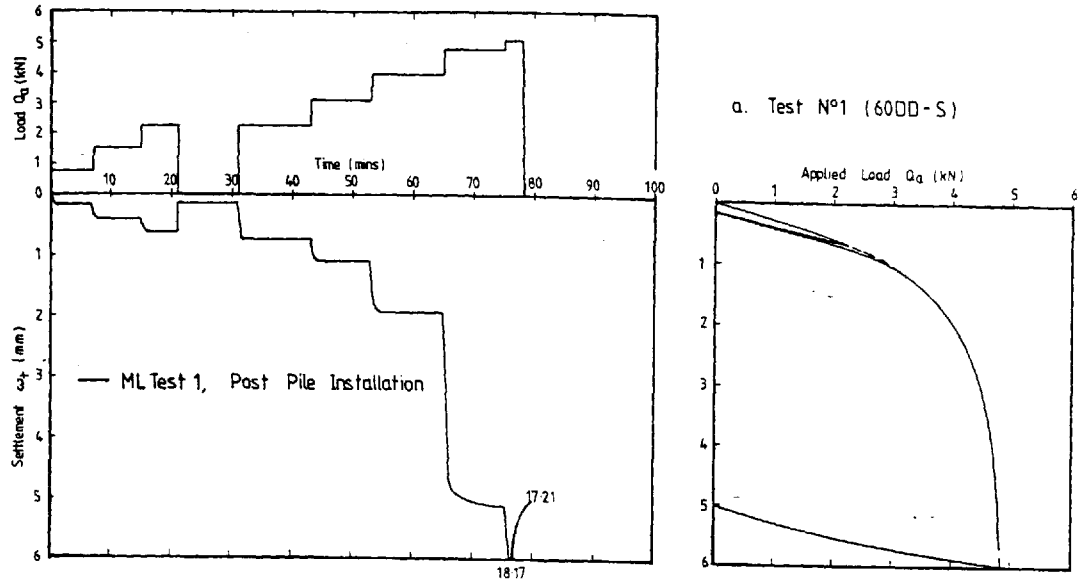

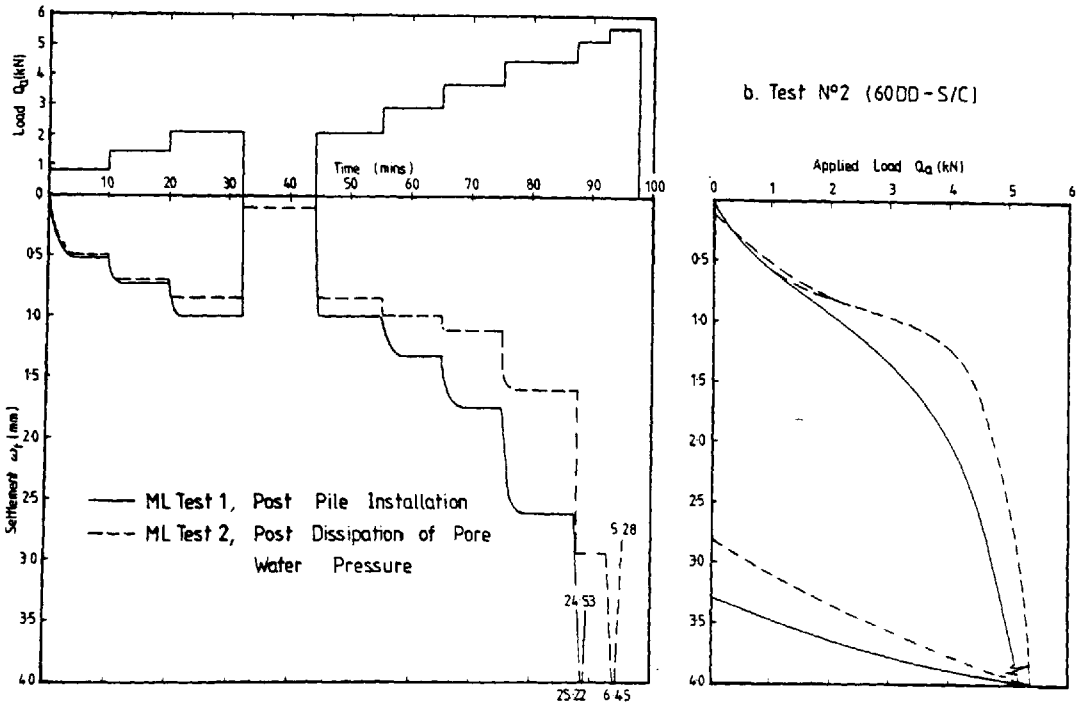

RESULTS OF MAINTAINED LOAD TESTS

FIGURE N° 6,6

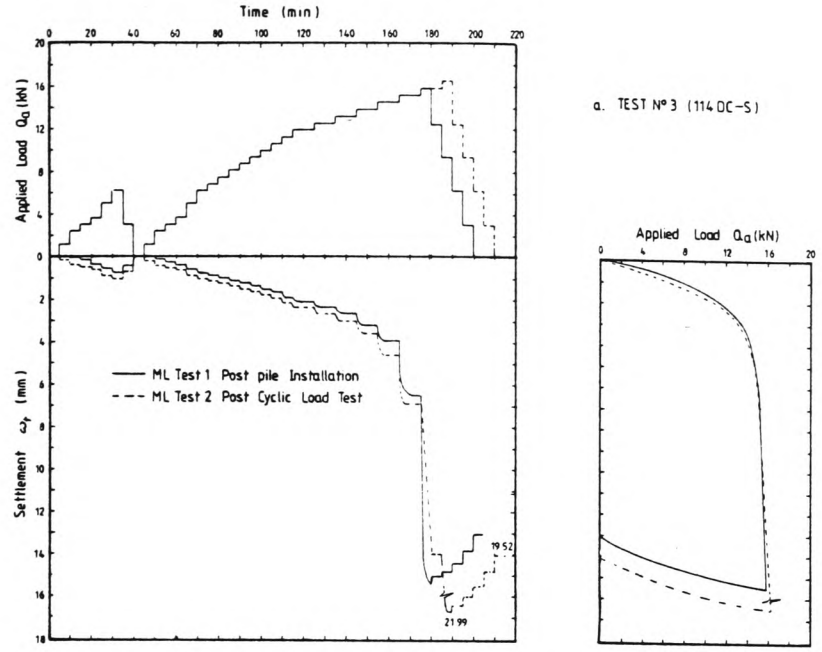

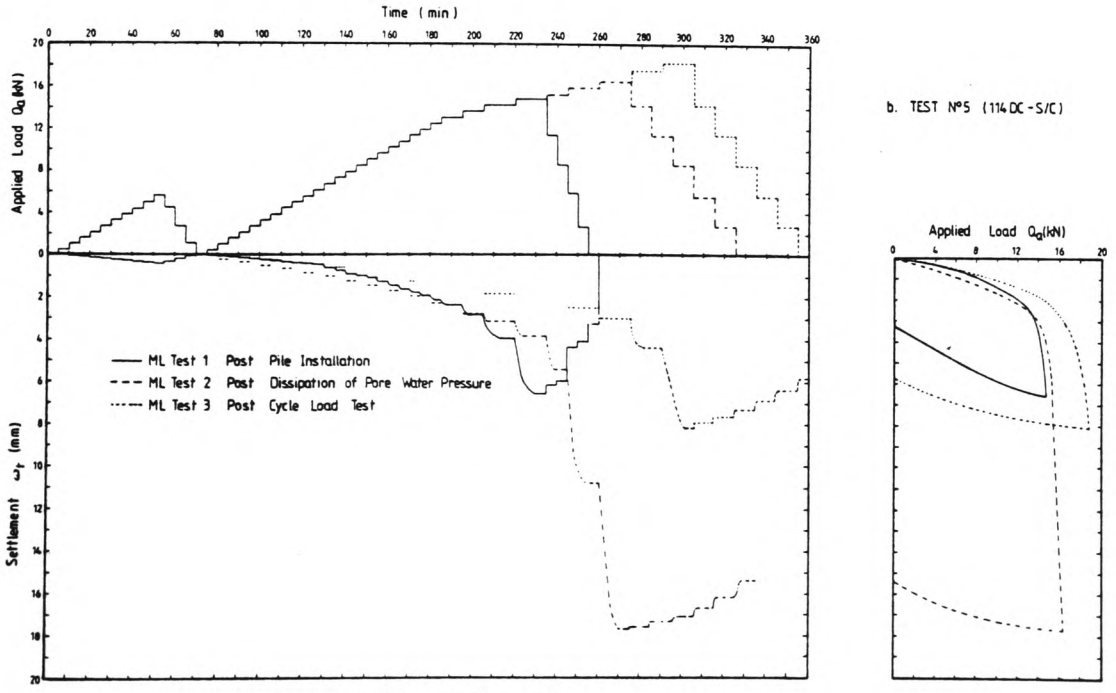

RESULTS OF MAINTAINED LOAD TESTS

FIGURE N° 6.7

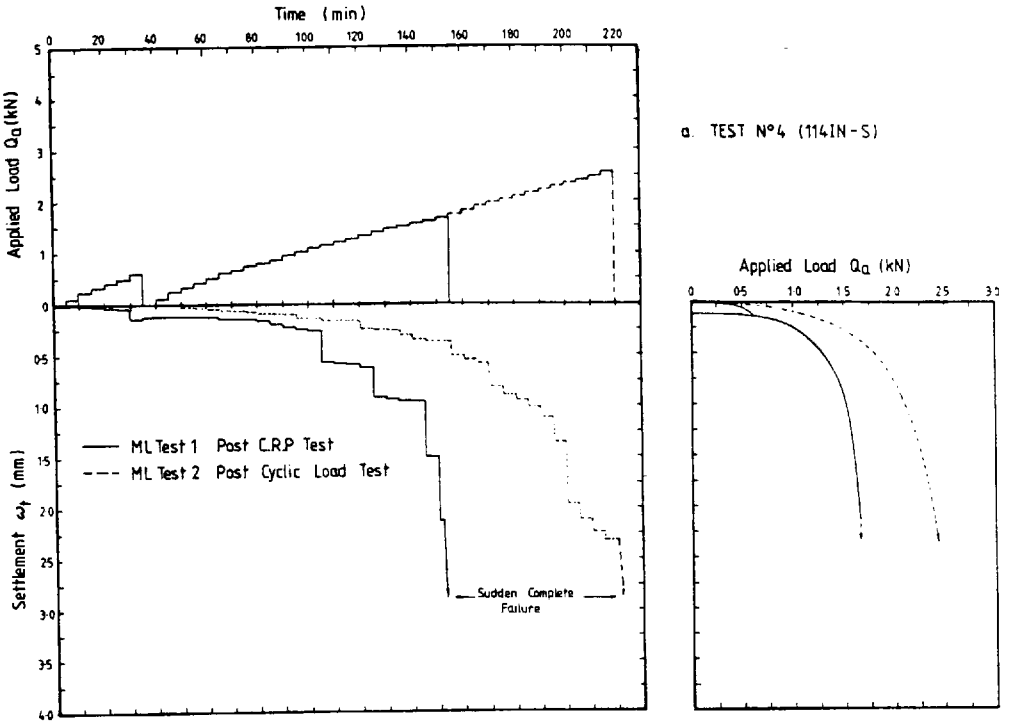

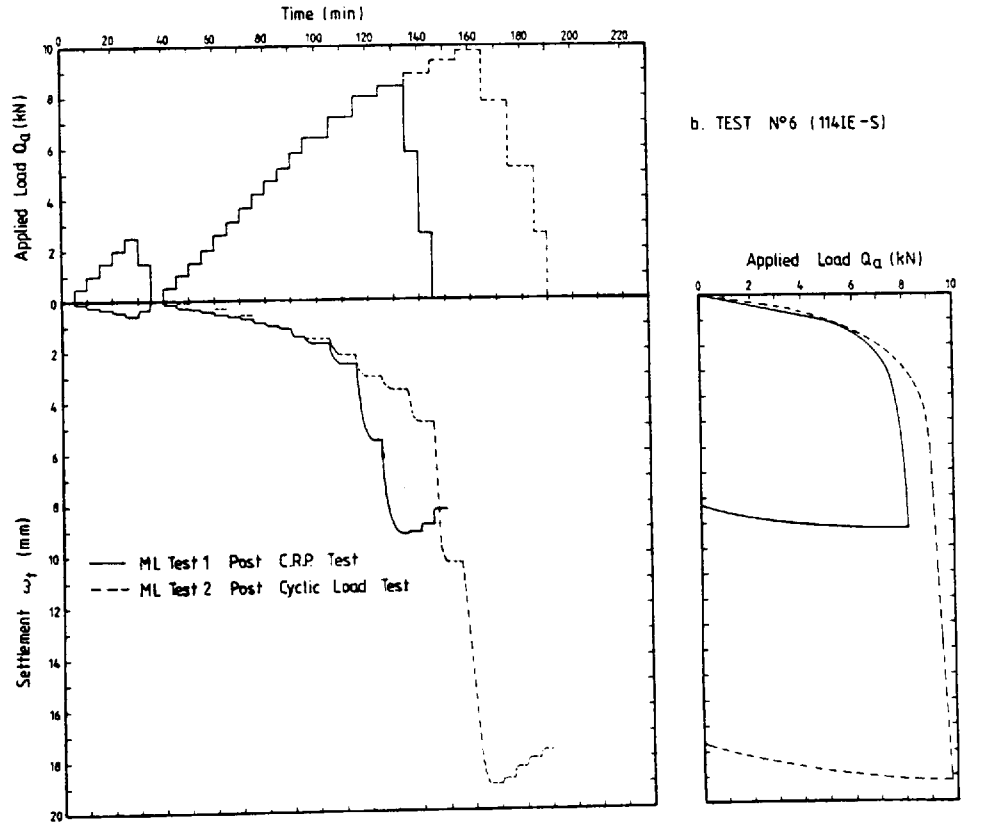

RESULTS OF MAINTAINED LOAD TESTS
FIGURE N° 6.8

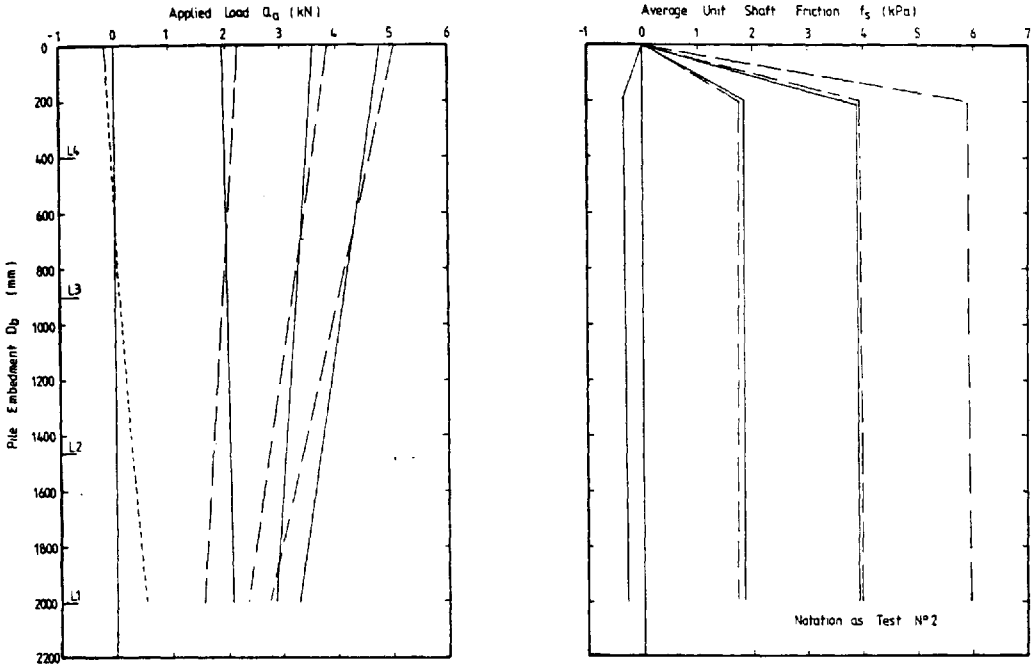

a. Test N° 1 (60 DD - S)

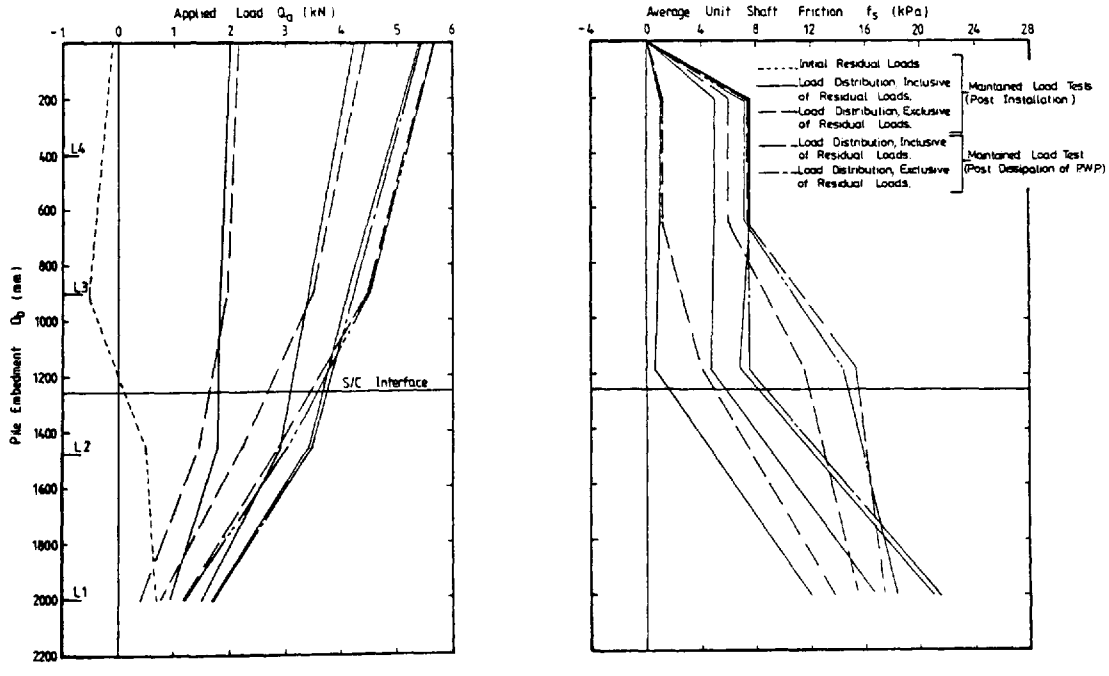

b. Test N° 2 (60 DD - S/C)

FIGURE N° 6.9 CHANGES IN DISTRIBUTION OF LOAD AND AVERAGE SHAFT FRICTION DURING A SERIES OF MAINTAINED LOAD TESTS

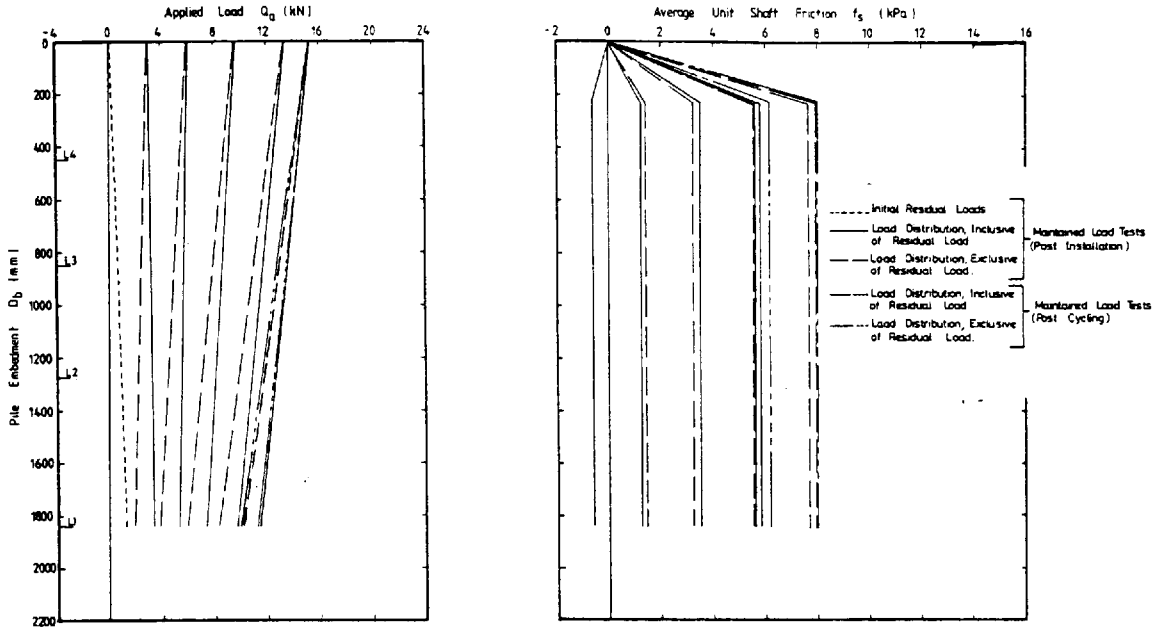

a. Test N° 3 (114 DC - S)

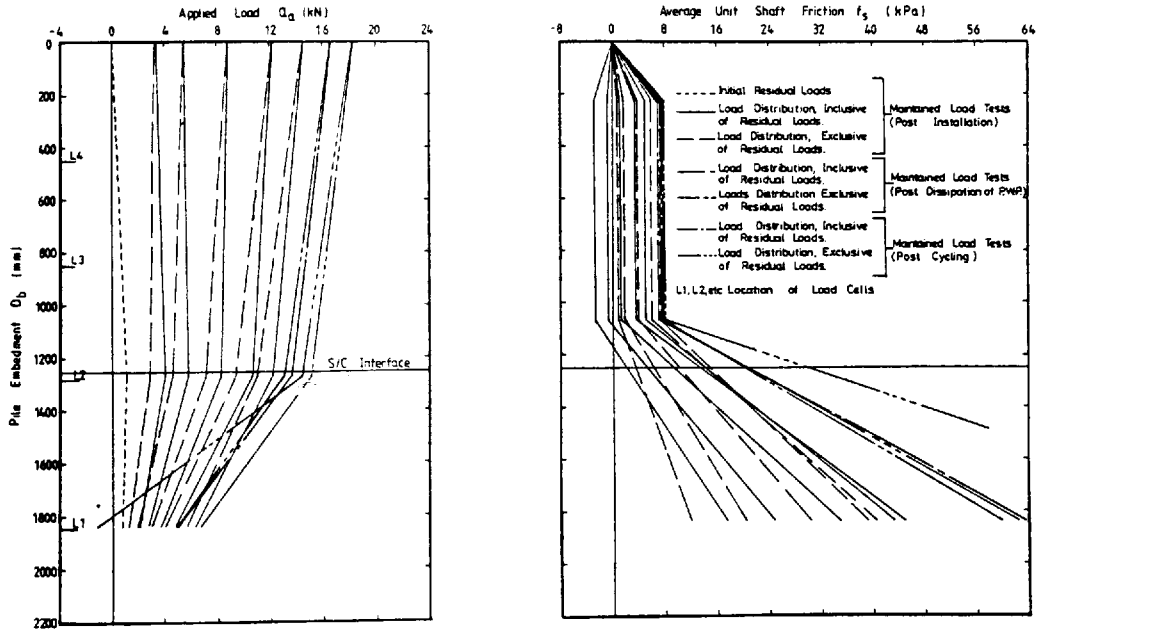

b Test N° 5 (114 DC - S/C)

FIGURE N°6.10 CHANGES IN DISTRIBUTION OF LOAD AND AVERAGE SHAFT FRICTION DURING A SERIES OF MAINTAINED LOAD TESTS

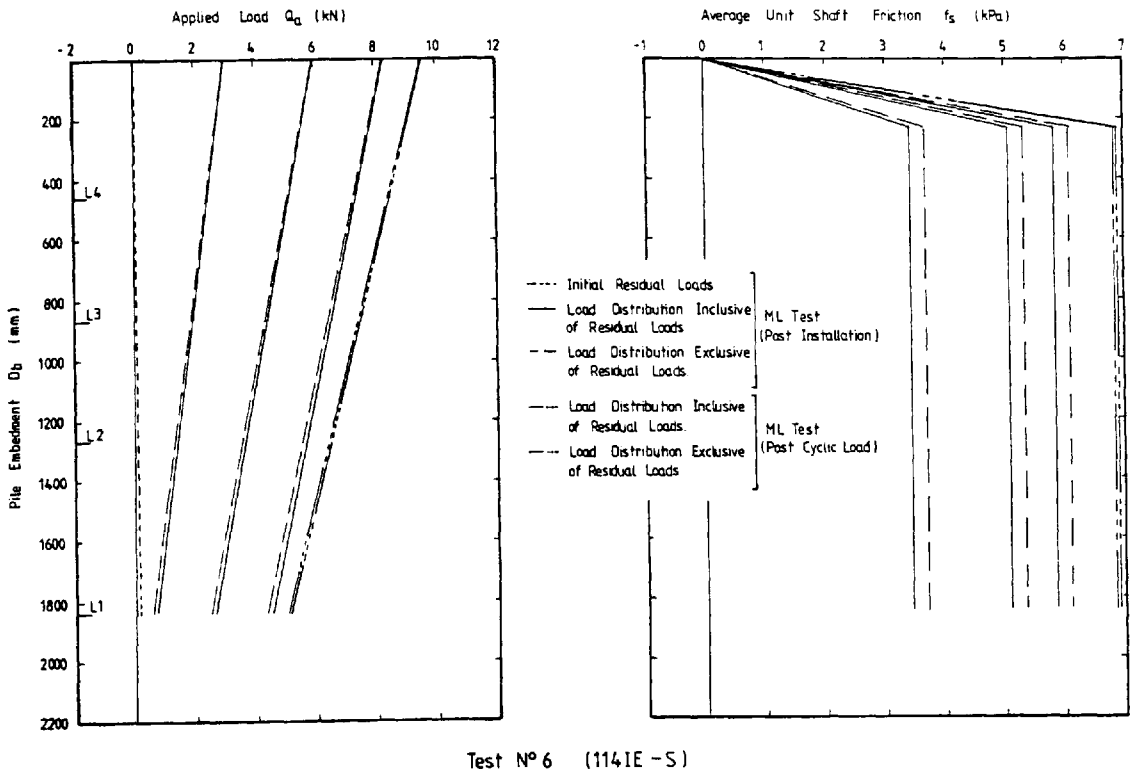

Test N° 6 (1141E - S)

FIGURE N°6.11 CHANGES IN DISTRIBUTION OF LOAD AND AVERAGE SHAFT FRICTION DURING A SERIES OF MAINTAINED LOAD TESTS

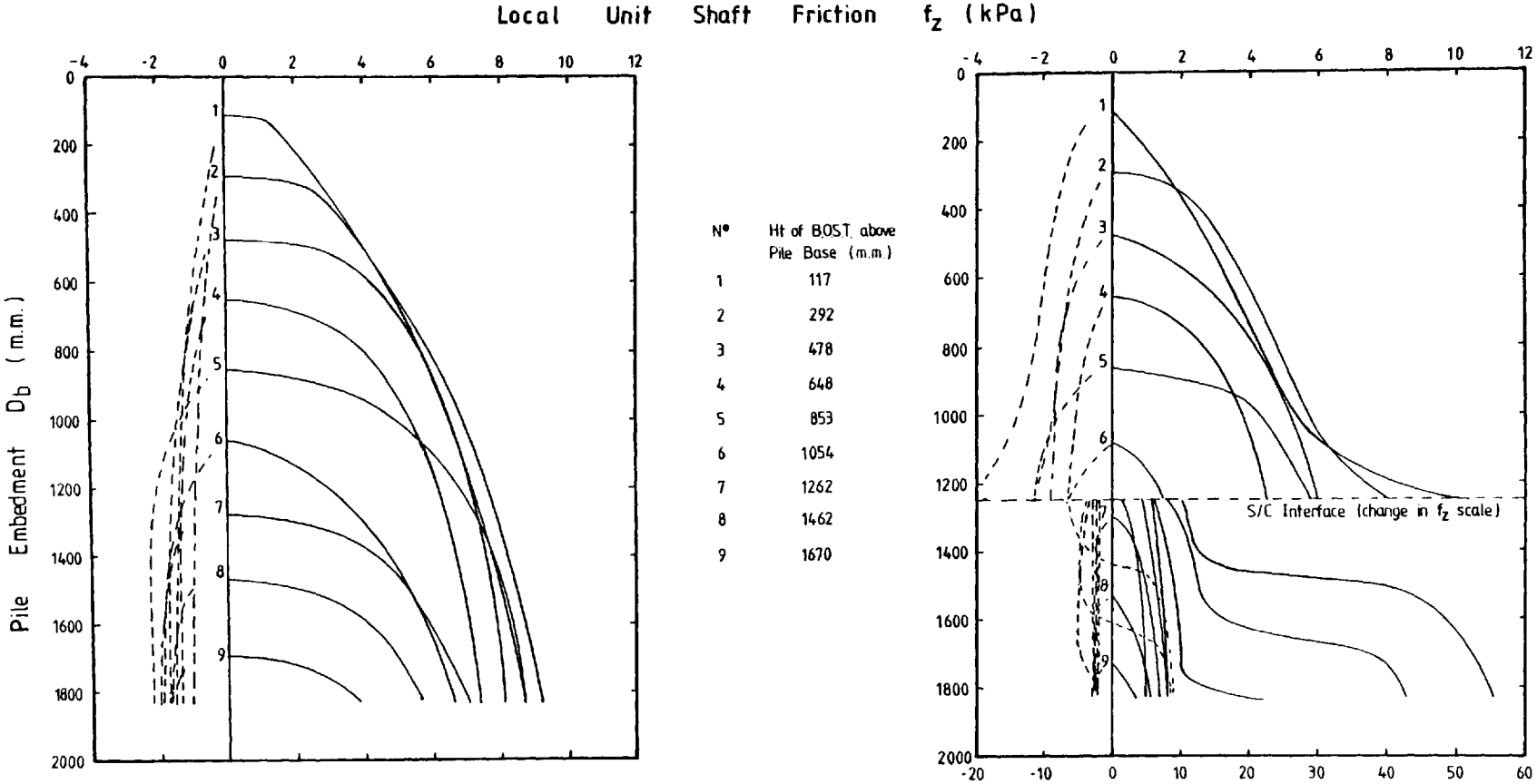

DEVELOPMENT OF LOCAL UNIT SHAFT FRICTION WITH PILE EMBEDMENT DURING INSTALLATION

FIGURE 6,12

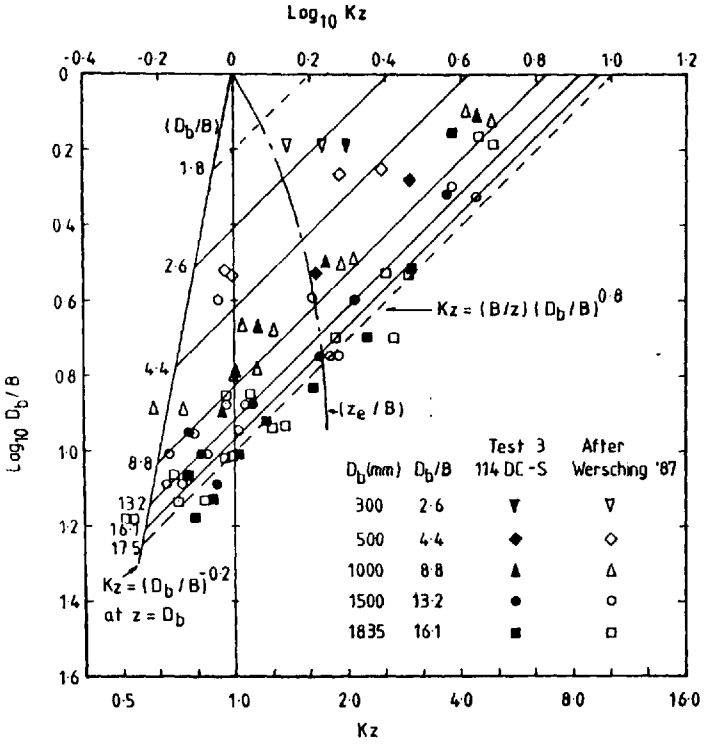

VARIATION IN THE LOCAL COEFFICIENT OF EARTH PRESSURE WITH DEPTH AND EMBEDMENT

FIGURE 6.13

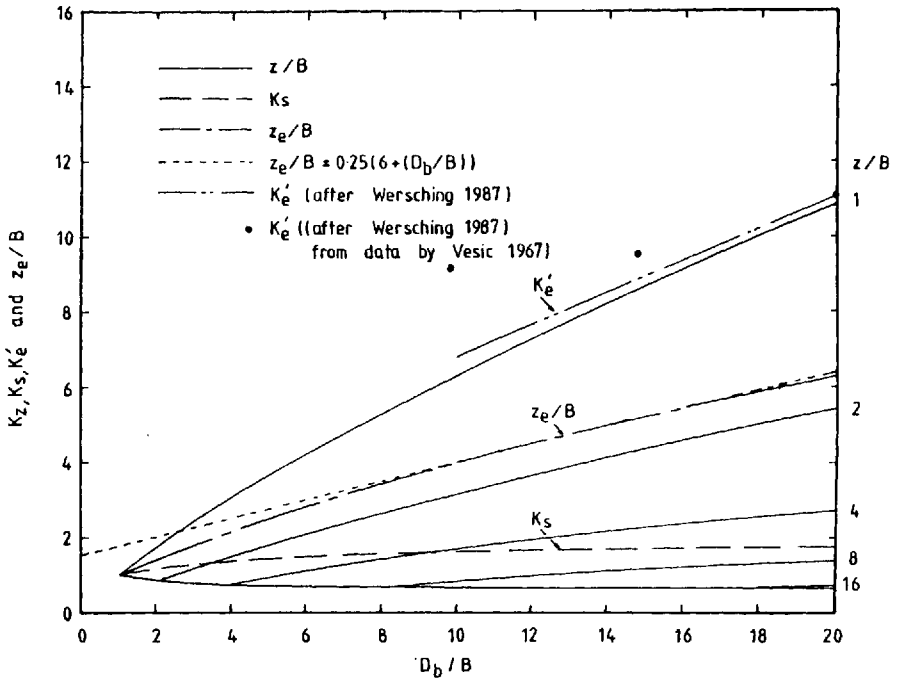

VARIATION IN THE LOCAL AND AVERAGE COEFFICIENTS OF EARTH PRESSURE (K_z AND K_s), DEPTH AT WHICH $K_z = K_s$ (z_e/B) AND THE SHAFT BEARING CAPACITY FACTOR K'_e WITH PILE EMBEDMENT

FIGURE 6.14

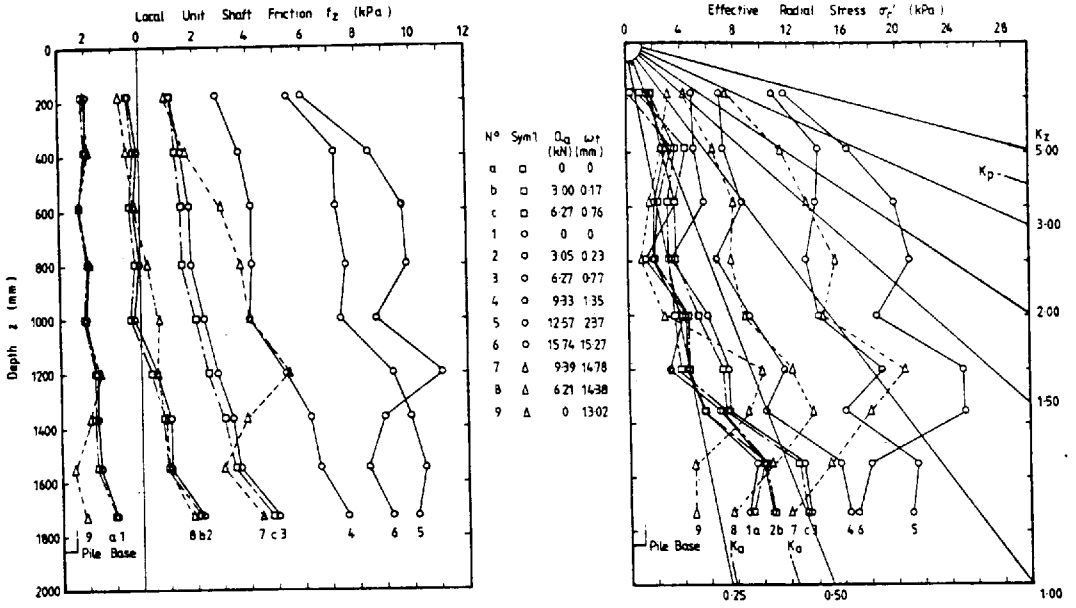

N°	Sym	Q_g (kN)	ω_t (mm)
a	□	0	0
b	□	3·00	0·17
c	□	6·27	0·76
1	○	0	0
2	○	3·05	0·23
3	○	6·27	0·77
4	○	9·33	1·35
5	○	12·57	2·37
6	○	15·74	15·27
7	△	9·39	14·78
8	△	6·21	14·38
9	△	0	13·02

a. Maintained Load Test Series 1 (Post Installation)

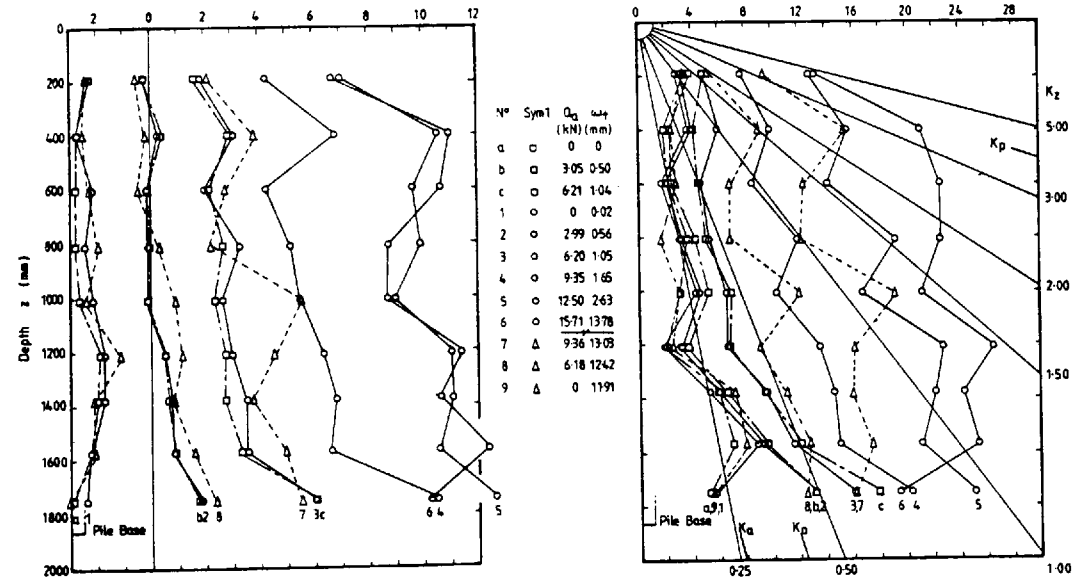

N°	Sym	Q_g (kN)	ω_t (mm)
a	□	0	0
b	□	3·05	0·50
c	□	6·21	1·04
1	○	0	0·02
2	○	2·99	0·56
3	○	6·20	1·05
4	○	9·35	1·65
5	○	12·50	2·63
6	○	15·71	13·78
7	△	9·36	13·03
8	△	6·18	12·42
9	△	0	11·91

b. Maintained Load Test Series 2 (Post Cyclic Loading)

TEST N°3 (114 DC – S.)

DEVELOPMENT OF LOCAL SHAFT FRICTION AND EFFECTIVE RADIAL STRESS DURING A SERIES OF MAINTAINED LOAD TESTS

FIGURE 6.15

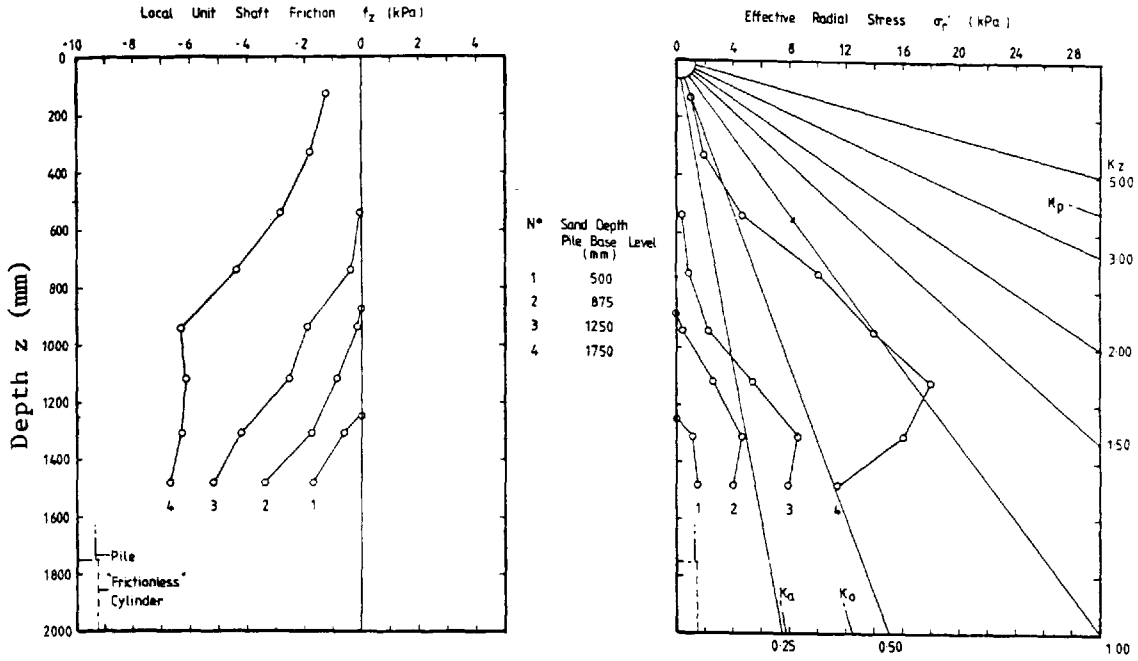

a. Test N°4 (114IN-S)

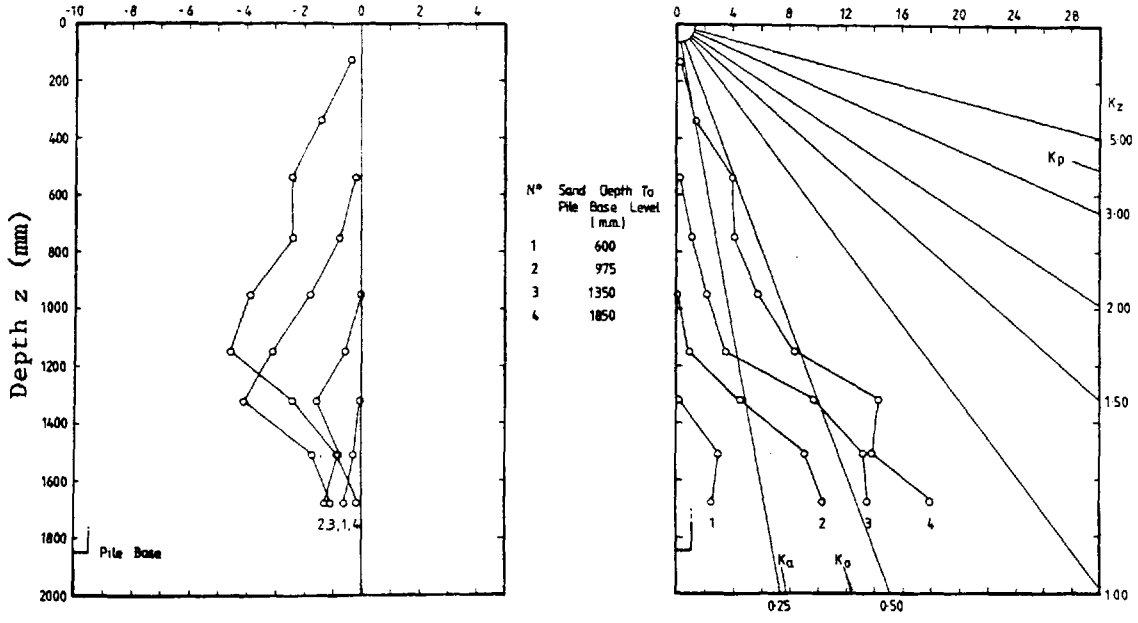

b. Test N°6 (114IE-S)

DEVELOPMENT OF LOCAL SHAFT FRICTION AND EFFECTIVE RADIAL STRESS DURING SAND PLACEMENT

FIGURE 6.16

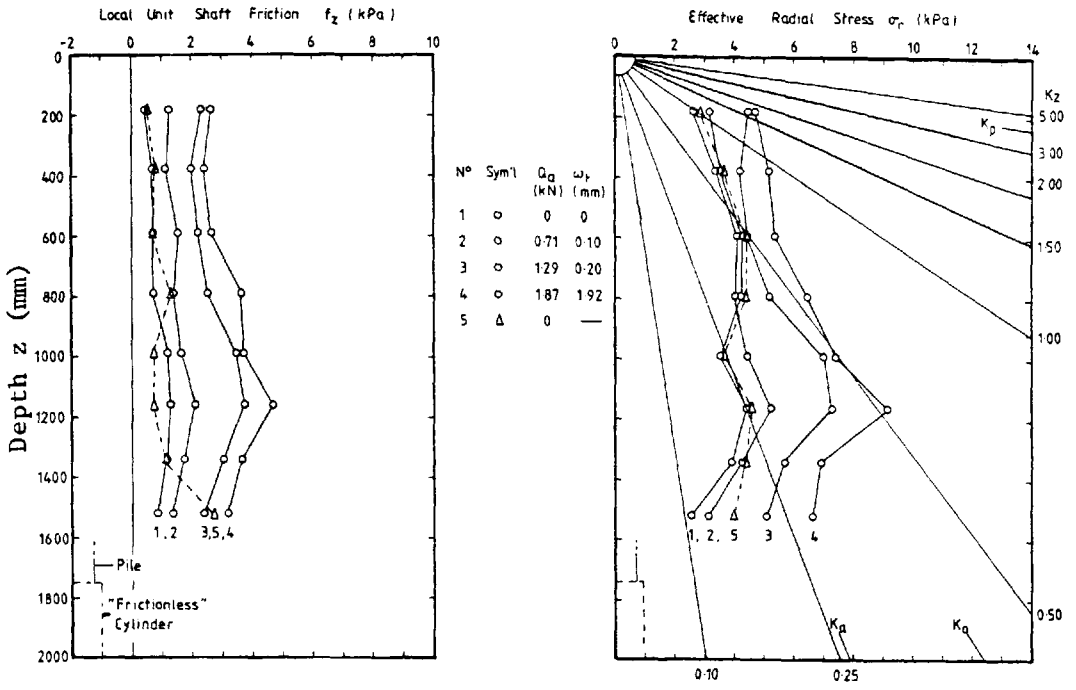

a. Maintained Load Test Series 1 (Post C.R.P. Test)

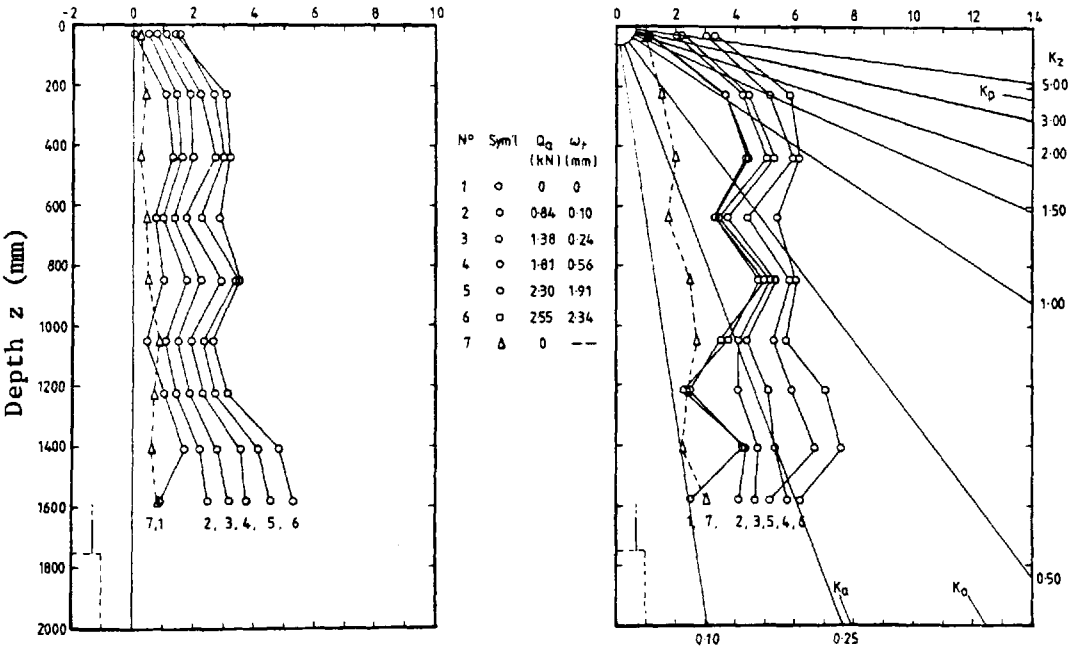

b. Maintained Load Test Series 2 (Post Cyclic Loading)

TEST N° 4 (114IN-S)

DEVELOPMENT OF LOCAL SHAFT FRICTION AND EFFECTIVE RADIAL STRESS DURING A SERIES OF MAINTAINED LOAD TESTS

FIGURE 6.17

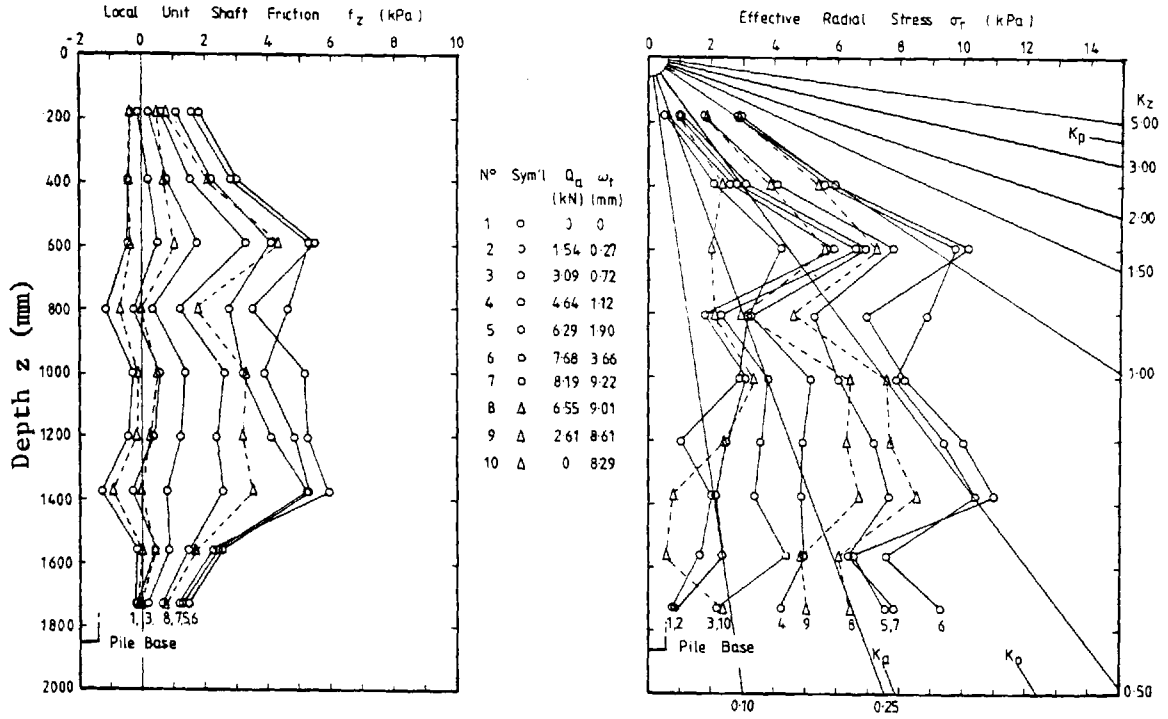

a. Maintained Load Test Series 1 (Post C.R.P. Test)

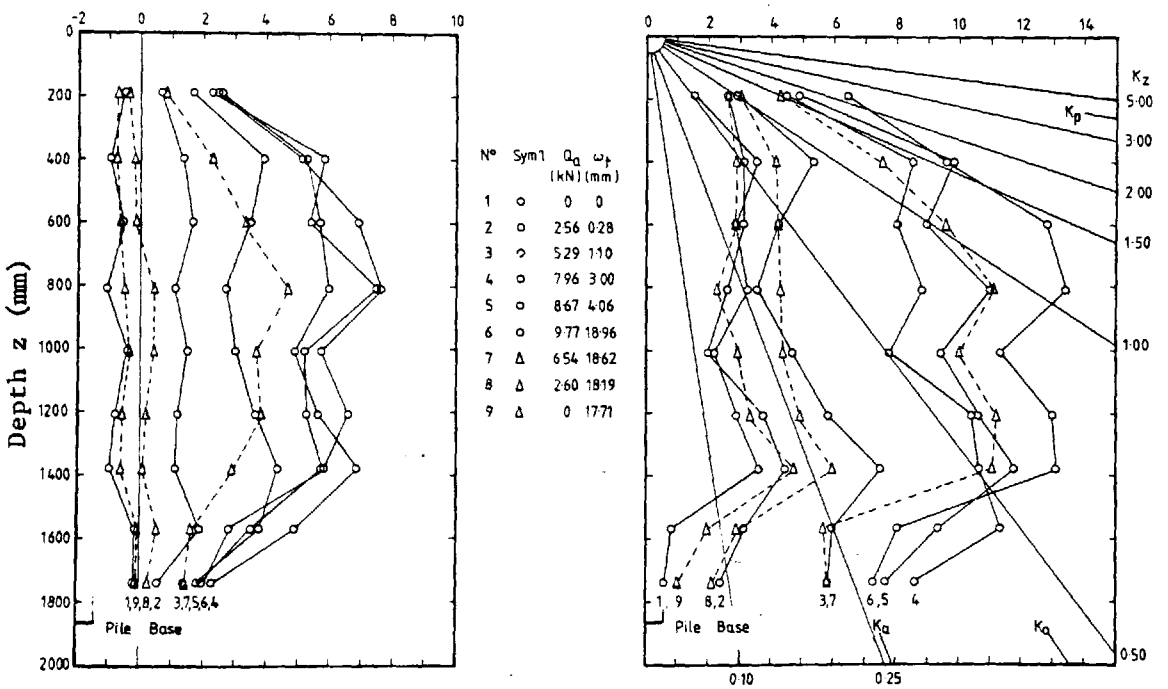

b. Maintained Load Test Series 2 (Post Cyclic Loading)

TEST N°6 (1141E-S)

DEVELOPMENT OF LOCAL SHAFT FRICTION AND EFFECTIVE RADIAL STRESS DURING A SERIES OF MAINTAINED LOAD TESTS

FIGURE 6.18

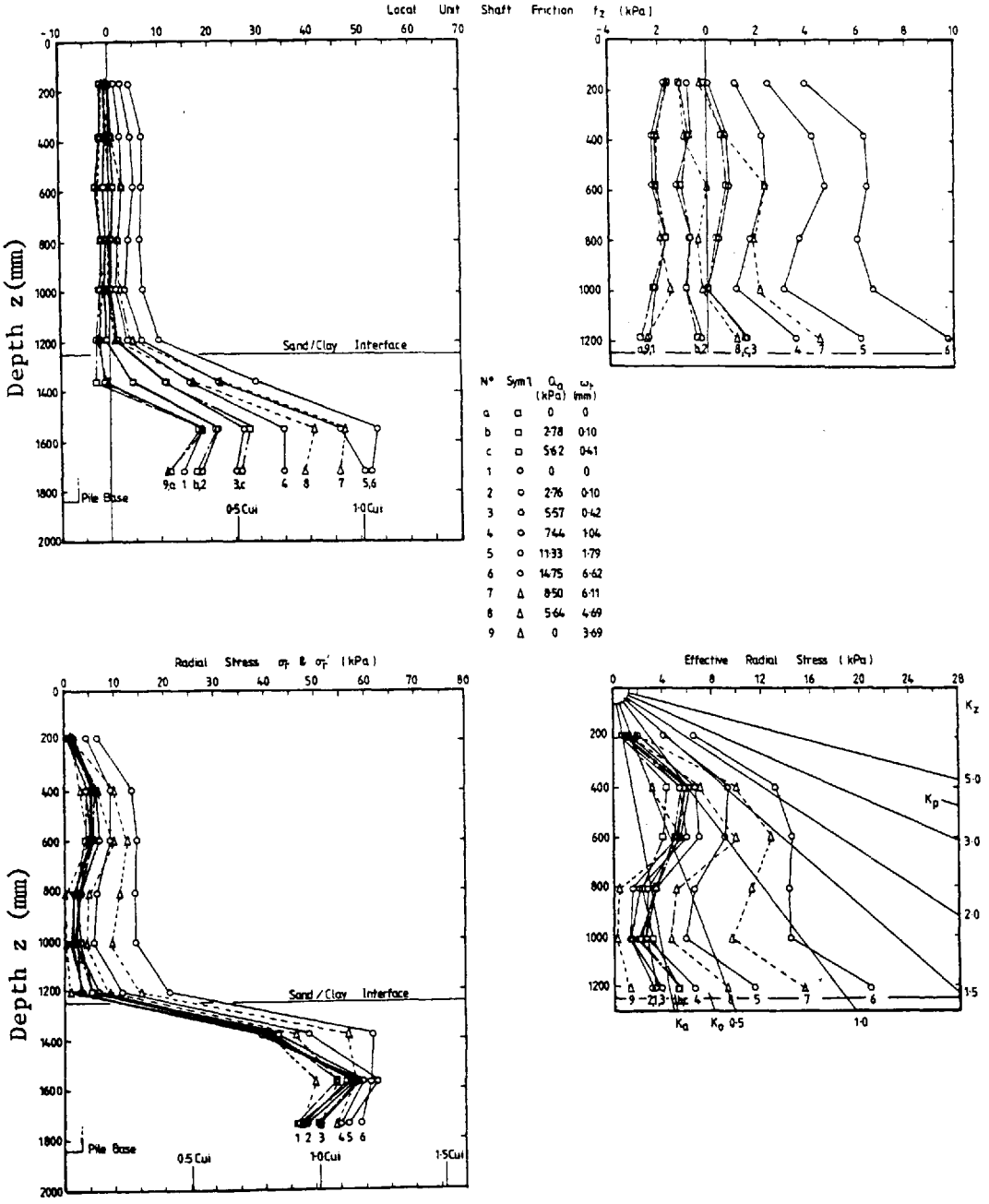

Maintained Load Test (Post-Installation)

TEST N°5 (114 DC - S/C)

DEVELOPMENT OF LOCAL SHAFT FRICTION AND RADIAL STRESS DURING A MAINTAINED LOAD TEST (POST- INSTALLATION)

FIGURE · 6.19

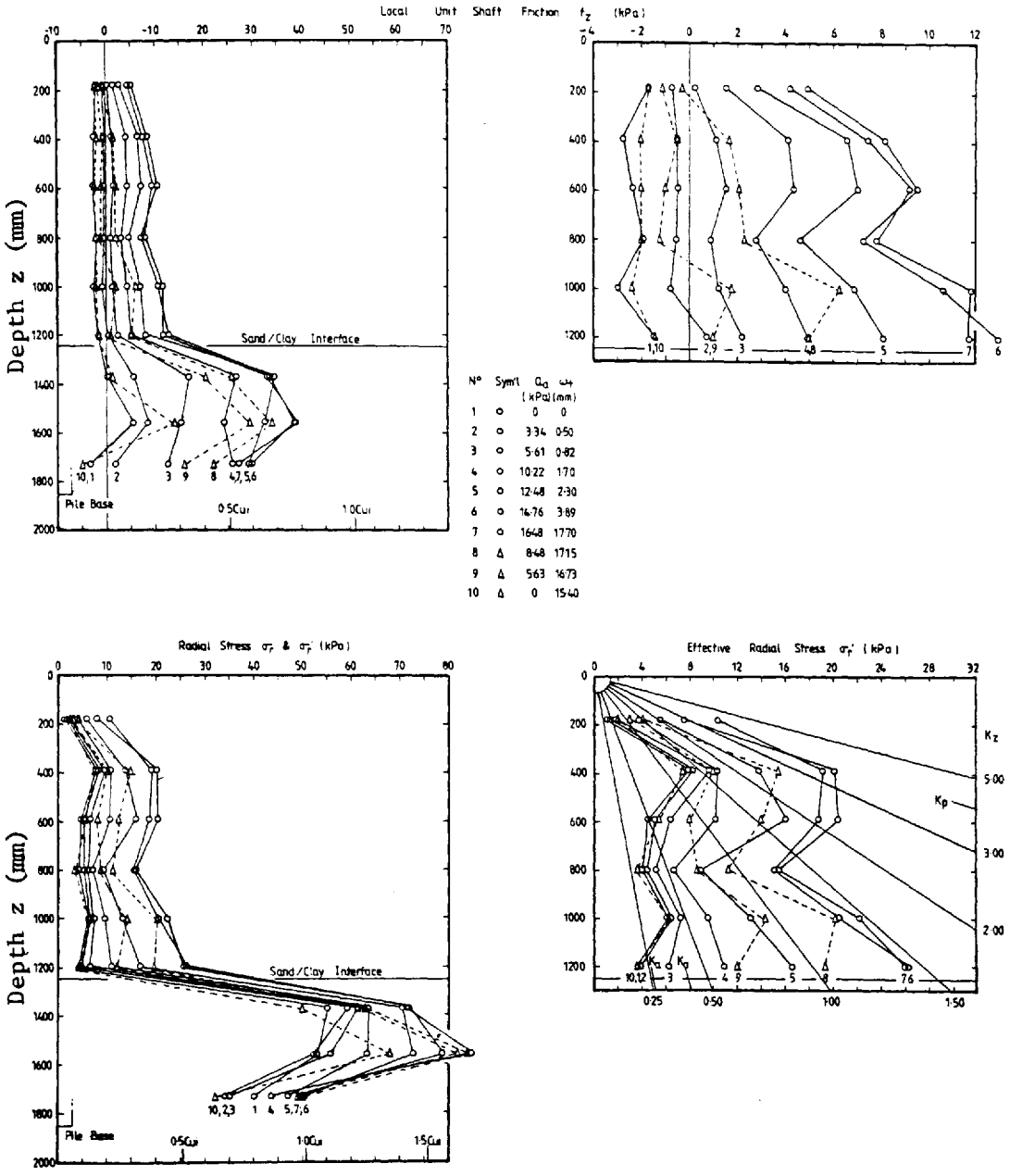

Maintained Load Test (Post - Dissipation of Pore Pressure)

TEST N° S (114 DC - S/C)

DEVELOPMENT OF LOCAL SHAFT FRICTION AND RADIAL STRESS DURING A MAINTAINED LOAD TEST (POST - DISSIPATION OF PORE PRESSURE)

FIGURE 6.20

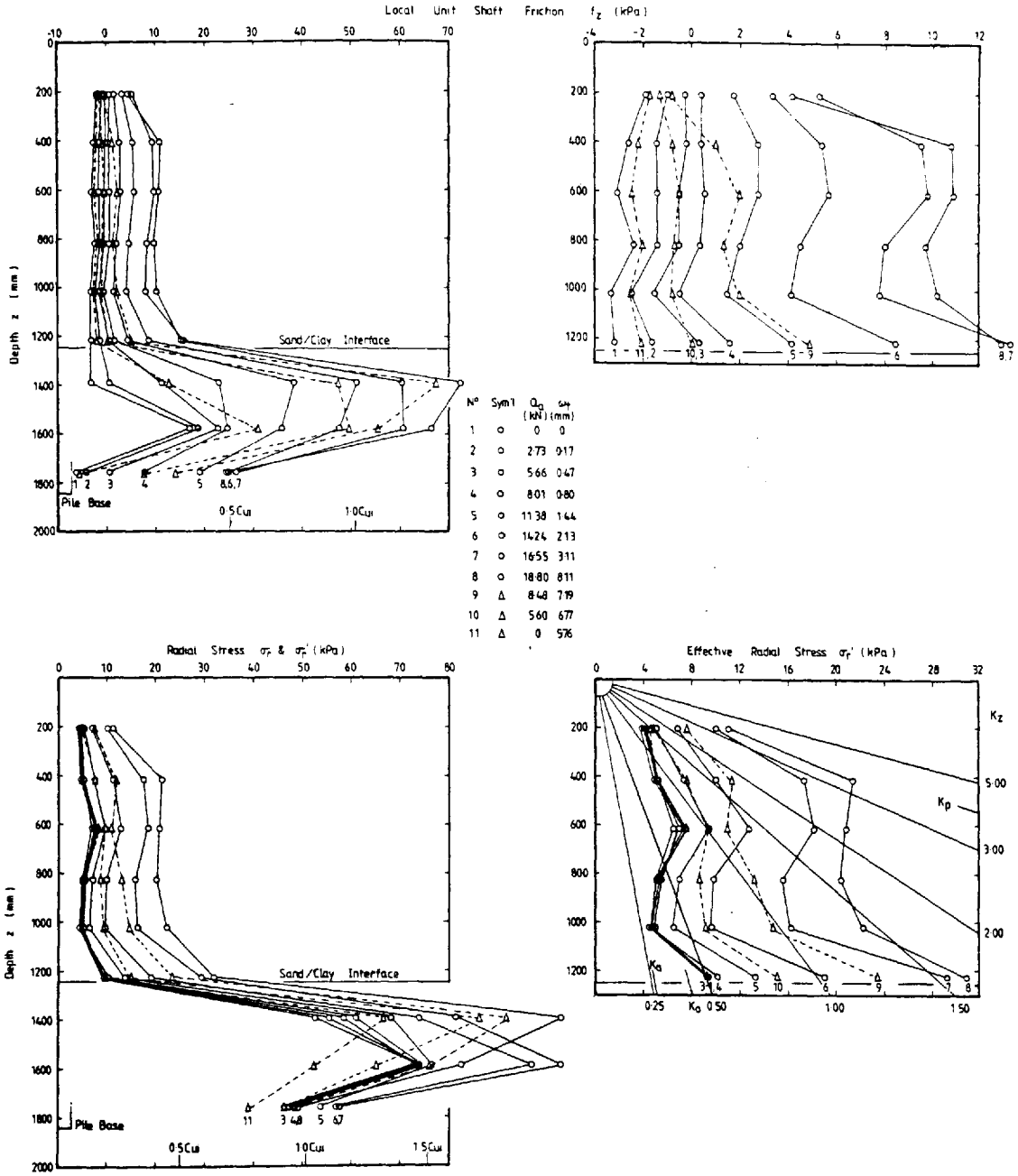

Maintained Load Test (Post-Cyclic Loading)

TEST N°5 (114 DC – S/C)

DEVELOPMENT OF LOCAL SHAFT FRICTION AND RADIAL STRESS DURING A MAINTAINED LOAD TEST (POST-CYCLIC LOADING)

FIGURE 6.21

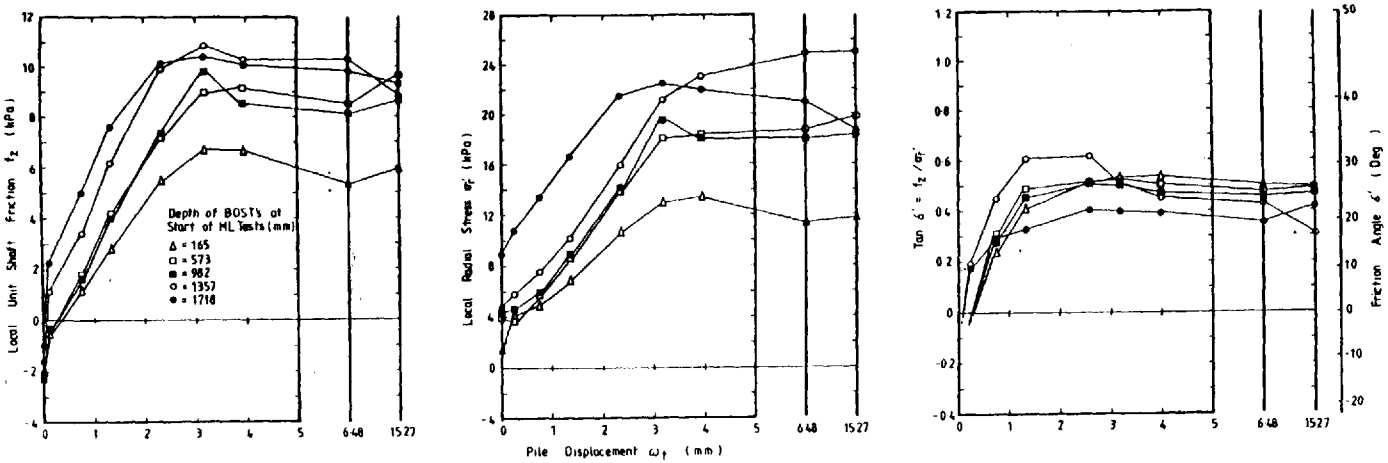

a. Maintained Load Test Series 1 (Post Installation)

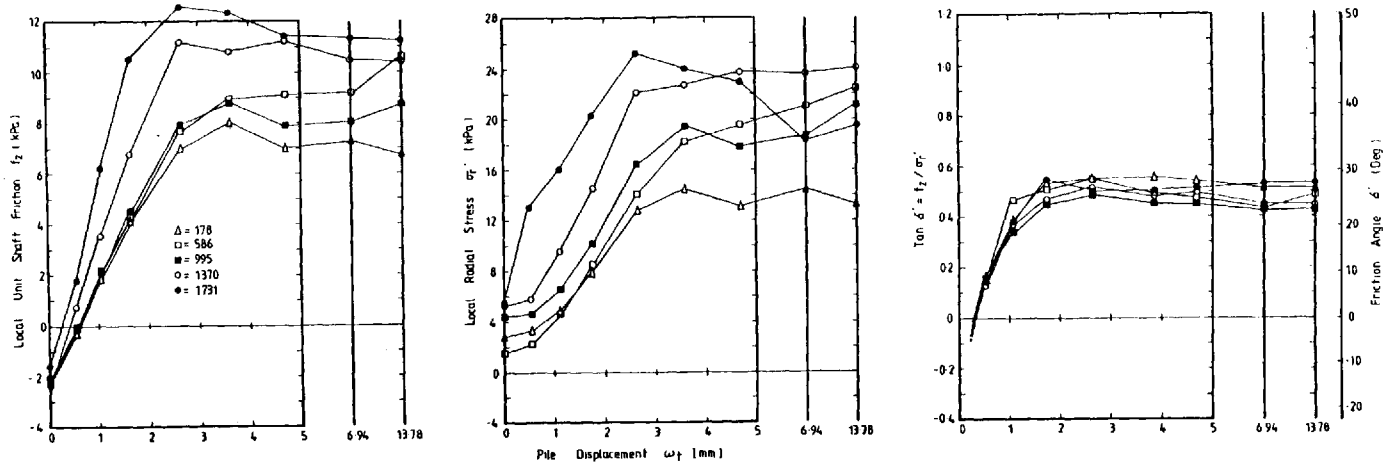

b. Maintained Load Test Series 2 (Post Cyclic Loading)

TEST N°3 (114 DC - S)

MOBILIZATION OF LOCAL UNIT SHAFT FRICTION, RADIAL STRESS AND FRICTION ANGLE AT VARIOUS LEVELS ALONG THE PILE SHAFT WITH PILE DISPLACEMENT DURING A SERIES OF MAINTAINED LOAD TESTS

FIGURE 6.22

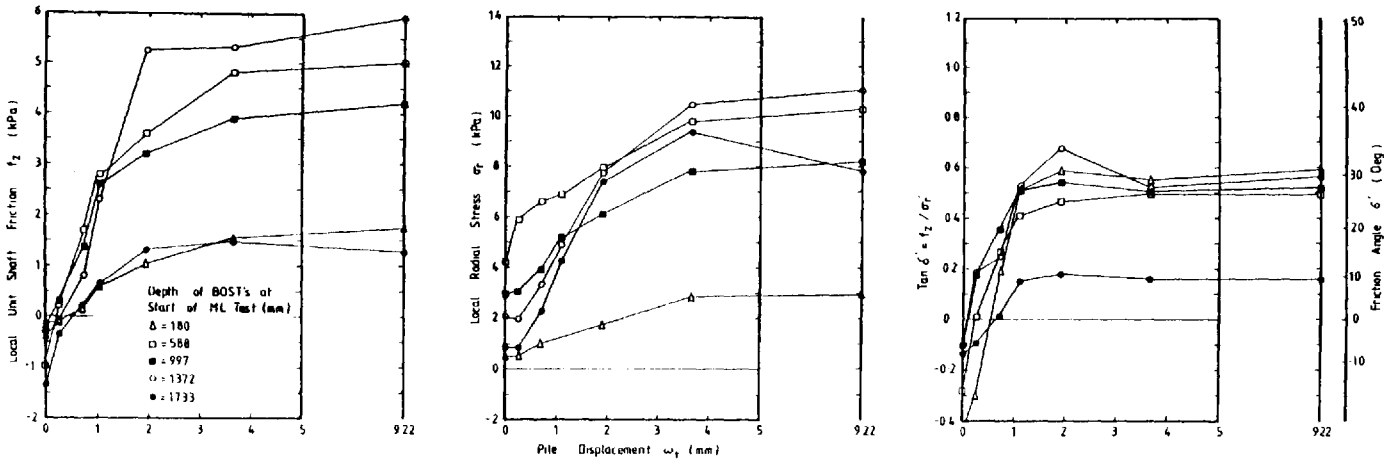

a. Maintained Load Test Series 1 (Post C.R.P. Test)

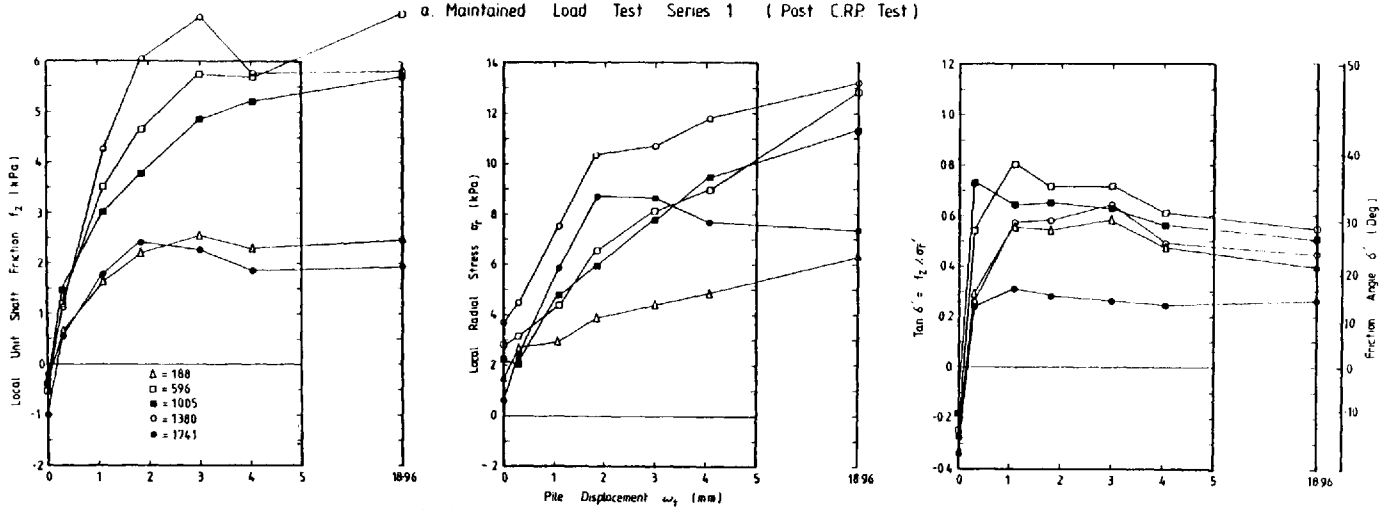

b. Maintained Load Test Series 2 (Post Cyclic Loading)

TEST N° 6 (114 IE - S)

MOBILIZATION OF LOCAL UNIT SHAFT FRICTION, RADIAL STRESS AND FRICTION ANGLE AT VARIOUS LEVELS ALONG THE PILE SHAFT WITH PILE DISPLACEMENT DURING A SERIES OF MAINTAINED LOAD TESTS

FIGURE 6,23

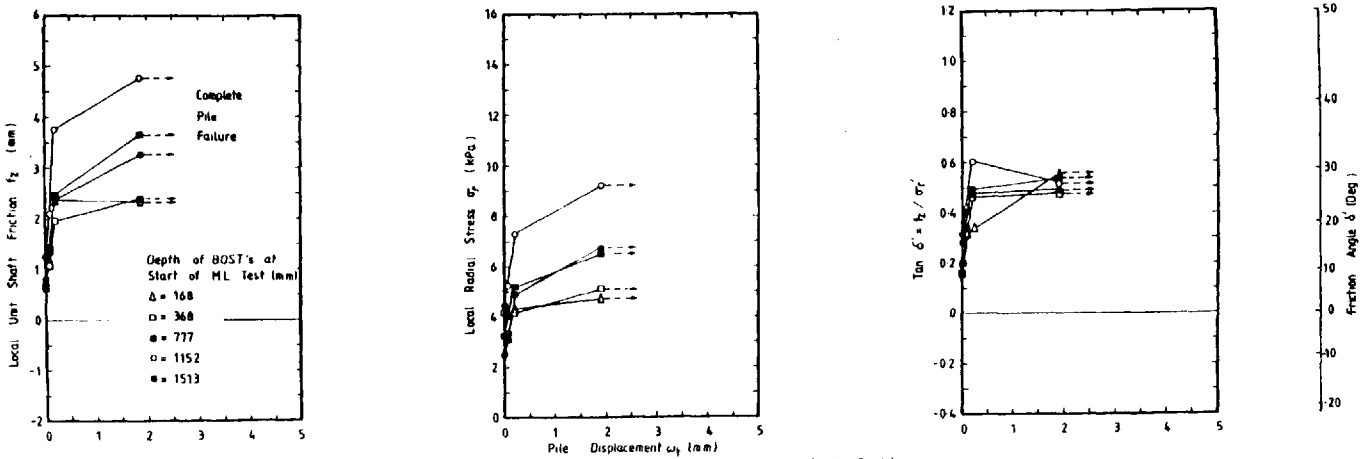

a. Maintained Load Test Series 1 (Post C.R.P. Test)

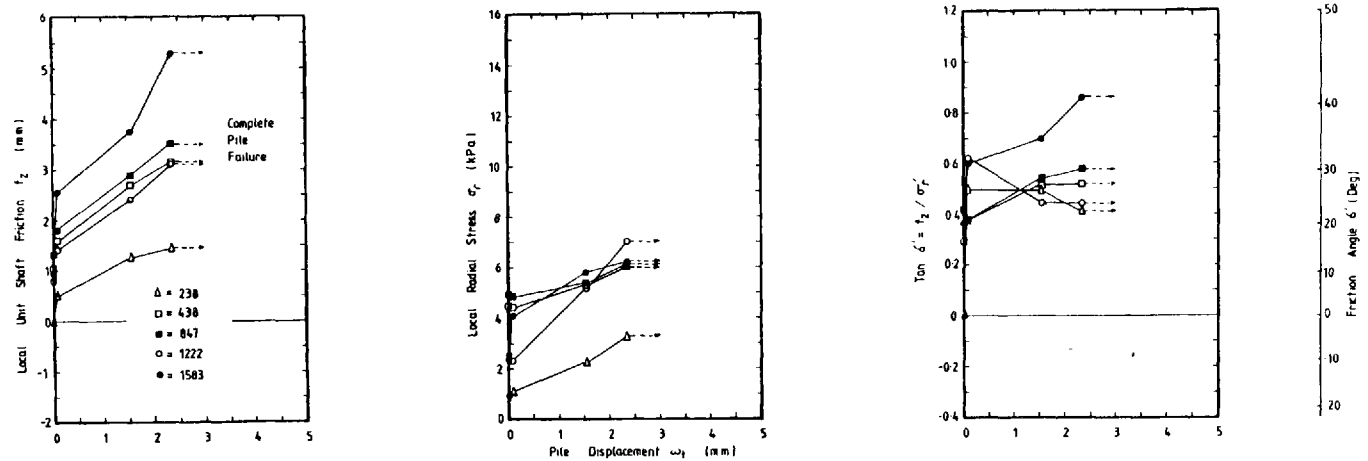

b. Maintained Load Test Series 2 (Post Cyclic Loading)

TEST N° 4 (1141N-S)

MOBILIZATION OF LOCAL UNIT SHAFT FRICTION, RADIAL STRESS AND FRICTION ANGLE AT VARIOUS LEVELS ALONG THE PILE SHAFT WITH PILE DISPLACEMENT DURING A SERIES OF MAINTAINED LOAD TESTS

FIGURE 6.24

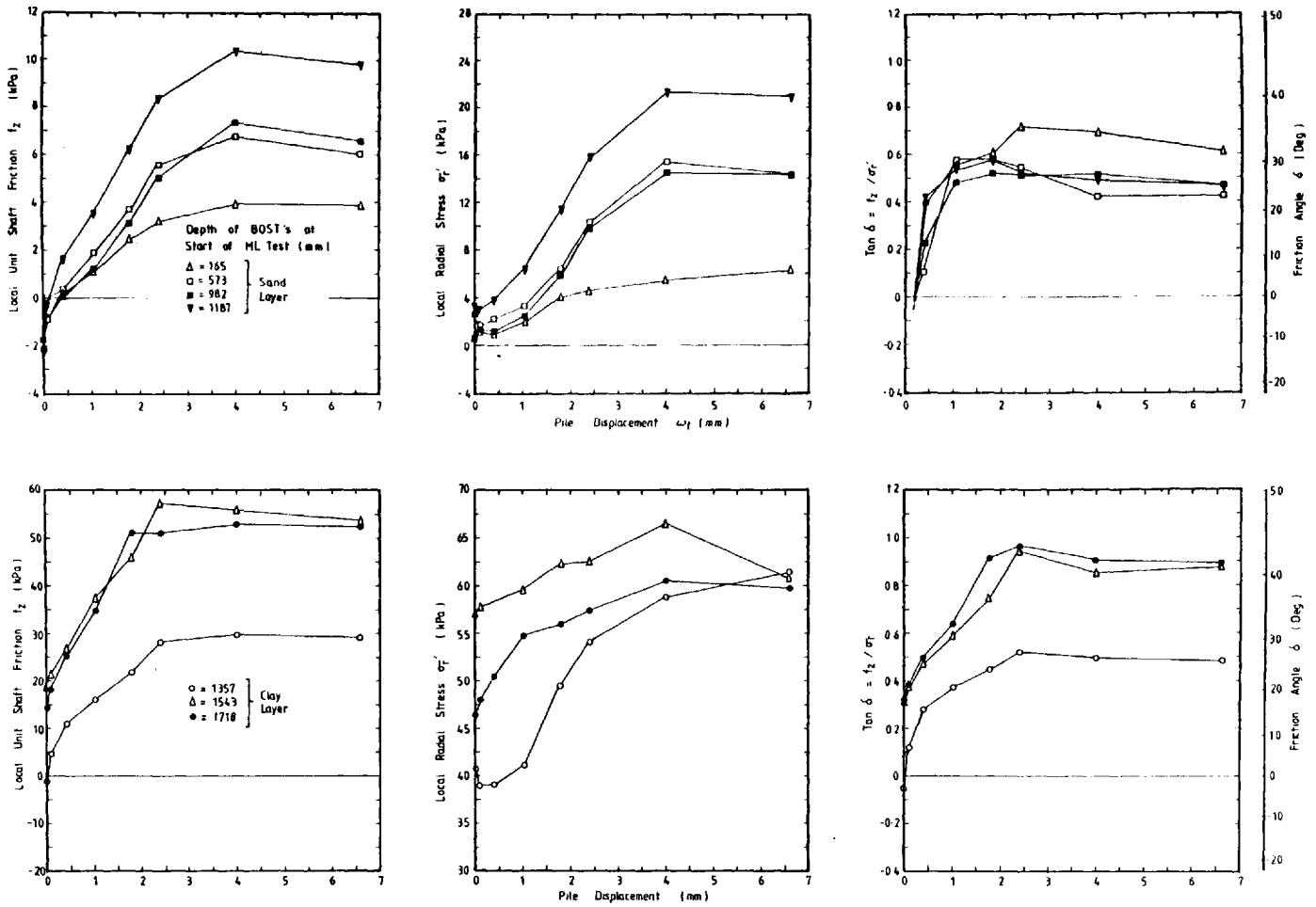

Maintained Load Test (Post - Installation)

TEST N°S (114DC - S/C)

MOBILIZATION OF LOCAL UNIT SHAFT FRICTION, RADIAL STRESS AND FRICTION ANGLE AT VARIOUS LEVELS ALONG THE PILE SHAFT WITH PILE DISPLACEMENT DURING A MAINTAINED LOAD TEST (POST INSTALLATION)

FIGURE 6,25

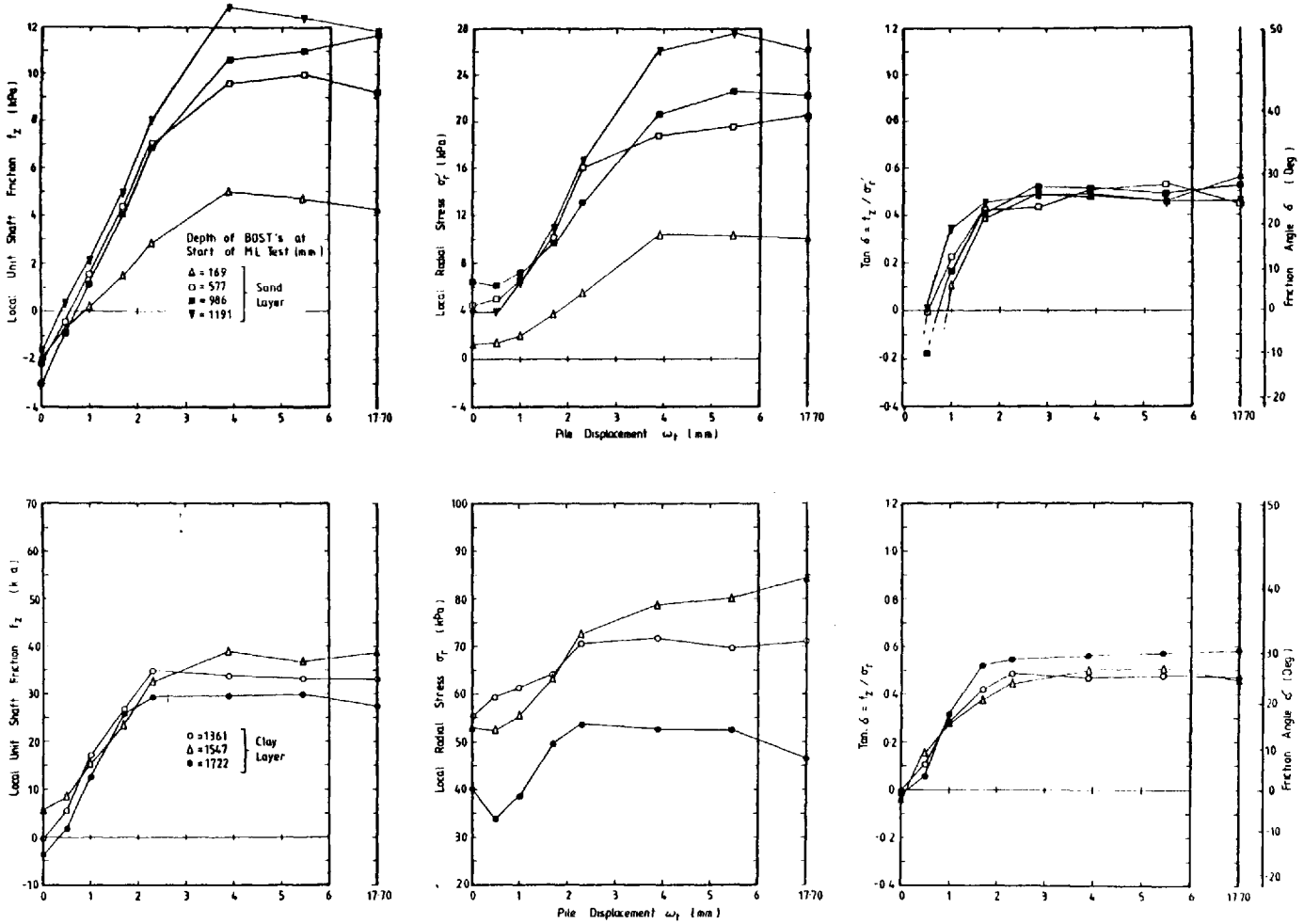

Maintained Load Test (Post - Dissipation of Pore Pressure)
TEST N°5 (114DC -S/C)

MOBILIZATION OF LOCAL UNIT SHAFT FRICTION, RADIAL STRESS AND FRICTION ANGLE AT VARIOUS LEVELS ALONG PILE SHAFT WITH PILE DISPLACEMENT DURING A MAINTAINED LOAD TEST (POST-DISSIPATION OF PORE PRESSURE)

FIGURE 6.26

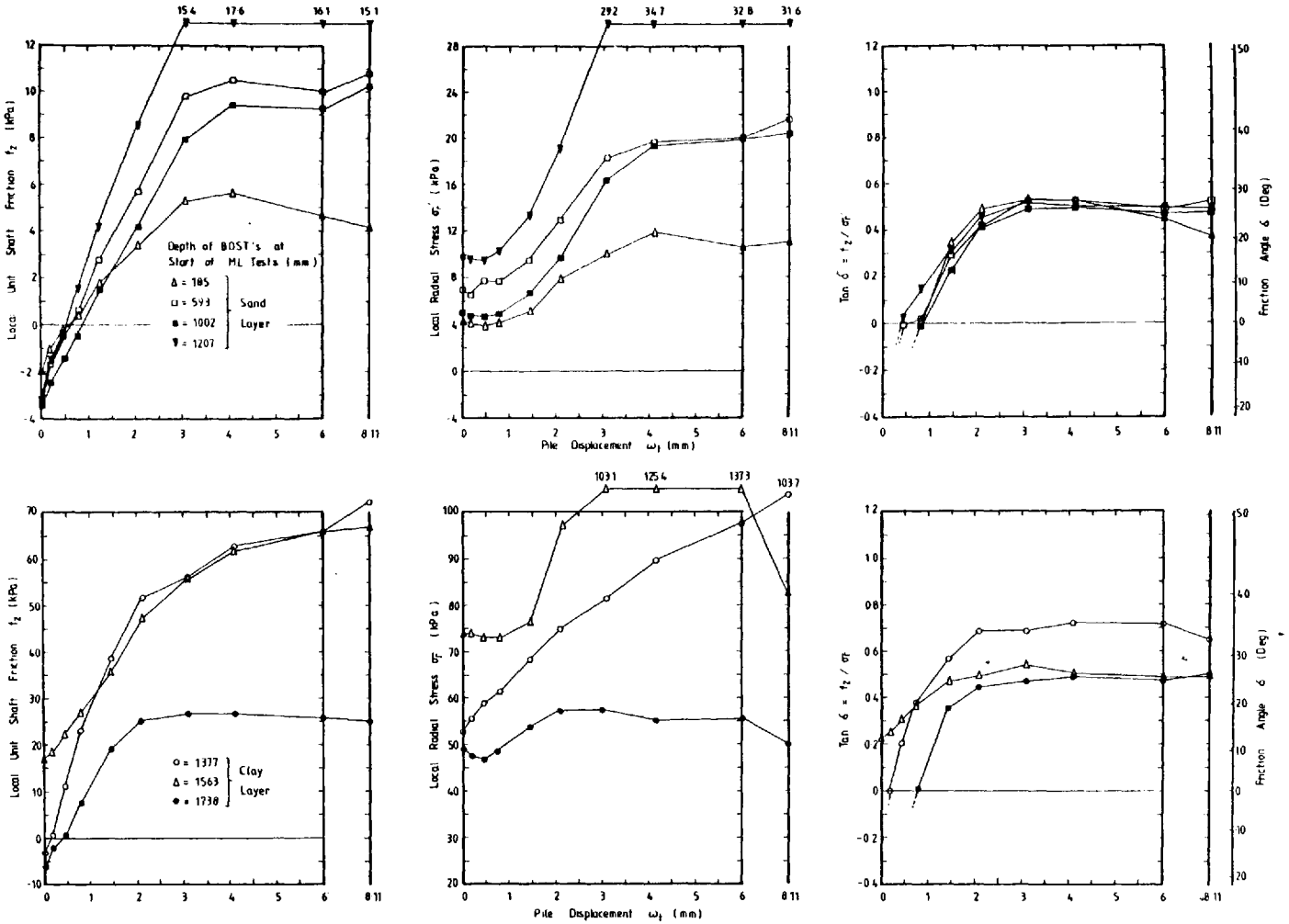

Maintained Load Test (Post-Cyclic Loading)
TEST N°5 (114DC-S/C)

MOBILIZATION OF LOCAL UNIT SHAFT FRICTION, RADIAL STRESS AND FRICTION ANGLE AT VARIOUS LEVELS ALONG THE PILE SHAFT WITH PILE DISPLACEMENT DURING A MAINTAINED LOAD TEST (POST CYCLIC LOADING)

FIGURE 6.27

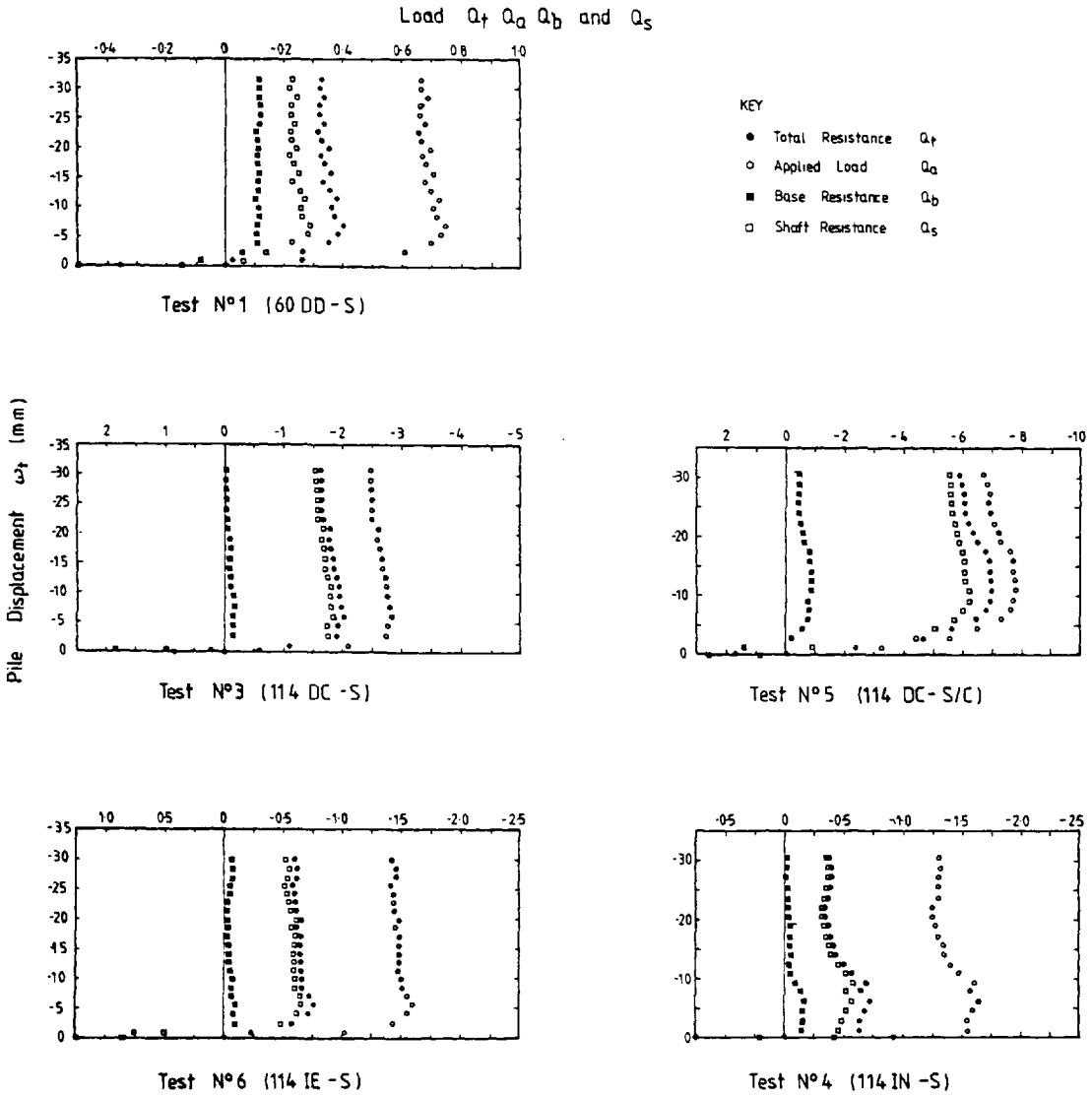

FIGURE N° 6.28 CONSTANT RATE OF UPLIFT TEST
(Rate = 1·524 mm / minute)

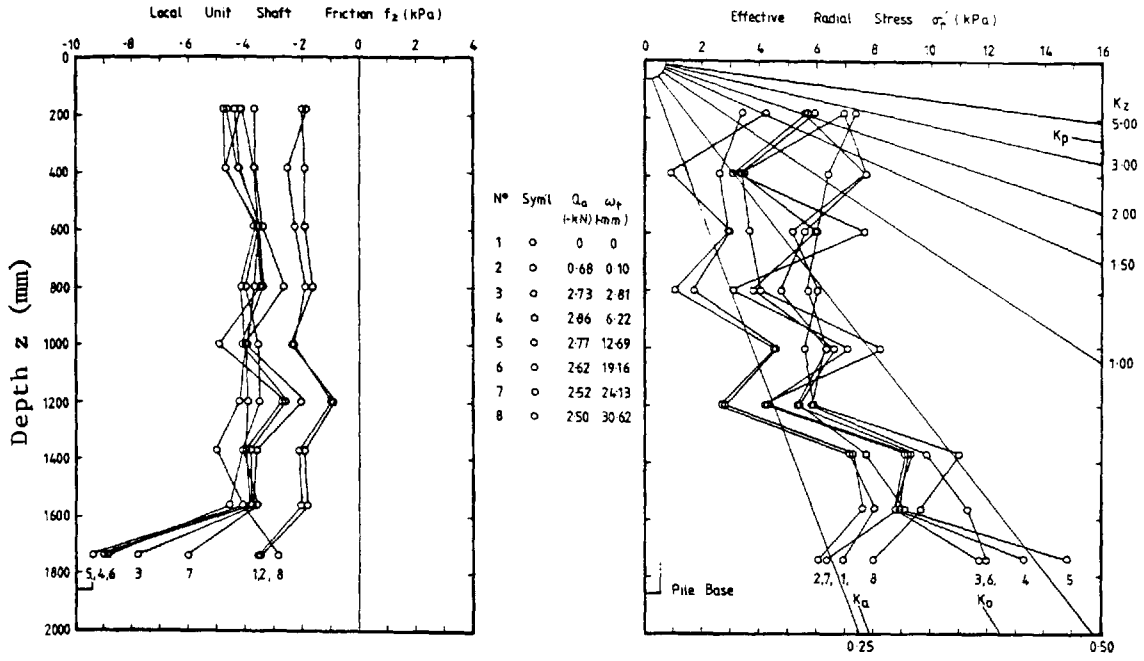

a. Test N° 3 (114DC - S)

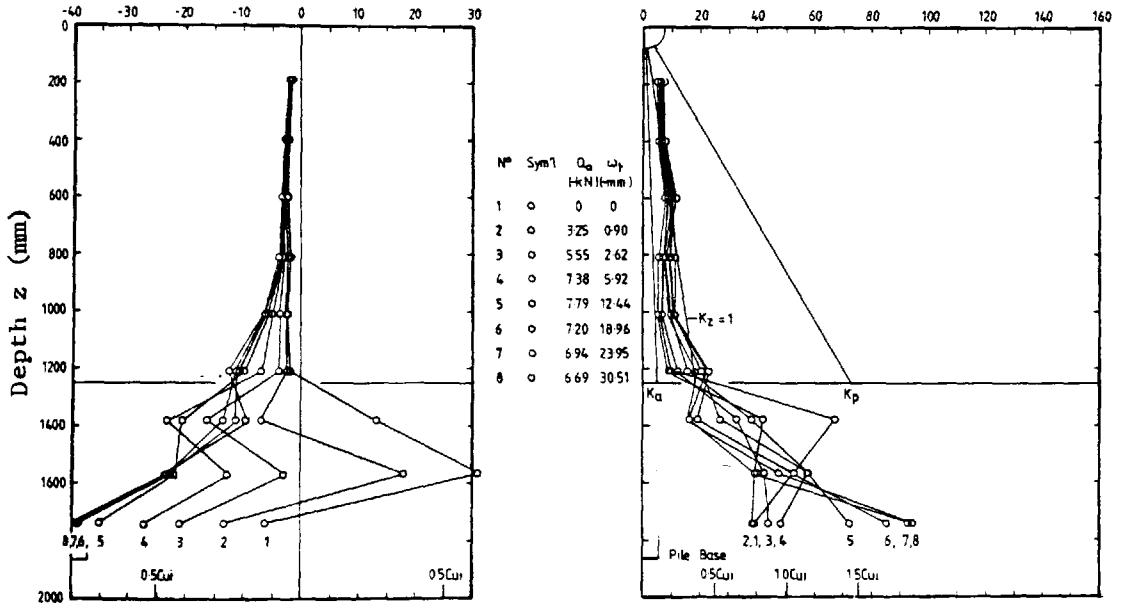

b. Test N° 5 (114 DC-S/C)

DEVELOPMENT OF LOCAL SHAFT FRICTION AND EFFECTIVE RADIAL STRESS DURING THE CONSTANT RATE OF UPLIFT TEST

FIGURE 6.29

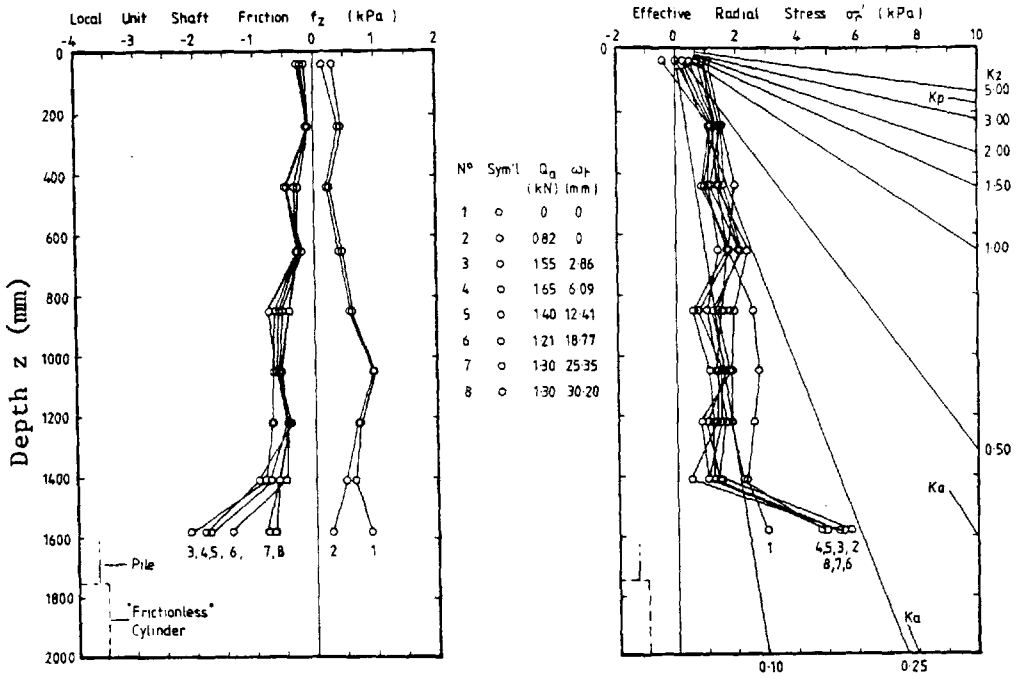

a. Test N° 4 (114IN-S)

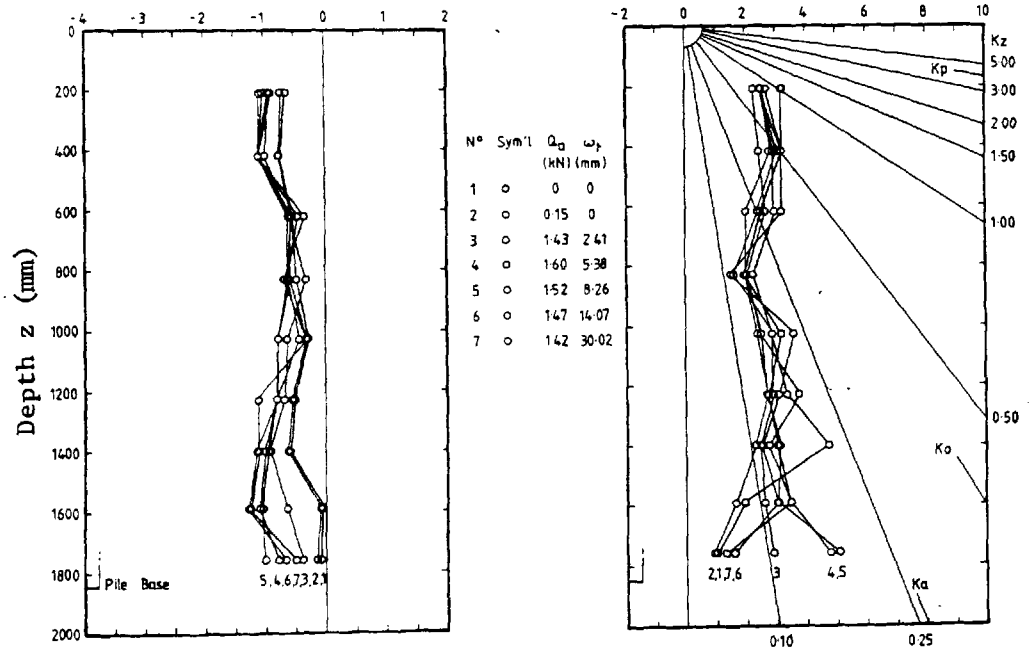

b. Test N°6 (114IE-S)

DEVELOPMENT OF LOCAL SHAFT FRICTION AND EFFECTIVE RADIAL STRESS DURING THE CONSTANT RATE OF UPLIFT TEST

FIGURE 6.30

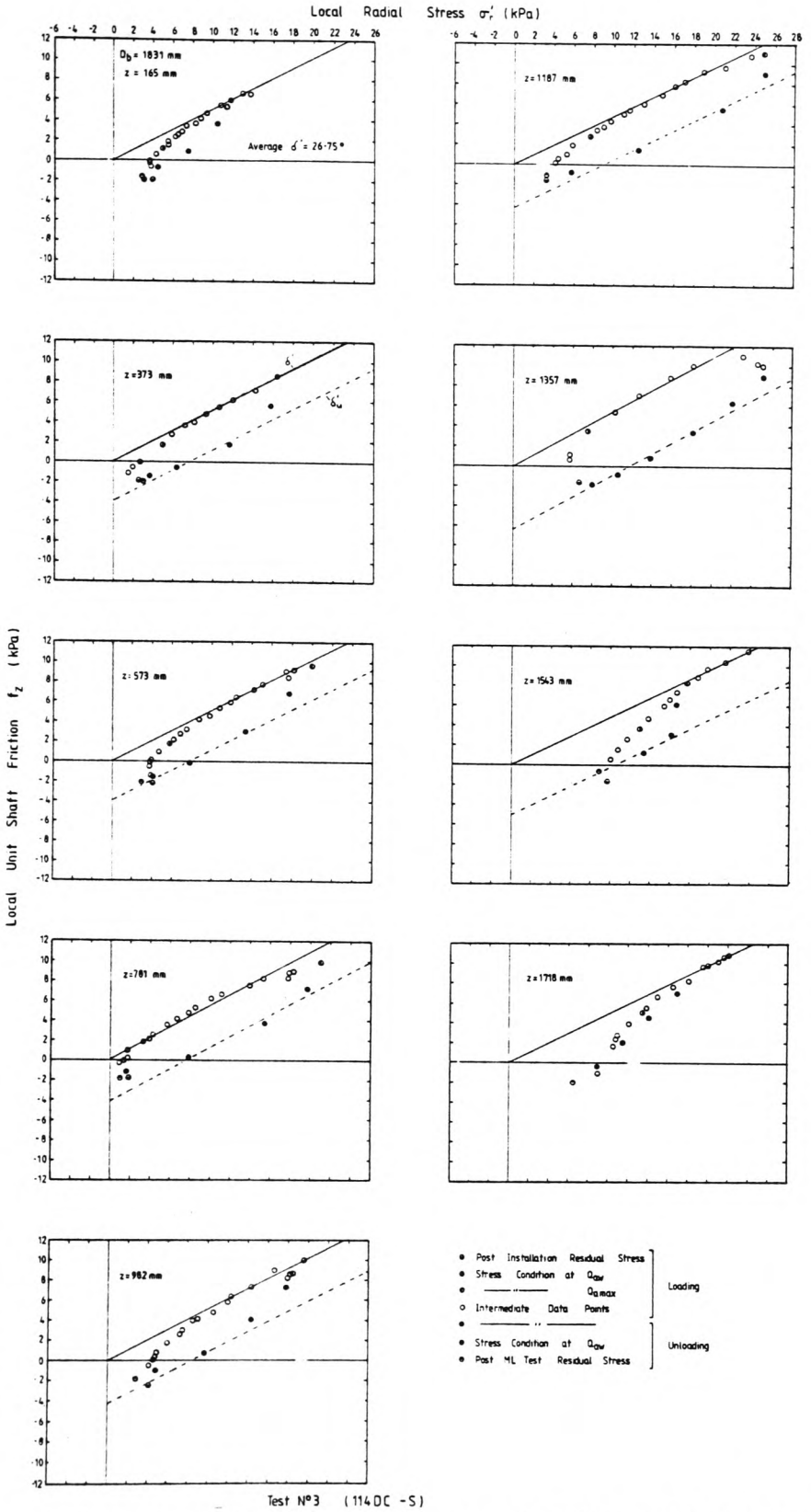

Test N°3 (114 DC - S)

DEVELOPMENT AND INTERDEPENDENCE OF THE LOCAL UNIT SHAFT FRICTION WITH THE LOCAL RADIAL STRESS AT VARIOUS LEVELS ALONG THE PILE SHAFT DURING THE MAINTAINED LOAD TEST (ML TEST POST INSTALLATION)

FIGURE N° 6,31

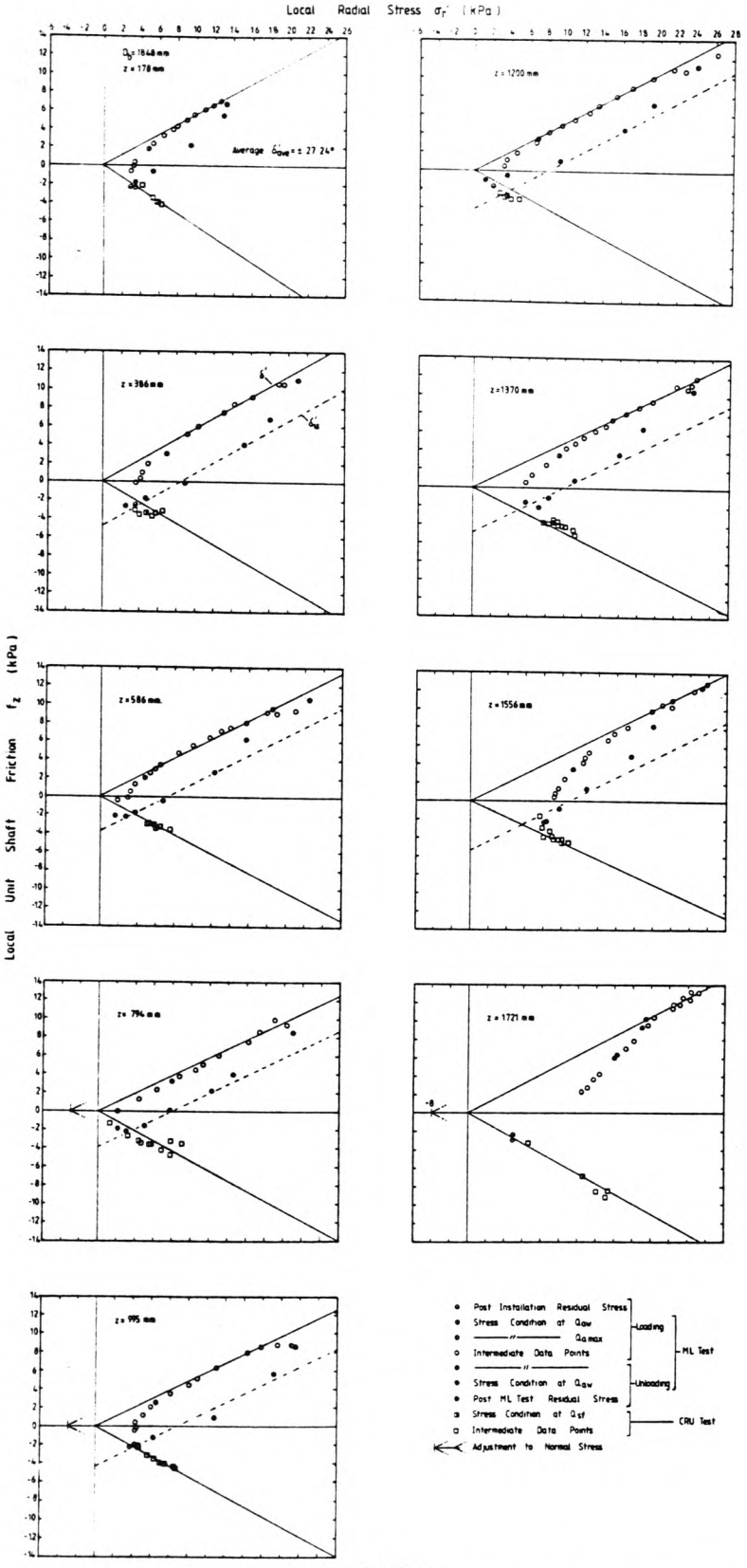

Test N°3 (114DC-S)

DEVELOPMENT AND INTERDEPENDENCE OF THE LOCAL UNIT SHAFT FRICTION WITH THE LOCAL RADIAL STRESS AT VARIOUS LEVELS ALONG THE PILE SHAFT DURING THE MAINTAINED LOAD AND CONSTANT RATE OF UPLIFT TESTS. (POST CYCLIC LOADING)

FIGURE N° 6.32

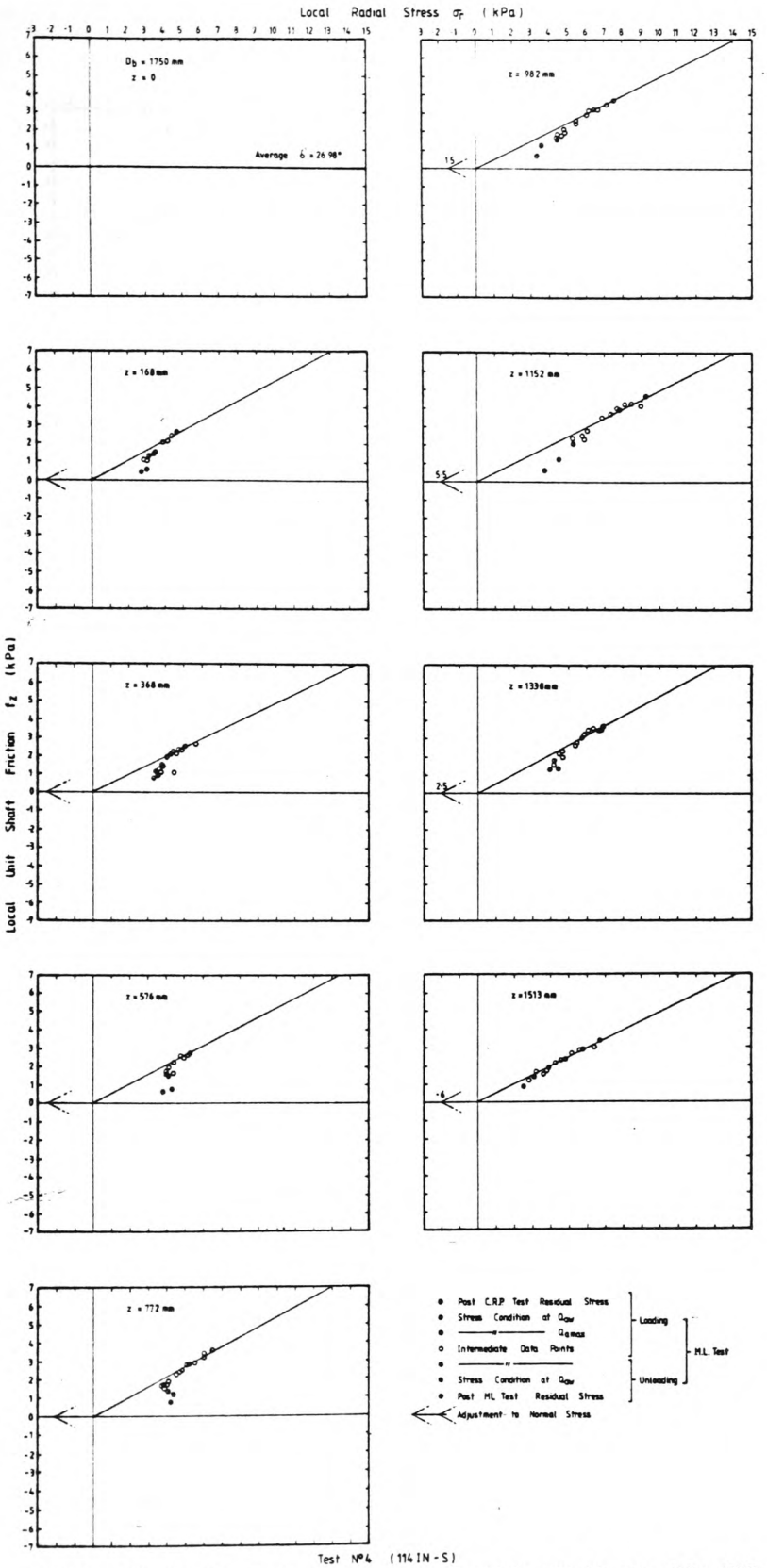

Test N°4 (114 IN - S)

DEVELOPMENT AND INTERDEPENDENCE OF THE LOCAL UNIT SHAFT FRICTION WITH THE LOCAL RADIAL STRESS AT VARIOUS LEVELS ALONG THE PILE SHAFT DURING THE MAINTAINED LOAD TEST (POST CRP TEST)

FIGURE N° 6.33

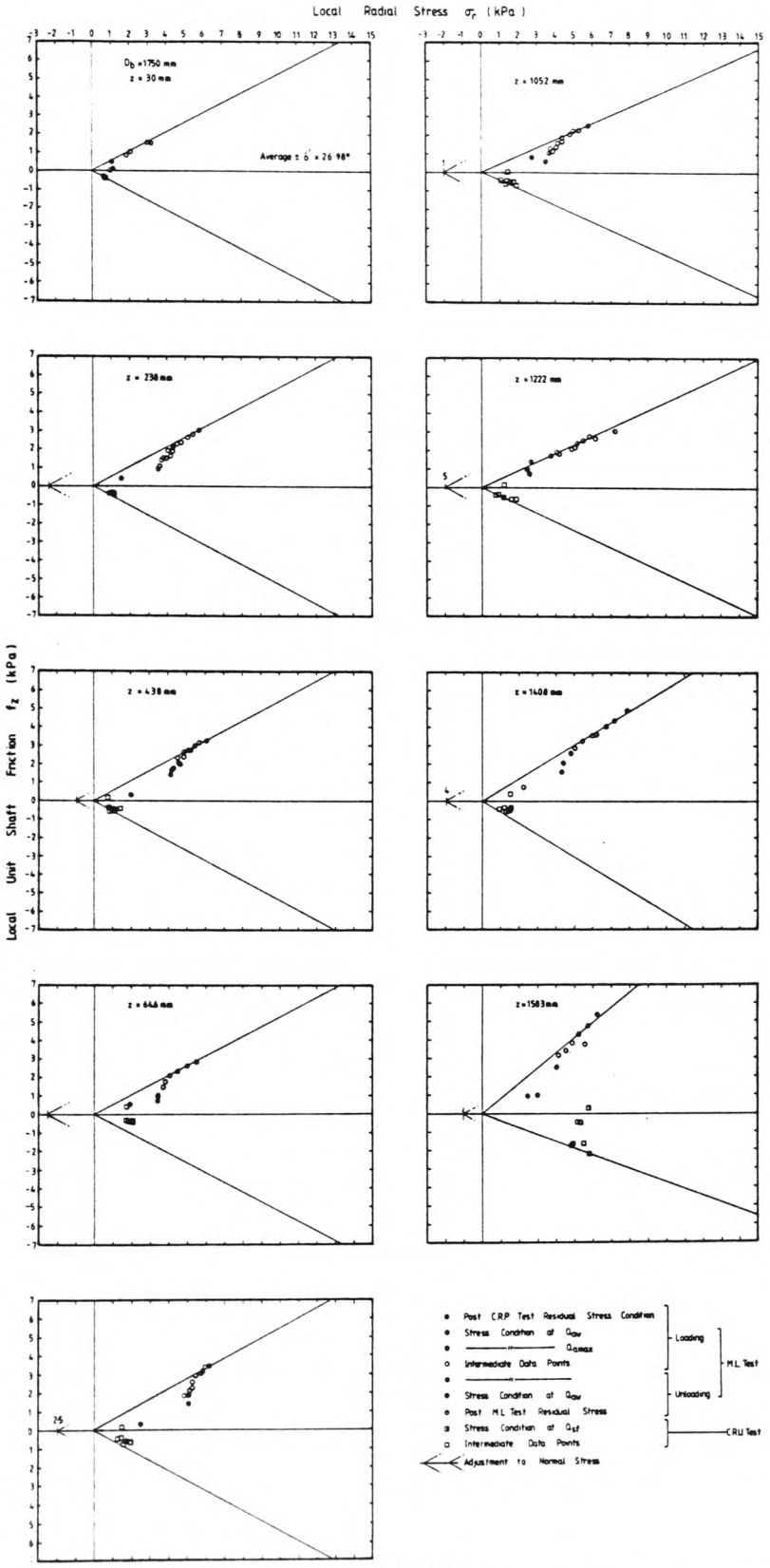

Test N°4 (114 IN - S)

DEVELOPMENT AND INTERDEPENDENCE OF THE LOCAL UNIT SHAFT FRICTION WITH THE LOCAL RADIAL STRESS AT VARIOUS LEVELS ALONG THE PILE SHAFT DURING THE MAINTAINED LOAD AND CONSTANT RATE OF UPLIFT TEST (POST CYCLIC LOADING)

FIGURE N°6.34

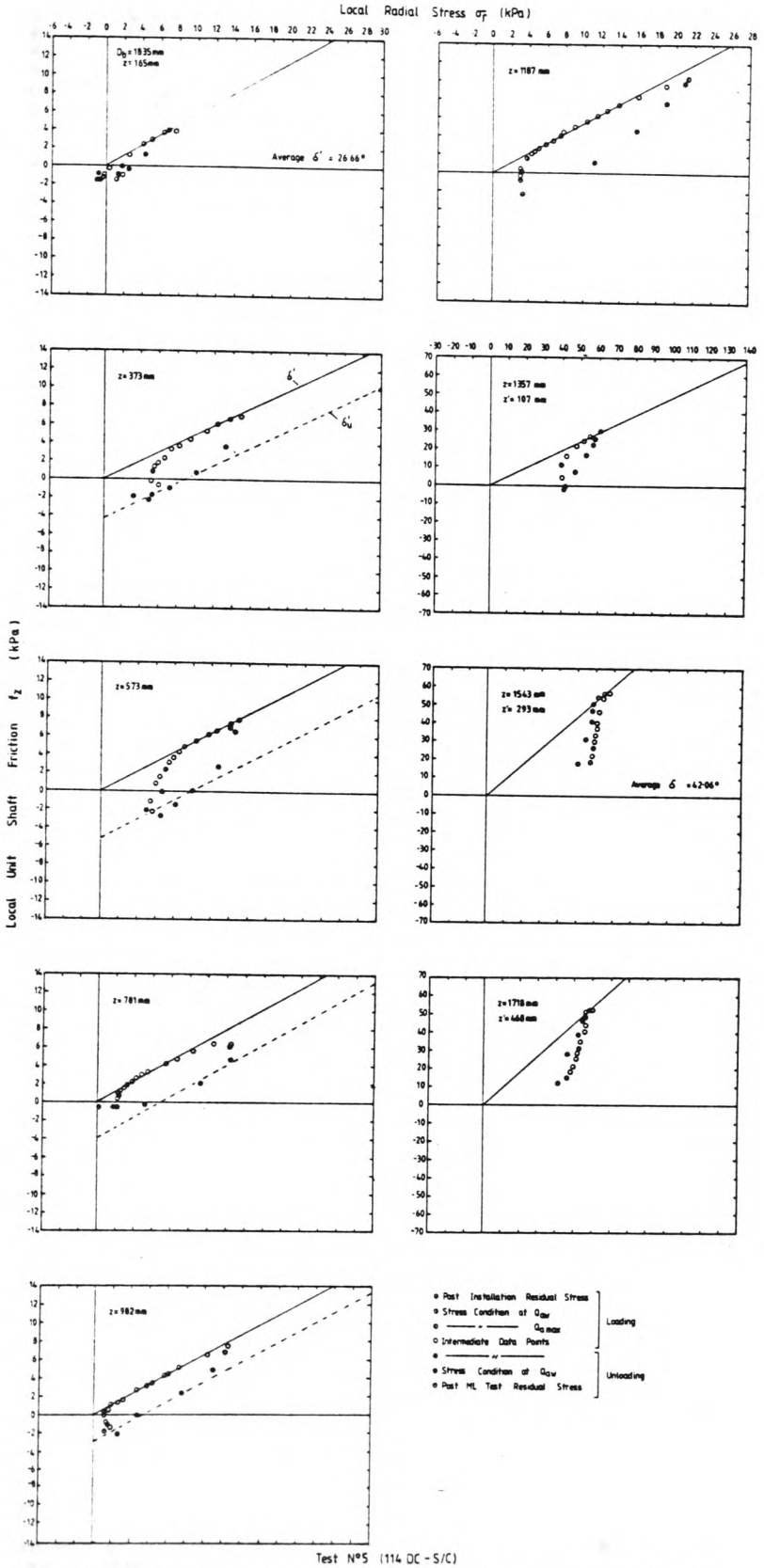

DEVELOPMENT AND INTERDEPENDENCE OF THE LOCAL UNIT SHAFT FRICTION WITH THE LOCAL RADIAL STRESS AT VARIOUS LEVELS ALONG THE PILE SHAFT DURING THE MAINTAINED LOAD TEST (ML TEST POST INSTALLATION)

FIGURE N° 6.35

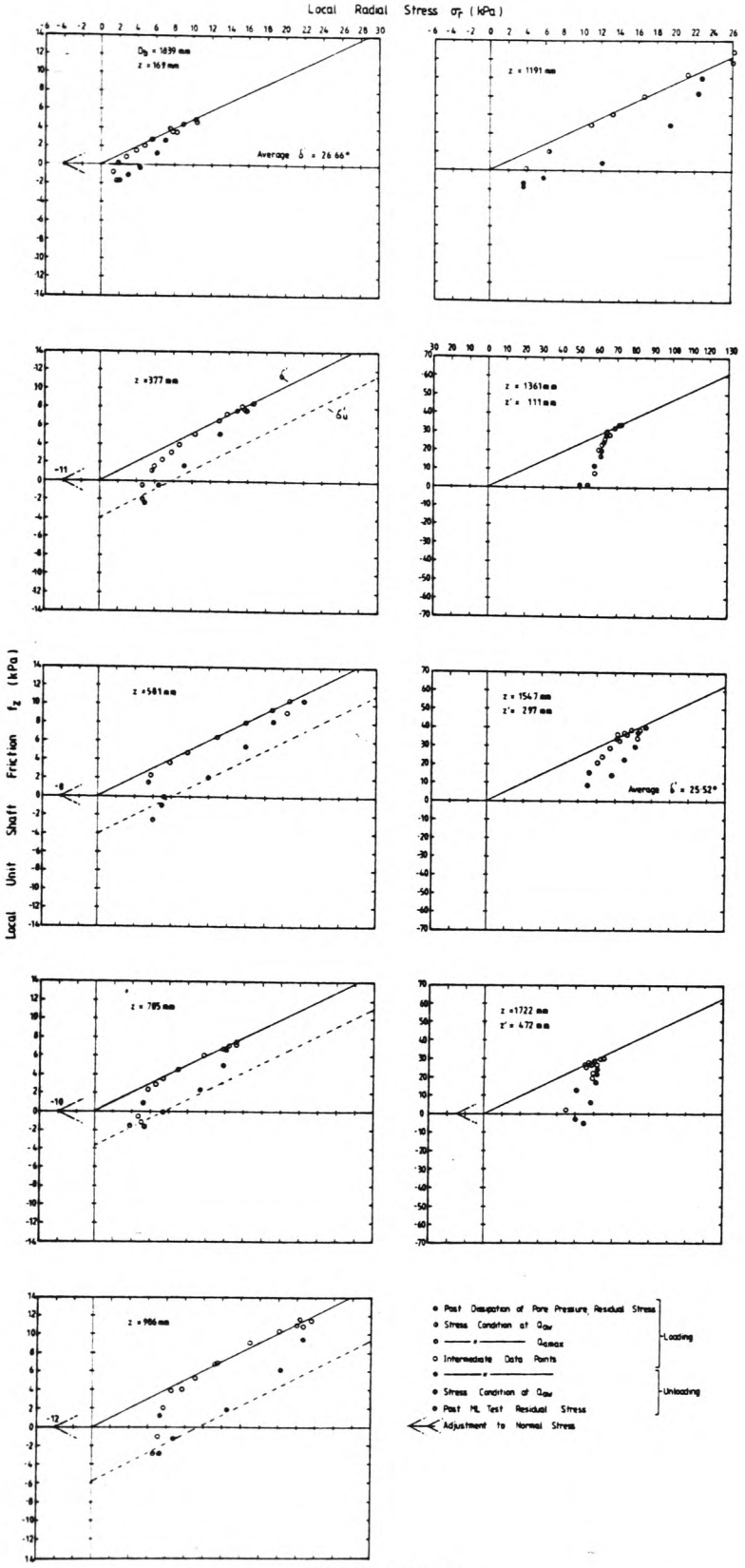

Test N°5 (114 DC-S/C)

DEVELOPMENT AND INTERDEPENDENCE OF THE LOCAL UNIT SHAFT FRICTION WITH THE LOCAL RADIAL STRESS AT VARIOUS LEVELS ALONG THE PILE SHAFT DURING THE MAINTAINED LOAD TEST
(M.L. TEST POST-DISSIPATION OF PORE PRESSURE)

FIGURE 6.36

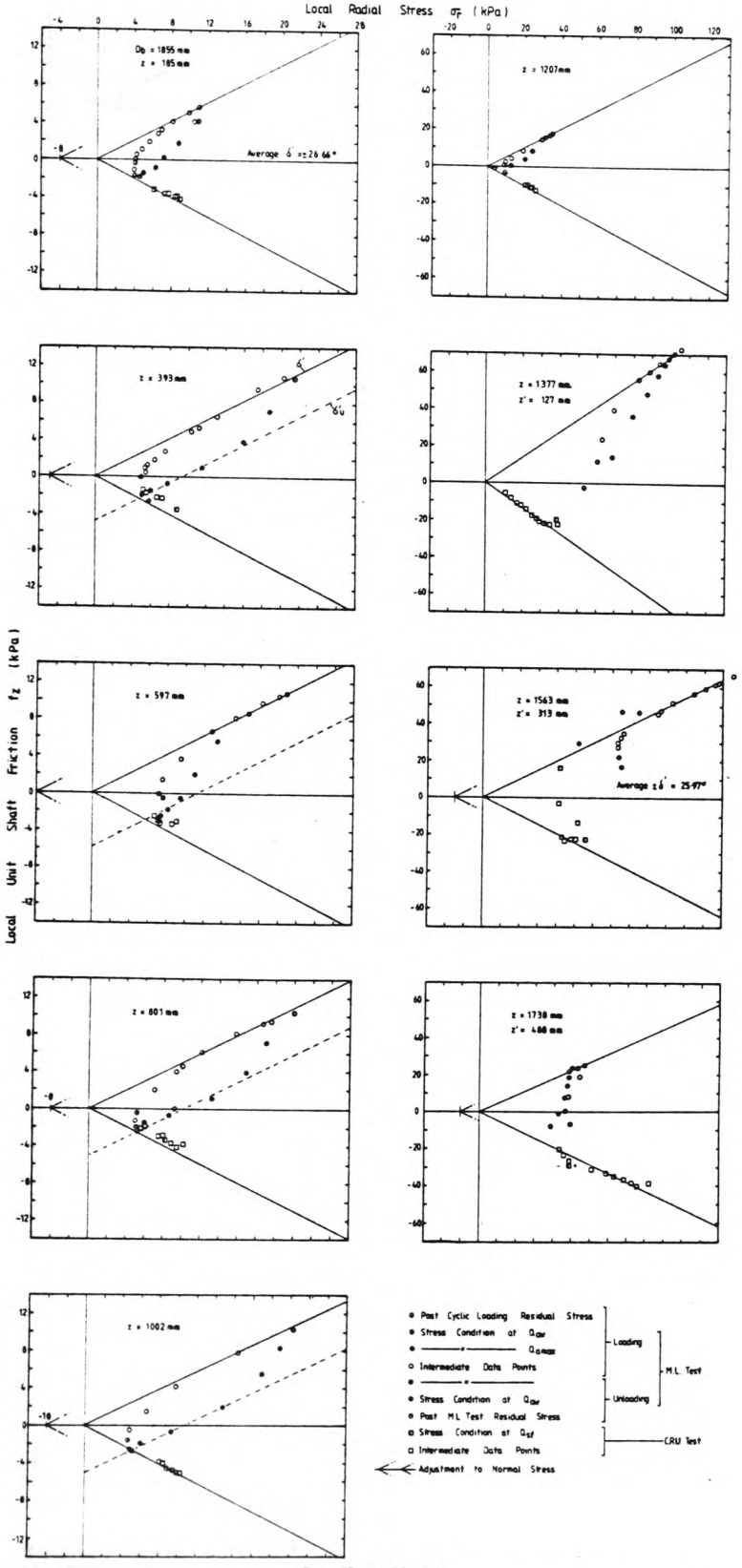

Test N°S (114 DC - S/C)

DEVELOPMENT AND INTERDEPENDENCE OF THE LOCAL UNIT SHAFT FRICTION WITH THE RADIAL STRESS AT VARIOUS LEVELS ALONG THE PILE SHAFT DURING THE MAINTAINED LOAD AND CONSTANT RATE OF UPLIFT TESTS (POST - CYCLIC LOADING)

FIGURE N° 6.37

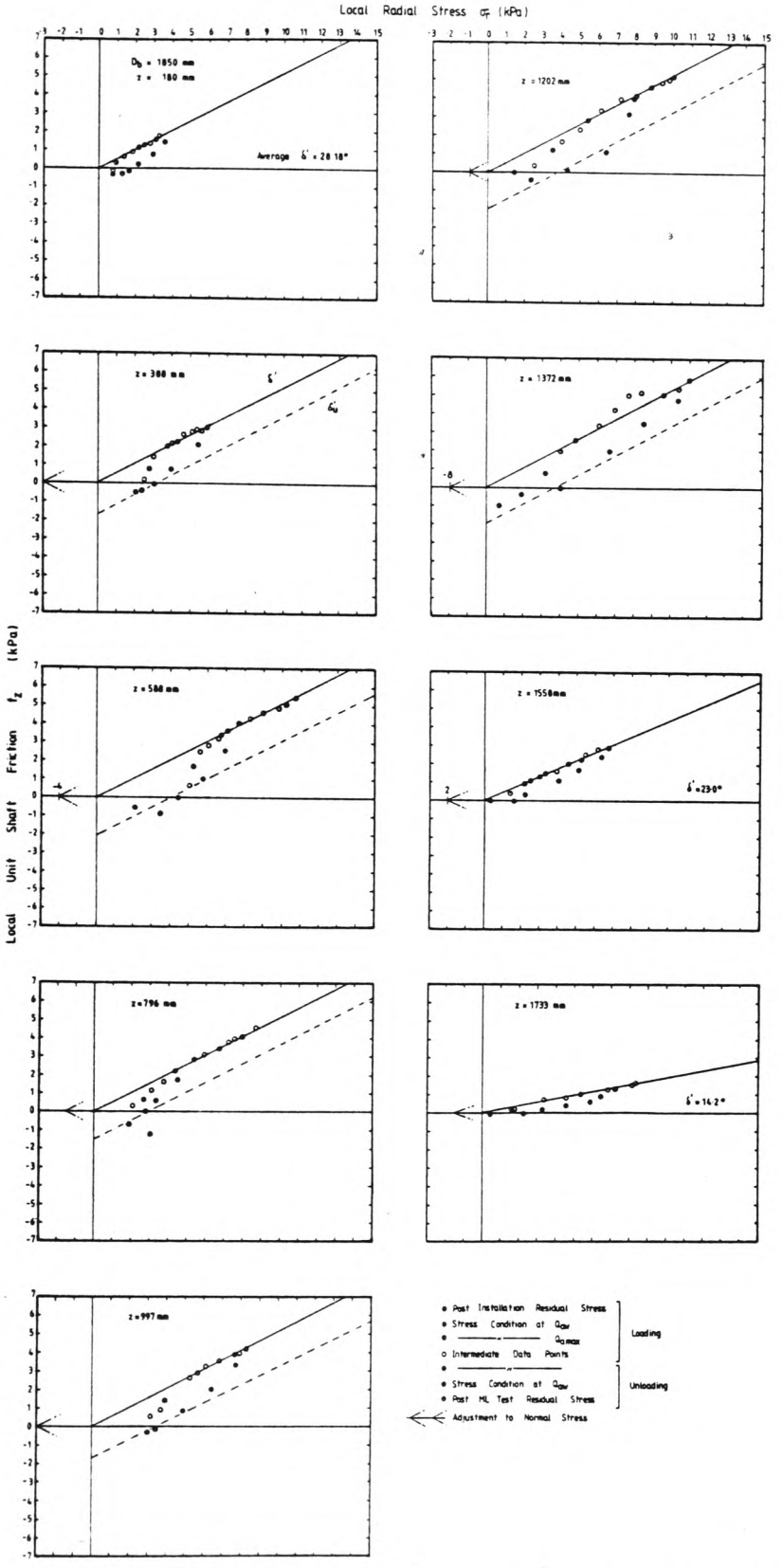

Test N°6 (114 IE-S)

DEVELOPMENT AND INTERDEPENDENCE OF THE LOCAL UNIT SHAFT FRICTION AND THE LOCAL RADIAL STRESS AT VARIOUS LEVELS ALONG THE PILE SHAFT DURING THE MAINTAINED LOAD TEST (ML TEST POST INSTALLATION)

FIGURE N° 6.38

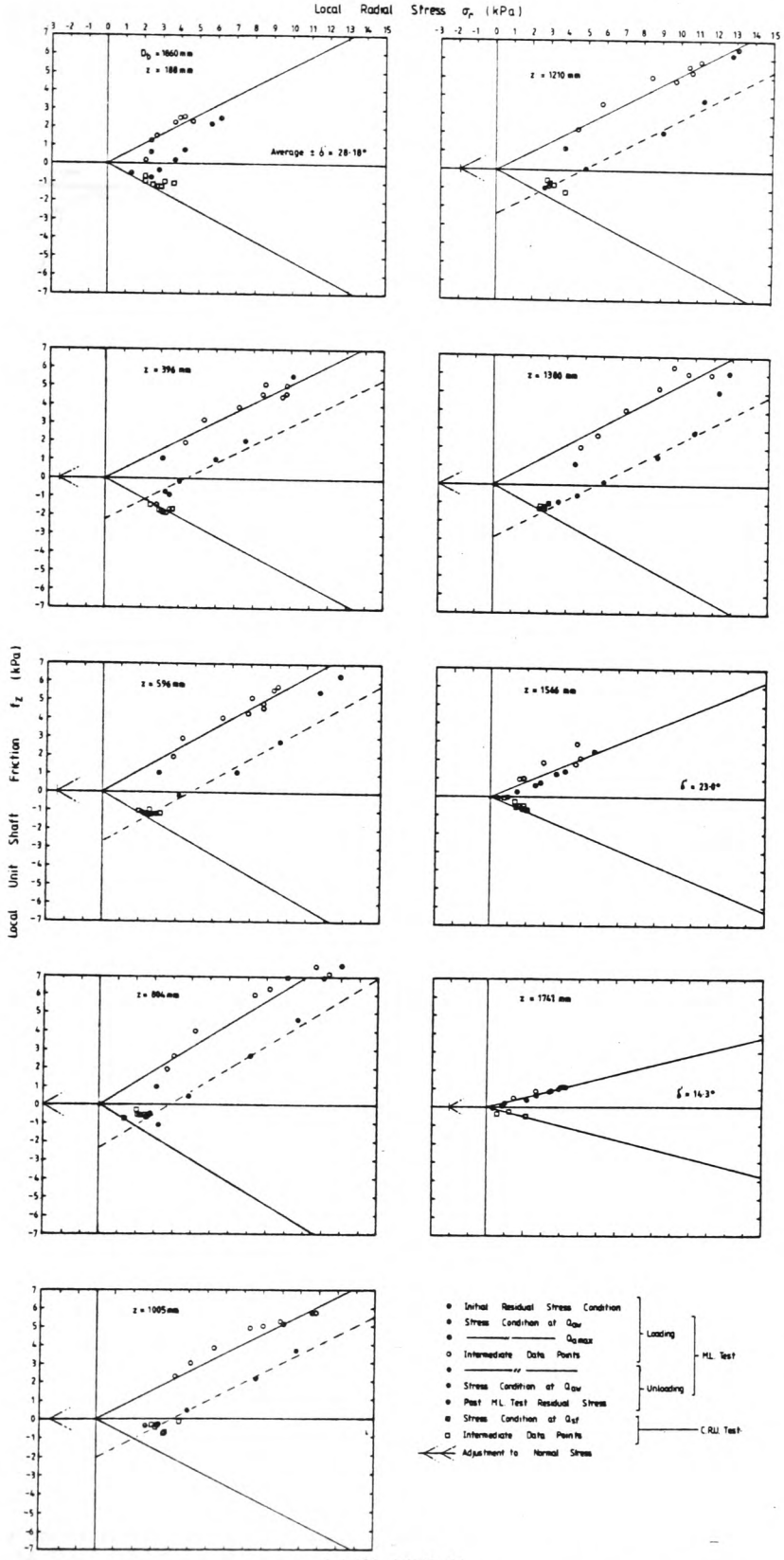

Test N° 6 (114 IE – S)

DEVELOPMENT AND INTERDEPENDENCE OF THE LOCAL UNIT SHAFT FRICTION WITH THE LOCAL RADIAL STRESS AT VARIOUS LEVELS ALONG THE PILE SHAFT DURING THE MAINTAINED LOAD AND CONSTANT RATE OF UPLIFT TESTS. (POST CYCLIC LOADING)

FIGURE N° 6.39

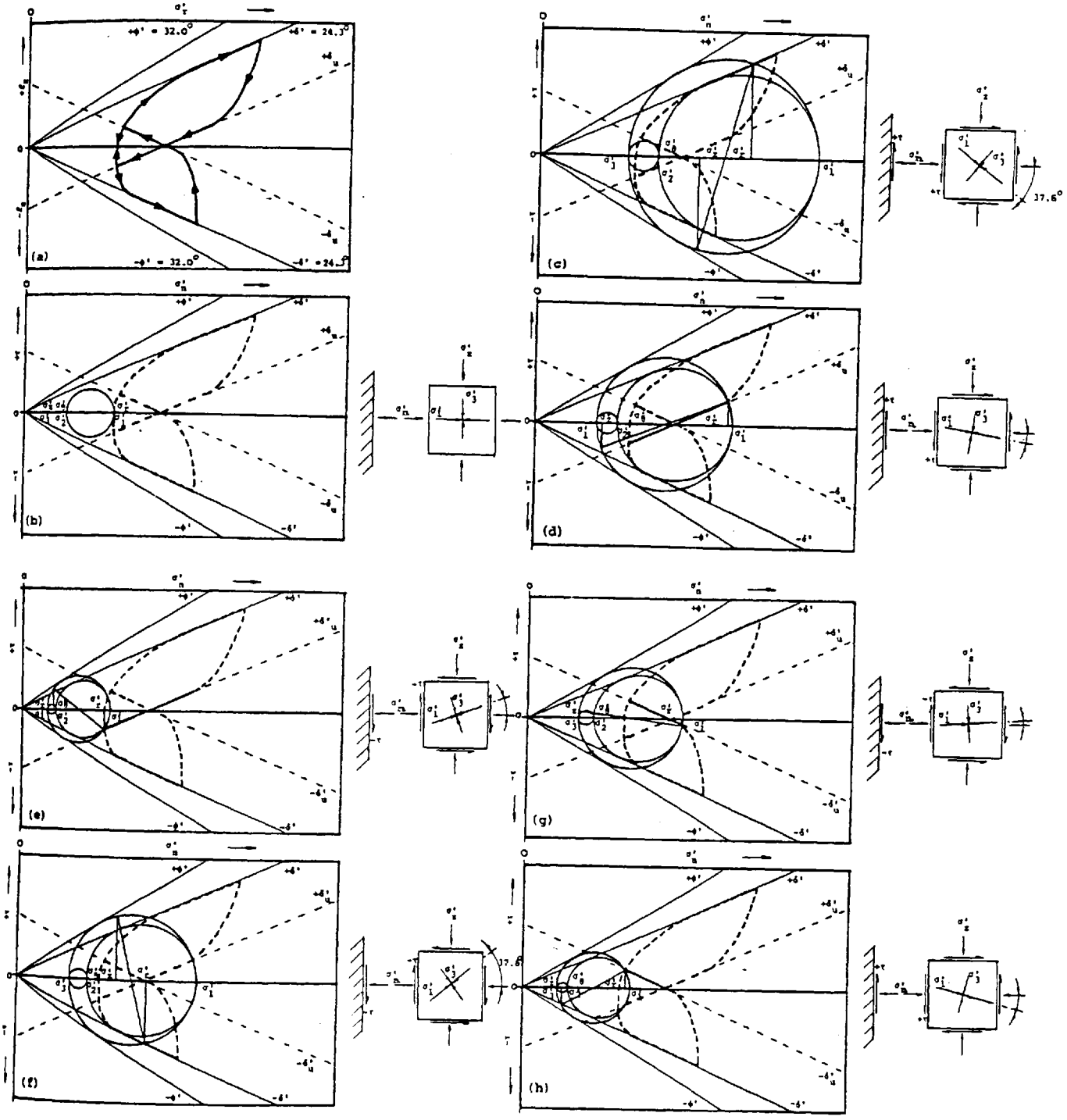

IDEALIZED EFFECTIVE STRESS HISTORY ACTING ON A PRISMATIC ELEMENT OF SAND ADJACENT TO THE PILE SHAFT DURING COMPRESSIVE AND TENSILE PILE LOADING

AFTER WERSCHING (1987)

FIGURE 6.40

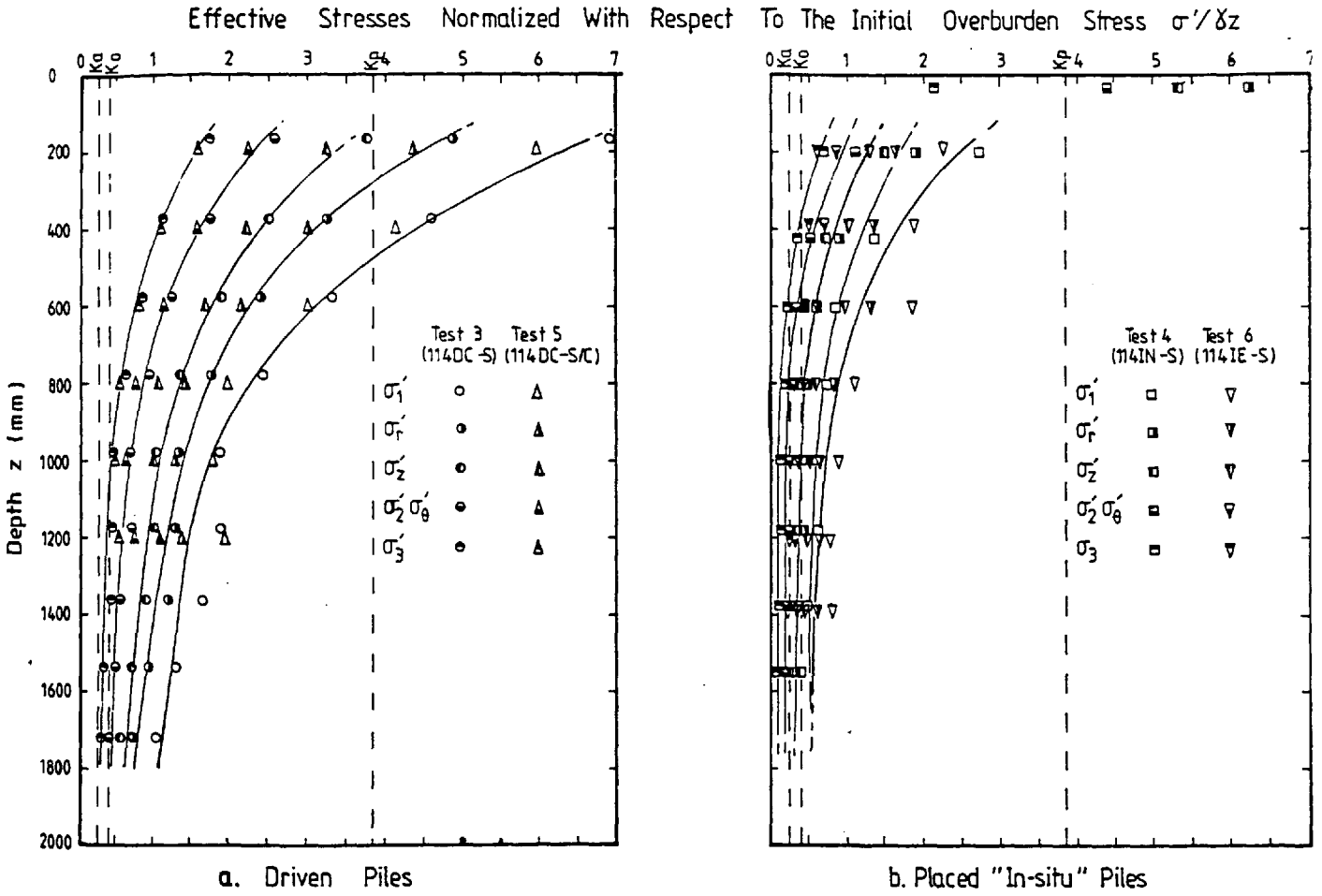

VARIATION IN THE NORMALIZED EFFECTIVE STRESSES ACTING ON A PRISMATIC ELEMENT OF SAND ADJACENT TO THE PILE SHAFT WITH DEPTH AT MAXIMUM APPLIED COMPRESSIVE LOAD

FIGURE N°6.41

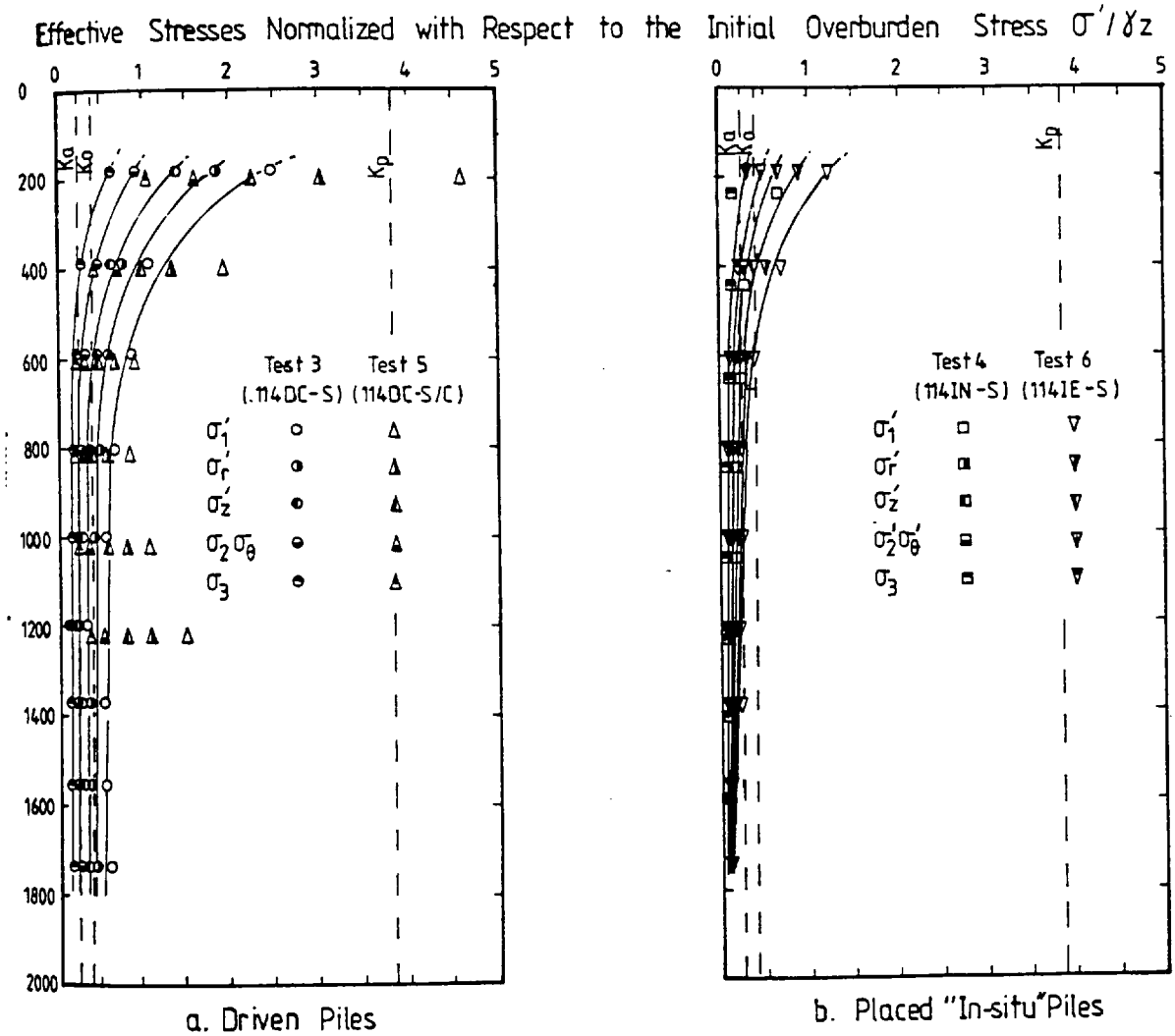

VARIATION IN THE NORMALIZED EFFECTIVE STRESSES ACTING ON A PRISMATIC ELEMENT OF SAND ADJACENT TO THE PILE SHAFT WITH DEPTH AT MAXIMUM TENSILE SHAFT RESISTANCE

FIGURE 6.42

CHAPTER 7

SOIL STRESSES AND DISPLACEMENTS

CHAPTER 7

SOIL STRESSES AND DISPLACEMENTS

7.0 Introduction

This chapter presents the development of soil stresses and displacements during pile installation and load testing. Some of these results have also been reported by Rowlands, Delpak and Robinson (1989), given in Appendix 7.1.

7.1 Sand Density.

In order to measure the "as placed" density and monitor the changes in sand density due to pile installation and load testing, a number of methods were used. The "as placed" in-situ density was monitored in three ways,

1. Prior to each sand layer being placed in position two C.B.R. moulds were located diagonally opposite each other at a radius of 960mm from the pile. The sand was placed to the required depth in the manner described in Chapter 5.2. On completion of the semi-full scale tests these C.B.R. moulds were retrieved, weighed and the sand displacement density determined.
2. An initial sand density check was also made using the sand/plaster method developed by Werscheing(1983) as discussed in section 3.9.2. These samples were hydrated 24 hours prior to the installation and testing procedures.
3. A mini Mackintosh Prospector probe developed by Kay(1980) was used to monitor any variation in sand density

throughout the depth of the sand layers. This was used at the formation of every 250mm layer of sand, at a radius of 960mm from the pile axis and penetrated to a depth of 500mm. The average of two probe tests per layer was taken.

The variations in sand density due to pile installation was determined at selected points using the sand/plaster method.

Apart from the initial density samples, all the sand/plaster samples were hydrated after pile installation and the first series of maintained load tests. This was to achieve compatibility and to make a comparison with previous work at the Polytechnic.

For tests 4 and 6 where the piles were already in position before placing the sand, the samples were hydrated after the final maintained load test. Any significant changes in density during these tests would be more predominant after load cycling rather than after the initial maintained load test.

7.1.1 Sand Density Prior To Pile Installation.

The mini-Mackintosh prospector probe results are illustrated in Figure 7.1. The number of blows per 500mm of sand are fairly constant throughout, indicating uniform sand placement. At the interface between the individual sand layers, where the sand was prepared for instrumentation, a marginal increase in the local blow count was observed. This indicates a slight densification of the sand forming a "crust" of between 25-50mm thick.

The initial sand density determined using the C.B.R. moulds and the sand/plaster technique are illustrated in Figures 7.2 and 7.3. The

tests using the C.B.R. moulds indicated that all the initial layer densities were in good agreement. This suggests a uniform mass of homogeneous sand for each test. The overall initial sand density results, obtained from the sand/plaster samples hydrated when the sand had been completely placed, indicate a slight density gradient. The trend is an increase in sand density with depth, which is acceptable due to compaction with a progressive increase in overburden stress.

This slight density gradient is considered insignificant and the average value for the sand mass was used for the analysis. The sand density samples on the outermost radii, hydrated after the completion of pile installation and loading, show parity with the initial sand density samples. This was observed for all the driven pile tests and indicates that this location is outside the pile driving influence zone.

7.1.2 Change In Sand Density Due To Pile Installation And Loading.

The recorded changes in sand density determined from the sand/plaster samples due to pile installation and loading for all 6 tests are shown in Figures 7.2 and 7.3. To make a comparison with previous work, carried out at the Polytechnic, the results from the driven pile tests were converted into volumetric strains, refer to Figure 7.4.

The variation in sand density due to the dynamically driven 60mm pile are given in Figures 7.2 and 7.4a. These clearly indicate an increase in density in the vicinity of the driven pile. Test 2 (sand/clay profile) shows a greater increase in the density than in test 1 (sand

only profile). The average volumetric strains over the equivalent depth of sand being 3.27% and 2.38% respectively for a r/B value of 2. The sand/clay interface may have contributed to this local increase in sand density due to the action of soil heave. This would counteract the natural downward movement of the sand causing extra local compressive strains around the pile.

The dynamic action of pile driving would possibly cause some reverberation through the pile and soil media, particularly in the clay. This would contribute to the agitation of the sand particles hence increasing the soil density.

For the tests on the 114mm pile, which was driven at a constant rate of 10mm/min, the sand density results are given in Figures 7.3 and 7.4b. The two tests, i.e. test 3(sand only profile) and test 5 (sand/clay profile) give average volumetric strains of 3.14% and 3.17% respectively at a r/B ratio of 1.4B. The similarity of the results reflects the nature of driving, particularly when compared to those subjected to the dynamic form of pile installation.

For the sand only profile both methods of installation affected sand densification around the pile in a similar manner. Along the majority of the pile shaft the volumetric strain ε_v was typically 2.5% (r=2B) for the 60mm pile and 2.75% (r=1.4B) for the 114mm pile. There was a reduction in ε_v near the uppermost section of te pile and around the pile base. Some of the sand density samples immediately below the base did show a negative volumetric strain (dilatancy). There is some ambiguity over the validity of these particular results. The samples retrieved did seem to be thinner and of increased diameter. This resulted in an increased surface area to volume ratio.

Werscheng(1987) concluded that this would give lower density values from the method, stating that the resultant greater portion of excess surface water to void water would effectively increase the calculated void ratio of the sample.

The volumetric strains and general trends of sand density distribution are in good agreement with Lake(1986) and Werscheng(1987). A comparison with their work is illustrated in Figures 7.4a and b.

Volumetric strain contours produced by Davidson et al(1981) and Robinsky and Morrison(1964) are presented in Figures 7.4c and 7.4d respectively. At the relevant r/B ratios of 1.4 and 2 the volumetric strains given by Davidson are 2-7% and Robinsky and Morrison values are 2-5%. The values reported in this thesis are in good agreement with these. From their work it is also evident that there is an increase in the sand density below the pile base although Davidson results do show dilatancy in the immediate vicinity of the base. This substantiates Werscheng's (1987) doubts over the value of the density samples immediately below pile base level.

The zones of increased density around the dynamically driven pile and the pile driven at a constant rate of penetration extended diametrically to 15B and 13B respectively. These are in good agreement to those produced by Lake(1986), 14B and Werscheng(1987), 13.2B. They are generally greater than those reported in other literature for loose sand, i.e. Robinsky and Morrison(1964), 10B, Broms(1966), 7-12B, Kishida(1967), 7B and Meyerhof(1959), 6B.

For the insitu pile tests (tests 4 and 6) the samples were hydrated

after load cycling. Although generally there was a marginal increase in sand density at r=1.4B. These values are insignificant bearing in mind the accuracy of the method. An important feature in test 4 was the effect of the frictionless cylinder. At the level of 1750mm a marked increase in sand density of 2% was recorded. The shoulder of the frictionless cylinder has acted as a boundary condition along with the surrounding sand. This was the intended simulated condition of the work produced by Kay(1980). An analogy could be made with the two layered soil system but the frictionless cylinder did not allow for any sand drag down or soil heave conditions.

7.2 Analysis Of The Red Keuper Marl Layer.

7.2.1 Initial As Placed Properties Of The Red Marl.

The clay was compacted into the wooden formwork as previously described in Chapter 5.2. After the formation of every 150mm layer of clay, four 38mm core samples were taken. Two of the samples were used to determine the apparent undrained cohesive strength in the unconfined compression apparatus. The moisture content, bulk density, void ratio, and degree of saturation were determined from the remaining samples.

The results from the two sand/clay profile tests are given in Figure 7.5. It illustrates a uniformity in the clay properties which indicates a consistent placement technique.

After completion of test 2 (60DD-S/C) the moisture content of the clay was generally found to be slightly below the optimum moisture of 18%, although a high degree of saturation was maintained throughout

test 2, refer to Figure 7.5. To increase the moisture content of the clay, in readiness for test 5, it was periodically "wetted" with a fine water spray whilst stored in the bins between tests. The clay was stored for a period of five weeks before test 5 was carried out. As can be seen from Figure 7.5 the moisture content was adjusted thus slightly lowering the undrained cohesive strength.

7.2.2 Examination Of The Clay After The Tests.

To analyse and inspect the effects of pile driving on the clay it had to be carefully dissected. Initially all the sand was removed from the tank with the pile left in-situ. This enabled one side of the secondary tank to be removed. The sectioned wood formwork inside was then systematically taken away allowing the clay to be carefully removed in small blocks. This process was carried out until a full diagonal section of clay was revealed. Throughout the process care was taken to cover all exposed clay with polythene to prevent loss of moisture content. All the samples for triaxial testing were tested on the same day as their retrieval from the clay mass. This was considered necessary since the wax coating method of storage had proved unreliable in moisture retention by previous researchers. The triaxial samples taken from test 5 to determine the effective stress parameters, were kept sealed in a humid environment.

Unfortunately all the photographic evidence taken during test 2 was destroyed during processing and only photographs from test 5 are presented here.

7.2.2.1 Structural Changes In The Clay Due To Pile Installation.

The structural changes observed in the clay are illustrated in Figure 7.6 supported by the relevant photographic evidence produced from test 5.

7.2.2.2 Soil Heave.

Evidence of soil heave at the sand/clay interface was present in both tests 2(60DD-S/C)and 5(114DD-S/C) but was more prominent in the former. This is probably due to the difference in the methods of pile driving. The dynamic method produces a "punching" intrusion into the clay, leading to a a sudden increase in local lateral stresses causing greater soil heave. In test 5 the constant rate of penetration method of installation (100mm increments) gave a slower pile entry into the clay, with the lateral stresses being more gradually set up and distributed throughout the clay body. Generally soil heave was evident at a radius of 2.75B from the pile axis. The displaced volume is only marginal in both test cases, heave being restricted by the overburden pressure of the sand. Also due to the time lag between pile installation and the soil dissection a reduction in the initial heave condition due to consolidation effects would be expected. This would be particularly prevalent in the soil adjacent to the pile where higher pore water pressures were generated.

Soil heave due to driven piles in clay is extensively reported although the magnitude of the ratio of initial heave volume to volume of embedded pile varies quite considerably from 30-100%, Poulos and Davis(1980). This variation may be attributed to variations in soil

and driving conditions. Cooke and Price(1973) reported a value of 66% for jacked piles in London clay.

7.2.2.3 Disturbance Zones Around The Pile Shaft And Toe.

Figure 7.6 and Plate 7.1 illustrate the areas of disturbance within the clay. Near the interface considerable distortion and drag down of the clay was evident. In particular a band of clay of approximately 15-20mm of heavily remoulded clay was visibly apparent around the circumferance of the pile. Within this band the clay particles seem completely reorientated in relation to the main body of the clay. This remoulded clay zone was evident throughout the length of the pile for both tests.

At the toe of the pile beneath the sand plug, further evidence of clay remoulding can be seen, refer to Figure7.6 and Plate 7.2. The clay has remoulded striations which follow the lines of the sand plug.

A number of authors have identified the various zones of remoulded clay, such as Tomlinson(1970), Randolph and Wroth(1982), Martins(1983) and Lake(1986). Tomlinson (1970) drove 168mm O.D. steel seamless tubes into London clay with an eventual L/B ratio of 32. From these tests a drag down of 3B was developed. Four of the test piles were exhumed and over the lower portion of the pile in particular a thin layer of clay between 1-6mm thickness had adhered to the pile. Further investigation revealed that the soil particles within this layer of clay were very strongly aligned at a small angle to the pile axis.

Martins(1983) carried out a series of small scale tests on 15mm model

piles in kaolin. This work involved a micro-fabric study of the clay within the disturbed zones, classified as A,B, and C. The boundary between the apparently undisturbed clay, zone C and the disturbed clay zones A and B lies at an approximate distance of about 0.2B from the pile shaft. Zone A being the most severely disturbed zone.

The visual observations made during tests 2 and 5 were in general agreement with these values, where the disturbed zone A and B ranged between 0.15B-0.35B.

There was little evidence of fissures and fracture lines in the clay radiating from the pile, of the magnitude and quantity reported by Lake (1986). It was suggested that the majority of the fissures were probably caused by stress relief due to the dismantling of the clay tank. The sudden stress relief was reduced by removing the formwork in sections. However during the removal of the clay there was still some evidence of fissures in the clay.

Massarsch and Broms(1977) postulate that cracks can occur in normally consolidated clay due to pile driving. These cracks increase the permeability of the clay local to the pile and cause a rapid dissipation in pore water pressure.

7.2.2.4 Moisture Content Profiles After Completion Of Tests.

After careful dissection of the whole clay block, a complete moisture content profile was taken for both tests 2 and 5.

The clay face was divided into a 100mm square grid. For each square on the grid two moisture content samples were taken. Before the samples were taken the face of the clay was cut back by 50mm. This

was to eliminate any errors in the results which may have arisen due to any moisture loss at the exposed clay face.

The full profiles are given in Figure 7.7. They illustrate that throughout the main body of the clay the moisture content remained similar to the initial values given in Figure 7.1. At the sand/clay interface however, there was a reduction in the clay moisture content which locally increased the undrained cohesive strength. Figures 7.6 to 7.8, illustrate that there was a migration of moisture from the clay into the overlying sand. For test 2, water had permeated through the vinyl membrane. This was evident in the earlier model pile tests, refer to 4.2.7.9, and was probably due to the formation of small cracks in the vinyl membrane from the soil heave deformation. As would be expected for test 5, where the vinyl membrane was not used, there was a more predominant migration of moisture into the sand. The wetted sand zone extended up to 150mm from the interface, refer to Plate 7.3. This is generally the accepted value of capillary rise expected in sand.

A small reduction in the clay moisture content was also observed locally around the sand plug at the toe of the piles. The sand plug can be then said to act as a sand-drain, increasing the rate of pore water pressure dissipation around the pile tip, refer to section 7.3.4. Lake(1986) reported a marked increase in the clay moisture content immediately beneath the sand plug. During his investigation he carried out a pull out test which could have caused a suction force at the pile tip which would have the effect of drawing moisture into the sand plug. The experiment was dismantled and the clay dissected immediately after the test. This allowed little time for

pore water stabilization within the clay. In the authors test series no pull out was performed on test 2 but was carried out for test 5. A stabilization period of generally 15 days was allowed before the experiments were dismantled. This was thought sufficient to erradicate any significant variation in moisture content.

7.2.2.5 Sand Drag Down Into The Clay

Sand dragdown into the underlying clay has been reported by various authors including Tomlinson (1970), Lake (1986) and Werscheng (1987) and was evident in the earlier 38mm model pile tests. For tests 2 and 5 the sand was pulled down to depths of 2.5B and 3.0B respectively, refer to Figure 7.6 and Plate 7.4. Tomlinson(1970) suggests that sand may be pulled down up to a distance of 3-4B. Plate 7.5 illustrates the adhesion of the sand and clay to the pile within this sand drag down zone. The annular ring of sand present at the sand/clay interface extends to approximately 0.5B-1.0B from the pile axis, which is in agreement with that suggested by Lake(1986).

7.2.2.6 Sand Plug At The Pile Base.

Meyerhof and Sastry(1978b), Lake(1986) and Werscheng(1987) have reported this phenomenon of a sand plug driven ahead of the pile base into clay in a two layered soil system. This predominantly wedge shaped sand plug fits generally into traditional failure patterns under deep foundation postulated by Prandtl in 1921. For tests 2 and 5 the sand plugs are slightly elongated and hemispherical in nature. They extend to approximately 0.6B below the pile and are slightly less than the diameter of the pile base, refer to Figure 7.6 and Plate 7.6.

The sand plug reported by Lake(1986) was barrel shaped and extended 0.8B below the pile base. The sand plug result of test 2 gives some credance to the hypothesis suggested by Lake (1986) that suction forces produced by the pull out tests caused a deformation in the plug. The significant difference in the sand moisture content could also be attributed to the effects of the pull-out test carried out during Lake's experiment. Lake(1986) reported a moisture content, ω=11.8%, whilst for test 2, by the author the moisture content was, ω=6.2%.

For test 5 the moisture content of the sand plug was 9.2%. A pull out test was carried out during this experiment, but seems to have had an insignificant effect on the shape of the sand plug. The shape is essentially the same as that reported by Werscching (1987).

7.2.2.7 Properties Of The Red Marl After Completion Of All Tests.

Of the 38mm samples taken during the removal of the clay from the tank three were used in undrained triaxial tests, the results of which are given in Figure 7.8. There is a small decrease in the moisture content profile near the surface of the clay, refer to section 7.2.2.4. This has given rise to a correspondingly significant local increase in the undrained shear strength of the clay. Throughout the rest of the body of the clay, there seems to be a slight drop in the shear strength compared with the initial values. This possibly illustrates some consolidation effects in the clay.

7.3 Generation And Dissipation Of Excess Pore Water Pressure.

The full history of the generation and dissipation of excess pore water pressures within the clay layer througthout tests 2 and 5, are given in Figures 7.9 and 7.10 respectively. Essentially the pattern was similar for the two tests. The principal differences were in the build up of pore water pressure during installation and the general rate of dissipation of this pressure. These may be attributed to the different methods of pile installation and the boundary conditions of the clay layer, which are discussed in the ensuing sections.

7.3.1 Generation Of Pore Water Pressure Due To Pile Installation.

Figures 7.11 and 7.12 illustrate the generation of pore water pressure at various levels within the clay at a constant radial distance equivalent to 1.5B for tests 2 and 5 respectively. The different method of pile driving has had a significant effect on the build up of the pore water pressure with respect to time. Also in test 2 the pile was fully driven within 4.5 hours as compared to 8.5 hours for test 5.

During test 5 an initial increase in pore water pressure was recorded at a pile penetration D_b of 200mm(2B) into the overlying sand. For test 2 this occured at a depth D_b of 240mm(4B). These values of D_b are in good agreement with the initial changes in overburden pressures recorded on the innermost radially distributed vertical pressure transducers, located at the sand/clay interface.

During pile installation for both tests 2 and 5 it is difficult and probably ambiguous to attempt to correlate the total increase in

overburden pressure developed at the sand/clay interface with the change in excess water pressure. The ambiguity lies with the duration of the peak applied load during installation. The duration of this load in relation to the time taken to perform an increment of pile installation is very small. This is particularly true for test 2 where a peak period increase in overburden pressure would almost be insignificant. It would therefore be more appropriate to compare residual values of the vertical pressure with the excess pore water pressure. To substantiate this during test 5 for a pile installation D_b of 1100mm(9.6B) a residual vertical pressure of 9KPa was recorded at r=1.5B. At the same radial distance, this compared to an increase in excess pore water pressure of 8KPa at z'=200mm(1.75B).

For both tests as the pile penetrated the clay and approached a level of piezometers, there was a significant increase in the pore water pressure. This was particularly evident when the pile tip passed a level of instruments, see Figures 7.11 and 7.12. These results suggest that a significant horizontal movement of the clay has occurred, setting up high lateral stresses, indicative of the high pore water pressures local to the pile. This is in general agreement with the principles of modelling pile installation as an expansion of a cavity within a soil media. (Ladanyi 1963). However the pore pressure at the pile/soil interface and the radial movement of the clay in the immediate vicinity of the pile were not monitored during the tests.

Due to the low pile penetrations into the clay and the apparent drainage effects of the sand plug, it is probable that there was an insignificant build up of pore water pressure at the pile/soil

interface. This makes a direct comparison with existing data on piles driven into a clay only profile unrealistic.

Throughout the embedded depth of the pile in the clay it was evident from both tests that the pore water pressures generated local to the pile tip were greater than those generated along its length. For test 2 the maximum pore water pressure at a radial distance of 1.5B local to the pile base and shaft were $0.36C_u$ and $0.27C_u$ respectively and $0.56C_u$ and $0.34C_u$ for test 5. It is suggested by various authors, Rigden(1979) and Roy et al(1981) that higher local stresses are set up around the pile tip.

Figure 7.13 illustrates the pore water pressures at pile base level normalised with the initial undrained shear strength of the clay. The larger pore pressures generated are more localised for the pile driven at a constant rate of penetration in test 5, than those produced in test 2, for the dynamically driven pile.

Figures 7.14 - 7.16 illustrate that within the radial limits of the piezometers the initial generation and radial distribution of the pore water pressure is logarithmic. This relationship is consistent throughout the embedded length of the pile and is of the form.

$$\Delta u = PC_{ui} - RC_{ui} \ln(2r/B) \quad \text{..... equation 7.1}$$

where P and R are values which describe the magnitude of the pore water pressure generated. Steenfelt et al (1979) prescribed such an equation which took the form of

$$\Delta u = 4C_u - 2C_u \ln(2r/B), \text{ where } C_u = 40kN/m^2 \quad \text{..... equation 7.2}$$

This equation was derived from a series of tests carried out on a 19mm diameter pile, jacked into reconstituted Kaolin clay. It was found that the overall results were in good agreement with those

predicted from a cavity expansion model.

Figure 7.15 illustrates that the pore water pressure generated within the clay local to the pile shaft were similar in magnitude for both tests 2 and 5. They give similar P and R values, with test 5 giving the larger relative pore water pressure values.

Clark and Meyerhof(1972) drove 76mm diameter piles into insensitive clays and found that the maximum build up in pore water pressure is a function of the soil type, pile size and material and driving time.

Based on the linear logarithmic relationship the ratios of uT5/uT2 are illustrated in Figure 7.17. They have been plotted for various radial distances during pile installation and loading at a depth equivalent to the pile base and mid shaft level. They indicate the variation in build-up of excess pore water pressure during pile installation, whilst the ratio of uT5/uT2 for loading was fairly constant at 2.5. This supports the previous statement by Clark and Meyerhof. At mid shaft level, the ratio of uT5/uT2 remains fairly constant for both pile installation and load testing.

There is a significant variation in the P and R values when compared to the equation given by Steenfelt et al (1979). The predicted values of excess pore water using their equation would be much greater. This also applied to the method developed by Lo and Stermac (1964). This is to be expected because of the effects of the sand local to the pile. Also due to the low L/B ratio and a significant amount of soil heave at the sand/clay interface, particularly during test 2, there would be an inherent reduction in the generation of pore water pressure. (i.e. a reduction in magnitude

of lateral only straining).

The effects of drainage channels attached to piles during installation was investigated by Holtz and Boman (1974). They developed a technique to reduce the excess pore water pressure generated during pile installation. This involved attaching paper plastic drains to wood piles. The excess pore water pressure generated during driving 13 test piles without drains and 48 piles with drains was measured. The results indicated at least a 50% relative reduction in excess pore pressure when drains were used.

The radial extent of any significant generation of pore water pressure was generally 8B and 5B for test 2 and 5 respectively. Test 5 demonstrated more localised effects on the pore water pressure. The boundary of the secondary clay tank, although tending to these limits seemed to have little effect on the overall results.

7.3.2 Generation of Pore Water Pressure During Load Tests.

The pore pressure generated during the load tests were lower by some 20-35% than the values produced by pile installation. Martins(1983) illustrates that the above value may be greater than 50%. This may be attributed to the lack of sudden lateral straining set up by pile installation.

The radial generation of pore water pressure again follows a logarithmic distribution in the same manner as the pile installation values. The P and R values in the general expression of equation 7.1 being 0.13 and 0.06 for test 2 and 0.38 and 0.18 for test 5 respectively; refer to Figures 7.15 and 7.16.

Between the radial limits of the instrumentation the log $\Delta u/\log_n 2r/B$ graphs shown in Figures 7.15b and 7.16 illustrate a linear relationship. This is true for both test 2 and test 5. The loading and installation values for the gradient of the line are similar and differing only in the magnitude of the excess pore water pressure generated. Due to the varying techniques and more localised effects of the generation of the pore water pressure between the two tests the value of Δu is different and is defined as;

	Installation	Loading
Test 2	$\Delta u=1.1C_{ui}(2r/B)^{-0.96}$	$\Delta u=0.2C_{ui}(2r/B)^{-0.96}$
Test 5	$\Delta u=6.2C_{ui}(2r/B)^{-2.30}$	$\Delta u=2.5C_{ui}(2r/B)^{-2.30}$

For r=1.5B the piezometer pressures local to the pile base are again higher than those distributed in the clay within to the embedded depth of the pile. The radial extent for the generation of excess pore water pressure was 5B and 3.5B for tests 2 and 5 respectively. As expected this is a significant reduction in the size of the influence zone generated during pile installation.

Other authors, such as Clark and Meyerhof(1972) Massarsch, Broms and Sandquish(1975) and Roy et al (1981) have also observed this.

In the final assessment of the pore water pressures generated during loading, ω_t the pile displacement during peak loads must be considered. If large values of ω_t occur then the lateral stress condition due to pile displacement increase accordingly. The location of the piezometers in the clay relative to the pile base are also affected by the progressive load testing. Where initially they may have been in the immediate influence zone of the pile base, due to subsequent load tests, causing an increase in D_b values, the

piezometers will become more remote from this zone. The third load test carried out during test 5 has generally lower pore pressure values local to the pile base and may be indicative of this point.

7.3.3 Generation Of Pore Water Pressure Due To Cyclic Loading.

Initially there was a steady increase in the pore water pressure during the cyclic load test. At the end of the 1600 cycles this value tended to a peak of 2kPa at r=1.5B and z'=600mm. (refer to Figure 7.18). Although this is only a marginal increase in magnitude and distribution of the pore pressure it again can be represented by a linear logarithmic function;-

$$\Delta u = 0.10C_{ui} - 0.05C_{ui}\ln(2r/B) \quad \text{..... equation 7.3}$$

The radial limit of any significant change in pore water pressure was similar to the maintained load test value of 5B. These small values in pore pressures would have little or no effect on any load test results and seems to be reflected in the subsequent maintained load test 3. Prech(1986) carried out cyclic load tests on a 273mm diameter piles driven into silty sand and silty clay. He found that the pore pressure at the soil/pile interface remained low (4kPa after 1000 cycles).

Briand and Felio (1986) studied the response of piles subjected to cyclic loading. They concluded that the pore pressures at the soil/pile interface do not increase during cyclic loading; in some cases a decrease in pore pressure was recorded as the shear transfer degraded. They also concluded that a cyclic threshold exists above which failure occurs by plunging or pull out of the pile. On average this threshold is claimed to be 80% of the ultimate capacity of the

pile. Cyclic loading below this threshold does not produce any significant decrease in the ultimate static capacity. For test 5 the cyclic load was 40% of the static capacity.

7.3.4 Dissipation Of Excess Pore Water Pressure.

The dissipation of excess pore water pressure after each pile installation and loading phase is illustrated in Figures 7.19 and 7.20 for tests 2 and 5 respectively.

After pile installation and the first series of maintained load tests the time taken for 85% dissipation of pore water pressure was 9 days for test 2 and 6.5 days for test 5. The significant variation in this period may probably be attributed to three main reasons;-

i. The variation in the size of the sand plug would be a contributory factor on the area of the drainage influence zone.

ii. In the upper portions of the clay the P.V.C membrane used at the sand/clay interface in test 2 has somewhat decreased the rate of dissipation although not totally restricting it.

iii. The more localised generation of pore pressure produced by test 5, in conjunction with point (i). has led to a quicker dissipation period.

The dissipation curves have been modelled using a two dimensional numerical technique. The predicted results from this method are also given in Figures 7.19 and 7.20. The method is based on the differential equation for two dimensional consolidation, for an isotropic, homogeneous soil, which is given by :

$$\delta u/\delta t = C_v((\delta^2 u/\delta r^2) + (\delta^2 u/\delta z^2))$$

The dissipation rate was calculated from the explicit finite difference solution of this equation.

To set up the finite difference consolidation grid the initial distribution of pore water pressures must be known. These values were deduced from previous equations derived from the actual pore water pressures generated during the tests given in section 7.4.4. The sand/clay interface was considered to be a free draining boundary. To be consistent with previous observations and assumptions the pile/soil interface was also considered to be in a free draining condition. The boundaries of the secondary clay tank are considered impermeable with an initial negligible value of pore water pressure. All the boundary conditions were assumed to be the same for both tests 2 and 5.

From the numerical technique, the predicted dissipation curves from the initial phase of pile installation and maintained load test 1, are in good agreement with the actual curves. For test 2 at a radial distance of r=1.5B and z'=250mm the predicted and actual curves are virtually identical. With increasing values of z' the predicted values of pore pressure are marginally less. This was probably an indication of the effects of the boundary conditions. Near the sand/clay interface and local to the pile base there was undoubtedly a true resemblance to the boundary conditions. Between these areas the influence of the boundary conditions was probably less acceptable for the particular case of test 2. In this zone there may be small initial values of pore pressure at the pile/soil interface.

The predicted and actual dissipation curves for test 5 are in close agreement throughout the depth of the clay. This indicates a good

assessment of the initial boundary conditions. Therefore the inherent conditions of test 5 with a low L/B ratio into the clay and the influence of the sand zones, the assumption of zero pore pressures at the pile/soil is reasonable. For higher values of L/B into the clay, as indicated by test 2, this assumption may be in error.

The dissipation curves after the second series of maintained load tests are also illustrated in Figures 7.19 and 7.20. 80% dissipation of pore pressure occurred within 2 and 3.5 days for tests 2 and 5 respectively. The larger initial pore presure being generated by test 5 which has the corresponding greater dissipation time.

Generally the numerical solution is in good agreement with the actual dissipation curve for both tests, particularly near the pile base. The more localised generation of the pore pressure due to loading has aided the exactness of the numerical solution. Near the sand/clay interface there is some discrepancy between the numerical solution and the actual dissipation curve. This may be attributed to the loss in moisture to the upper sand layer. It would cause the degree of saturation to fall, and some suction effects local to the sand/clay interface.

7.4 Stresses Generated On A Horizontal Plane Within A Soil Profile.

The instruments used to monitor the radial shear and effective vertical stresses developed during pile installation and the subsequent load tests were the interface shear stress transducer (I.S.S.T.s) and the Nottingham diaphragm pressure transducer (D.P.T.s). These are described in Chapter 3.

For Test 1,2,3, and 5 (driven pile tests) the instruments were placed on or at the equivalent depth of the sand/clay interface. In Tests 4 and 6 they were located at the initial equivalent depth of the pile base.

7.4.1 Pile Installation.

7.4.1.1 Effective Vertical Stresses In A Homogeneous Sand Profile.

Only the residual values of the change in effective vertical stress, $\Delta\sigma'_{zi}$ could be monitored during Test 1. This was due to the nature of pile installation as previously described in section 7.3.1. The radial distribution of $\Delta\sigma'_{zi}$ for tests 3 is illustrated in Figures 7.21 and 7.22a and is described in this section.

The figures illustrate that there was a positive build up in $\Delta\sigma'_{zi}$ at radial distances from the pile axis of 180mm and 280mm during the initial stages of pile installation. At a radial distance of 480mm a slight negative $\Delta\sigma'_{zi}$ was recorded for a pile penetration of 340mm (3B); thereafter it tended towards a positive increase.

This is contrary to reports of similar tests carried out by Mogami and Kishida(1961), Kishida(1964) and Werscheing(1987) where a general reduction in $\Delta\sigma'_{zi}$, was recorded across a horizontal plane during the initial stages of pile penetration although some sceptism about this result was expressed by Werscheing (1987).

With further pile penetration $\Delta\sigma'_{zi}$ increased in magnitude but diminished in value with radial distance, r, from the pile axis. A peak value in $\Delta\sigma'_{zi}$ of 4.5kPa was observed at a pile penetration (D_b) of 775mm, at a radial distance of 480mm(4.2B) from the pile axis.

Subsequent peak values of 12kPa and 40kPa occurred at r=280mm(2.5B) and 180mm(1.6B) for pile penetration depths of 850mm and 950mm respectively.

After these peak values were reached there was a significant reduction in $\Delta\sigma'_{zi}$, with further pile penetration. The peak reduction in $\Delta\sigma'_{zi}$ was reached at the outer limit first at a pile penetration of 950mm and tended towards zero. At r=280mm a peak reduction of -2kPa occurred for a D_b of 1150mm whilst at r=180mm $\Delta\sigma'_{zi}$ reduced to -14kPa at a pile penetration of 1200mm. This radial variation in $\Delta\sigma'_{zi}$ is indicative of a bulbous stress distribution under the pile base.

Kishida(1964) and Werscheing(1987) state that $\Delta\sigma'_{zi}$ equalled the effective overburden pressure at a radial distance of 4.5B and 3.2B respectively at pile failure when the pile base was 2.8B above the D.P.T.s. This was in good agreement with a value of 3.5B produced from test 3.

As the pile approached the level of instruments, there was a marginal increase in the effective overburden pressure, but when the pile base reached the depth of 1250mm $\Delta\sigma'_{zi}$ again tended towards the effective overburden pressure at each radial location. For pile penetrations greater than 1250mm there was again a marked reduction in $\Delta\sigma'_{zi}$, making $\Delta\sigma'_{zi}$ less than the effective overburden pressure, particularly at radial distances of 180mm and 280mm. For pile penetrations greater than 3.0B below the instrumentation level $\Delta\sigma'_{zi}$ at all radii tended to new constant values. This seems compatible with the work of Touma and Reese(1974) where it was suggested a discontinuity in the sand displacements around the base of a pile produced flow and arching zones which reduce the effective overburden pressure near to the pile.

A similar trend in the build up of $\Delta\sigma'_{zi}$ below pile base level and a reduction in $\Delta\sigma'_{zi}$ above pile base level was observed by Vesic (1969). The variation in the radial patterns of $\Delta\sigma'_{zi}$ generally confirms the observations made by Wersching(1987).

7.4.1.2 Residual Effective Vertical Stresses.

The change in residual effective vertical stresses at a depth of 1250mm during pile installation for Tests 1 and 3 are illustrated in Figure 7.21b.

All the D.P.T.s exhibited a small negative residual $\Delta\sigma_{zi}$ value during both tests for pile embedment depths of 200mm. At a radial distance of r=180mm the residual value of $\Delta\sigma'_{zi}$ for test 1 continued to reduce with further pile penetration until a constant limiting negative value was reached at a pile penetration of 900mm. It remained relatively constant to a pile embedment depth of 1050mm. In Test 3 the residual stress at the same radial location exhibited a small positive value from a pile penetration of 275mm. From a depth of 800mm it again increased until it reached a peak value of 4.0kPa at a pile embedment of 900mm. It then decreased to a final residual value of -12.5kPa at the end of pile installation.

These variations in residual stresses may possibly be explained with reference to the development in vertical soil displacements illustrated in Figure 7.33. During test 1 no vertical displacements were recorded at the depth of 1250mm until the pile had penetrated to a depth of 1000mm, i.e. the limit at which the residual $\Delta\sigma'_{zi}$ had reached a constant limiting value. Below this penetration level the residual $\Delta\sigma'_{zi}$ values were influenced by the bulb of pressure and

vertical elastic recovery. In Test 3 the vertical displacements at a level of 1250mm first became evident at a pile penetration of 275mm. This generally corresponded to the point of inflection in the residual $\Delta\sigma'_{zi}$ values which then became positive. This increase in residual $\Delta\sigma'_{zi}$ was related to the elastic recovery of the soil.

Kishida(1964) postulated that the stresses caused by pushing a pile can be divided into two components:-

i.e. $T\sigma_z = D\sigma_z + L\sigma_z$

where $T\sigma_z$ = total vertical stress in the sand

$D\sigma_z$ = vertical stress caused by the displacement of sand (Displacement stress)

$L\sigma_z$ = vertical stress caused by the pushing load (Load stress).

For Tests 1 and 3 the influence of the bulbs of pressure became evident at pile embedment depths of 1000mm and 750mm respectively. As the pile approached the level of instruments in test 3 the residual stress reduced to -4kPa at D_b=1250mm. For test 1 the residual stress was -10kPa. For further pile penetrations below 1250mm the residual stress generally continued to reduce and reached a constant limiting value of -14kPa at a pile penetration of 1600mm during test 1 and approached a limiting value of -13kPa for test 3 at the end of pile installation.

At a radial distance of r=280mm the development of the residual stress during pile installation was similar to that at r=180mm, but the values were significantly less during test 1 at this radial location. For test 3 the residual stress values were of the same order of magnitude.

During test 1 there was a significant decrease in the residual stress at the radial distance of 480mm. Marginal signs of residual stress were evident during the latter stages of pile penetration for this test. At r=480mm during test 3 residual stress values were more in evidence and tended to a -3kPa at the end of pile installation.

These residual stress values indicated the influence of the pile diameter on the development of radial vertical stress. The methods of driving may have also influenced the build up in stress values. The dynamic method possibly causing a more localised effect due to the punching action of pile installation. This would be particularly evident during the earlier stages of pile installation where the blow number/pile penetration was low.

7.4.1.3 Effective Vertical Stress Developed In A Layered Soil Profile

For test 2 only the residual values in effective vertical stress were monitored due to the method of installation as previously stated. During test 5 the change in effective vertical stresses were monitored. This data is presented in Figure 7.21a and 7.22a and is discussed here.

For Test 5 the $\Delta\sigma'_{zi}$-D_b profile across the interface exhibited a similar trend to test 3 to a pile embedment depth of 1000mm. For radial distances of r=160mm and 480mm the peak $\Delta\sigma'_{zi}$ values were 40kPa and 5kPa respectively. At a radial distance of r=280mm the peak value of $\Delta\sigma'_{zi}$ was 20kPa i.e. significantly higher than in test 3.

The magnitude of this stress varied quite considerably from test 3 after the peak values in $\Delta\sigma'_{zi}$ were reached. At r=180mm and at a pile

penetration of 1000mm $\Delta\sigma'_{zi}$ began to reduce rapidly in magnitude until it reached a value of 12.5kPa. This was again synonymous in effect to a bulbous pressure distribution below the pile base. The greater elastic response of the clay at the interface became more apparent at a pile embedment depth of 1225mm. Also as the pile penetrated the clay the discontinuity in the sand displacements around the pile base which were evident during Test 3 and in the work of Touma and Reese(1974) were not apparent in Test 5. The boundary interface layer had restricted the sand flow zone. As the pile base and sand cone driven ahead of the pile entered the clay, the action of the soil heave became a predominent influence on the $\Delta\sigma'_{zi}$-D_b profile. As the heave occurred the vertical effective pressure increased to a peak value of 30kPa at a pile penetration of 1300m.

With reference to Figure 7.21, the similarity in the effective stress profiles upto D_b=1000mm between test 3 and 5 was reflected in their respective vertical displacement profiles. The divergence in the $\Delta\sigma'$-$D_b$profiles with further pile embedment was once again reflected in the vertical displacements where at a depth of 1250mm extension strains were recorded in test 3 and compression strains in test 5.

As the pile base approached the interface level, $\Delta\sigma'_{zi}$ decreased with radial distance from the pile axis. Peak $\Delta\sigma'_{zi}$ values of 20kPa and 5kPa occurred at pile penetrations of 900mm and 650mm for r=280mm and 480mm respectively. This again was in keeping with a bulbous stress distribution of stress below pile base level.

Following the maximum value in $\Delta\sigma'_{zi}$ due to soil heave there was again a sharp reduction in $\Delta\sigma'_{zi}$, at a radial distance of r=180mm. This correlated to some extent to the settlement of the interface, which

in turn corresponded to vertical extensive strains again being exhibited in this region.

The effective vertical stress tended to a value slightly less than the overburden pressure close to full pile embedment. The trend in the stress profiles at r=280mm and 480mm was again similar to that displayed at r=180mm but of a diminished order of magnitude. At full pile embeddment $\Delta\sigma'_{zi}$ was -2kPa and 2kPa at r=280mm and 480mm respectively.

A significant difference between test 3 and 5 at full pile embedment was the final value in the overburden pressure. The final values of $\Delta\sigma'_{zi}$ at r=180mm were -2kPa and -11kPa for tests 3 and 5 respectively. The difference in these values being approximately equal to $K_o\sigma'_{zi}$. The clay layer in test 5 had effectively acted as a boundary layer and prevented the development of sand arching and flow regions around the pile base which seemingly reduced the $\Delta\sigma'_{zi}$ during test 3.

7.4.1.4 Residual Effective Vertical Stress In A Layered Soil.

The residual values for tests 2 and 5 are illustrated in Figure 7.21b. Generally the residual $\Delta\sigma'_{zi}$- D_b profiles remained positive throughout pile installation for both tests 2 and 5. The peaks and troughs in these profiles correlated to the associated trends in the $\Delta\sigma'_{zi}$-D_b profiles. For pile embedment values of less than 1250mm and at r=180mm the peak values in residual $\Delta\sigma'_{zi}$ were 15kPa at D_b=900mm and 5kPa at D_b=750mm for test 5 and 2 respectively. These values are markedly higher when compared to the residual $\Delta\sigma'_{zi}$ values obtained from the sand only profile tests. This was probably due to higher elastic displacement recovery values obtained at the sand/clay interface.

After the pile base had penetrated the sand/clay interface a high residual $\Delta\sigma'_{zi}$ was obtained, which demonstrated the semi permanent effect of soil heave. These peak residual values of 10kPa were obtained at penetration depths of 1500mm and 1375mm for test 2 ans 5 respectively at r=180mm. Similar, but reduced effects were displayed at r=280mm and 480mm.

At final pile penetration depths the residual values remained positive across the whole interface during both tests. At r=180mm during test 2 the residual $\Delta\sigma'_{zi}$ tended to the effective overburden pressure. At the greater radial distances this value was limited to 5kPa.

In test 5 the residual $\Delta\sigma'_{zi}$ value tended to 10kPa ($K_o\sigma'_{zi}$) at r=180mm at the end of pile installation. The associated residual stress values at r=280mm and 480mm were 3kPa and 3.5kPa respectively.

7.4.1.5 Radial Shear Stresses In A Homogeneous Sand Profile.

The radial shear stresses (τ_i) were only monitored during test 3. The location of the stress transducers were compatible to those of the D.P.T.s with the inclusion of instruments placed at r=380mm. Figures 7.22b and 7.23a illustrate the τ_i-D_b stress distribution.

During the initial phase of pile installation there was a slight negative value in τ_i at a radial distance of r=180mm. To a D_b value of 200mm there was no significant development in radial shear stress. After this point was reached there was a gradual increase in τ_i, decreasing with radial distance from the pile. A peak value in shear stress of 10kPa was first reached at the outer radius of 480mm for a pile penetration of 900mm. Subsequent peak values of 20kPa, 32kPa,

and 50kPa were obtained at radii of 380mm, 280mm and 180mm, for D_b values of 850mm, 900mm, and 1050mm respectively.

As the pile approached the level of instruments there was a sudden reduction in the radial shear stress at all radii. This may be associated with an equalisation of the relative radial sand movement as the pile penetrated the level of instruments; refer to radial displacement Figure 7.35. A peak reduction in shear stress τ_i was obtained at all radii when the pile base was equal to the depth of instrumentation. This was equivalent to the maximum radial displacement of the sand, neutralised relative radial displacement. Once the pile had passed through the level of instruments there was again an increase in τ_i. At r=180mm this value increased to 4kPa at all radii.

For further pile penetration a steady state in τ_i was reached, and as the pile installation was drawing to a conclusion a slight reduction in τ_i was evident. (At the end of pile installation the direction of τ_i was complementary to the local shear stress, f_z, along the pile shaft).

7.4.1.6 Residual Radial Shear Stress In A Homogeneous Sand.

The associated residual radial shear stress is presented in Figure 7.23b. The first evidence of residual τ_i is at a pile penetration of approximately 300mm. There was a general increase in residual τ_i, for further pile penetrations at all radial locations. At r=480mm a maximum value in residual τ_i was 5kPa at a D_b of 1000mm. At closer radial distances to the pile the peak residual τ_i increased, with a maximum value of 20kPa at r=180mm. These values were a reflection of

the τ_i values and may be asociated with lateral elastic recovery of the soil.

As the pile approached the level of instruments there was a reduction in the residual radial shear stress. This reduced value reached a peak when the pile base was equal in depth to the instrumentation level. At r=180mm the residual τ_i was -5kPa and was similar in magnitude to the τ_i value. This reflects the laterally strained condition of the soil due to the intrusion of the pile. The residual $\tau_i$diminished in value with radial distance at this particular level. With further pile penetration there was again a recovery in residual τ_i. At r=180mm its value increased to 1kPa. With increasing radial location the residual τ_i tended to a neutral position of τ_i =0kPa. After reaching these peak values at approximately 1500mm a virtual steady state in residual τ_i was reached.

7.4.1.7 Development Of Shear Stresses Within A Layered Soil Profile.

The I.S.S.T.s were located at the sand/clay interface in both tests 2 and 5. Only the residual shear stresses for test 2 could be recorded and arepresented in Figure 7.23b. For test 5 the radial shear stress $\tau_i$and residual values were recorded during the pile installation.

The τ_i-D_b profile for test 5 was similar in appearance to that of test 3 but the peak values attained were much less, particularly closer to the pile. At a radial distance of 180mm and pile embedment of 1050mm the peak radial shear stress was 35kPa, some 40% of that produced in test 3. The comparative percentage differences decreased with increasing radial distance from the pile. When the pile base was at the interface level a maximum negative shear τ_i value of -20kPa

was experienced. Peak values decreased with radial distribution and were reached at successively greater depths. A steady state was reached towards the end of the pile installation, where the radial shear stresses across the interface tended towards values of between 2kPa and -2kPa. There was again a slight reduction in τ_i towards the end of the pile installation. The directon of which was complementary to the local shaft friction, f_z along the pile shaft.

7.4.1.8 Residual Radial Shear Stresses Within A Layered Soil Profile.

During test 2 the residual τ_i was insignificant until a pile embedment depth of 600mm. This correlated to the depth at which the mobilisation of radial displacement occured, refer to Figure 7.35. Although residual τ_i was evident at further pile penetration depths it was not until the pile approached the sand/clay interface that any significant change was observed. At a radial distance of 180mm residual τ_i reached a peak of -15kPa at a depth of 1425mm. At subsequent pile embedments there was a reduction in τ_i which tended towards τ_i=0 for all radial locations.

For test 5 the shape of the residual τ_i-D_b profile was complementary to the τ_i-D_b profile with reduced values in τ_i. At the radial location of 180mm and pile embedment of 1000mm a peak residual τ_i value of -7.5kPa was recorded. Peak values again reduced with increased radial location. At r=480mm the residual τ_i only marginally deviated from the neutral axis by 1kPa.

As the pile passed through the sand/clay interface a maximum τ_i of +17.5kPa was reached at r=180mm and D_b =1300mm. At this radial location there was an increase in residual τ_i to a depth of 1500mm.

For pile penetrations greater than this depth a steady limiting value in residual τ_i was reached. This reduced in value towards the end of pile penetration. On the outer radial limits once the pile had passed the level of instruments there was a continuous reduction in residual shear stress τ_i, the rate of which decreased with pile penetration. Residual τ_i was complimentary to the residual f_z on the pile shaft at the end of pile installation.

7.4.2 Vertical Effective Stress Generated Around And Below A Vertically Loaded Pile.

Wersching(1987) presented the probable distribution of change in vertical effective stress generated within a sand mass by a pile of unit length, loaded to plunging failure in a dimensionless coefficient, "I" form. This coefficient was determined using equation 7.4 and plotted against dimensionless coefficients r/D_b and z/D_b. The resultant distribution of "I" evaluated throughout pile installation for test 3 is illustrated in Figure 7.24 along with those presented by Wersching(1987)

$$I = \frac{\Delta\sigma'_{zi}\, D_b^2}{Q_t} \quad \text{..... Equation 7.4}$$

where $\Delta\sigma'_{zi}$ = change in effective vertical stress.

D_b = Pile embedment

Q_t = Total pile resistance.

Also illustrated in Figure 7.24 are the "I" coefficients calculated by Wersching using equations for "I" derived by Geddes(1966). They were evaluated for a uniform vertical subsurface line load of unit length, where Q_b/Q_t=0.86, for test 3 Q_b/Q_t=0.83, which was the average value during pile installation.

The stress coefficients were similar to those produced by Werschingh(1987) and exhibited similar features stated by the aforementioned author, which were:-

1. A bulbous distribution of stress coefficients below the pile, which reduced in intensity with increased distance from the pile.
2. The development of a region above the pile base within which the stress coefficients were negative.
3. A transition zone between the regions defined in 1 and 2. The stress coefficients within this zone tended to zero.

These stress coefficient zones correlated favourably with the proposed theoretical solution produced after Geddes(1966). The experimental values of "I" tended to be greater under the pile base than the theoretical solution. This observation was made by Geddes(1966) when a comparison was made between the Boussinesq solution for "I" under a pile base and that derived from the Mindlin equations.

7.4.3. A Two Dimensional Analysis Of The Stresses Generated On Or At The Equivalent Depth Of The Sand/Clay Interface During Pile Installation.

Throughout pile installation, the two dimensional stress histories acting on a horizontal plane at a depth of 1250mm during test 3 and 5 are illustrated in Figures 7.25 and 7.26 repectively. The vertical stress history was taken as the sum of the initial overburden pressure plus the change in effective stress $\Delta\sigma'_{zi}$, given in Figure 7.21. The radial shear stresses were taken as the direct readings given in Figure 7.23. These stresses were assumed to be compatible at

the equivalent radii on the horizontal plane. For the initial "at rest" state the stress history was assumed to be $\sigma'_{ri}=K_o\sigma'_{zi}$, where σ'_{zi} was taken as equivalent to the initial effective overburden pressure.

7.4.3.1 Two Dimensional Analysis Of The Stresses In A Sand Only Profile During Pile Installation.

The stress path of τ_i against σ'_{zi} during pile installation for test 3 is illustrated in Figure 7.25. It shows that at a radial distance of r=180mm, as the pile approached the layer of instrumentation, an assumed state of shear failure existed within the soil. The stress path within this region appeared to follow along an arc of a Mohr circle. A straight line tangential to this circle which passed through the origin subtended an angle ψ, equal to 56.4 degrees. This was the proposed failure envelope for shear failure acting within the sand due to a constantly penetrating pile. It would be logical to expect $\psi=\phi'$ but no satisfactory explanation can be offered at this stage as to why ψ was much greater than ϕ'.

At a radial distance of 200mm the stress path exhibited similar properties to that outlined above, with ψ=53.5 degrees. The stress profile at r=480mm did not develop to a state of shear failure. The consistency in the profile form and the proportional magnitude of the stress profiles at the various radii does not suggest that the readings at any one point were spurious in any manner.

By using the stress path profiles and selecting various points of interest on these lines, it was possible to plot the direction of the major principal stress σ'_1, in relation to pile penetration D_b, this is illustrated in Figure 7.27. From this relationship the direction

of the major principal stress appeared to emanate from a point on average 117mm(1.0B) below the pile base. This is fairly consistent with the formation of a dense sand cone "active wedge" below the flat base of a driven pile.

Meyerhof(1959) stated that the elastic major principal stress developed directly below and acted radially from the pile base.

As the pile approached the level of instrumentation it appeared from the direction of σ_1' that there was the development of a radial shear zone. This complements the classical theory of the active wedge and radial shear zone development below a deep foundation.

7.4.3.2 Two Dimensional Analysis Of The Stresses On A Sand/Clay Interface During Pile Installation.

The variation in τ_i and σ'_{zi} during pile installation for test 5 is presented on Figure 7.26. As the pile approached the sand/clay interface it was again evident that shear failure was occurring. The stress path formed failure envelopes where ψ=31degrees at r=180mm and 35 degrees at r=280mm. This was approximately equal to ϕ' and indicated that shear failure developed within the sand. For a radial distance of r=480mm shear failure was not evident.

A significant feature of this test was the development of shear failure in the reverse direction when the pile entered the clay layer. This illustrated a discontinuity in lateral movement between the sand and clay. (i.e. greater lateral movement within the clay)

Appropriate points were again selected on the stress profile to plot the direction of the principal stress σ_1' in relation to pile

penetration D_b.

The results of σ_1'-D_b are shown in Figure 7.27. The direction of the principal stress emanated from a point of 0.6B below pile base level. This coincidentally corresponded to the size of the sand plug exhumed from the clay at the end of the test. Although it is envisaged that during pile penetration through the sand, the sand plug would be more conical in nature.

Due to the shear failure occuring in the reverse direction the principal stress σ_1' could be determined as the pile approached the sand/clay interface. This illustrated a reversal in the direction of σ_1'which emanated from a point 1.0B below the pile base. From the direction of this stress along with the complementary shear stresses at this point, it can be envisaged that this was in fact within a radial shear zone. This tentatively agrees with the theory postulated by Meyerhof(1959) that radial shear zones develop to at least pile base level.

7.4.3.3 Changes In Stress Within A Soil Profile Due To Pile Installation.

The following sequence in the change in stress due to pile installation for test 3 was similar to that postulated by Werscheing (1987) for a sand/clay profile. However for test 5 significant deviations occured in the stress path to that described by Werscheing. It is suggested that these changes were due to the boundary effects of the clay layer and the incompatibility in lateral and vertical movement between the two soil types.

The following stress changes are thought to act on an element of sand at

a depth of 11B within a radius of 2.0B from the pile axis. Before pile installation occurs the initial "at rest" stresses were assured to be $\sigma'_{ri}=K_o\ \sigma'_{zi}$ where σ'_{zi} was equal to the initial effective overburden pressure.

At the onset of pile installation the intensity of both σ'_{zi} and τ_i increased, accompanied by an anti-clockwise rotation of the principal stresses. At a pile penetration of 1000mm and at a radial location of 180mm σ'_{ri} equalled σ'_{zi} which corresponded to a maximum value in σ_{zi} . This was true for both tests 3 and 5 although during test 5 the radial shear stress value of τ_i was much reduced. With further pile penetration, τ_i increased with a reducton in the σ'_{zi} value. The rotation of the principal stresses remained in an anti-clockwise direction. As the pile approached the instrumentaion layer there was a sudden reduction in the radial shear stress accompanying the decreasing σ'_{zi} value. This was reflected in the stress path profile at the relevant pile embedment depths of 1075mm and 1050mm for tests 3 and 5 respectively. From this point there was a significant difference in their respective stress path profiles. The stress profiles follow to a reasonable extent along the arcs of Mohr circles which were tangential to the ψ envelopes.

During test 3 as the pile approached to within 50mm of the instrumentation layer there was a significant drop in the τ_i value, accompanied by a small decrease in σ'_{zi} . At a depth of 1200mm, τ_i reduced below zero value and a marginal increase in σ'_{zi} was experienced. Throughout this period a rapid clockwise rotation of the principal stress planes occured, reverting back to the original stress condition where σ'_{zi} was greater than σ'_{ri}.

During this phase the stress profile intercepted the abscissa at a σ'_{zi} value of 17.5kPa. The marginal increase in σ'_{zi} may be associated with the development of radial shear zones. Once the pile had passed the level of instruments, there was again a reversal in the direction of τ_i with a significant decrease in σ'_{zi} which may be associated with the development of flow and arching zone (Touma and Reese 1974). With further pile penetration a reversed and reducing value of σ'_{zi} was observed with an anti-clockwise rotation of the principal stresses. The initial stress condition of σ'_{zi} greater than σ'_{ri} was in force where σ'_{zi} approached the original σ'_{ri} value.

During test 5 when the pile approached to within 50mm of the sand/clay interface at r=180mm, there was a drop in the τ_i value with a corresponding drop in σ'_{zi}. The stress path intercepted the abscissa at 37.5kPa. This was considerably greater than that experienced during test 3 and demonstrates the boundary effects of the clay layer.

During this phase the principal stress plane underwent a rapid clockwise rotation. As the pile approached the sand/clay interface the direction of τ_i changed and a significant increase in σ'_{zi} was observed. This stress behaviour was indicative of soil heave at the sand/clay interface and the greater outward radial displacement of the clay surface relative to the overlying sand.

When the pile base penetrated the interface level there was a significant increase in σ'_{zi} with an associated smaller variation in τ_i. The stress profile in this region rests on an arc of a Mohr circle tangential to the ψ envelope. It is suggested that at this point a

reversed shear failure occured. With further pile penetration the value of τ_i reversed and σ'_{zi} decreased in magnitude as the effect of heave and lateral movement subsided. Nearing the end of pile installation the initial shear stress state was reinstated, where σ'_{zi} was geater than σ'_{ri}. The rotation of the pricipal stresses at this stage was anti-clockwise. The value of σ'_{zi} was only slightly less than the initial at rest state σ'_{zi}. This illustrated that the clay acted as a boundary, restraining any sand flow and hence eliminating any significant reduction in σ'_{zi} as demonstrated in test 3.

Nearing the end of pile installation in both tests a quasi steady state of stress was observed to act across the instrumentation level. Similar reasoning to that outlined above may be applied to the state of stress recorded at r=280mm, as previously mentioned there was no development of shear failure at r=480mm.

7.4.3.4 Steady State Stress Profiles Acting On A Horizontal Plane At A Depth Of 1250mm Within A Soil Profile.

To determine the steady state stresses acting on a horizontal plane within a soil body it was initially assumed that the radial variation in σ'_{ri} within the sand was inversely proportional to the radius. This enabled a two dimensional stress profile to be determined at radial distances of 180mm and 280mm for both tests. At the pile/soil interface σ'_{ri} was readily determined from the B.O.S.T.s at the level of the sand/clay interface during pile installation.

For test 3 the estimated values for σ'_{ri} at radius 180mm and 280mm were determined and the steady state stresses plotted on Figure 7.25.

The resultant Mohr circles were effectively tangential to the ψ envelope which suggested that the sand within a radial distance of 280mm was in a state of shear failure.

The estimated values for σ'_{ri} determined using an initial σ'_{ri} values from the B.O.S.T.s for test 5 did not give realistic steady state conditions. They were too large in magnitude. This suggested that the initial σ'_r determined from the B.O.S.T.s was excessive and not compatible with the rest of the soil profile. This was feasible due to the wedging action of the sand particles local to the pile at the sand/clay interface. This would have been caused by the conical annulus of sand around the pile, which was dragged down into the clay during installation, refer to Figure 7.6. The steady state condition was assumed to be in a state of shear failure similar to the test 3 case.

Beyond a radial distance of 280mm the stress state within the soil profiles was not considered sufficient to cause shear failure. For radial limits in excess of 480mm the stresses within the soil probably tended towards the at rest states where $\sigma'_{ri} = K_o\sigma'_{zi}$.

For the steady state condition the variation in magnitude of the major stresses and the corresponding rotation of the principal stresses, acting across the horizontal plane of instrumentation are illustrated in Figure 7.28. The stresses within the sand at the pile/soil interface were correlated from results produced by the B.O.S.T. where applicable.

The steady state stresses produced for test 3 appear fairly consistent in relation to the contact stresses at the soil/pile

interface. The shear stress values τ_i reduce virtually in a linear manner with radial distance from the pile axis. For test 5 the τ_i values are linear from 180mm outwards but were much greater at the soil/pile interface, an expected result of the wedging action discussed earlier. A comparison of the σ'_{ri} and σ'_{zi} values between the two tests clearly indicates the variation in final magnitude of their respective values at plunging failure. Consider for example σ'_{zi}, where for test 5 it was limiting to the effective overburden pressure, whilst during test 3 it tended to $K_o\sigma'_{zi}$ for reasons given earlier.

7.4.4 Maintained Load Test.

Throughout the maintained load tests the change in vertical and radial shear stresses were monitored and are presented in Figures 7.29 and 7.30 respectively. The changes in the effective vertical stresses were small and generally within the limits of accuracy of the transducers. However their values did display certain trends which were consistent and proved their repeatability throughout the series of tests. The radial shear stresses were generally relatively small in magnitude particularly at low applied loads, but again displayed consistency and repeatability. The datum values for vertical and radial stresses during the various maintained load tests were deduced by averaging initial zero values taken at the beginning of each maintained load test under zero applied load. Also displayed on each test diagram is the initial datum in relation to the effective overburden pressure and the maximum increase in stress values.

7.4.4.1 Development Of Effective Vertical Stresses In A Sand Only Profile. (Driven Piles)

Throughout the maintained load tests the magnitude of σ'_{zi} was small with peak values being reached at maximum applied loads. The distribution of σ'_{zi} was fairly linear during test 1 although this fact was not particularly evident during test 3. Maximum values in σ'_{zi} were attained nearest the pile and diminished in magnitude with radial distance from the pile axis. The increase in σ'_{zi} may be attributed to compressive straining within the soil which was also evident in the vertical soil displacements, refer to Figure 7.41.

Cyclic loading carried out during test 3 prior to the maintained load test 2 had little effect on the magnitude of σ'_{zi} although the datum base did change marginally. In relation to the initial effective overburden pressure, the initial datum values in σ'_{zi} are significantly less.

7.4.4.2 Development In Effective Vertical Stresses In A Sand only Profile. (In-Situ Piles)

The D.P.T.s for these particular tests were situated at the pile base level. During the initial maintained load test series carried out in test 4 there was generally an initial relief in the overburden pressure on the inner most radially located D.P.T.s. This possibly resulted from the development of arching and the simulated "bin effect".

The second series of load tests carried out after the cyclic load tests illustrated a reverse effect in the build up of σ'_{zi} . It

demonstrated an initial collapse of the "bin effect" with an increase in local σ'_{zi} near to the pile and a relief in σ'_{zi} on the outer radii. The effect being locally restored at pile failure. This probably resulted from the effects of the cyclic load and the boundary effect of the sand below pile base level.

There was a general reduction on σ'_{zi} around the base of the pile during the load test carried out during test 6. The relief in σ'_{zi} was greatest near to the pile and diminished with radial distance from the pile axis. This adds some credence to the development of a flow zone around the pile base due to incompatibility in soil displacements causing a relief in overburden pressure.

7.4.4.3 Development Of Vertical Stresses In A Layered Soil (Driven Piles).

During the initial stages of load testing for both tests 2 and 5 there was an initial reduction in the σ'_{zi} values. Again these values were lowest nearer the pile. This tied in with the development of extensive strains within the sand above the sand/clay interface, resulting from incompatibility in the vertical displacement between the two soils.

During the first load test after pile installation the effect was exaggerated due to the probable effects caused by consolidation, when the effective stress of the clay was increasing. Towards pile failure there was generally an increase in the $\Delta\sigma'_{zi}$ and were typically greater with closer proximity to the pile. This could be related to the pile displacements at these loads. The large displacements increased the stress level within the clay which had a net effect of

increasing the $\Delta\sigma'_{zi}$ at the interface, similar to the effect caused during installation. This effect was typical throughout all the maintained load tests.

Once the piles were unloaded there was a general recovery in $\Delta\sigma'_{zi}$, which correlated to the displacement recovery readings.

7.4.4.4 Development Of Radial Shear Stresses In A Sand Only Profile (Driven Piles)

The development of radial shear stress throughout the two maintained load tests, carried out during tests 3 indicated a negative τ_i value. These values are comparable with the general outward movement of soil indicated by the radial displacements shown in Figure 7.46 . Peak negative values in τ_i (=7.5kPa) were recorded on the innermost transducers r=180mm at maximum applied loads. Values in τ_i diminished with increased radial distance from the pile axis. The value of τ_i during pre and post cyclic loading were compatible at each stage of the applied load. When the total load was released at the end of each load test, the τ_i value at each radial location returned to its original residual value to within reasonable limits of accuracy of the transducers, (full lateral elastic recovery).

7.4.4.5 Development Of Radial Shear Stresses In A Sand Only Profile (In-situ Piles)

The general trends in τ_i developed during the maintained load tests carried out for tests 4 and 6 were very similar to those of test 3. The magnitude of τ_i was much less than that developed during test 3. A significant feature in the value of τ_i is that it seems related to

the applied load. This implied that τ_i is more of a function of the arching stresses developed within the granular soil, rather than the product of soil movement. The ratio of Q_{amax} . to τ_{imax} . at a radial distance of 180mm(1.6B) limits to a value of 2 during these 3 tests.

7.4.4.6 Development Of Radial Shear Stresses In A Sand/Clay Profile (Driven Piles)

The development of radial shear stress during test 2 and 5 displayed negative τ_i values. These values at maximum applied loads were -6kPa and -9.75kPa for tests 2 and 5 respectively at a radial location of 180mm from the pile axis. The values of τ_i developed during test 5 were greater than those produced from tests 3, (sand only test) and demonstrated the boundary effects of the clay. The magnitude of τ_i was greatest at the innermost radius and diminished in value at increased radial distance from the pile axis per increment of load. The direction of τ_i can also be linked with the radial displacement diagram illustrared in Figure 7.46. The change of $\tau_{i_{max}}$. as compared to the initial residual values in τ_i is also made under each relevant diagram.

7.4.5 Changes In Vertical Stress And Radial Shear Stress During The Uplift Test.

The changes in effective vertical stress and radial shear stress during the constant rate of uplift test are illustrated in Figures 7.31 and 7.32 respectively. The magnitude of these stresses were again small and generally within the limits of accuracy of the instrumentation. However these changes did display trends which could be related to displacements within the soil media. Also illustrated

in the diagrams are the post residual effective vertical stresses and radial shear stresses deduced from averaging the last three scans of the maintained load test under zero applied load. The total change in these stresses near the end of the pull out test were also plotted to display their total change.

7.4.5.1 Change In Effective Vertical Stress In A Sand Only Profile.

The initial change in $\Delta\sigma'_{zi}$ during the 114mm diameter pile tests illustrated a general relief in stress. This was followed by an increase in $\Delta\sigma'_{zi}$ where compressive straining within the sand occured. For test 1 the compressive straining was evident from the first incidence of applied load. The general trend was then a reduction in $\Delta\sigma'_{zi}$ with further pile pull out. This indicated a relief in stress and was probably related to the flow of sand around the pile base filling the cavity caused by the test. Following the initial relief of stress during the early stages of test 4 there was a positive build up in $\Delta\sigma'_{zi}$across the whole of the instrumentation level. Due to the nature of the test no cavity appeared around the base of the pile, hence there was no stress relief in this area. The increase in $\Delta\sigma'_{zi}$ possibly indicated failure occuring in the sand releasing a positive increase in $\Delta\sigma'_{zi}$.

Test 6 displayed an unique change in $\Delta\sigma'_{zi}$ with increasing radial location from the pile axis. During the early stages of the pull out test there was a significant reduction in $\Delta\sigma'_{zi}$ at a radial distance of r=280mm. At the inner and outer most radial location of the D.P.T.s there was an insignificant change in $\Delta\sigma'_{zi}$ but a gradual reduction in $\Delta\sigma'_{zi}$ was displayed during further withdrawal of the pile. This set the trend in the stress profile throughout the pull

out test. The maximum reduction in σ'_{zi} at r=280mm was 4.75kPa. The general trend indicated that the stress relief was related to the release in the action of the radial shear zone. On completion of the pull out test there was an increase in σ'_{zi} at the outer radii limit. At r=180mm there was a reduction in σ'_{zi} which may be associated with a loosening of the sand local to this area. This may be due to sand flow into the cavity caused by the pile extraction and being forced down on pile release at the end of the test.

7.4.5.2 Changes In Effective Vertical Stress In A Two Layered Soil Media.

During the early stages of the pull out test carried out on test 5 σ'_{zi}displayed a positive increase in value. This was in agreement with the relative vertical displacements at this period in the last test. A peak value of 2.75kPa was reached for a pile displacement of -5.92mm, at a radial distance of 180mm. This value diminished with increased radial position from the pile axis. With further pile withdrawal there was a general reduction in $\Delta\sigma'_{zi}$ across the sand/clay interface. Examination of the vertical displacement results from this period onwards, shows marginal increases in soil displacement at the interface, whereas in the sand above a steady uplift was displayed. The result of this was the production of extensive straining causing a reduction in σ'_{zi} reflected in the D.P.T.s results.

7.4.5.3 Development Of Radial Shear Stress Within A Sand Profile.

The change in radial shear stress during test 3 and 4 implied that the sand was drawn towards the pile which ties in with the radial displacement results, refer to Figure 7.49.

The greatest change in τ_i was detected on the transducers nearest the piles, and decreased with increased values in r. The magnitude of τ_i tended to upper limits of 0.75kPa and 5.5kPa for tests 3 and 4 respectively during the initial stages of uplift and only increased marginally thereafter. This implied that there was a significant relief of stress due to the sudden uplift and with further extractions of the pile, only marginal releases in τ_i were detected.

An interesting feature when comparing the magnitude of τ_i between tests 3 and 4 was that τ_i was significantly larger in the latter. This was a function of the boundary conditions at the location of the transducers. This does give rise to possible speculation over the magnitude of the results, although they were true values within the context of the tests.

Test 6 produced a trend in τ_i that was significantly different to the previous two tests. The τ_i values were all negative with a peak value of -4kPa at a radial location of 180mm for a pile displacement of 30mm. The majority of the change in τ_i took place over the initial phases of pile retraction, tending to a displacement limit of -6mm, with smaller increments of τ_i thereafter. This trend in τ_i can be linked with a greater stress relief in the sand below pile base level. When this was compared with the change in vertical stress levels there was a marked similarity in the trends, which can be correlated to stress relief in the radial shear zone due to the upward movement of the pile. A feature of the 3 tests 3,4 and 6 is that when the pile was retracted the peaked final values in radial shear tended to the zero datum.

7.4.5.4. Development Of Radial Shear Stress At The Sand /Clay Interface.

τ_i reduced in magnitude during the initial stages of the pile uplift test. It reached a peak value of +2.75kPa at a radial distance of 180mm from the pile axis for a pile displacement of -10.80mm. This again illustrated the relief in stress and an apparent movement of sand inwards towards the pile shaft. This was reflected in the radial displacements within the sand at a depth just above the sand/clay interface. With further pile withdrawal there was a reduction in τ_i which corresponded to a reduced Q_a. This probably corresponded to shear failure at the soil pile interface causing a release in the uplift stress generated within the soil hence a reduction in sand movement.

7.5 Soil Displacements

Both the vertical and radial soil displacements were monitored throughout the experimental programme. Vertical displacements were measured using the electrolytic levels and the radial movement was monitored by the "terra plates" and displacement transducers.

7.5.1 Pile Installation

7.5.1.1 Vertical Displacements In A Homogeneous Sand Profile.

The vertical displacements (V) generated within the sand during pile installation for test 1 and 3 are illustrated in Figures 7.33 and 7.34. For test 3 during the initial stages of pile installation there was evidence of surface soil heave (0.10mm) at a radial distance r=310mm to a pile penetration of 210mm. There was no evidence of this

during test 1. With further pile penetration sand settlement occured, the rate of which diminished with increased D_b values tending to an apparent steady quasi constant limiting value.

Subsurface vertical displacement first became evident at a radial distance of r=180mm when the pile base was typically 5B-7B away from any one particular level of instruments. With further pile penetration within this region there was a rapid increase in vertical displacement. The greatest magnitude in V being at r=180mm, this diminished with greater values of r thus displaying a dished effect in sand movement. As the pile base approached to within 2.5B of the instrumentation level there was a marked reduction in the vertical movement. At a D_b value of typically 1.0B subsurface heave started to occur at the innermost radially located electrolytic levels. This correlated to the depth of the "active wedge" formed beneath the pile base. It is suggested that from this point onwards that the sand layer beneath the pile was in a state of rupture caused by the punching action of the active wedge. This relates to work by Robinsky and Morriston (1964) where it was estimated that the onset of rupture occured at 1.0B below pile base level.

Sub-surface heave was detected up to radial limits of r=240mm (4B) and r=460mm (4B) for test 1 and 3 respectively. At a depth of 1250mm peak heave values of 0.50mm and 0.75mm were recorded for tests 1 and 3 and were reached at pile penetration depths of 1350mm and 1250mm for the respective tests. With further pile penetrations sub surface heave subsided and once again a downward movement was reinstated within the sand. The rate of vertical displacement diminished with further pile penetration seemingly tending to a quasi steady limiting value.

7.5.1.2 Vertical Soil Displacements In A Layered Soil Profile.

During pile installation up to a depth of 1000mm the general trends in the V-D_b profiles were similar to the sand only tests.

For tests 5 during the initial stages of pile installation surface heave was evident at a radial distance of 310mm. This was not detected during test 2. After a pile embedment depth of 210mm soil heave at the surface ceased and the soil displacements were in a downward direction. They were evident at a radial distance of 960mm toward the end of pile installation where again they appeared to be tending to a quasi constant limiting value.

For D_b values greater than 1100mm the boundary effect and heave at the sand/clay interface had a substantial effect on the V-D_b profiles which was particularly evident in the electrolytic level results located at depths of 1000mm and 1250mm within the soil strata. As the pile approached and entered the interface layer a marked increase in soil heave was observed at the sand/clay interface.

With further pile penetration through the interface layer there was a significant decrease in the rate of soil heave. For both tests heave was evident up to a radial distance of 460mm from the pile axis but decreased in magnitude with increased r values. During tests 2 a peak uplift value of 1.25mm was obtained at a pile penetration of 1650mm, at a radial distance (r) of 120mm (2B). For test 5 the heave was 3mm for a D_b value of 1600mm at r=160mm (1.4B) These were twice the values stated by Lake (1986) and Wersching (1987) (0.70mm and 1.4mm respectively) which validates the latters disputation on the performance of the type (0714) electrolytic levels. The resultant

compressive straining is reflected in σ'_{zi} results, refer to section 7.4.3. The marked increase in the upward movement at the interface was reflected in the restrained development of vertical displacements within the body of sand. This was evident when a comparison was made in the V-D_b profiles produced during tests 3 and 5. With further pile penetration the vertical displacement reverted back to a downward movement which was evident throughout the sand profile. Towards the latter stages of test 2 a significant increase in downward vertical displacement was displayed within the overlying sand but not particularly so at the interface level. Probably this was due to the method of driving. Where an increased number of blows/pile penetration were required to drive the pile into the clay causing greater agitation and settlement local to the pile.

7.5.1.3 Radial Displacements In A Homogeneous Sand Profile.

The radial displacements "R" generated within the sand during pile installation are illustrated in Figures 7.35 and 7.36. From the onset of pile installation radial movement was detected at a depth of 375mm during both tests 1 and 3. At greater depths within the sand lateral soil movement was evident when the pile base was on average at depths of 500mm (8.3B) and 900mm (7.9B) for tests 1 and 3 respectively. This correlated to the initial development of vertical soil displacement. As the pile base approached a level of instruments, the outward lateral movement increased rapidly. This was true across the plane of measurement but diminished in value with greater radial distance from the pile axis. Throughout both tests the lateral movement outwards peaked when the pile base was at or just below the instrumentation level. This indicated the full compressive expansion

of the soil with the introduction of the pile. The magnitude and build up of radial movement was apparently independent of any soil heave but was affected by the pile diameter and tentatively agrees with expanding cavity theory. The small lateral movements developed after this stage were probably due to the local development of radial shear zones, refer to section 7.4.3.

Further pile penetration resulted in a reversal in the direction of radial movement indicating some relief in the compressive strain. This was again evident at all radial locations with reduced values at greater radial distances from the pile axis. The change in direction of radial movement was more prominent in test 1 and was probably a result of the method of driving. Towards the end of pile installation for both tests the radial movement tended to a quasi constant value, a feature which was also prevalent in the vertical displacement profiles.

From the R-D_b profiles the magnitude of radial displacement at the innermost radial located instrumentation throughout the body of the sand are similar within the context of the respective tests. With increased values in r the radial movement was greater within the upper portion of the sand. This movement apparently decreased with increased depth within the sand. This was a feature which was common in the vertical displacement V-D_b profiles. A comparison in the R-D_b profiles between the 2 tests illustrates that the ratio of R/B at a radial distance of 2B from the pile axis on average gave a common value of 0.04.

7.5.1.4 Radial Displacement In A Layered Soil Profile

The results are given in Figures 7.35 and 7.36. The R-D_b profiles illustrate radial movement within the sand layer. They display very similar trends to those given for tests 1 and 3. An important feature of test 2 was that towards the end of pile installation at a D_b value of 1575mm onwards there was a significant increase in the radial movement of the sand towards the pile axis. This was evident throughout the sand layer which increased in magnitude with closer proximity to the pile. A result which was again reflected in the vertical soil movement and a probable result of the incresed blow count/pile penetration within the clay. An extension of the R-D_b profile within this region, shown by the dotted line in Figure 7.36, indicated the R-D_b profiles would tend to a steady value. This latter point was also reflected in the R-D_b profiles for test 5 but the movement of sand towards the pile was less and tended to a steady state across the horizontal plane when the pile base was 1.0B below the instruments located at depths of z=625mm and z=1125mm. The instruments near the sand surface again showed greater latitude in movement and achieved a steady state condition at a greater depth below the level of instruments similar to the sand only tests. The R-D_b profiles also demonstrate that the occurrence of soil heave at the interface had little effect on radial soil movement which was primarily a function of the pile intrusion into the soil profile. The R-D_b profile for test 5 illustrates very clearly how the radial movement within the sand at all radial location diminished with depth.

7.5.1.5 Radial Displacements Within A Sand Due To Pile Installation.

At each radial location within the body of sand an average value in peak radial displacements was evaluated seperately for the 60mm and 114mm pile tests. The resultant values were normalised with the pile radius, (2r/B). These are illustrated in Figure 7.37 along with values produced by Davidson et al(1981) and Wersching (1987).

Wersching (1987) evaluated radial displacement values by proportioning out the change in volume of the sand from the vertical displacements. It was also assumed that at radii greater than 4.0B no lateral displacement occured.

The dimensionless radial displacement (2R/B) at any radius (2r/B) within a soil subjected to $\varepsilon_z=\varepsilon_v=0$ can be evaluated using equation 7.5 for a closed ended pile after Randolph et al(1979);-

$$2R/B = ((2r/B)^2 - 1)^{0.5} - 2r/B \quad \ldots\ldots\ldots \text{ equation 7.5}$$

Wersching (1987) used the result of this equation to predict lateral displacement in a loose sand. This was achieved by the introduction of an empirical compaction factor which gave the following relationship:

$$2R/B = C^{(2r/B)}(2R/B), \quad \varepsilon_z=\varepsilon_v=0 \quad \ldots\ldots\ldots \text{ equation 7.6}$$

He found that acceptable agreement between the theoretical and his deduced experimental values was achieved when C=0.78. To fit the normalised direct peak values measured during the 60mm and 114mm tests a C value of 0.85 was evaluated. This is shown in Figure 7.37 along with the predicted curve given by Randolph et al(1979)

During the 114mm pile tests only a marginal relief in the peak radial compressive strain was evident. This would have had little effect on

the predicted value of peak lateral movement. However during the dynamic test the reduction in compressive strain was rather more significant which would require a further adjustment to the compaction factor C.

7.5.1.6 Two Dimensional Strain Development Within The Soil Per Unit Pile Penetration.

Two dimensional strain development on an initially horizontal plane at a depth of 1250mm (11.0B) due to pile installation is shown in Figures 7.38 and 7.39 for a 60mm and 114mm diameter piles respectively. The development of vertical strains at the sand/clay interface were also plotted on the respective figures. They are based on a steady state displacement field existing around the base of the pile whilst penetrating through an homogeneous sand. This assumption may be slightly presumptuous particularly in the case of the dynamically driven pile. The development of vertical strains within the sand only profile are similar for both methods of driving. Generally there seems to be a slight translation in the strain profile form involving the negative strain development. For the dynamically driven pile peak extensive straining occured at 1.33B above pile base level at a radial distance of 120mm(2.0B) from the pile axis. For the constantly driven 114mm pile this occured around base level at r=160mm(1.4B). However at these radial distances for the respective methods of driving peak compressive straining tended to a value of 2B below pile base level.

During the sand/clay tests the magnitude of the peak compressive strains were significantly less, particularly for that of the dynamically driven pile.They were also slightly out of phase with

those produced during the sand only tests. This drop in magnitude may be attributed to the greater elastic properties of the underlying clay. In the case of the 60mm pile the method of driving may have been a contributory factor.

At the sand/clay interface peak extensive strains were greater than those produced by the sand only tests again a reflection in the properties of the clay.

Beyond the influence of the pile base within a sand only profile the vertical strains tended to a steady compressive state.

These results are in agreement with the work of Wersching (1987). Vesic (1965) produced strain profiles based on the work of Robinsky and Morrison (1964) and it suggests that the strains within the sand close to the pile base were extensive. Robinsky and Morrison (1964) postulate that sand movement close to the pile decreases the sand density within this region. This may be the case but through the complex development of arching the resultant vertical displacement at greater radii may lead to compressive straining within the soil as evidently shown in the 60mm and 114mm pile tests.

The ratio of maximum vertical compressive strain to the maximum extensive strain was generally around the order or 2 which broadly agrees with Vesic (1965)

Superimposed onto the vertical displacement strains produced from the 114mm pile tests are the relative details in the build up of the effective vertical stress. It illustrates a good correlation existing between the recorded stress levels and the development of strain within the limits of the instrumentation.

Radial strain development was deduced from the instrumentation layer located at a depth of 1125mm. The trend in development of radial strain was similar for both methods of pile installation. For the 60mm pile tests there was an apparent upward vertical translation of the profile relative to the pile base when compared to the 114mm pile test, similar to the vertical displacement strains.

The development of radial strain for the sand/clay tests at the same level of instrumentation showed little variation from the sand only tests. For clarity the strain values were therefore not plotted on the relevant figures. Peak radial strain for the dynamically driven pile occured at 1.25B below the pile base at a radial location of r=2B from the pile axis. At the same radial location peak radial strain occured at a distance of 2B below the pile base for a constantly driven pile.

Within the limit of instrumentation the strains developed around the pile shaft remote from the influence of the pile base were extensive in nature. Thus indicating a relief in lateral compression. The peak shear stress development across the plane of instrumentation at a depth of 1250mm within the soil was superimposed on the radial strain figure of the 114mm pile. A good correlation seemed to exist between those two entities within the limits of the instruments.

Making relevant assumptions the resultant strain vectors of the vertical and radial strains were evaluated and are illustrated in Figures 7.38 and 7.39. They show two dimensional strain development around the base of continuously penetrating pile through a loose sand. The strains generally radiate from beneath the base of the

pile. They principally acted within a zone stretching approximately 6B below the pile base and up to a radial zone of 4B from the pile base axis, although minor strain development was detected outside this region. Above pile base level a steady state in strain development was evident.

7.5.1.7 Vertical and Radial Displacement Zones Around The Base Of A Continuously Penetrating Pile In Homogeneous Sand.

To indicate the extent and movement of sand to a continuously penetrating pile, prominent points were selected from the $V\text{-}D_b$ and $R\text{-}D_b$ profiles. These were then plotted relative to the pile base and are illustrated in Figures 7.40a and b for the 60mm and 114mm piles respectively. The zones were fairly consistent for both pile driving methods. Although due to the larger driving increments during the dynamic method the boundary of the zones were not so distinguishable. The vertical soil movement exhibited a spear shaped region with six fairly distinct zones, the outer limits of which tended to 6B from the pile axis. The extent of the radial zones was again of the order of 6B. Three zones were evident although due to the nature of the dynamic tests the final zone could also be divided into 2 distinct areas.

For the vertical movement the six distinct zones were first defined by Wersching (1987) and are included here for comparison and completeness.

Zone I Increasing rate of downward displacement

Zone II Reducing rate of downward displacement

Zone III Increasing rate of upward displacement

Zone IV Reducing rate of upward displacement

Zone V Increasing rate of downward displacement

Zone VI Steady rate of downward displacement.

The boundaries between these zones were significant in terms of ε_z defined by relative points of the V-D_b profiles.

I-II Maximum compressive strain.

This appeared to emanate from around the pile base. The radial limit of this boundary defined by the point of convergence with boundary V-VI, generally extended to a radius of 6B from the pile axis and 3B below the pile base.

II-III Zero strain.

This appeared to originate from a point normal to the active sand cone at its mid height extending radially to 4-5B and at a depth approaching 1.5B

III-IV Maximum extensive strain.

This region appears to extend from the pile base level and runs through the points of intersection of boundary II-III and IV-V and I=II and V=VI.

IV-V Zero strain

The point of origin of this boundary differs between the 2 types of pile installation. For the dynamically driven pile it originates from a point approximately 1.75B above pile base level. Whilst for the pile driven at a constant rate it appears to emante from just above pile base level. Both appear to extend to the radial limits of boundary II-III.

V-VI Onset of steady state compressive strain.

For the piles driven dynamically and at a constant rate of

penetration, the onset of steady state compressive strain extends from points approximately 4B and 1B respectively above pile base level and intersects the boundary I-II at a radial distance of 6B.

The boundary II-V identified the limit of the minimum rate of change of compressive strains generated within the sand. At the inner limit compressive strains were reduced to zero coinciding with an inflexion point in the V-D_b profile, before again increasing with an inflexion point in the V-D_b profile, before again increasing. At the outer limit, the development of V with D_b was unaffected by the passage of the pile base.

These zones defined by Werschning (1987) correlate well to both type of pile installation. Although zones I,II and III were in accord in location and extent below pile base level for the dynamically driven pile, zones IV,V and VI were enlarged in extent above pile base level.

Four specific zones of radial movement within the sand were identified for the dynamic pile installation method. For the constant rate of penetration method only three zones were evident. The zones were as follows:

A - Increasing rate of outward radial movement

B - reducing rate of outward movement

C - Increasing rate of inward movement.

C'- Steady rate of inward movement.

The boundaries between these zones were significant in terms of ε_r.

A-B Maximum Compressive Strain.

This appeared to emanate from the face of the active sand cone formed

ahead of the pile and extended to the limit of 6B from the pile axis and 2B below pile base level.

B-C/C' Zero Strain.

This appeared to originate from the pile shaft at points of 1.0B and 0.5B above the pile base for the 60mm and 114mm piles respectively. It extended at a slightly depressed elevation to a radial limit of 6B. In the case of the 114mm pile the boundary also signified the onset of steady state extensive strain.

C - C' Steady Rate of Strain.

For the dynamically installed 60mm pile this boundary signified the point of steady state extensive strain, ϵ_r. It appeared to initiate from a point on the pile shaft 6B above the pile base level and tended to-wards the outer limit of boundary B/C. Beyond the radial limit of 6B from the pile axis the radial strain generated within the sand was considered to be negligible.

7.5.2 Maintained Load Test

The vertical soil displacements generated within the soil due to the initial maintained load tests carried out after pile installation are illustrated in Figure 7.41. The vertical displacements produced from the maintained load tests carried out after cyclic loading were very similar to the post installation results and are therefore not included here. However as a comparative exercise the variation in the vertical displacement after the dissipation of pore water pressure for the two layered soil profile have been included to illustrate the consolidation effects of the clay layer.

The magnitude of the vertical displacements were those recorded at

the end of each load increment and the excess of the values produced from pile installation.

The vertical displacements recorded during the first cycle of applied loads up to the working load demonstrated virtual total elastic recovery and have been ommitted for clarity.

7.5.2.1 Homogeneous Sand Profile.

The vertical soil displacement generated from the pile tests with end bearing illustrated a downward trend in movement which diminished with radial distance from the pile axis. The magnitude of the displacements produced from test 3 were similar to a comparable test carried out by Wersching (1987). However a significant difference between the relative vertical displacement between the two innermost radially located electrolytic levels was observed. The effect of this is discussed in section 7.5.2.3. Yoshimi and Kishida (1981) suggest that no slip ocurs between a metal/sand interface regardless of the conditions until the mobilized value of tan δ' was in excess of 0.7-0.8 tan δ'. For values of load up to and including the working load this was generally the case. Hence the vertical soil displacement at the pile/soil interface could be equated to ω_t up to the applied working load.

On release of the failure load elastic recovery was evident within the soil. For the driven piles at the innermost radially located electrolytic level the elastic recovery was in the range of 42-64% of the total displacement produced by Q_{amax}.

The larger elastic recovery was exhibited in the soil surrounding the dynamically driven pile. For the in-situ pile with end bearing, test

6, the elastic recovery within the soil was only marginal at 9% of the total displacement. The increased density of the sand due to pile driving resulted in an increased elastic recovery. The vertical soil displacements developed during test 4 were small in magnitude. This was expected in relation to the low applied load and small values in pile displacement.

7.5.2.2 Layered Soil Profile.

The vertical soil displacements generated during test 2 and 5, exhibited greater orders of magnitude in comparison with the sand only tests. The vertical displacements increased with depth with significantly greater displacements being recorded at the sand/clay interface. This may be accounted for by the differential frictional forces set up along the pile shaft by the two types of soil. The clays greater cohesive qualities draging the soil down, with greater resultant vertical displacements. This was particularly evident in test 5. The trend in progressively greater displacements with increased depth would lead to extensive straining in the soil above the sand/clay interface. This would lead to a reduction in the effective vertical stress, a fact which was illustrated earlier in section 7.4.4.3.

On release of the failure load a variation in the recovery of the soil was evident. At the sand/clay interface, the greater elastic recovery of the clay lead to an 85% recovery of the maximum vertical displacement produced from the application of Q_{amax}, at a radial location of r=120mm and r=160mm for tests 2 and 5 respectively. The soil displacement recovery within the main body of the sand was similar to the sand only tests, ranging from 54%-62% of the maximum

recorded values at the innermost radially located electrolytic levels.

The variation in the vertical soil displacement recovery at the sand/clay interface would lead to local compressive straining within the soil. The resultant effect of this would be an increase in the effective overburden pressure which correlated to the results produced by the vertical pressure transducers reported in section 7.4.4.3.

Figure 7.42 illustrates the vertical soil displacement which evolved during the pore water pressure dissipation period. Greater consolidation effects were evident with closer proximity to the pile which correlated to the magnitude of the pore pressure gradient set up within the clay due to the pile installation.

The development of vertical soil movement during the maintained load test carried out after the pore water pressure dissipation period is illustrated in Figure 7.43. The trend and magnitude in the vertical displacement being similar to those exhibited during the first maintained load test. However the recovery in the vertical displacement did appear to be significantly different within the body of the sand layer.The magnitude of the percentage recovery was of the same order as that experienced at the sand/clay interface and was generally 79%-85%.

7.5.2.3 Semi Normalised Vertical Displacement Profile From The Maintained Load Test.

By relating the soil displacements around a pile under working load conditions, Cooke et al (1979) evaluated the distribution of the

shear modulus of a soil in a stressed zone around the loaded pile. Werscheing (1987) adopted this method to evaluate the distribution of shear modulus around a driven pile in a loose sand. By plotting the parameters V/Q_a and $2r/B$ on a logarithmic scale he found a linear relationship existed between them, except at r=160mm. Scepticism was shown in Werscheing's work on the reliability of the results of the type 0714 electrolytic levels used at this radius. As stated in section 7.5.2.1 a variation in relative vertical displacements at this radii was noted between the present work and that of Werscheing (1987)

When the results of the parameters V/Q_a and $2r/B$ deduced from tests 1-6 were plotted in a logarithmic scale a good linear relationship was found to exist at all radii. The type 0714 electrolytic level being replaced by the type 0716. The resultant functions of the logarithmic plots of V/Qa and 2r/B for the sand only tests are illustrated in Figures 7.44 along with the actual calculated values V/Qa at the various locations of the electrolytic levels. The average value of the four functions was evaluated and is given in equation 7.7

$$V/Q_a = 0.061\ (2r/B)^{-1.45} \quad \text{.....equation 7.7}$$

This was also plotted on Figure 7.44 and is in reasonable agreement with the results for both the driven and in-situ pile tests.

7.5.2.4 Variation In The Shear Modulus Of Homogeneous Sand With Radius From The Pile Axis At Working Load.

Poulos and Davis (1980) in analysing results of pile tests in sand, assuming that the soil modulus remained constant with depth, calculated the elastic soil modulus in loose sand to range from

27.5-55.0 MN/m^2 for a driven pile. This gives a corresponding range in shear modulus, G of 10.6-21.2MN/m^2 . The initial tangent shear moduli derived from the drained triaxial tests gave an average G value of 15.8 MN/m^2. The shear modulus within the soil were calculated using equation 7.8.

$$G = \frac{T_o \; B}{2r(V2-V1)} \quad \text{..... equation 7.8}$$

where V1 and V2 are the vertical displacements bounding the annulus of soil under consideration of width r.

Up to the working load no slip at the pile/soil interface was assumed (refer to section 7.5.2.3) Therefore V2 at the interface was assumed to equal the pile displacement.

The deduced values for tests 3 and 6 are illustrated in Figure 7.45 and show generally decreased values in the shear modulus with proximity to the pile. A back analysis of the derivation of equation 7.7 was also carried out to give the average variation in shear modulus with radial distribution.

This was in good agreement with the actual calculated values and intercepted the tangent modulus at a radius of 1100mm from the pile axis. The range in shear modulus for tests 1 and 4 were also evaluated and were 0.13-14.40MN/m^2 and 1.15-338MN/m^2 respectively. For the two layered soil profile tests the shear modulus in sand was evaluated up to a depth of 1000mm and ranged from 0.08-4.80MN/m^2 and 0.28-5.92MN/m^2 for test 2 and 5 respectively. The lower values being encountered nearer to the pile shaft.

7.5.2.5 Radial Displacement Within The Homogeneous Sand.

The radial movement generated within the sand during the maintained load test is illustrated in Figure 7.46. The values plotted are those recorded at the end of each load increment and the excess of those values produced from pile installation. The magnitude of the radial movement was generally in excess of 10 times less than the vertical movement and within the limits of accuracy of the instrumentation. However the trends in movement were fairly consistent throughout the testing programme.

During the initial increments of load there was an apparent movement of the sand towards the pile causing a relief in the compressive strain caused during pile installaton for the driven piles. As the applied load increased beyond the working load the radial movement acted outwards away from the pile. This trend was generally the case for all the tests and was particularly prevalent in the sand layer above the clay.

7.5.3 Cyclic Load Test.

The cyclic load testing was only carried out during the 114mm pile tests. Figures 7.47 and 7.48 illustrate the development of vertical and radial movement with the sand due to a cyclic load equivalent to the working load of the pile.

7.5.3.1 Vertical Soil Displacements In A Homogeneous Sand Profile.

The vertical movement developed during test 3 and 6 displayed a continuous degradation in the downward direction. The magnitude of this movement was quite significant. For test 3 at a radial distance

of 160mm the total displacement generated after 1600 cycles were on average 11 times greater than the total displacement at pile load failure during the maintained load test. The equivalent displacements during test 6 were 5.5 times greater.

A similar trend in vertical displacement was initially experienced in test 4. However at the end of the 1600 cycles heave conditions were evident. The results of this test may be spurious in nature and no explanation can be offered for this displacement pattern.

7.5.3.2 Vertical Displacement In A Two layered Soil System.

Due to the boundary layer effect of the sand/clay interface the development of vertical displacements during test 5 were significantly different to those of test 3. At a comparable depth of 500mm the vertical displacement was reduced by some 80% between the two tests. The vertical movement within the sand was further restrained with increasing proximity to the sand/clay interface. For a depth of 1000mm the vertical movement was 90% less than that generated during test 3.

At the sand/clay interface there was only a relatively small development of vertical displacement. For the first 400 cycles the vertical displacement was 0.035mm at a radial distance of 160mm from the pile axis. At greater values of r the vertical displacement was negligible. With further application of the cyclic load heave developed at the interface and at the end of the 1600 load cycles the vertical displacement at r=160mm had reduced to 0.015mm.

7.5.3.3 Radial Movement Within The Homogeneous Sand.

The significant feature in the radial displacement was the order of magnitude was much greater than that generated during the maintained load tests as in the case of vertical movement. The sand movement was towards the pile which was consistent with the direction of radial displacement up to the application of Q_{aw} during the maintained load tests. Radial movement was most prominent in the upper layers of the sand and decreased with depth and radial distance from the pile axis.

7.5.4 Constant Rate Of Uplift Test.

The results shown in Figures 7.49 and 7.50 represent the excess vertical and radial displacement generated during the constant rate of uplift test.

7.5.4.1 Vertical Displacement In A Homogeneous Sand Profile.

For the driven pile tests the initial vertical movement generated within the sand at the innermost radially located instruments was generally in an upward direction. For test 3 this trend in movement continued throughout the test although at greater radii the vertical movement progressed in a downward direction. During test 1 at approximately Qsf the general trend in vertical movement was down at all radial locations. This suggests a collapse within the stress transfer mechanism within the sand. A similar trend can be partially detected in test 3 at a radial location of 310mm and a depth of 1000mm.

Another possible explanation for this progression in downward vertical movement would be the ingress of sand towards and into the

void formed below the base of the pile. Although the results of test 4 possibly contradict this.

The in-situ pile tests indicate an overall downward trend in vertical movement throughout the pull out test. Although a slight "pull up" in vertical displacement was detected at a radial distance of 160mm from the pile axis at Q_{sf} during test 4. The pattern of movement does suggest that vertical displacements in the upward direction are more localised. This being a possible consequence of the variation in the radial density gradient between the driven and in-situ pile tests. This also suggests that the trend and pattern of vertical movement is more of a consequence of a mechanism within the soil body, rather than the effects of the void below the base as test 4 suggests.

7.5.4.2 Vertical Movement In A Layered Soil Profile.

The trend in vertical movement within the sand and at the sand/clay interface was progressively upwards throughout the "pull out" test. The magnitude of these displacements at z=1000mm and 1250mm were of the order of 3 times greater than those detected during test 3. At a depth 500mm the values were generally twice as large. The greater vertical movement was a reflection on the properties of the clay relative to those of the sand. Compressive straining was also a product of this vertical movement, the pattern of which was reflected in the effective vertical stress results, refer to section 7.3

7.5.4.3 Radial Movement Within The Sand.

The development of radial soil displacements during the constant rate of uplift test is illustrated in Figure 7.50. The values of R are small and within the limits of the instrumentation. The results

indicate a general movement of sand towards the pile. By equating this pattern of movement to the radial shear stress results, a compatibility in the direction of sand movement is observed.

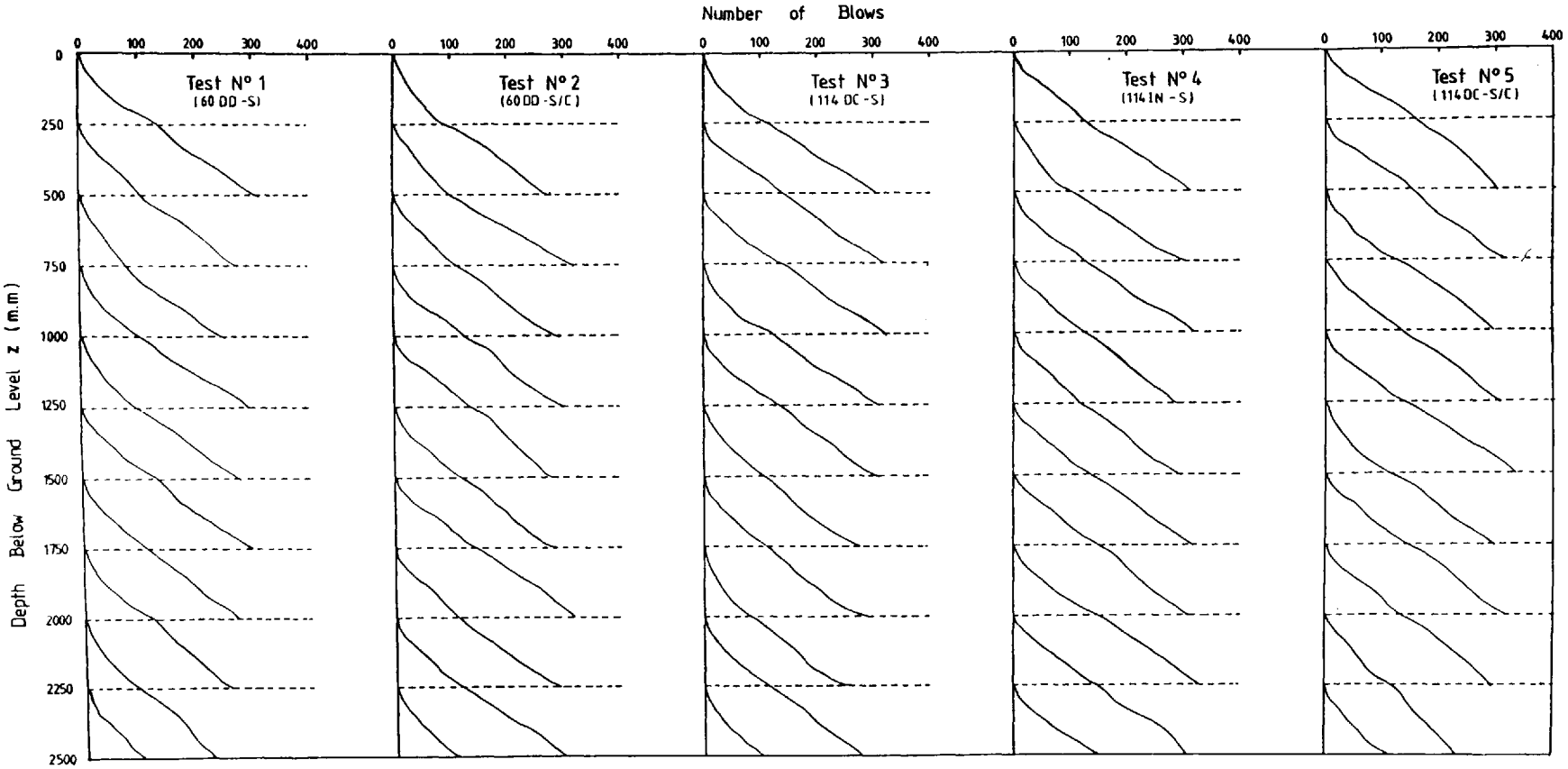

FIGURE N° 7.1 'MINI-MAC' PROBE TEST RESULTS

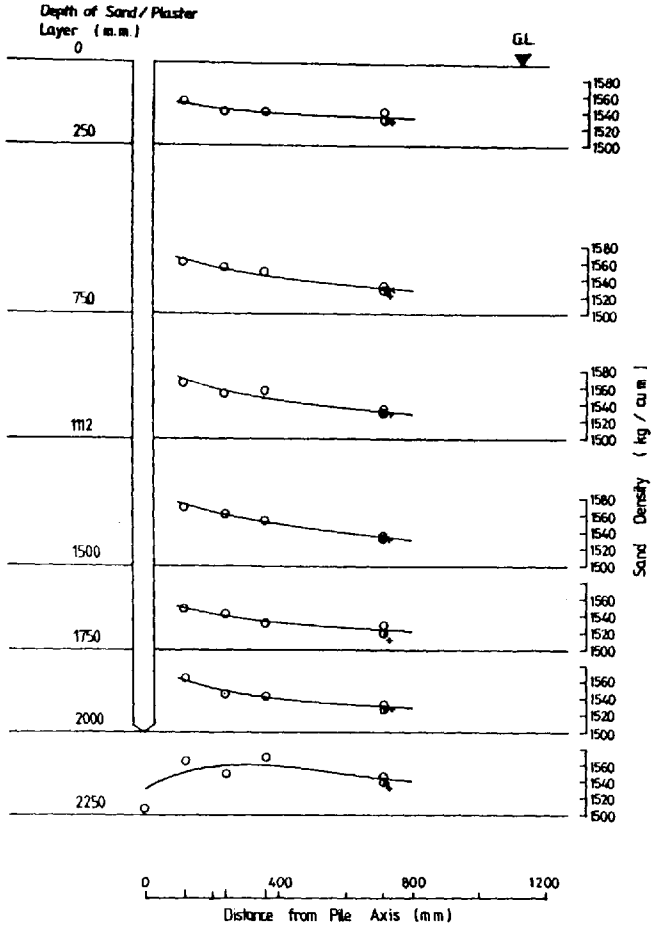

Test N°1 60 DD-S

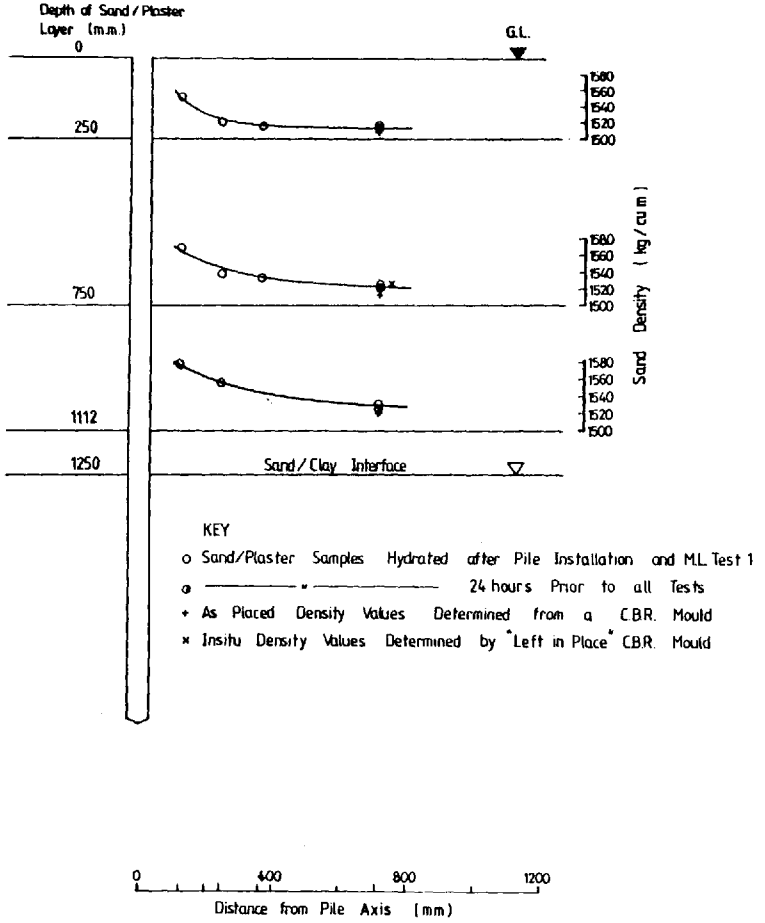

Test N°2 60 DD-S/C

FIGURE N° 7,2 CHANGES IN SOIL DENSITY DUE TO PILE INSTALLATION

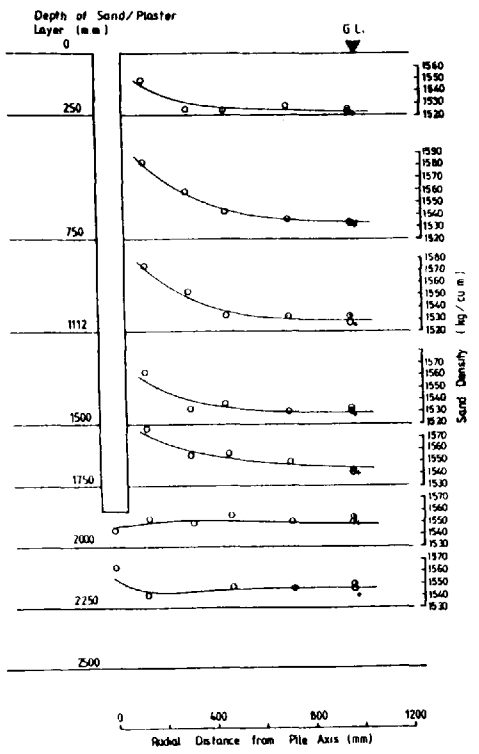

Test N°3 114 DC-S

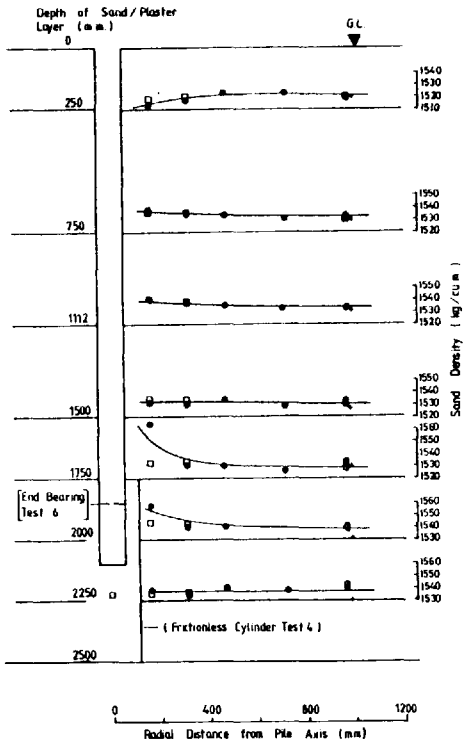

Test N°4 114 IN-S & Test N°6 114IE-S

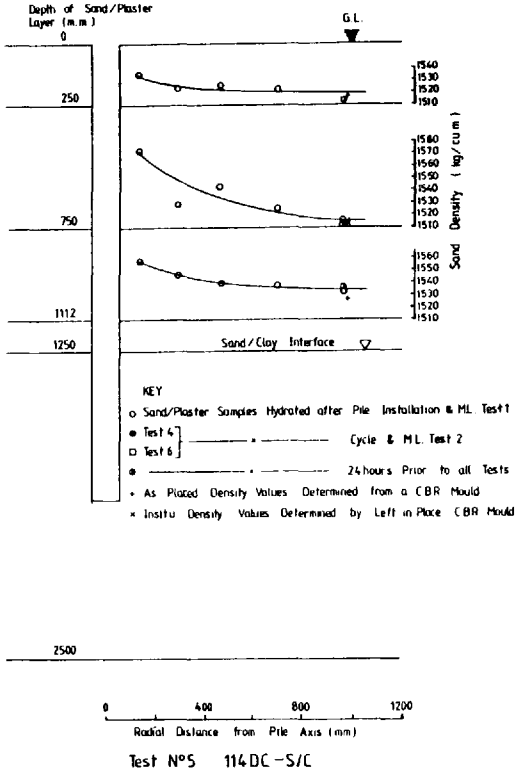

Test N°5 114DC-S/C

FIGURE N° 7.3 CHANGES IN SOIL DENSITY DUE TO PILE INSTALLATION (& CYCLIC LOADING)

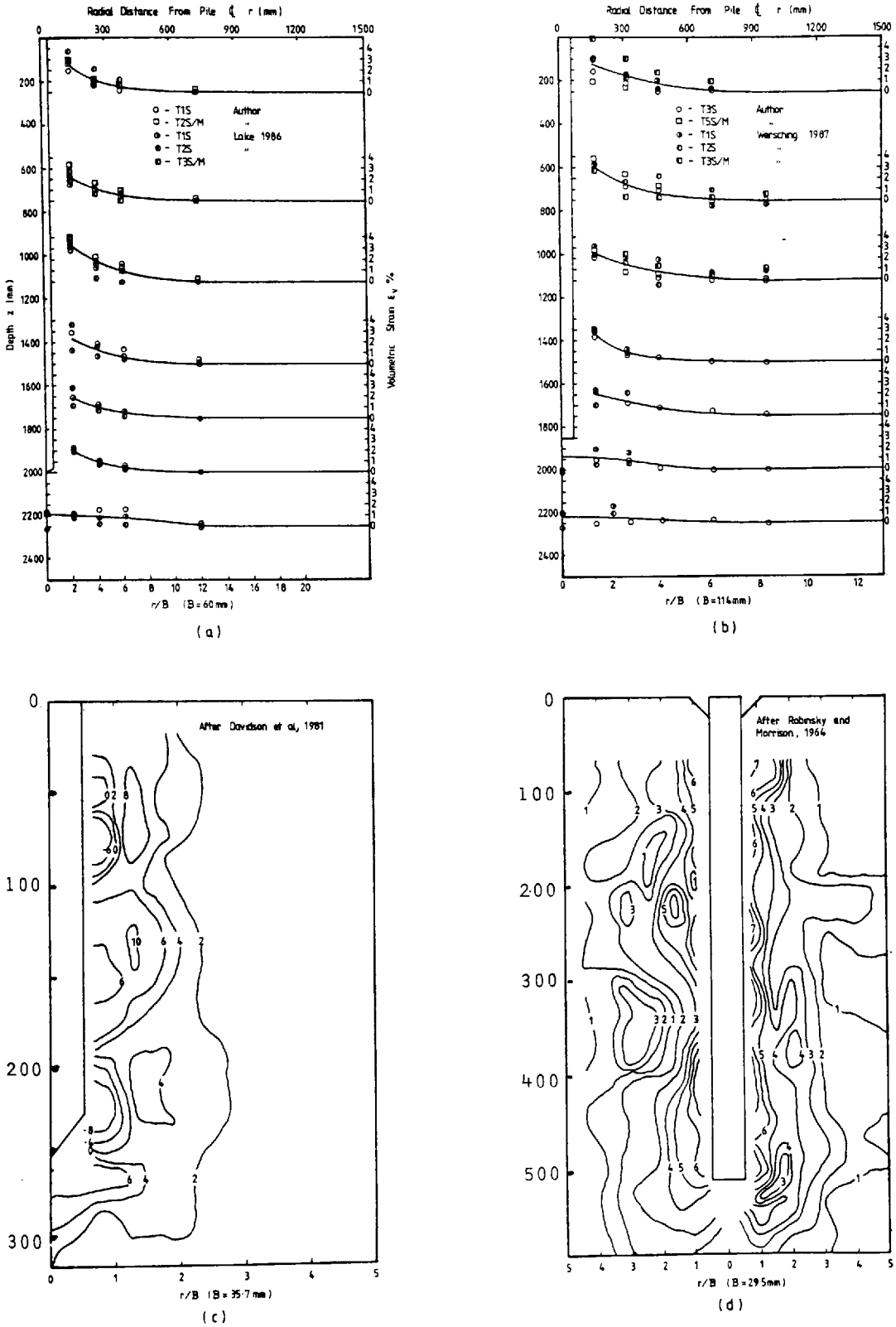

FIGURE 7.4 VOLUMETRIC STRAINS (%) IN LOOSE SAND DUE TO PILE INSTALLATION

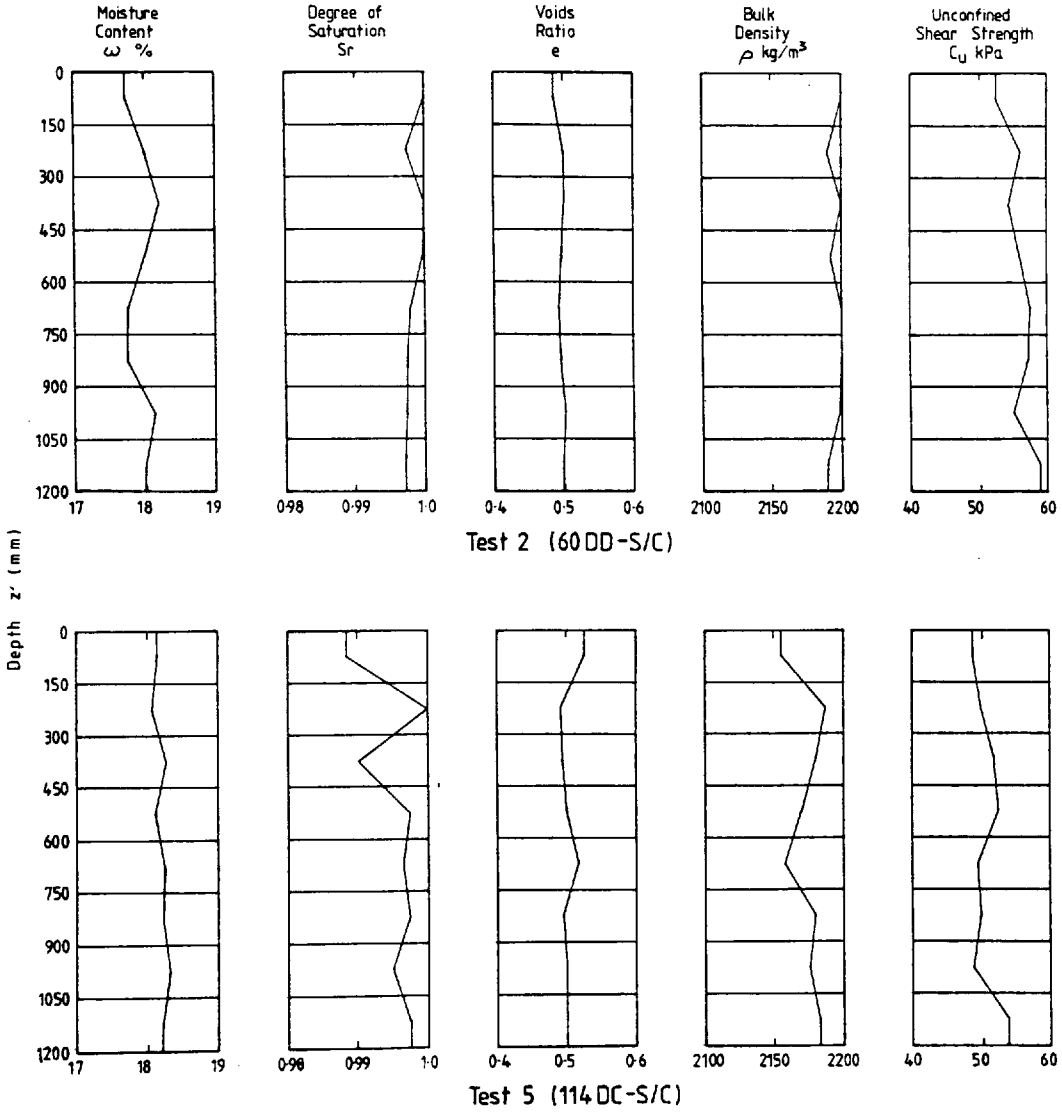

AS PLACED PROPERTIES OF THE RED MARL

FIGURE N° 7.5

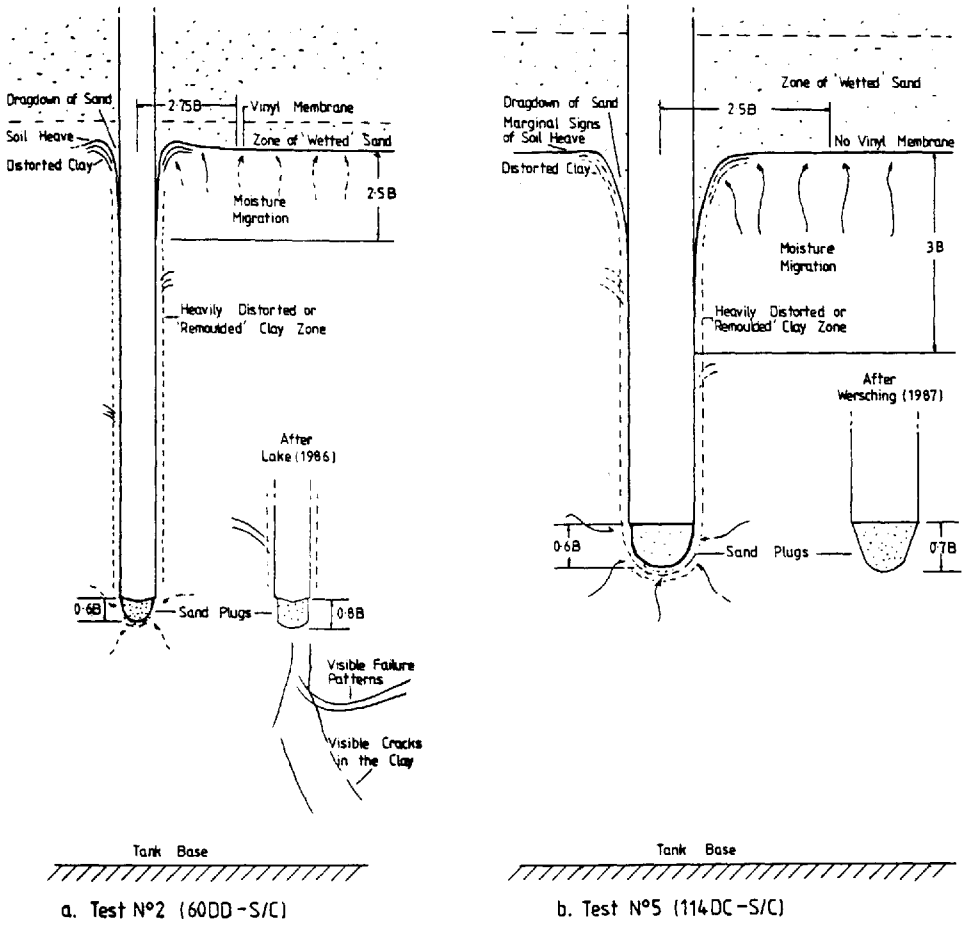

STRUCTURAL CHANGES IN THE CLAY DUE TO PILE INSTALLATION

FIGURE N° 7.6

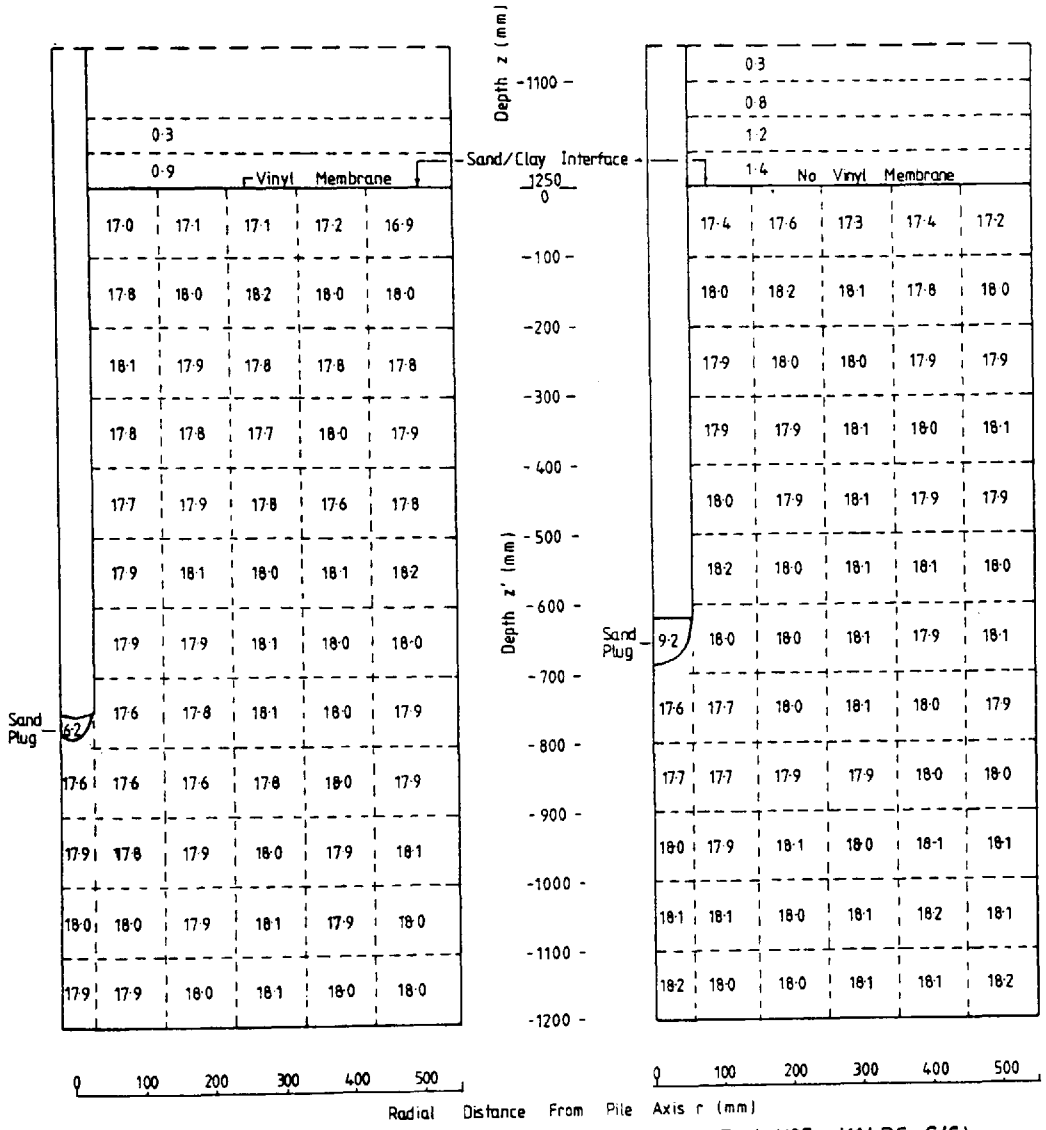

Test N°2 (6000 -S/C)

Test N°5 (1140C -S/C)

SAND - CLAY MOISTURE CONTENT (ω %) PROFILE AFTER PILE INSTALLATION AND COMPLETION OF ALL LOAD TESTS

FIGURE N° 7.7

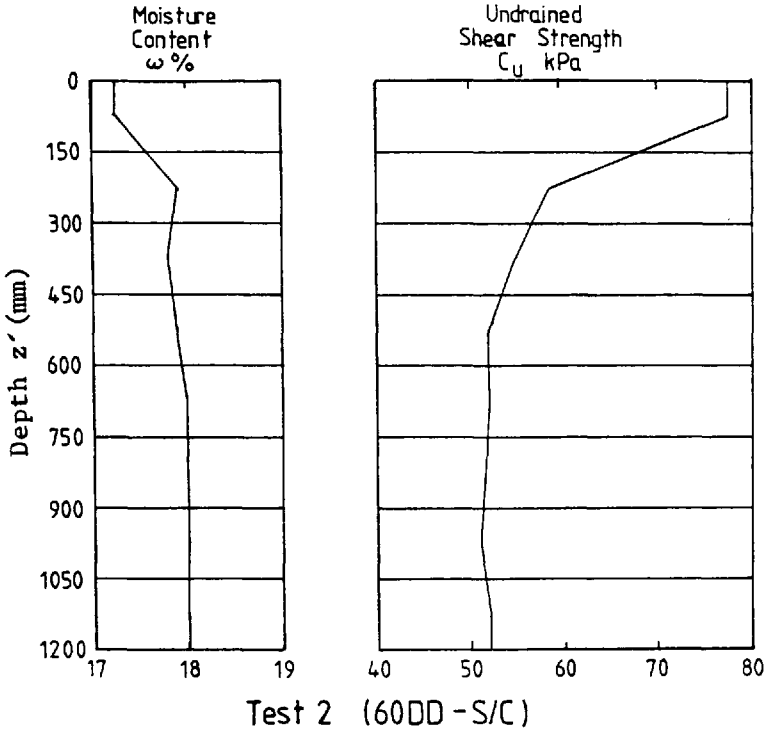

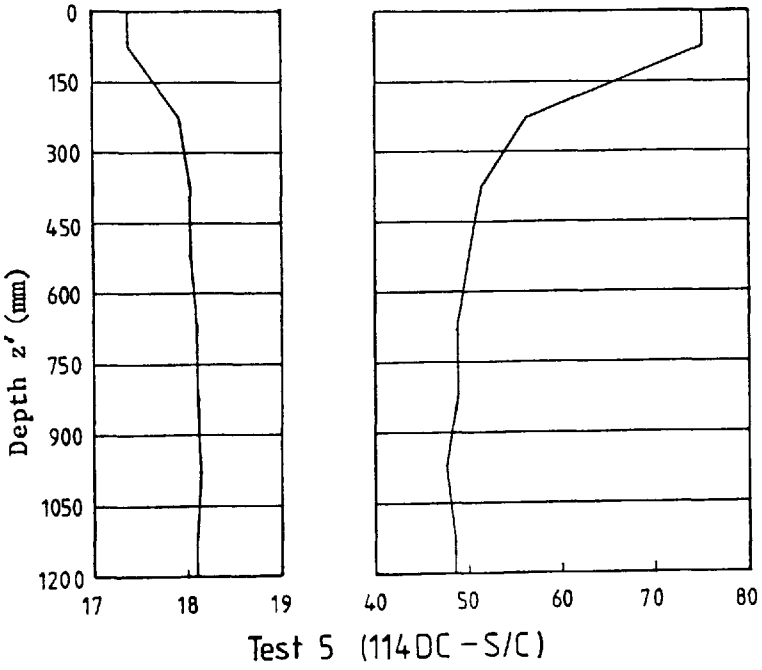

FINAL PROPERTIES OF THE RED MARL AFTER PILE INSTALLATION AND COMPLETION OF ALL LOAD TESTS

FIGURE N° 7.8

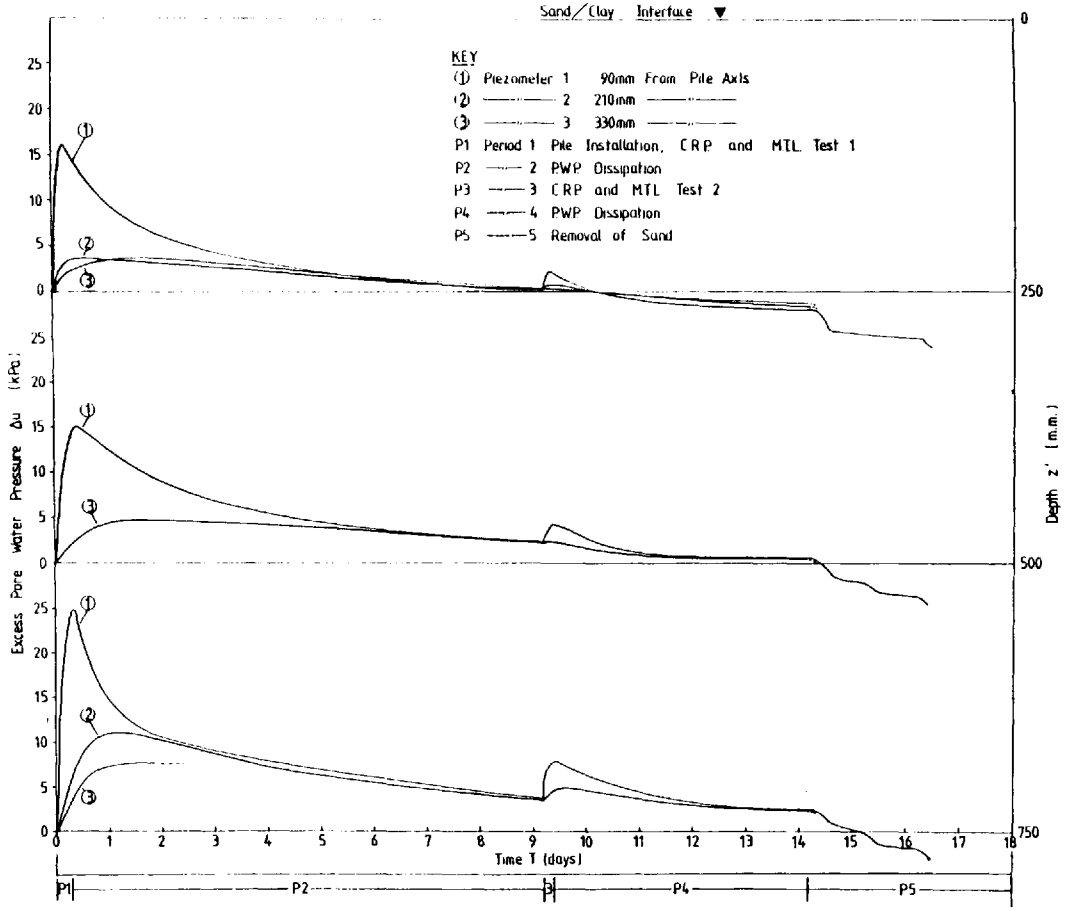

GENERATION AND DISSIPATION OF EXCESS PORE WATER PRESSURE DURING INSTALLATION, AND A SERIES OF C.R.P. AND MAINTAINED LOAD TESTS
TEST N°2 (60 DD-S/C)
FIGURE N° 7.9

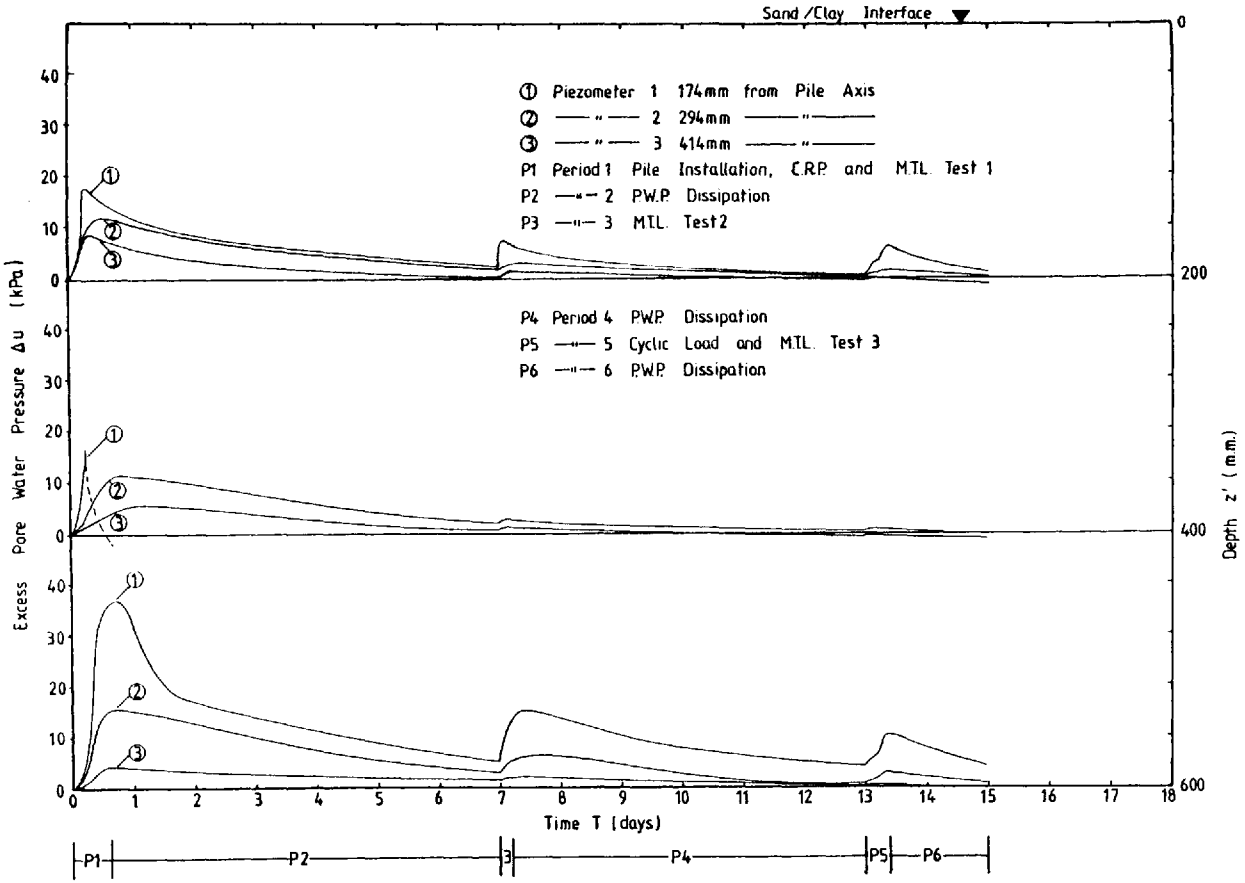

GENERATION AND DISSIPATION OF EXCESS PORE WATER PRESSURE DURING INSTALLATION, ' AND A SERIES OF C.R.P., CYCLIC AND MAINTAINED LOAD TESTS.
TEST N°5 (114 DC - S/C)

FIGURE N° 7.10

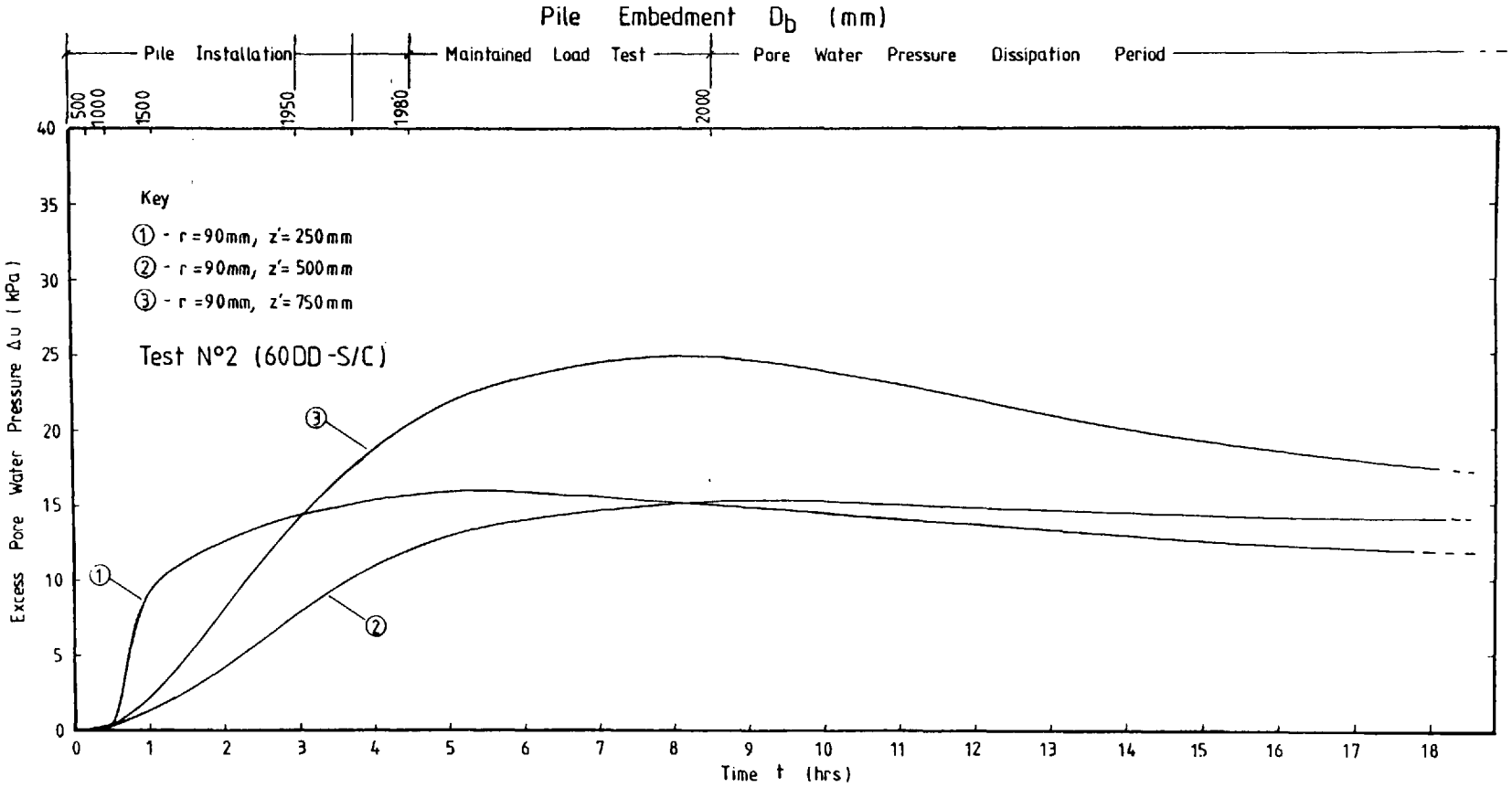

DEVELOPMENT OF EXCESS PORE WATER PRESSURE WITHIN THE CLAY AT A RADIAL DISTANCE, r = 1·5B DURING PILE INSTALLATION AND A MAINTAINED LOAD TEST

FIGURE N° 7.11

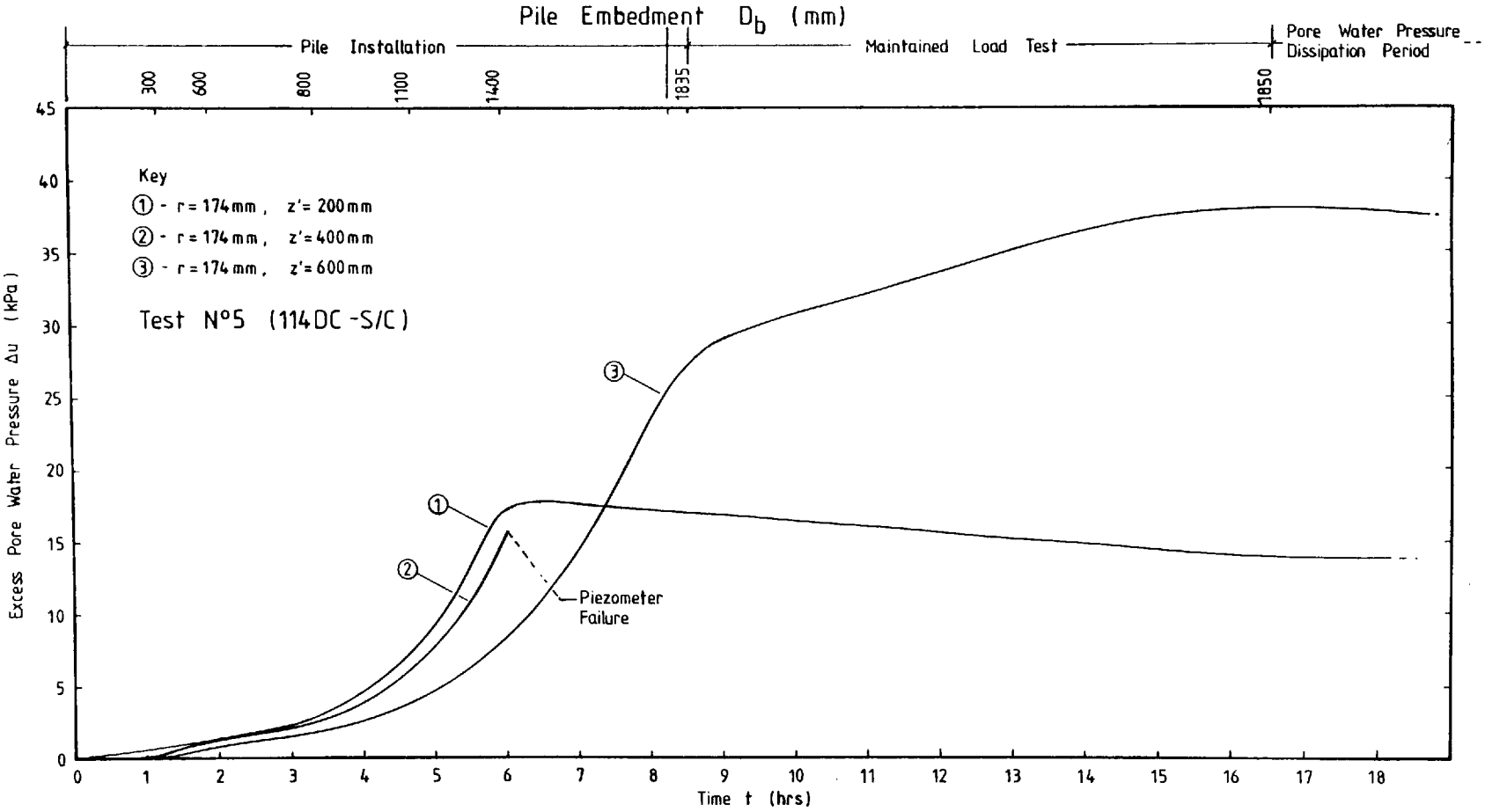

DEVELOPMENT OF EXCESS PORE WATER PRESSURE WITHIN THE CLAY AT A RADIAL DISTANCE r = 1·5 B DURING PILE INSTALLATION AND A MAINTAINED LOAD TEST

FIGURE N° 7.12

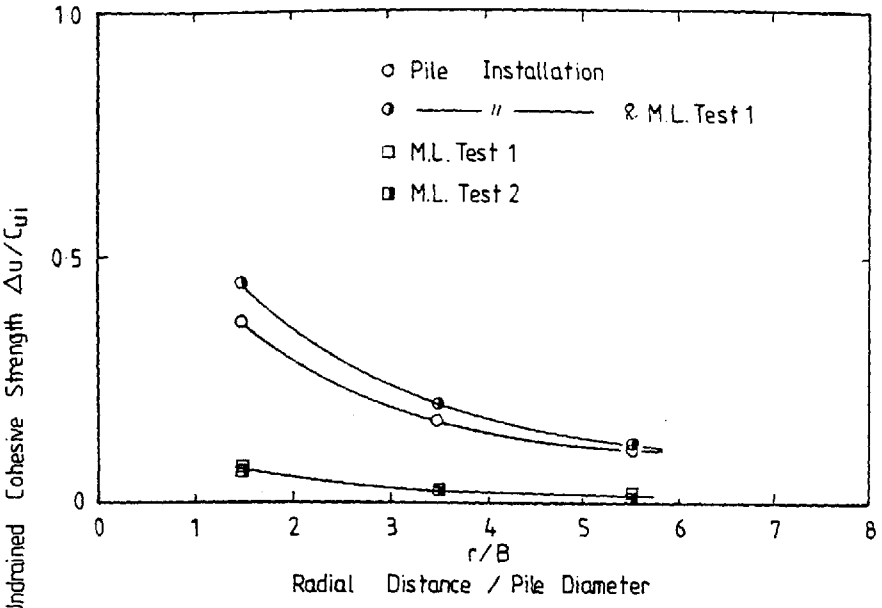

Test 2 (60DD-S/C)

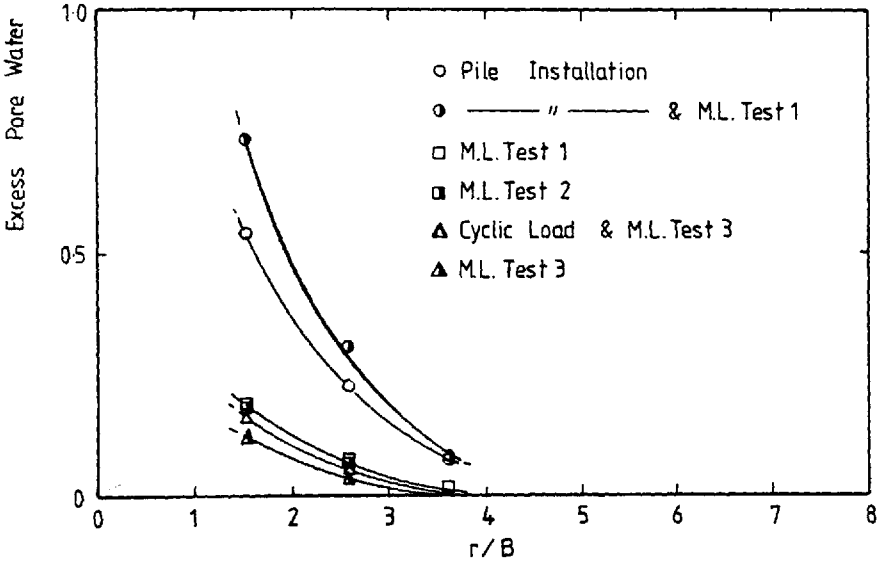

Test 5 (114DC-S/C)

RADIAL DISTRIBUTION OF EXCESS PORE WATER PRESSURE AT A DEPTH IN THE CLAY EQUIVALENT TO THE PILE BASE LEVEL, DURING INSTALLATION, CYCLIC AND MAINTAINED LOAD TESTS

FIGURE 7.13

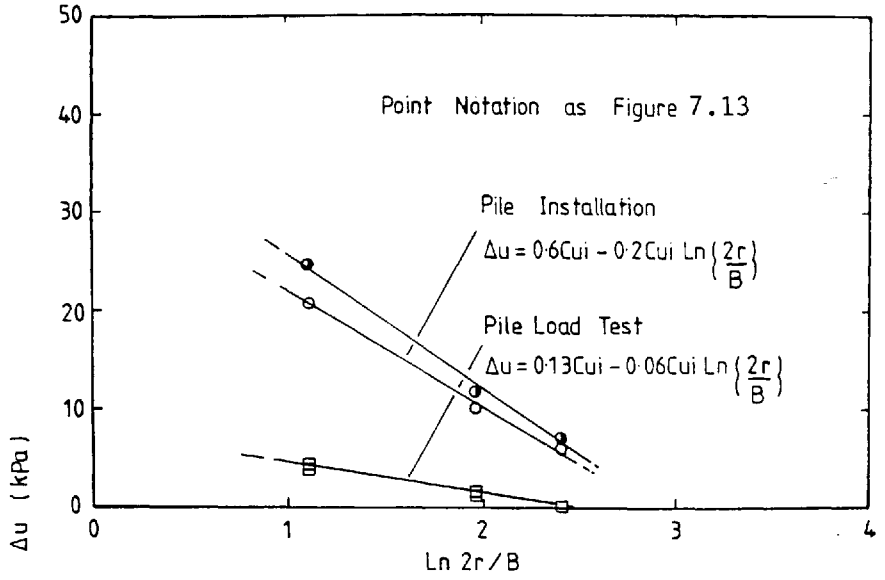

Test 2 (60 DD-S/C)

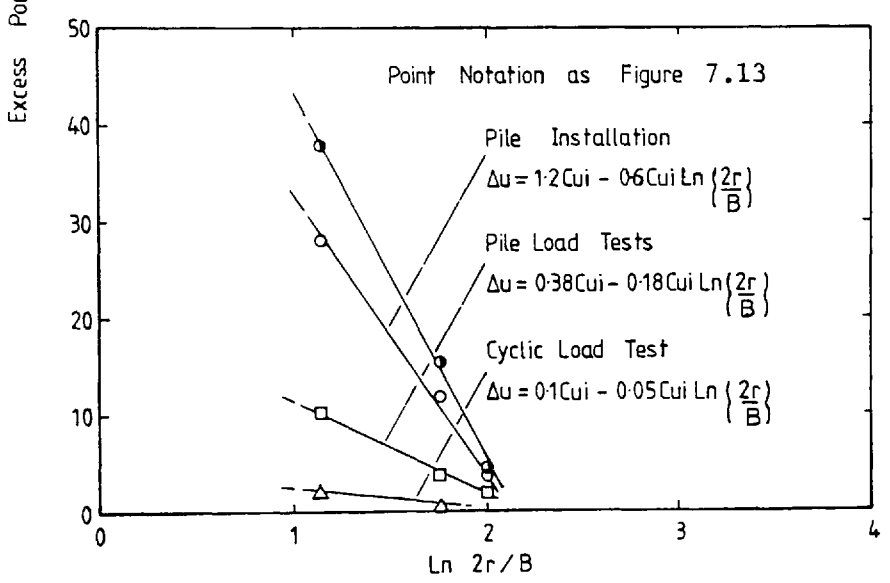

Test 5 (114 DC-S/C)

LOGARITHMIC RADIAL DISTRIBUTION OF EXCESS PORE WATER PRESSURE GENERATED AT A DEPTH IN THE CLAY EQUIVALENT TO THE PILE BASE LEVEL, DURING PILE INSTALLATION, CYCLIC AND MAINTAINED LOAD TESTS

FIGURE 7.14

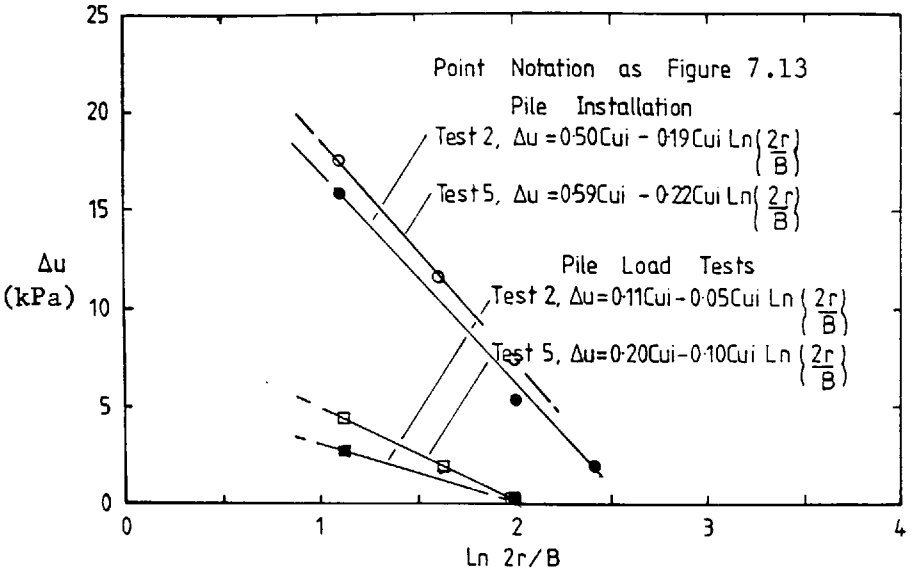

FIGURE a

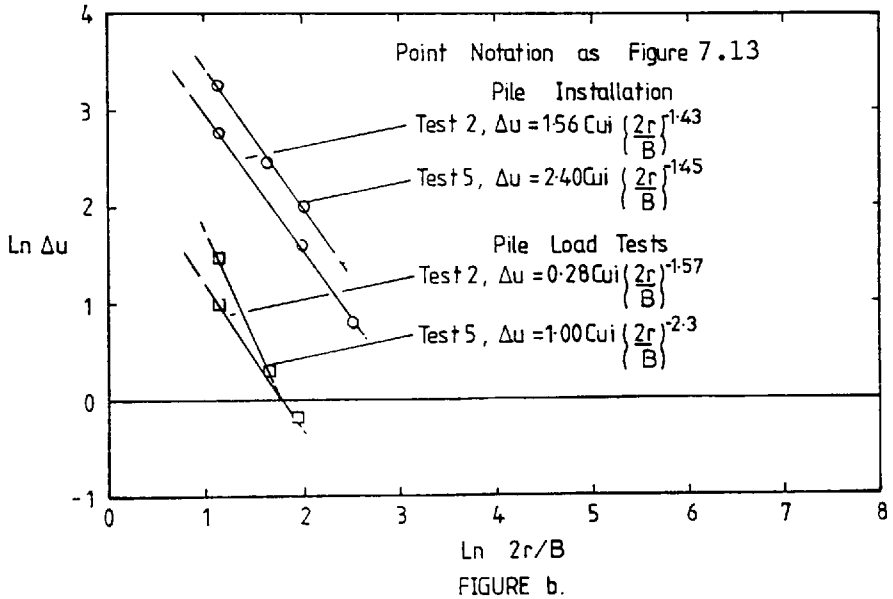

FIGURE b.

LOGARITHMIC RADIAL DISTRIBUTION OF EXCESS PORE WATER PRESSURE GENERATED WITHIN THE CLAY DURING PILE INSTALLATION, CYCLIC AND MAINTAINED LOAD TESTS

FIGURE 7.15

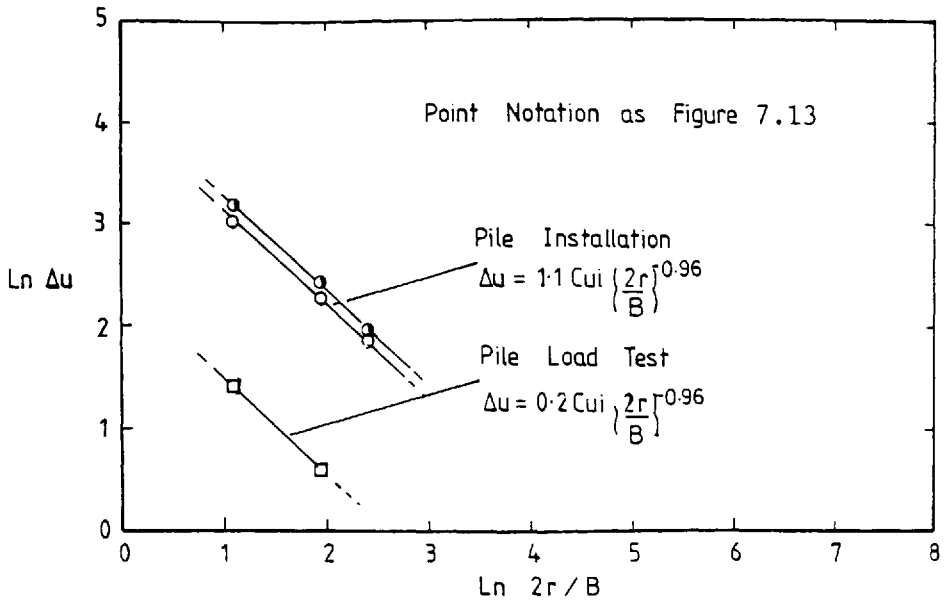

Test 2 (60DD-S/C)

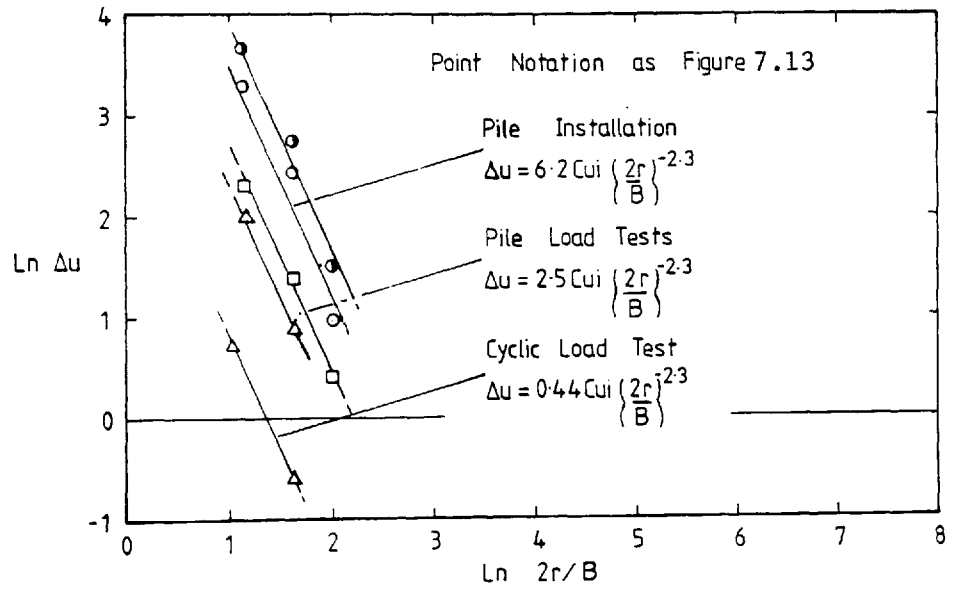

Test 5 (114DC-S/C)

LINEAR LOGARITHMIC REPRESENTATION OF PEAK EXCESS PORE WATER PRESSURE WITH RADIAL DISTRIBUTION

FIGURE 7.16

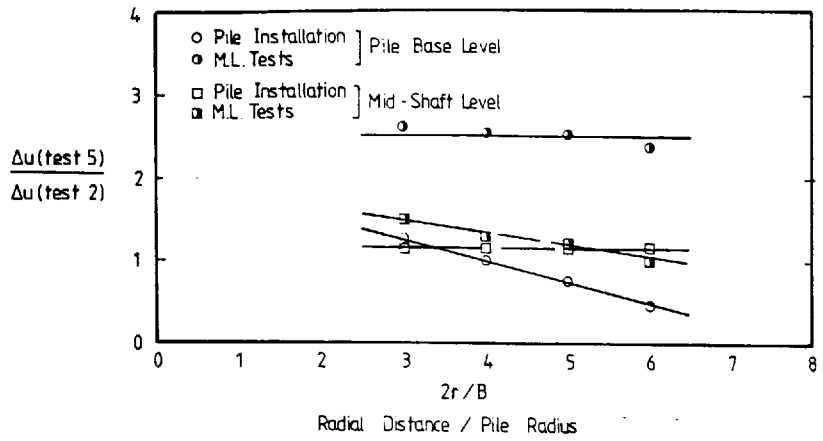

Radial Distribution Of The Ratio Of Excess Pore Pressures From Tests 2 & 5 During Pile Installation And Maintained Load Tests

FIGURE 7.17

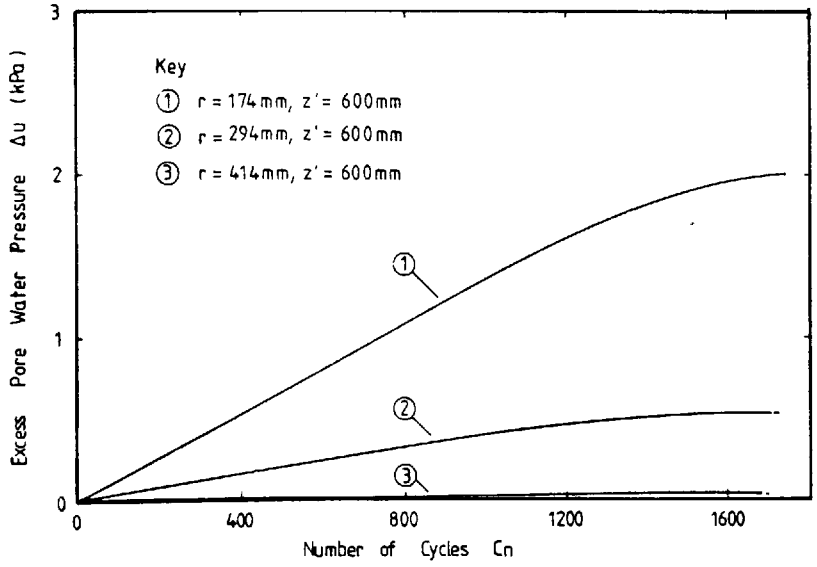

Test N°5 (114DC-S/C)

RADIAL DEVELOPMENT OF EXCESS PORE WATER PRESSURE AT A DEPTH IN THE CLAY EQUIVALENT TO THE PILE BASE LEVEL, DURING CYCLIC LOADING

FIGURE N° 7.18

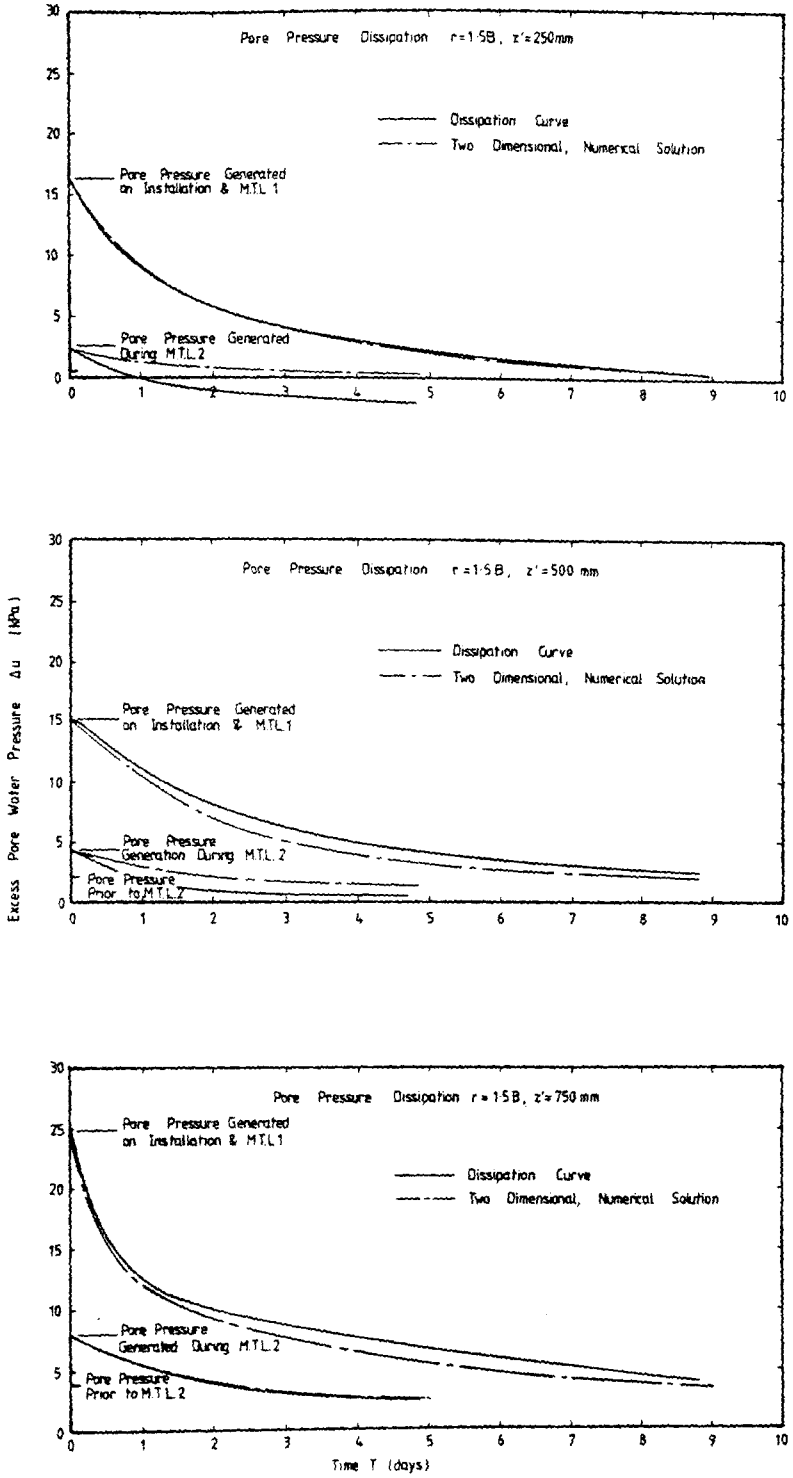

Test N°2 (6000-S/C)

DISSIPATION OF EXCESS PORE PRESSURE AT A RADIAL DISTANCE r=1·5B THROUGHOUT THE PILE EMBEDMENT DEPTH, z', IN THE CLAY

FIGURE N° 7.19

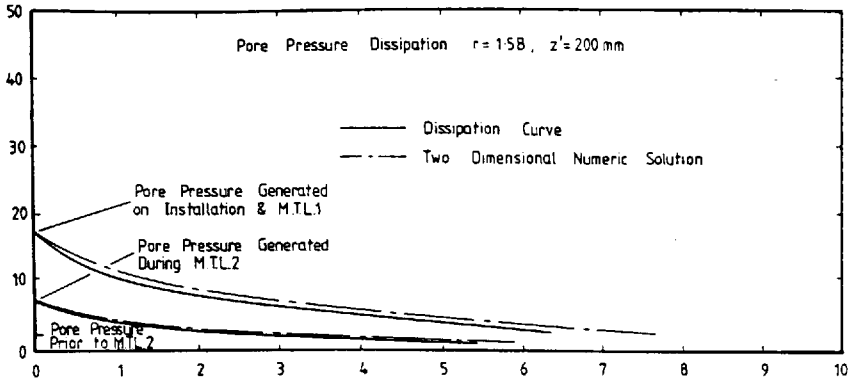

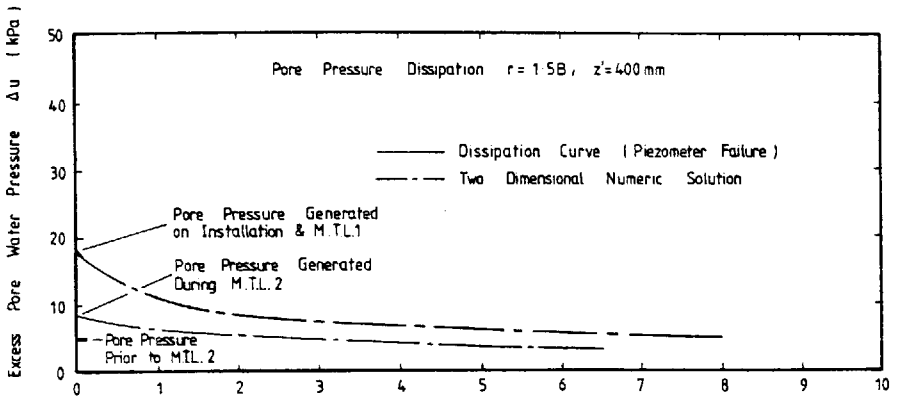

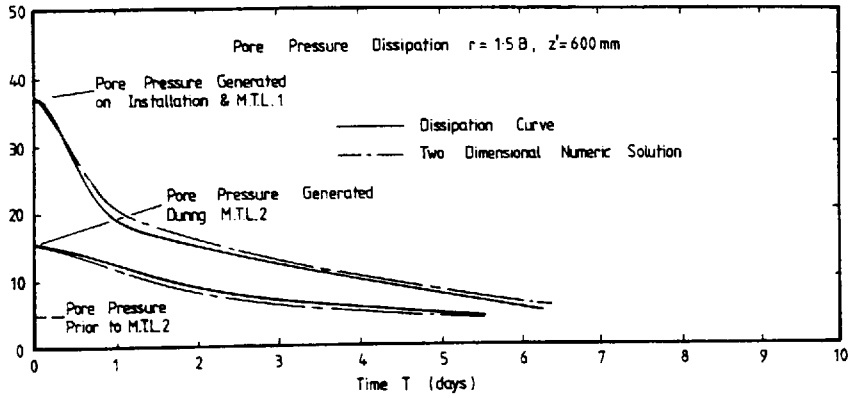

Test N°5 (114DC-S/C)

DISSIPATION OF EXCESS PORE WATER PRESSURE AT A RADIAL DISTANCE r = 1·5B, THROUGHOUT THE PILE EMBEDMENT DEPTH, z', IN THE CLAY

FIGURE N° 7.20

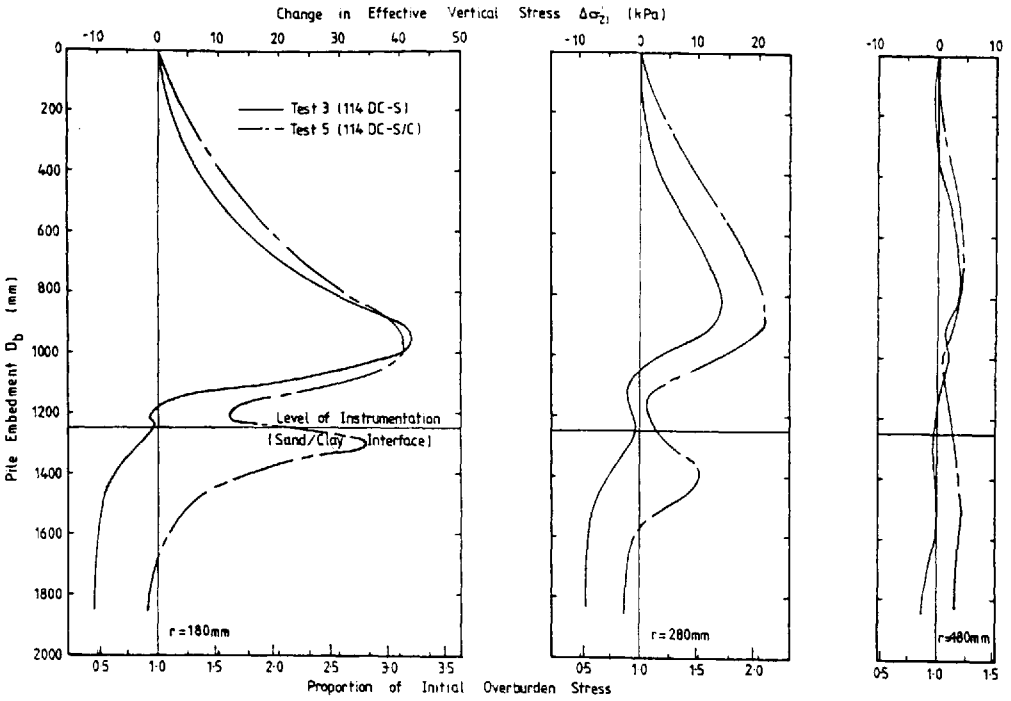

a. Vertical Stress History During Pile Installation

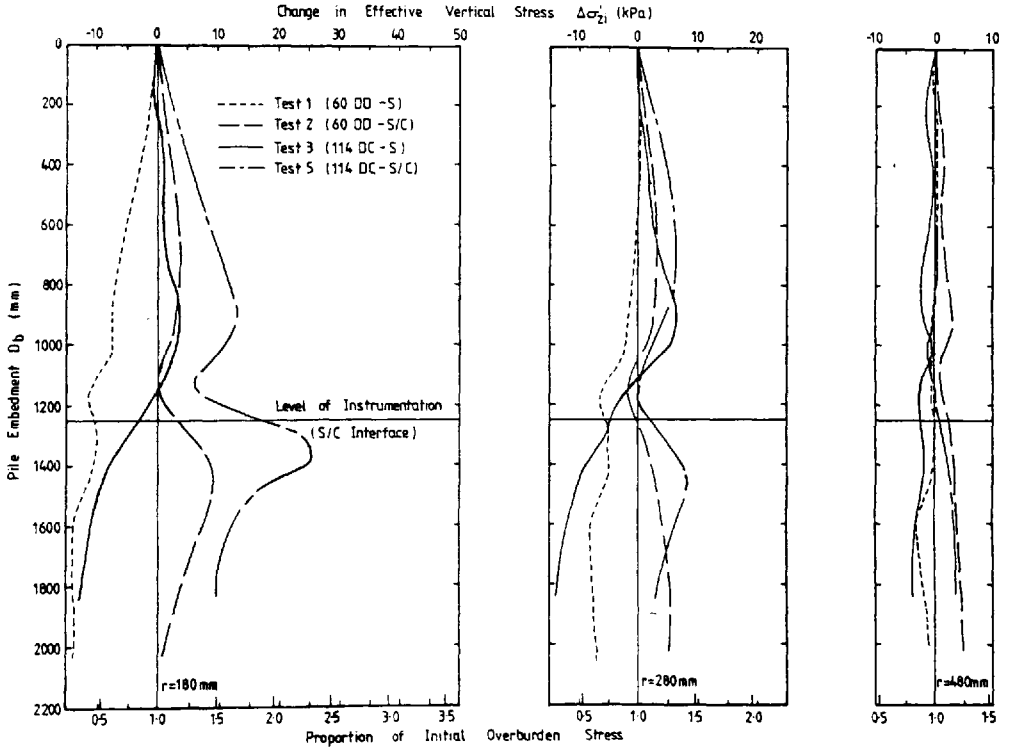

b. Residual Vertical Stress History During Pile Installation

FIGURE N°7.21 CHANGES IN EFFECTIVE VERTICAL STRESS AND RESIDUAL EFFECTIVE VERTICAL STRESS ACROSS A HORIZONTAL PLANE WITHIN THE SOIL PROFILE DURING PILE INSTALLATION

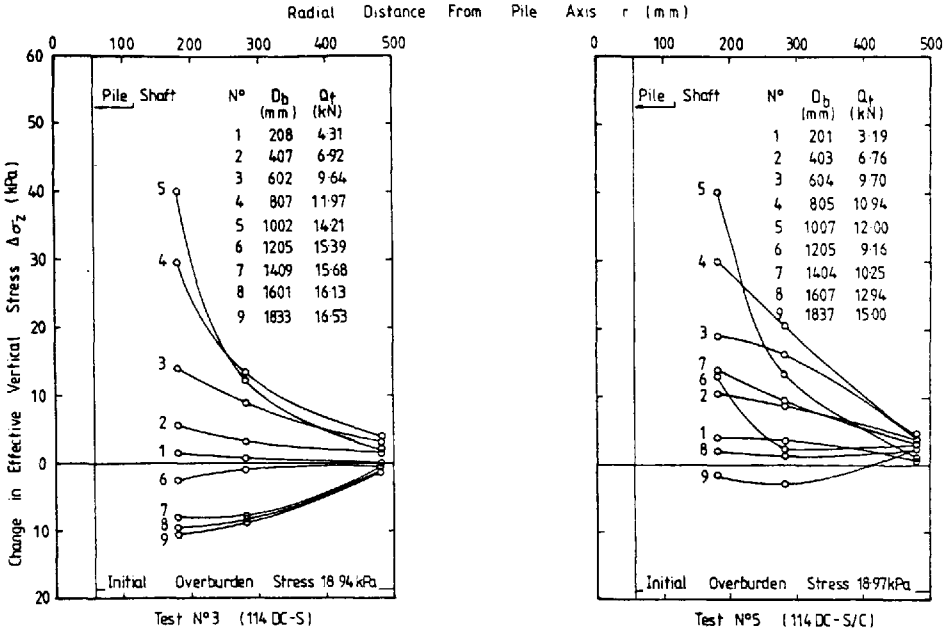

a. Effective Vertical Stress History During Pile Installation

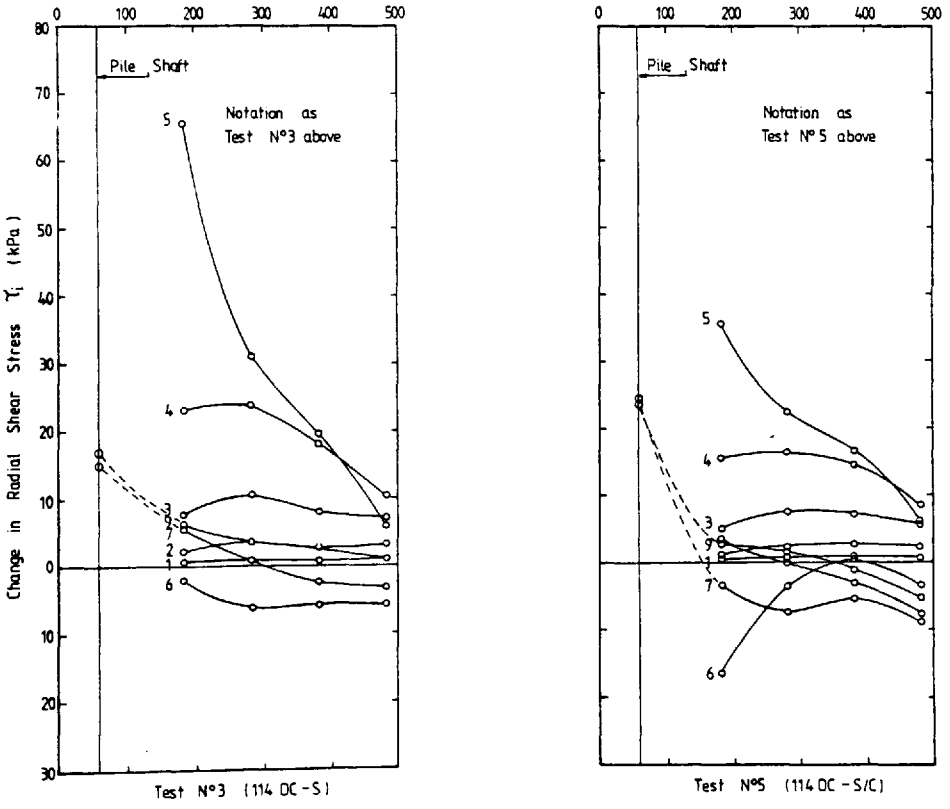

b. Radial Shear Stress History During Pile Installation

FIGURE N°7.22 CHANGE IN EFFECTIVE VERTICAL STRESS AND RADIAL SHEAR STRESS ACROSS A HORIZONTAL PLANE WITHIN THE SOIL PROFILE DURING PILE INSTALLATION

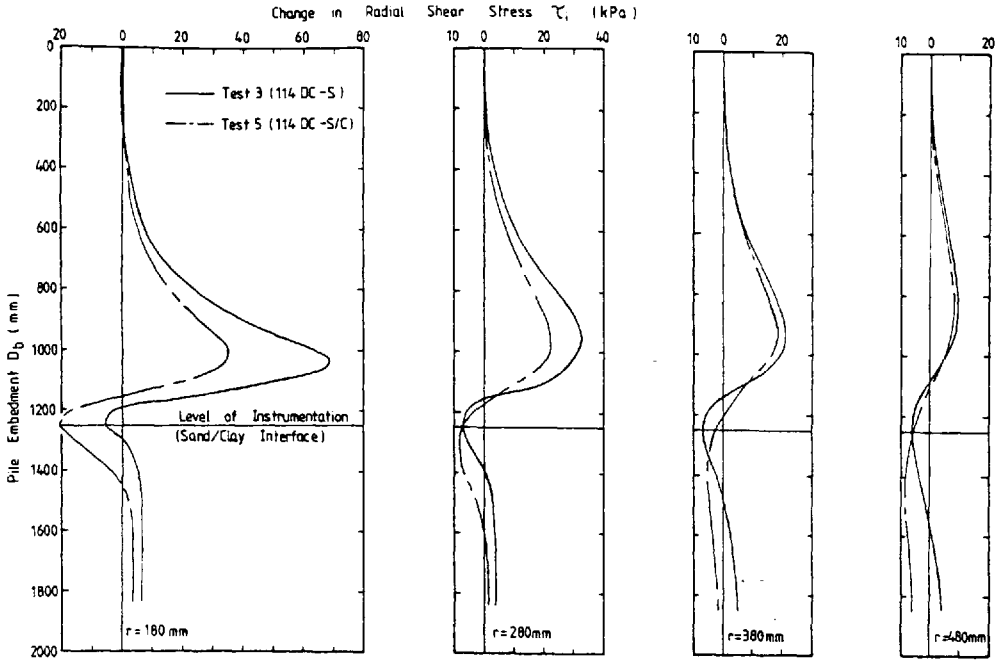

a. Radial Shear Stress History During Pile Installation

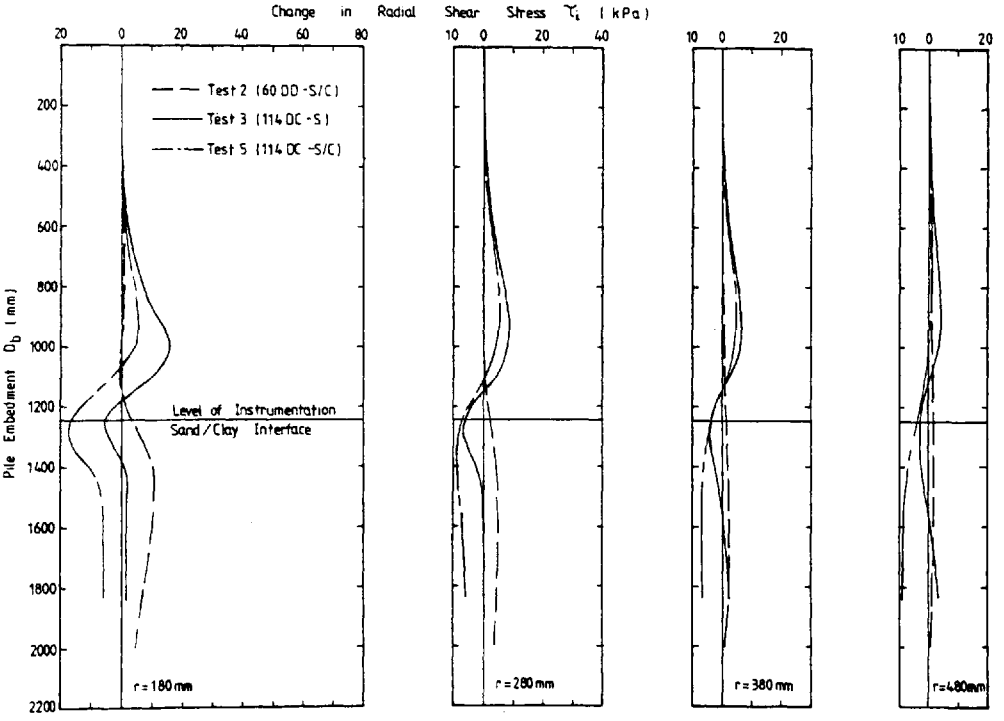

b. Residual Radial Shear Stress History During Pile Installation

FIGURE Nº 7.23 CHANGE IN RADIAL SHEAR STRESS AND RESIDUAL RADIAL SHEAR STRESS ACROSS A HORIZONTAL PLANE WITHIN THE SOIL PROFILE DURING PILE INSTALLATION

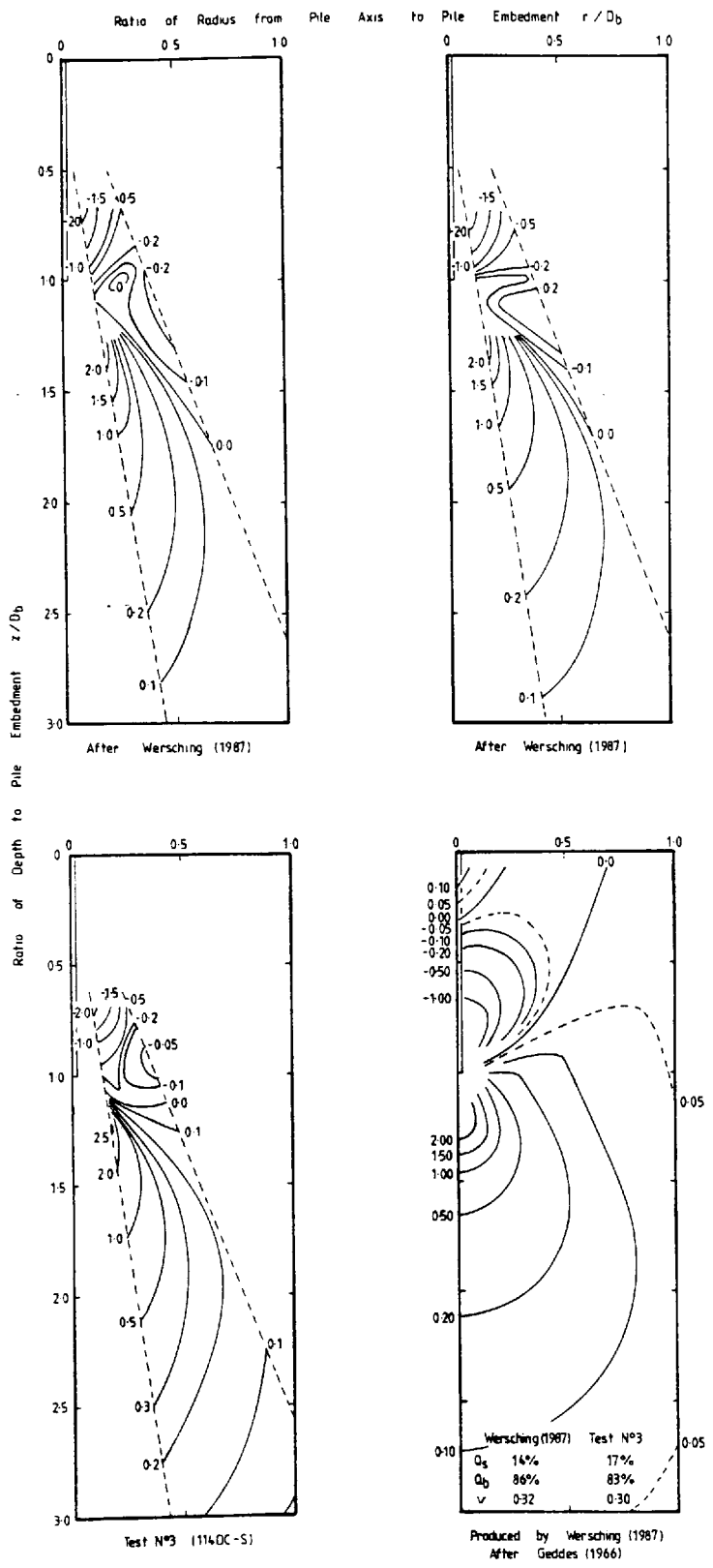

EXPERIMENTAL AND THEORETICAL DIMENSIONLESS STRESS COEFFICIENTS FOR THE CHANGE IN EFFECTIVE VERTICAL STRESS INDUCED IN LOOSE SAND BY A VERTICALLY LOADED PILE

FIGURE 7.24

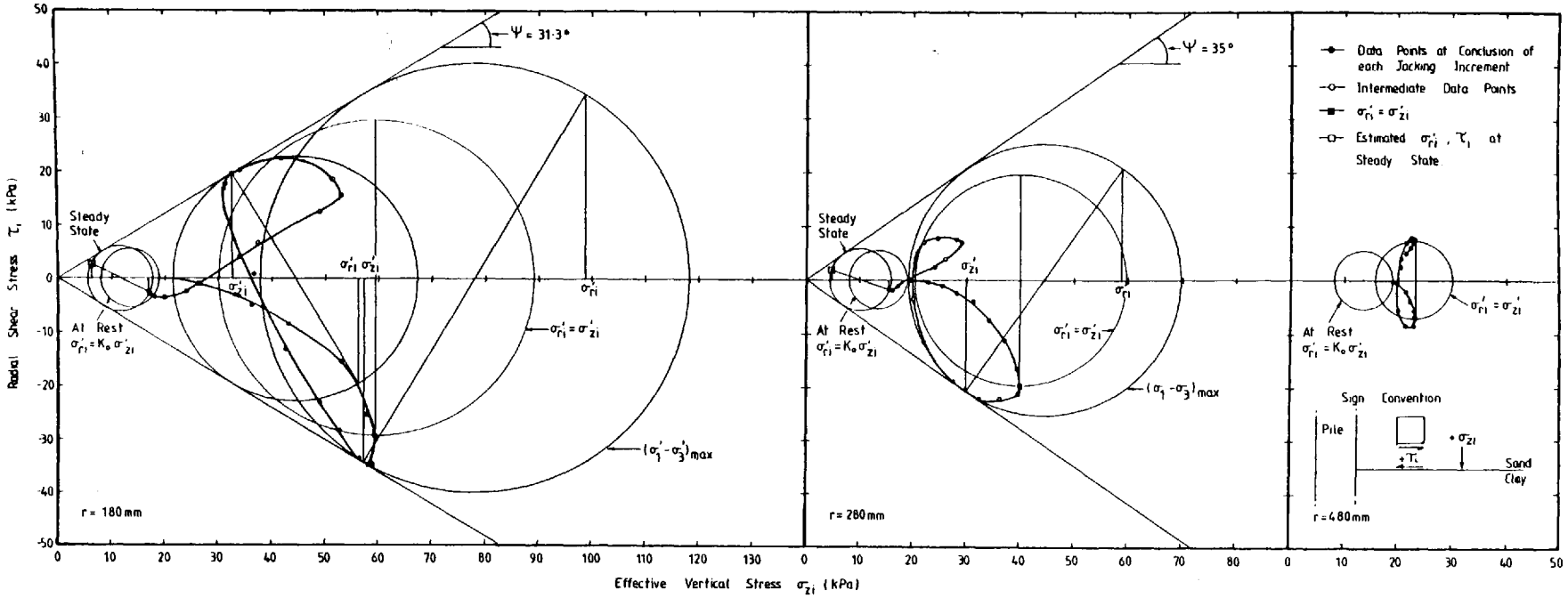

TWO DIMENSIONAL EFFECTIVE STRESS HISTORY ACTING ON AN ELEMENT OF SAND ADJACENT TO THE SAND/CLAY INTERFACE DURING PILE INSTALLATION

FIGURE N° 7.25

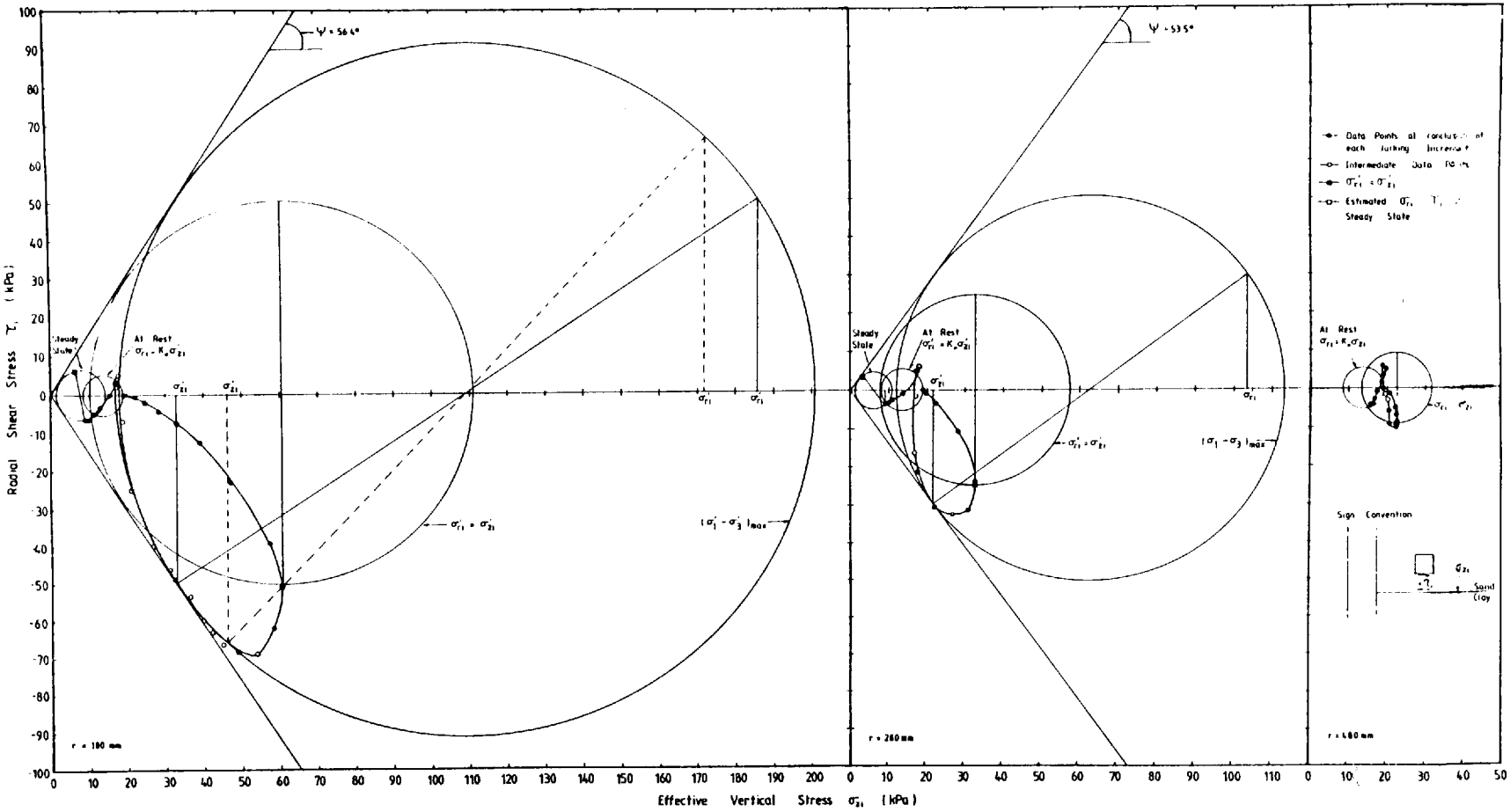

TWO DIMENSIONAL EFFECTIVE STRESS HISTORY ACTING ON AN ELEMENT OF SAND ADJACENT TO THE SAND/CLAY INTERFACE DURING PILE INSTALLATION

FIGURE N° 7.26

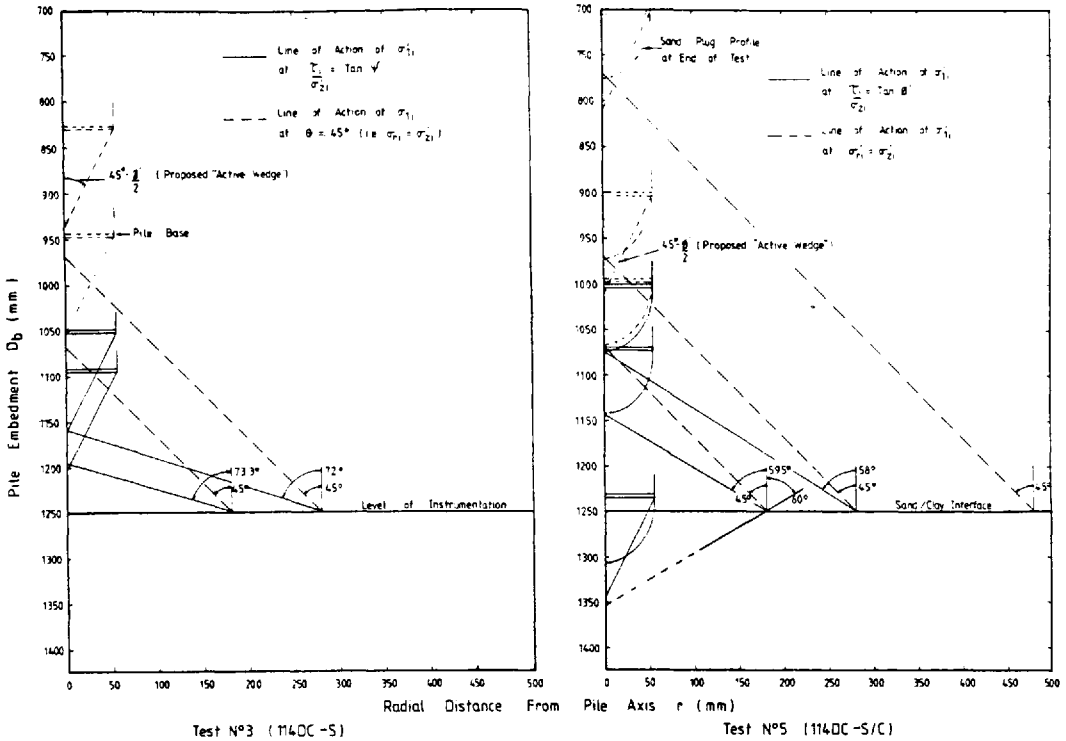

SOIL/PILE GEOMETRIES ASSOCIATED WITH THE MAXIMUM MAJOR EFFECTIVE PRINCIPAL STRESS AND THE ONSET OF SHEAR FAILURE IN A PLANE AT A DEPTH, z = 1250 mm

FIGURE N° 7.27

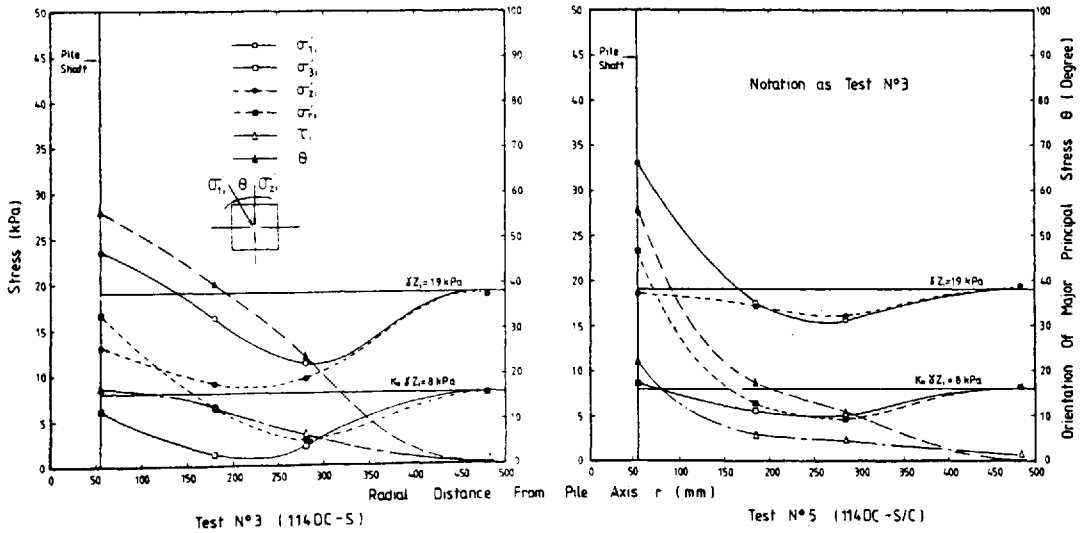

STEADY STATE EFFECTIVE STRESS PROFILE ACTING ACROSS THE SAND/CLAY INTERFACE ASSOCIATED WITH THE FULLY EMBEDDED PILE LOADED TO PLUNGING FAILURE

FIGURE N° 7.28

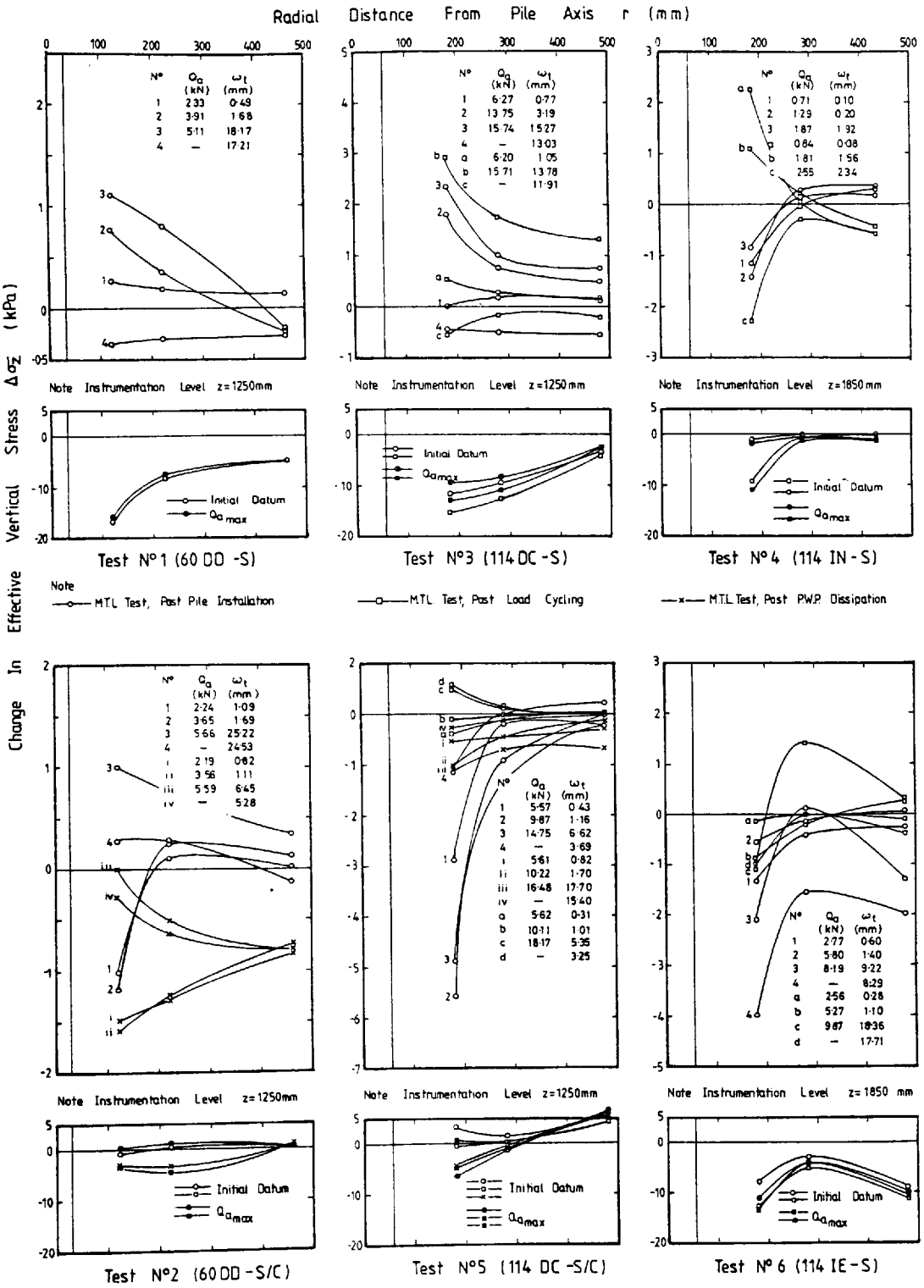

FIGURE N° 7.29 CHANGE IN EFFECTIVE VERTICAL STRESS ACROSS A HORIZONTAL PLANE WITHIN THE SOIL PROFILE DURING A SERIES OF MAINTAINED LOAD TESTS

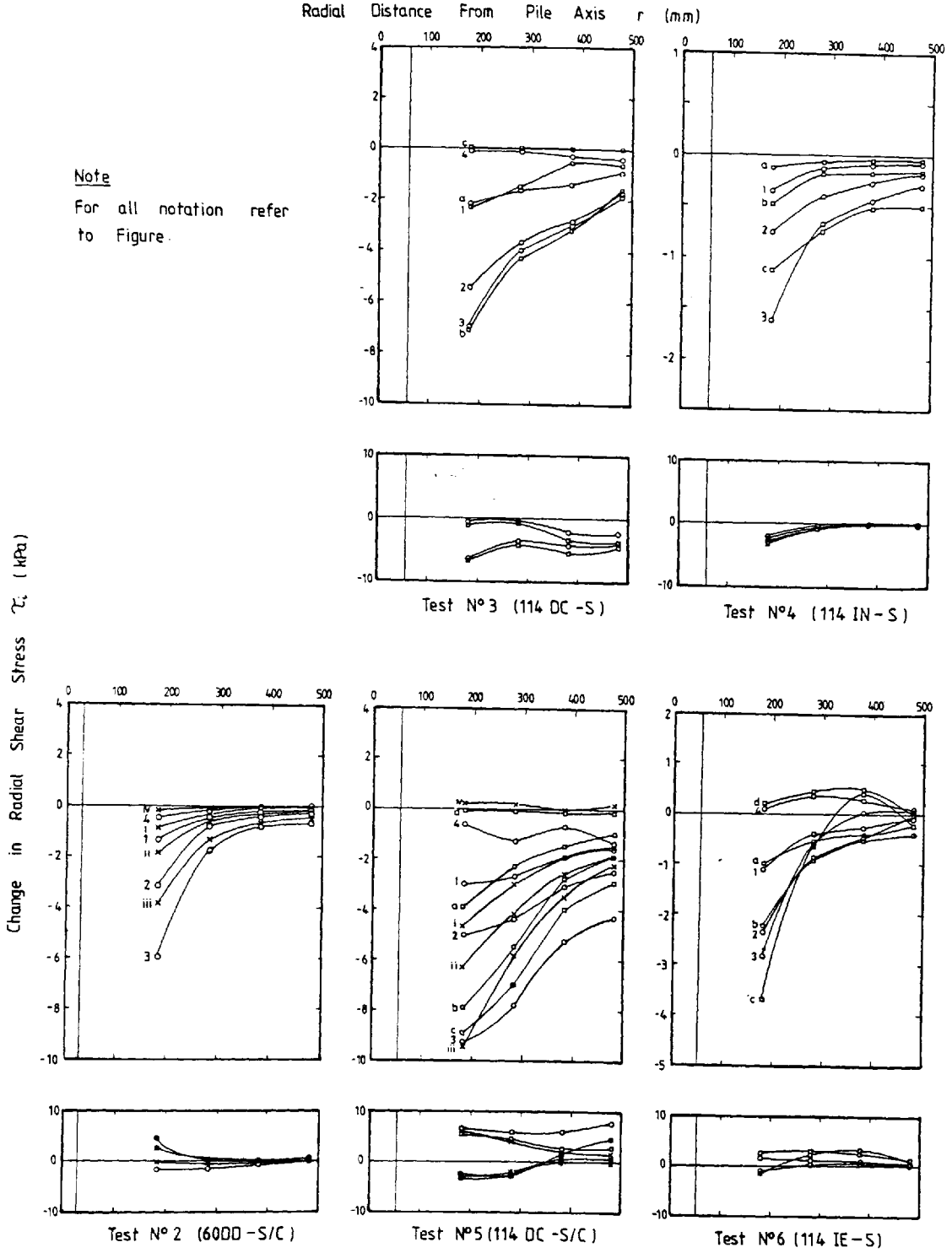

FIGURE N° 7.30 CHANGE IN RADIAL SHEAR STRESS ACROSS A HORIZONTAL PLANE WITHIN THE SOIL PROFILE DURING A SERIES OF MAINTAINED LOAD TESTS

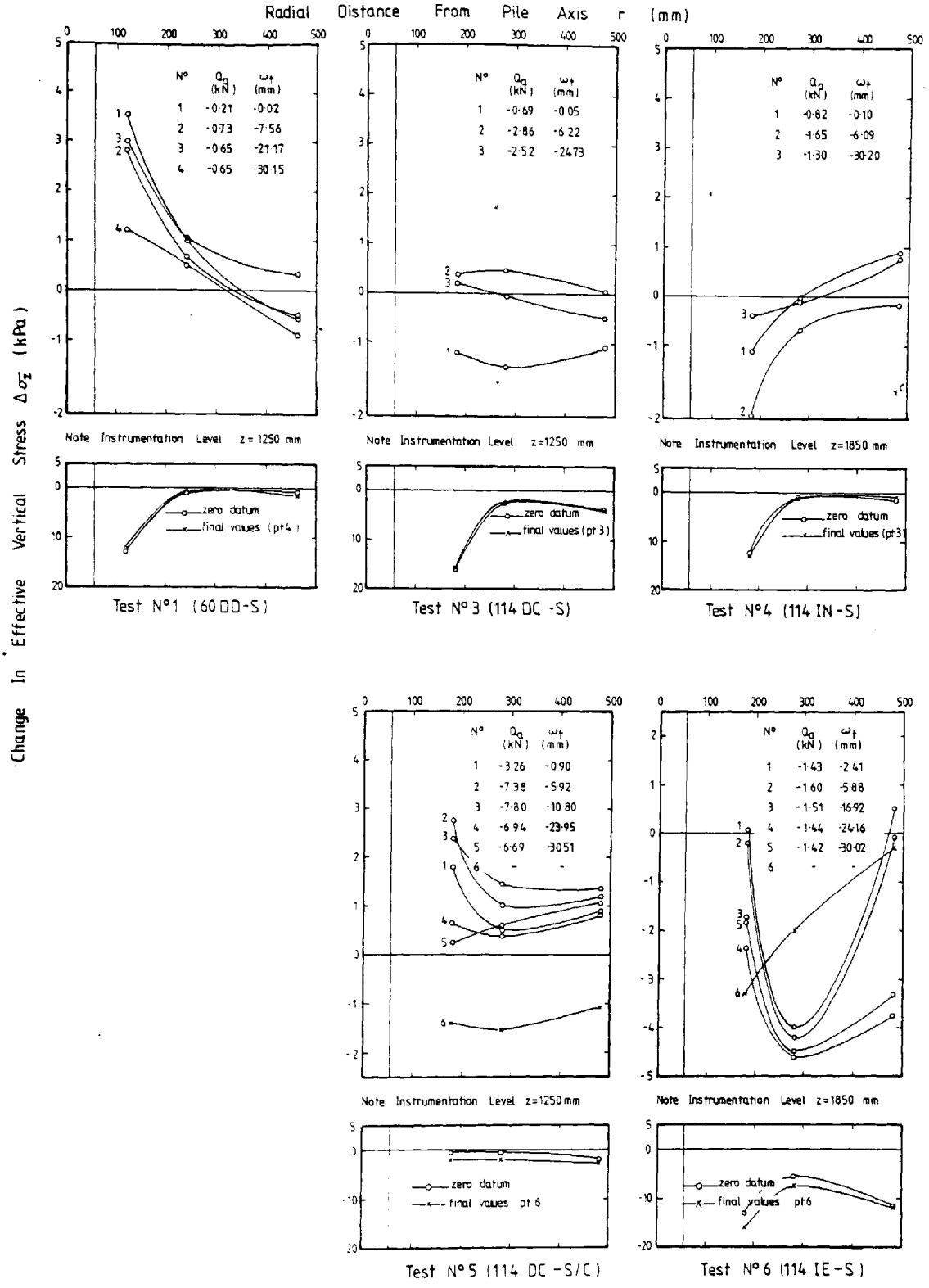

FIGURE N° 7.31 CHANGE IN EFFECTIVE VERTICAL STRESS ACROSS A HORIZONTAL PLANE WITHIN THE SOIL PROFILE DURING THE CONSTANT RATE OF UPLIFT TEST

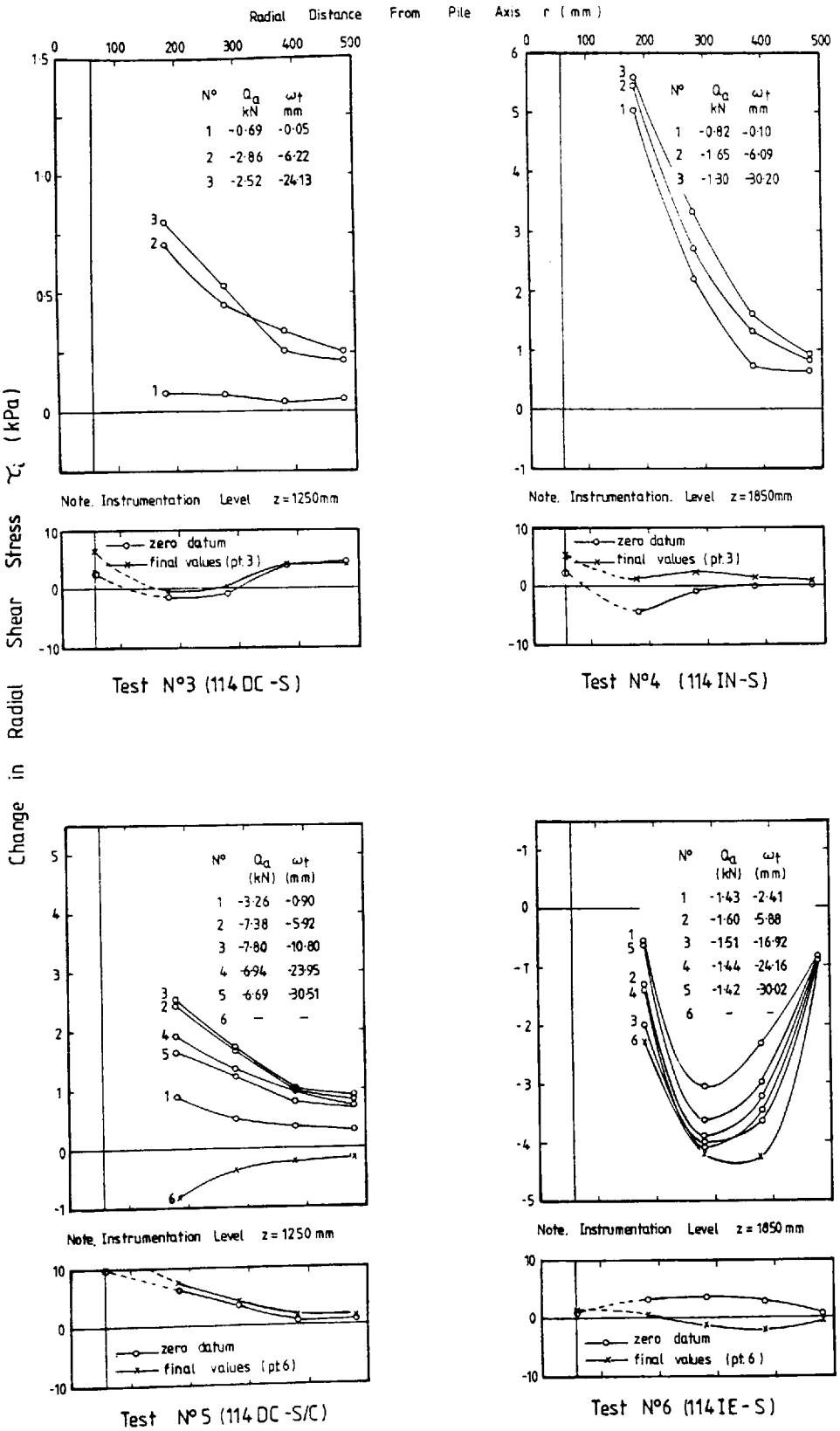

FIGURE N° 7.32 CHANGE IN RADIAL SHEAR STRESS ACROSS A HORIZONTAL PLANE WITHIN THE SOIL PROFILE DURING THE CONSTANT RATE OF UPLIFT TEST

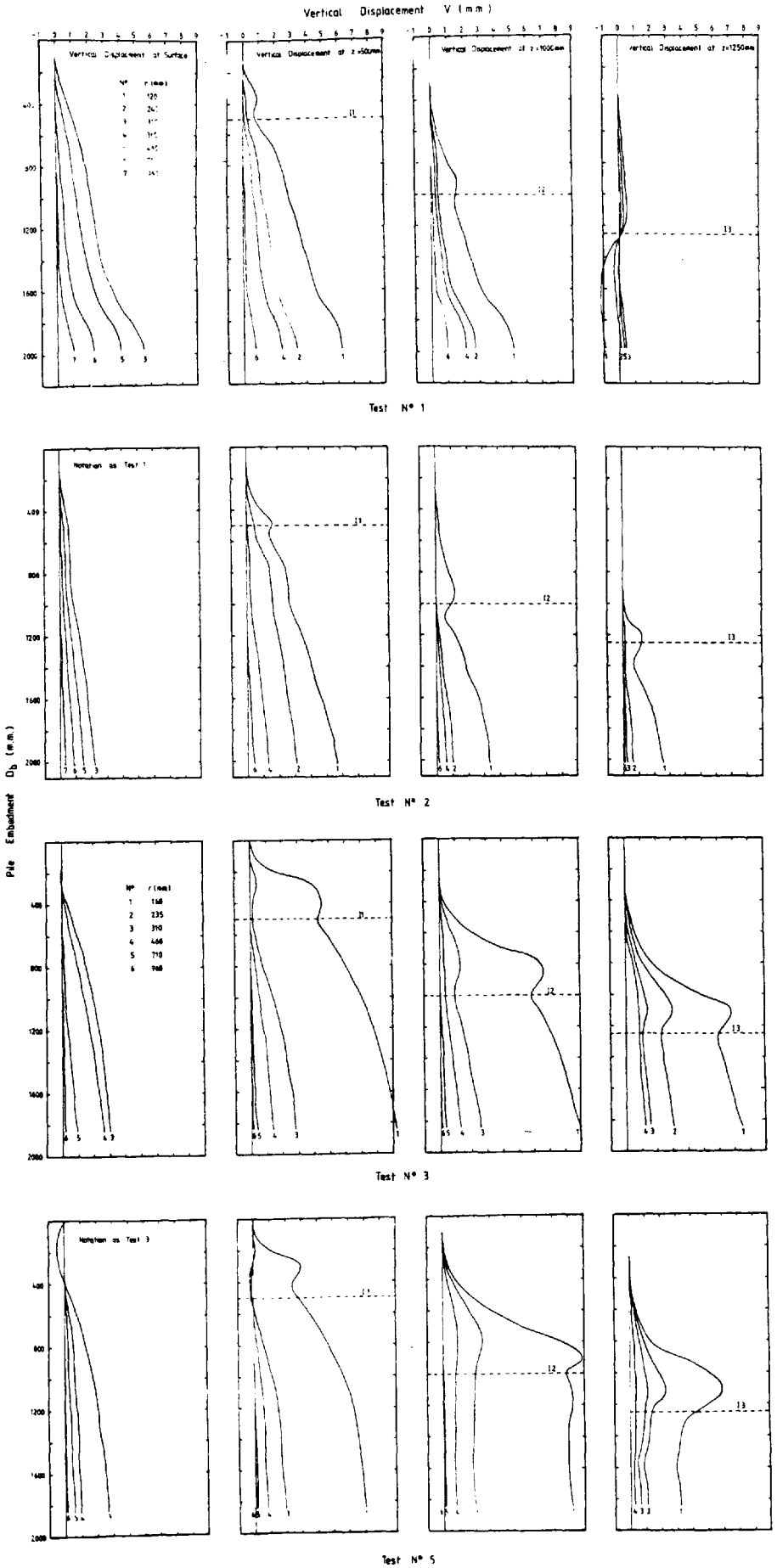

FIGURE 7.33 DEVELOPMENT OF VERTICAL SOIL DISPLACEMENTS DURING PILE INSTALLATION

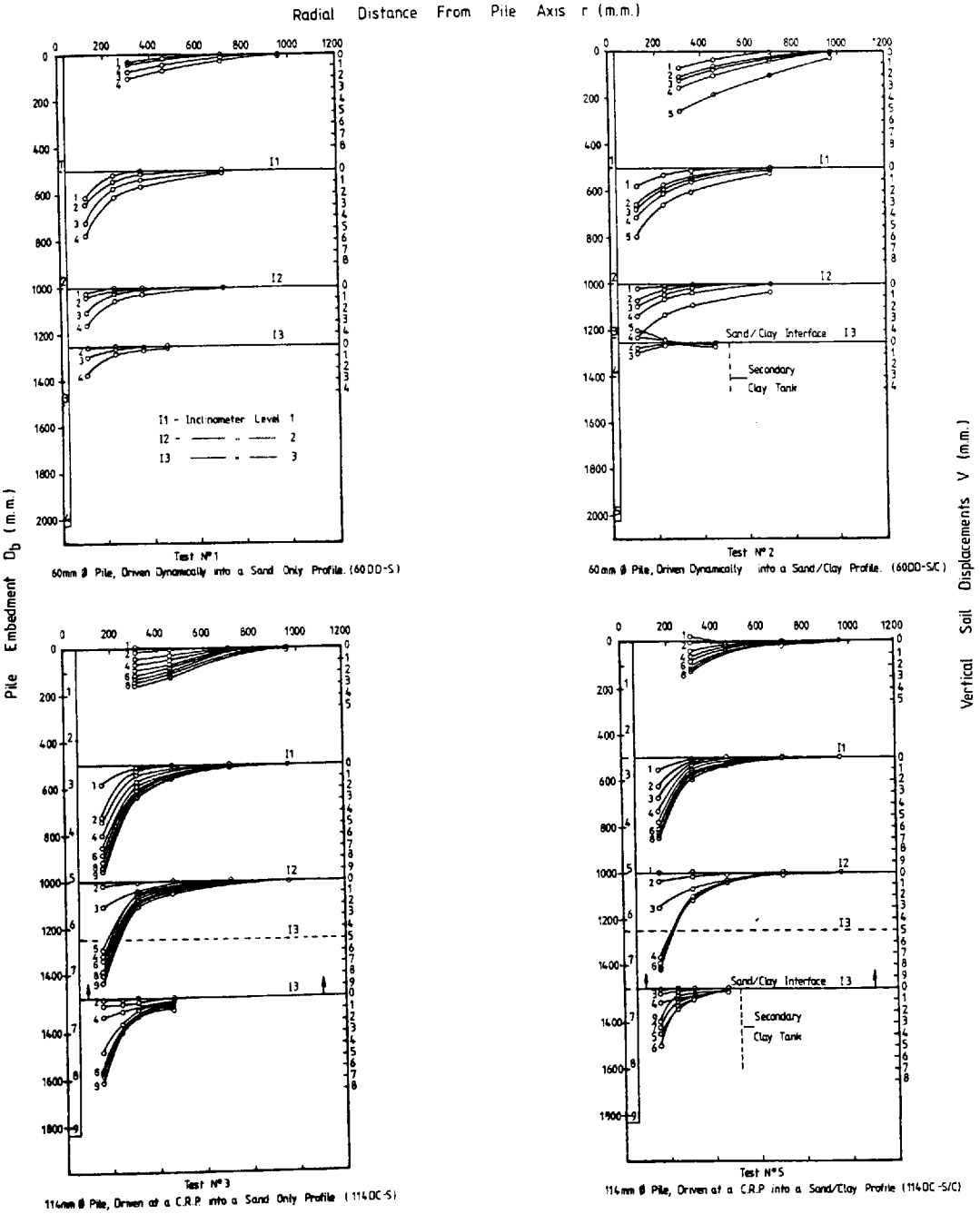

FIGURE 7.34 DEVELOPMENT OF VERTICAL SOIL DISPLACEMENT DURING PILE INSTALLATION

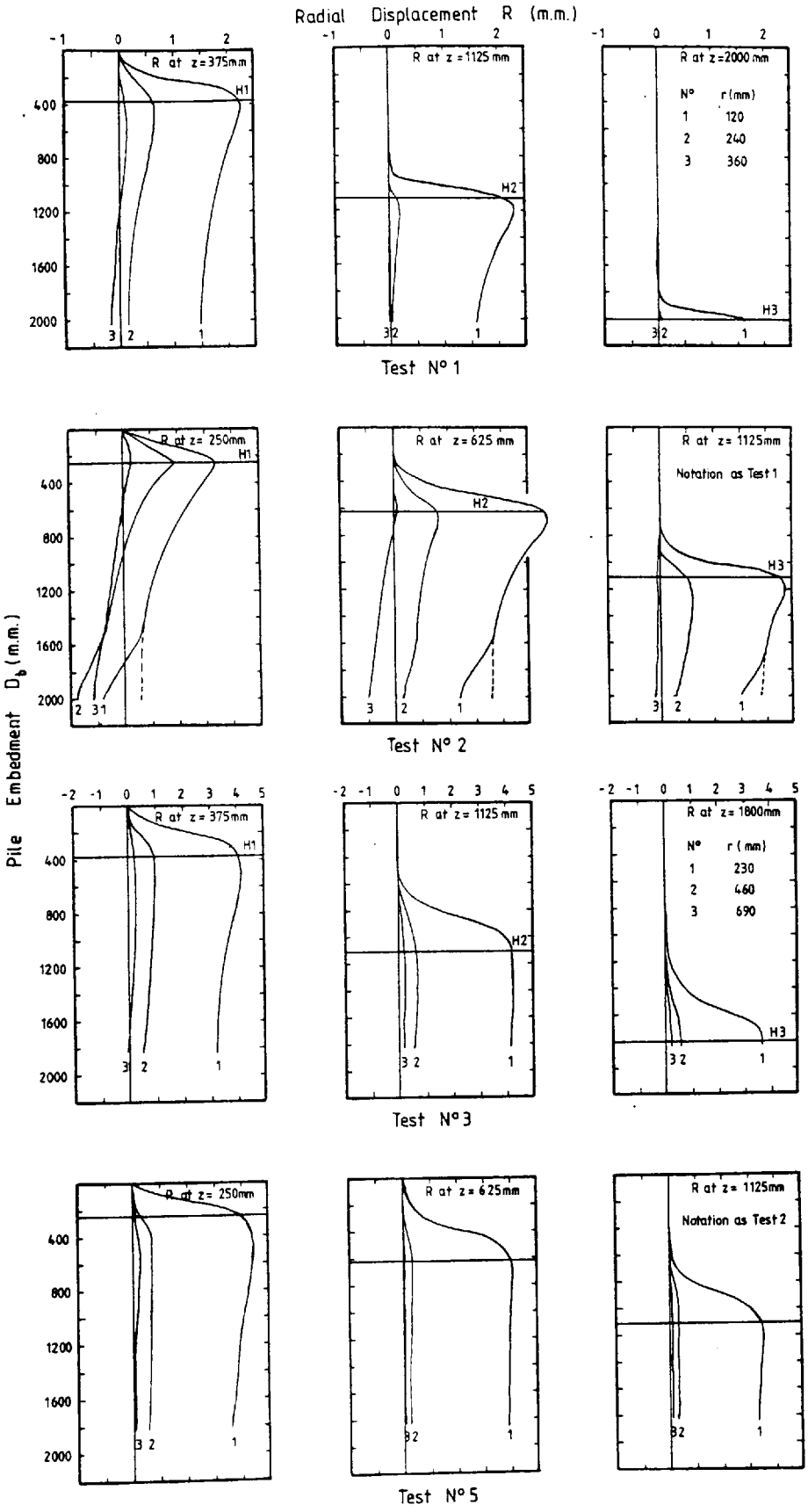

FIGURE 7.35 DEVELOPMENT OF RADIAL SOIL DISPLACEMENTS DURING PILE INSTALLATION

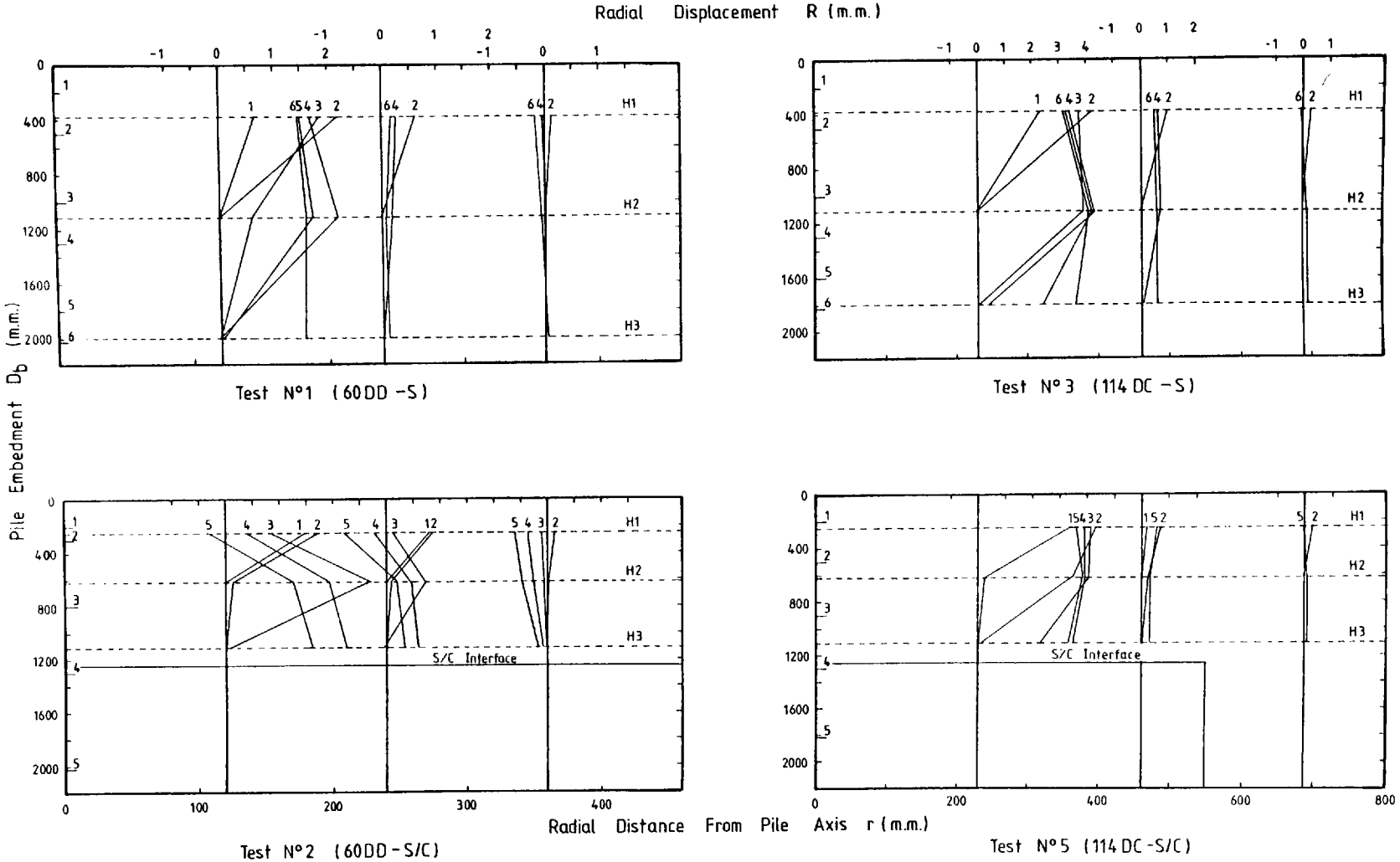

FIGURE N°7.36 DEVELOPMENT OF RADIAL SOIL DISPLACEMENTS DURING PILE INSTALLATION

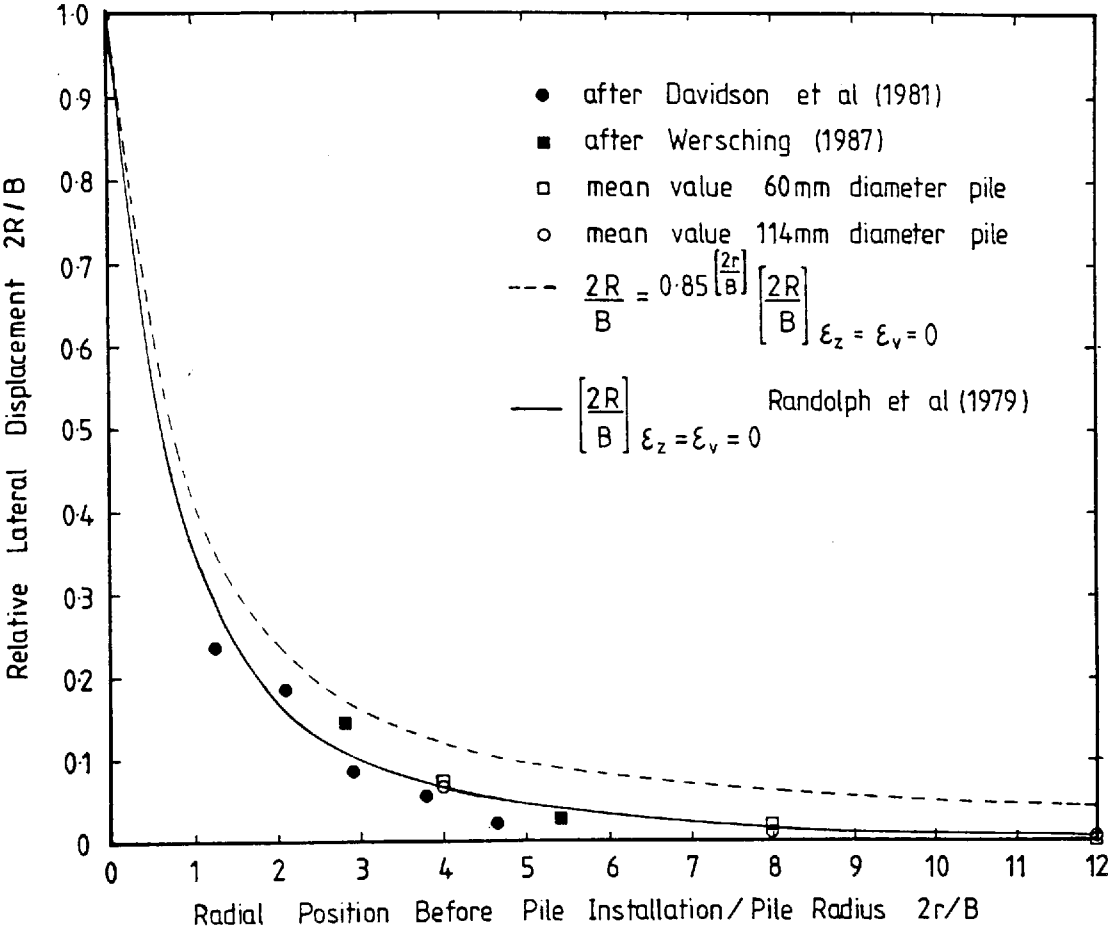

NORMALIZED RADIAL DISPLACEMENTS IN LOOSE SAND DUE TO PILE INSTALLATION

FIGURE N° 7.37

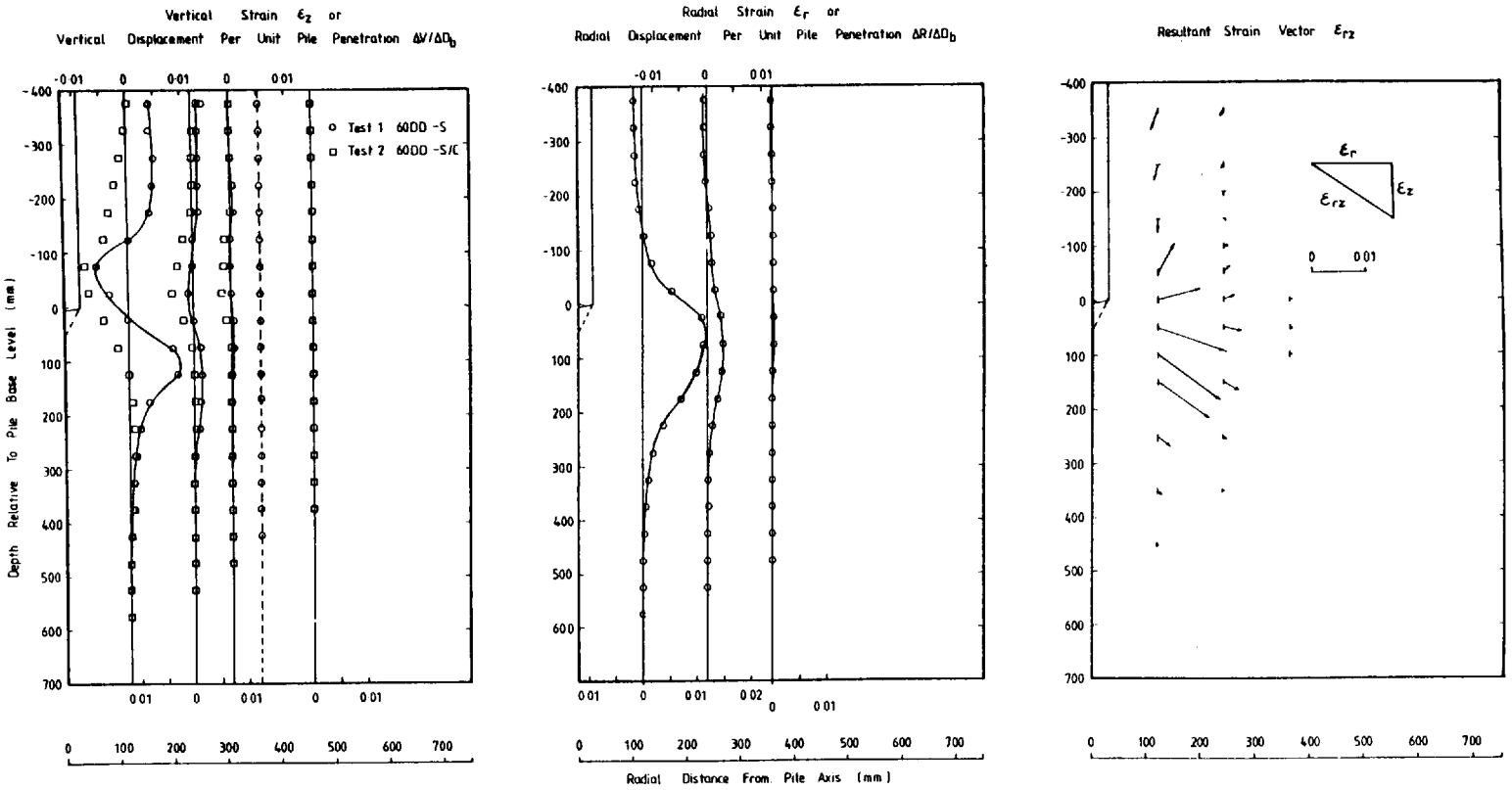

TWO DIMENSIONAL STRAIN DEVELOPMENT AROUND THE BASE OF A DYNAMICALLY DRIVEN PILE IN A LOOSE SAND

FIGURE N° 7.38

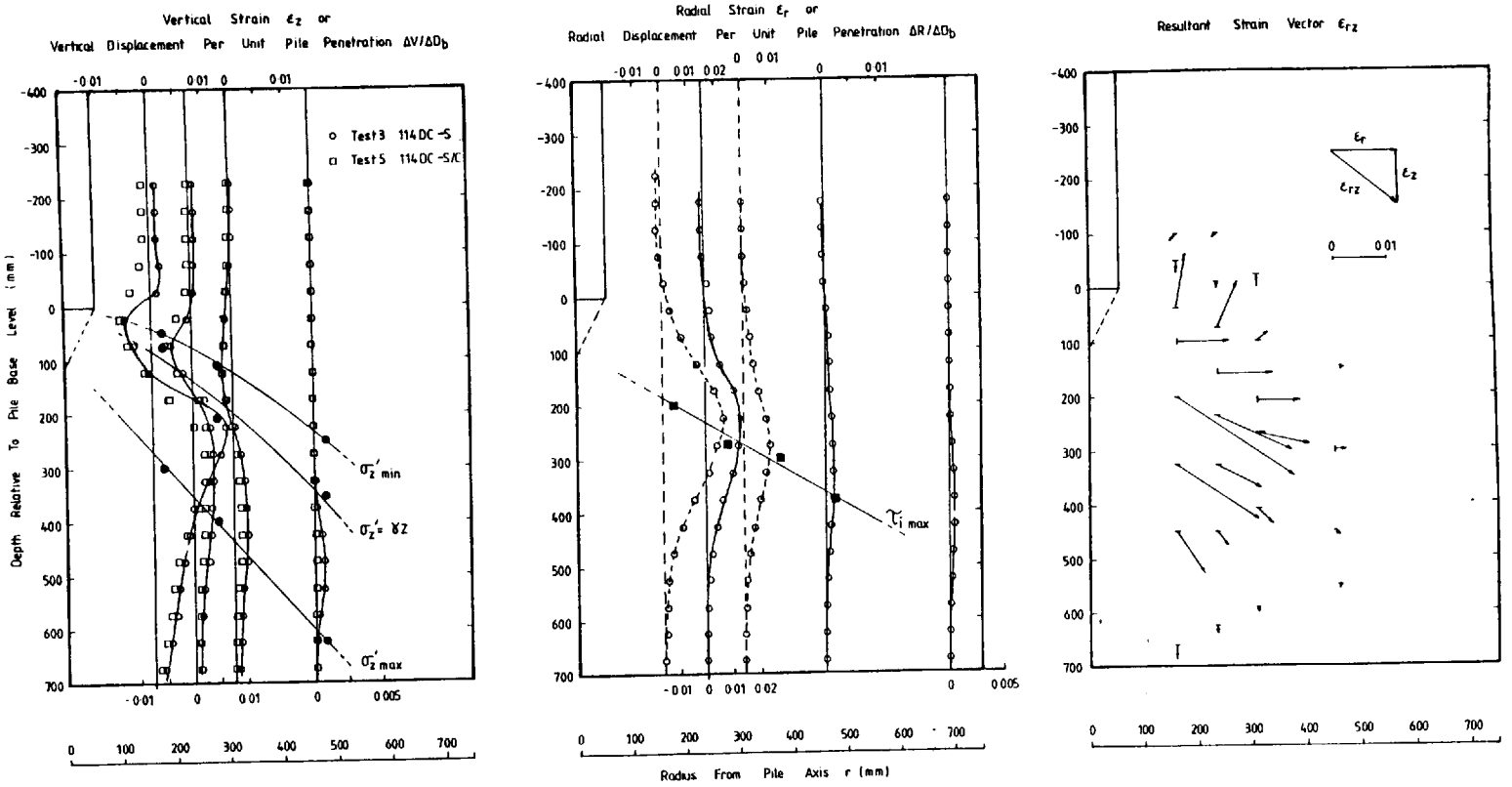

TWO DIMENSIONAL STRAIN DEVELOPMENT AROUND THE BASE OF A CONTINUOUSLY PENETRATING PILE IN A LOOSE SAND

FIGURE N° 7.39

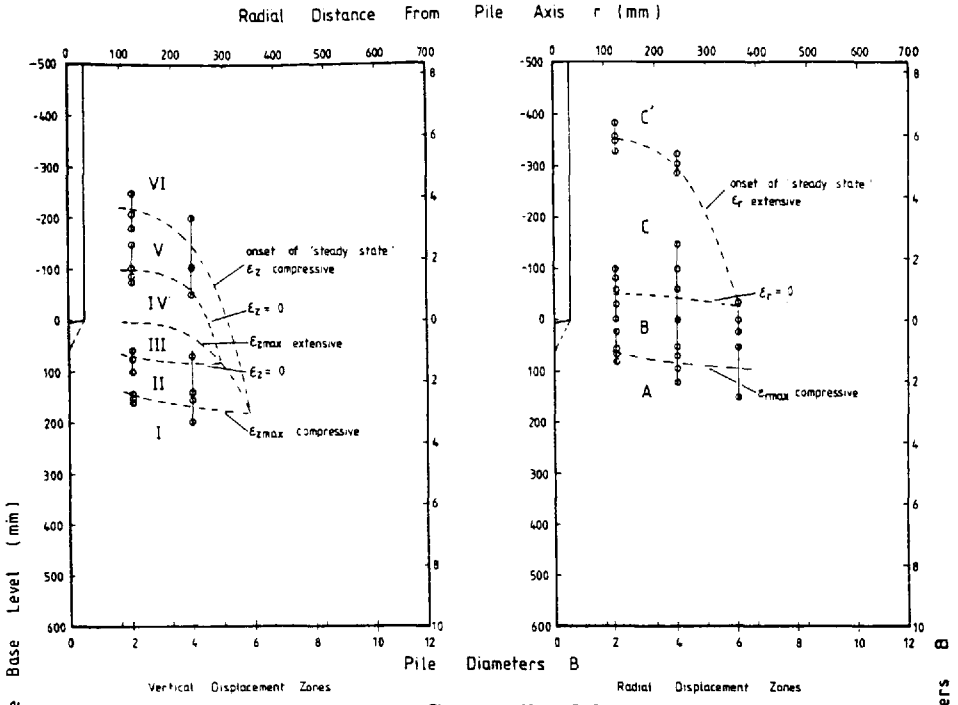

Figure a. 60mm Ø Pile

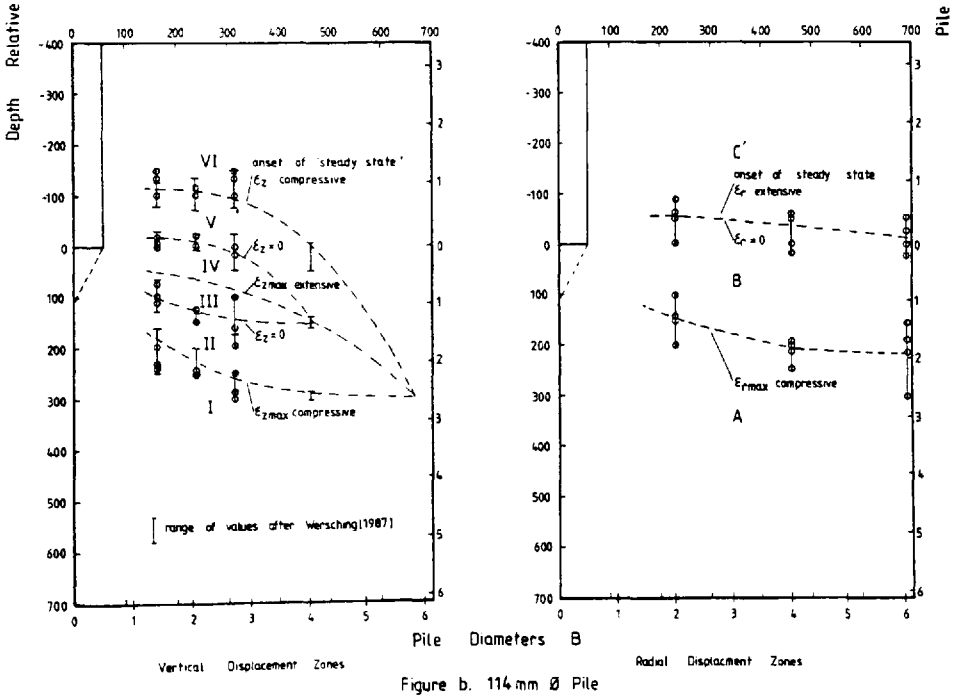

Figure b. 114mm Ø Pile

VERTICAL AND RADIAL DISPLACEMENT ZONES AROUND THE BASE OF A CONTINUOUSLY PENETRATING PILE IN LOOSE SAND

FIGURE N° 7.40

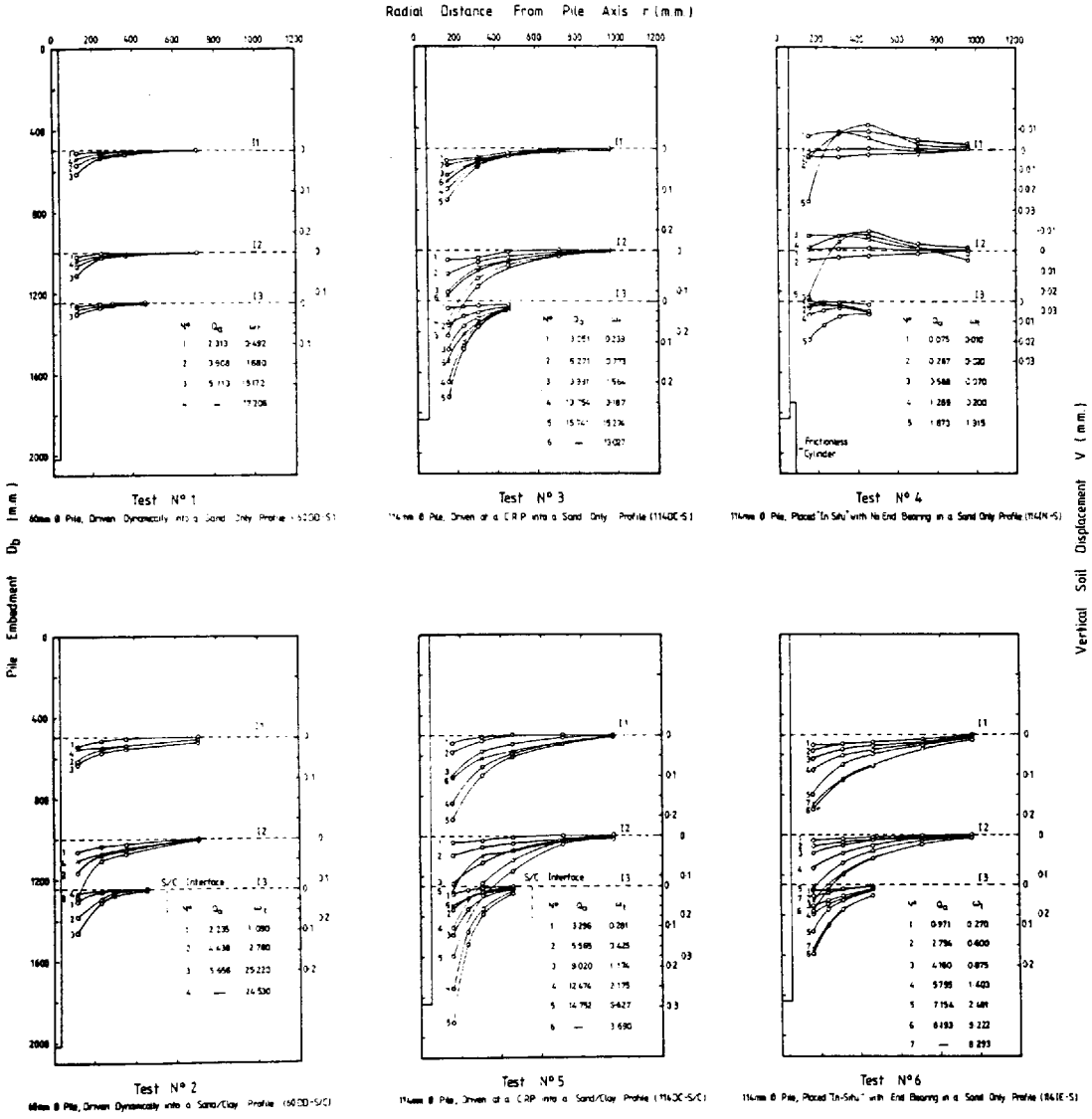

FIGURE N° 7.41 DEVELOPMENT OF VERTICAL SOIL DISPLACEMENT DURING THE MAINTAINED LOAD TEST (M.T.L. TEST SERIES 1)

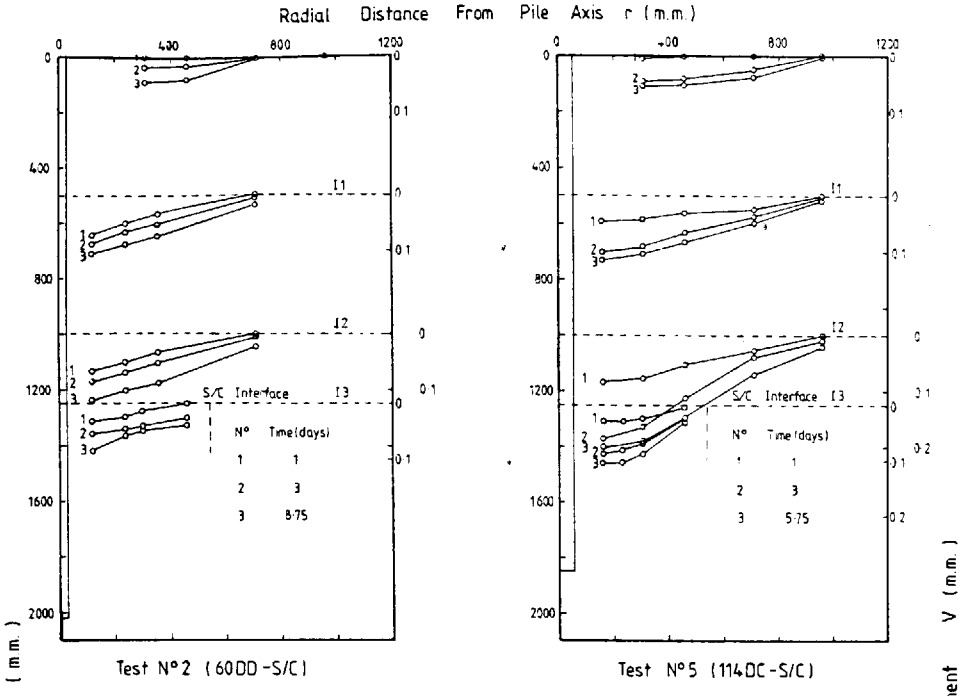

FIGURE 7.42 DEVELOPMENT OF VERTICAL SOIL DISPLACEMENTS DURING DISSIPATION OF PORE WATER PRESSURE

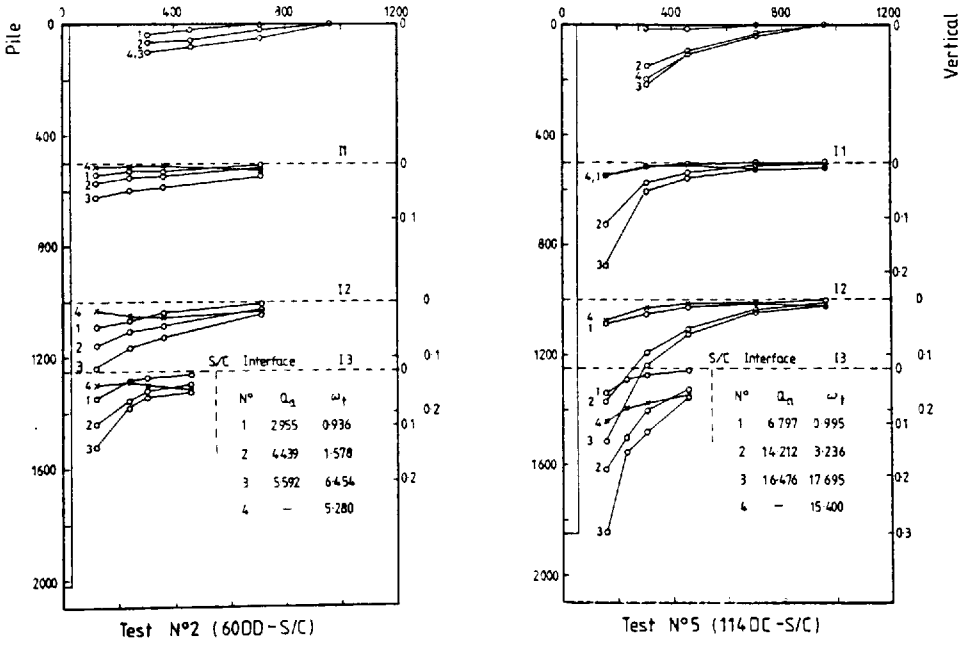

FIGURE 7.43 DEVELOPMENT OF VERTICAL SOIL DISPLACEMENTS DURING THE MAINTAINED LOAD TEST (M.T.L. TEST SERIES 2)

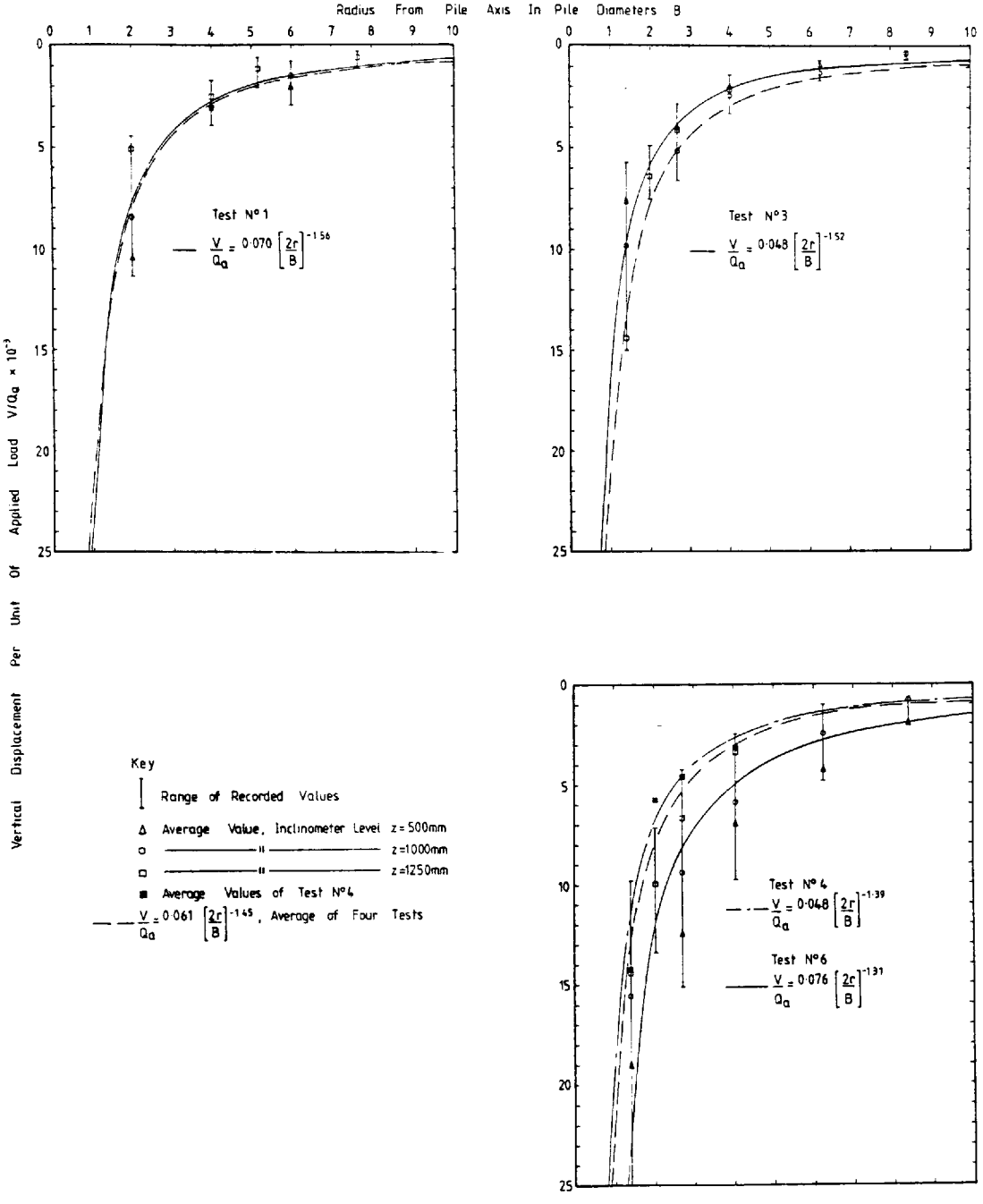

NORMALISED SOIL VERTICAL DISPLACEMENT PER UNIT OF APPLIED LOAD DURING THE MAINTAINED LOAD TEST

FIGURE N° 7.44

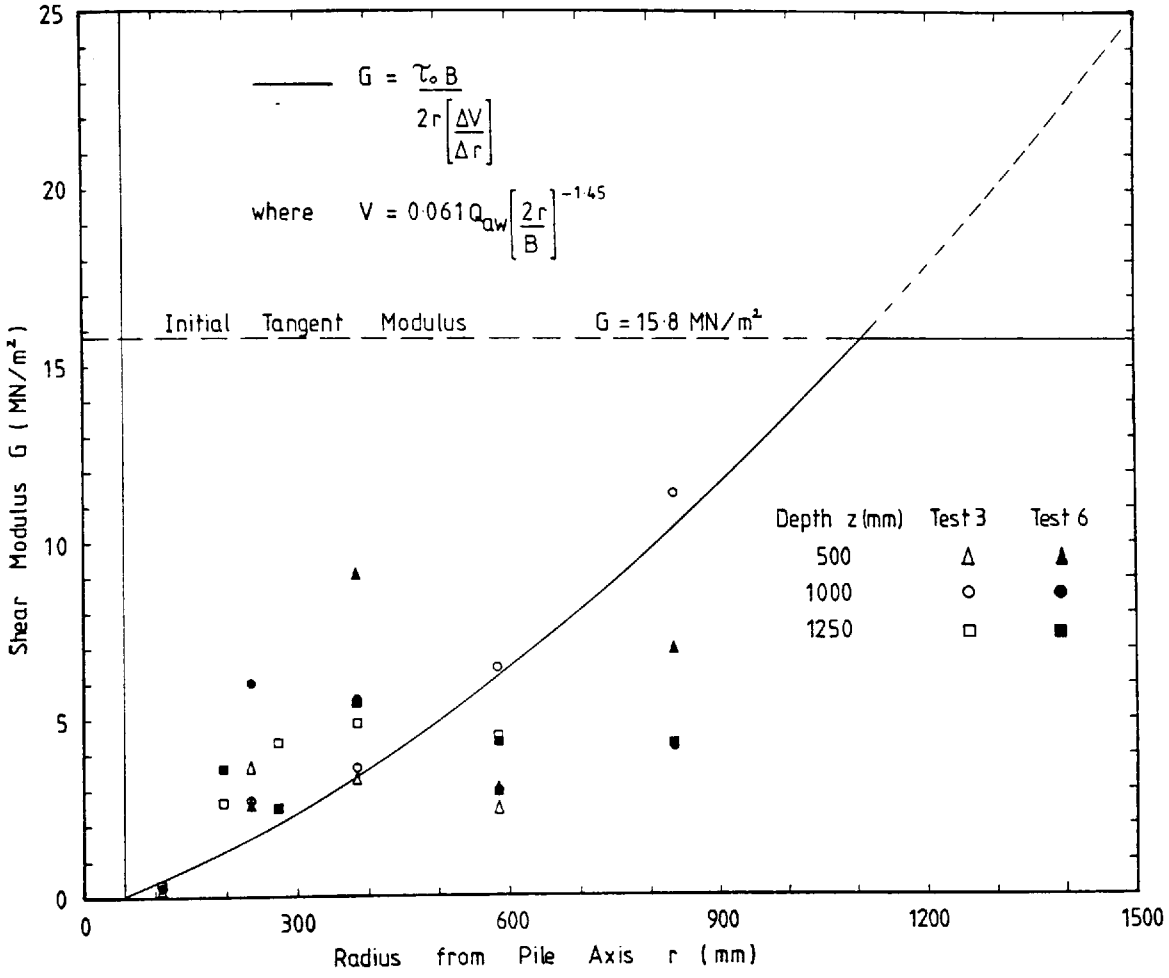

VARIATION IN SOIL SHEAR MODULUS WITH RADIUS FROM THE PILE AXIS AT WORKING LOAD

FIGURE 7.45

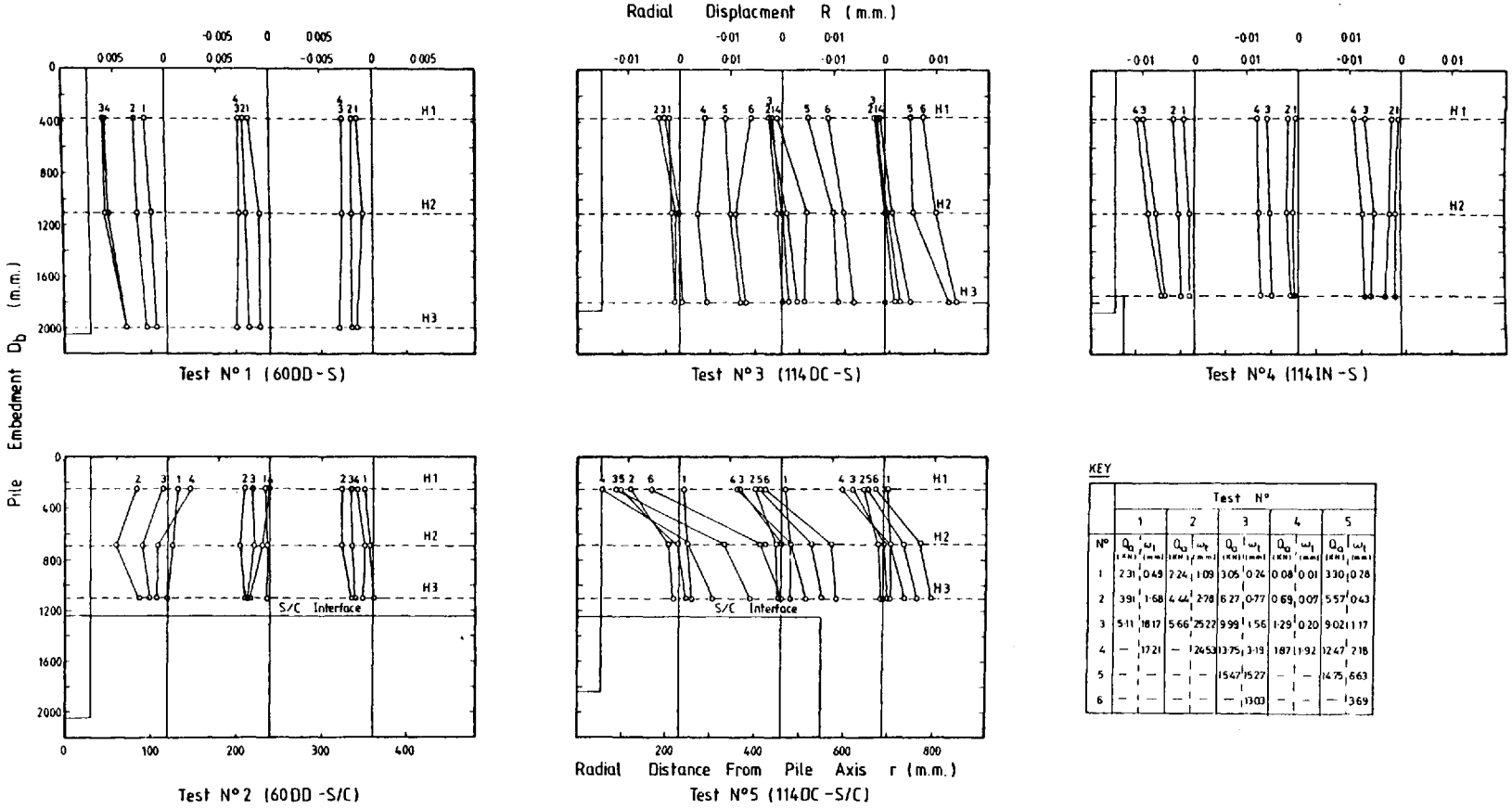

N°	1 Q_b (KN)	1 ω_b (mm)	2 Q_b (KN)	2 ω_b (mm)	3 Q_b (KN)	3 ω_b (mm)	4 Q_b (KN)	4 ω_b (mm)	5 Q_b (KN)	5 ω_b (mm)
1	2.31	0.49	2.24	1.09	3.05	0.24	0.08	0.01	3.30	0.78
2	3.91	1.68	4.42	2.78	6.27	0.77	0.69	0.07	5.57	0.43
3	5.11	18.17	5.66	25.22	9.99	1.56	1.29	0.20	9.02	1.17
4	—	17.21	—	24.53	13.75	3.19	1.87	1.92	12.47	2.18
5	—	—	—	—	15.47	15.27	—	—	14.75	6.63
6	—	—	—	—	—	13.03	—	—	—	3.69

FIGURE N°7.46 DEVELOPMENT OF RADIAL SOIL DISPLACEMENT DURING THE MAINTAINED LOAD TEST (M.T.L. TEST SERIES 1)

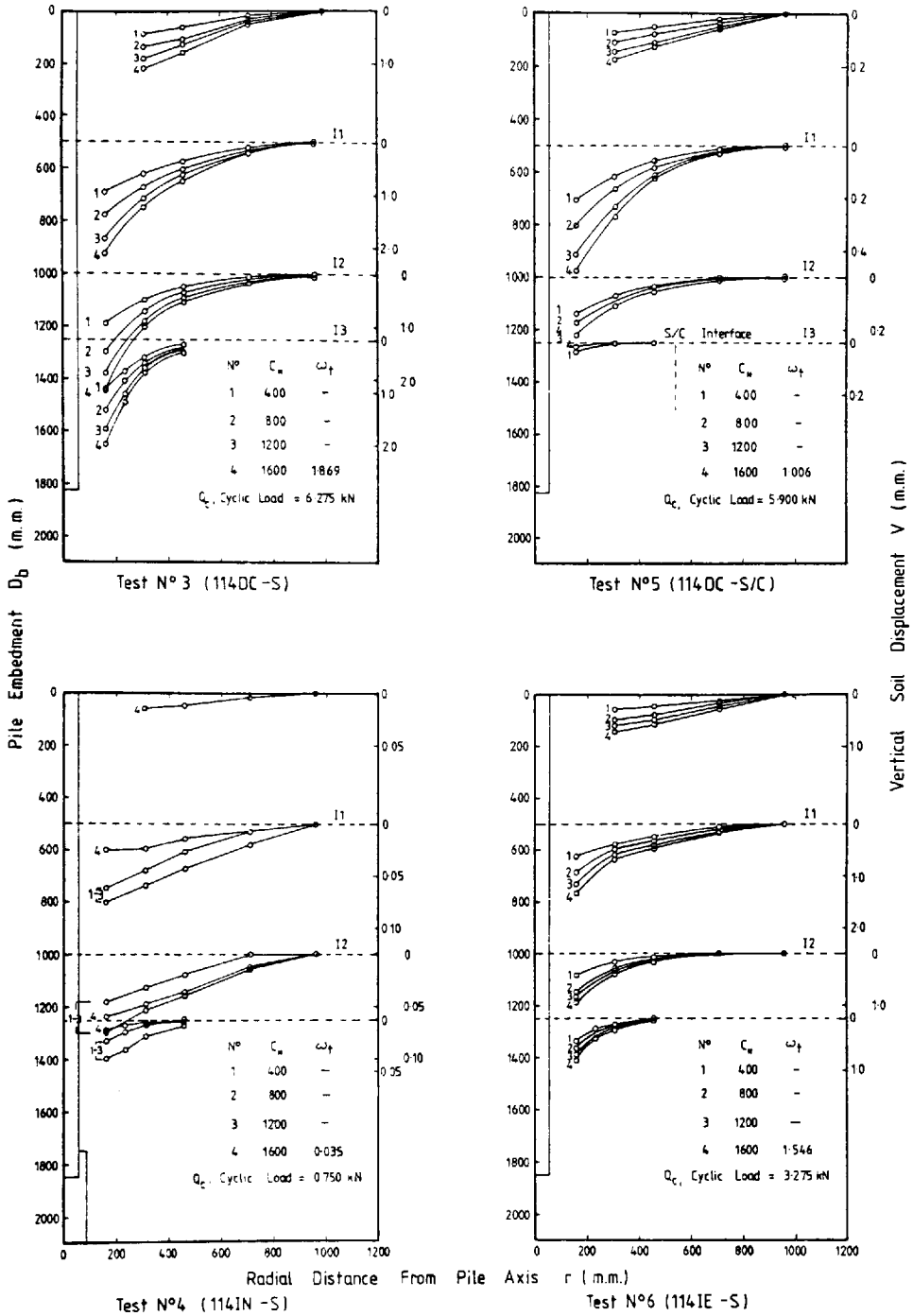

FIGURE N°7.47 DEVELOPMENT OF VERTICAL SOIL DISPLACEMENT DURING CYCLIC LOADING

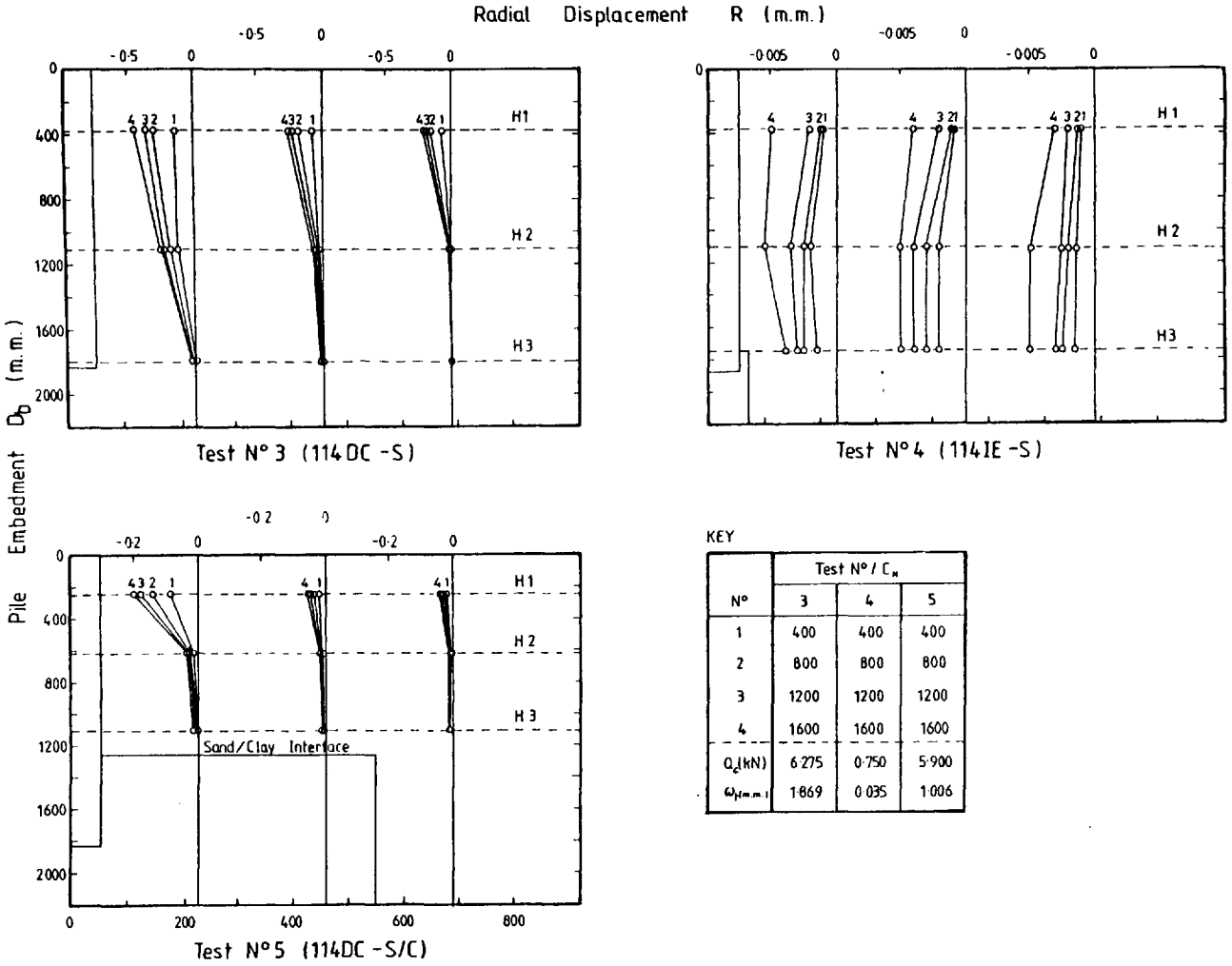

KEY

N°	Test N° / C_u		
	3	4	5
1	400	400	400
2	800	800	800
3	1200	1200	1200
4	1600	1600	1600
Q_c(kN)	6·275	0·750	5·900
$\omega_{(m.m.)}$	1·869	0·035	1·006

FIGURE N° 7.48 DEVELOPMENT OF RADIAL SOIL DISPLACEMENTS DURING CYCLIC LOADING

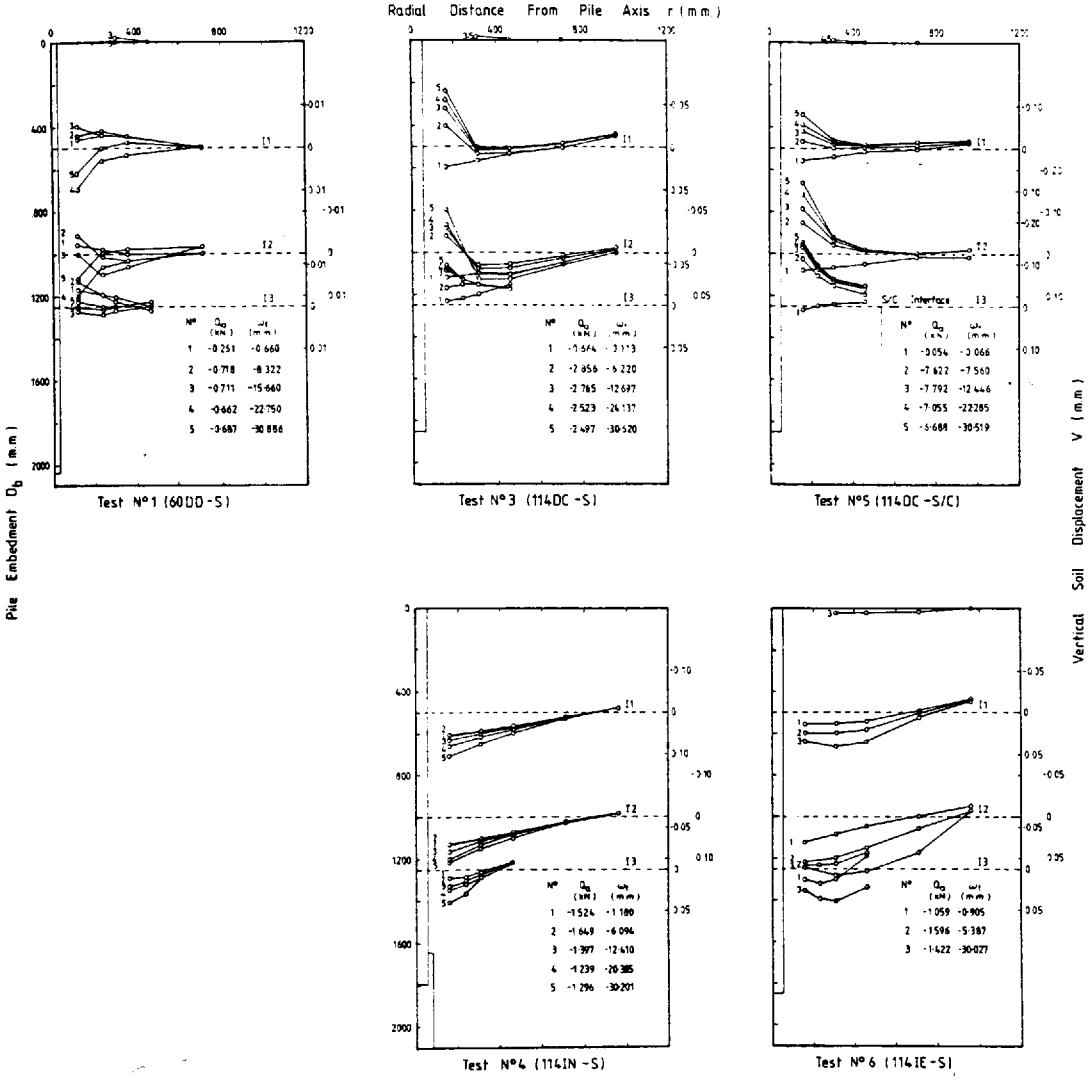

FIGURE N° 7.49 DEVELOPMENT OF VERTICAL SOIL DISPLACEMENT DURING THE CONSTANT RATE OF UPLIFT TEST

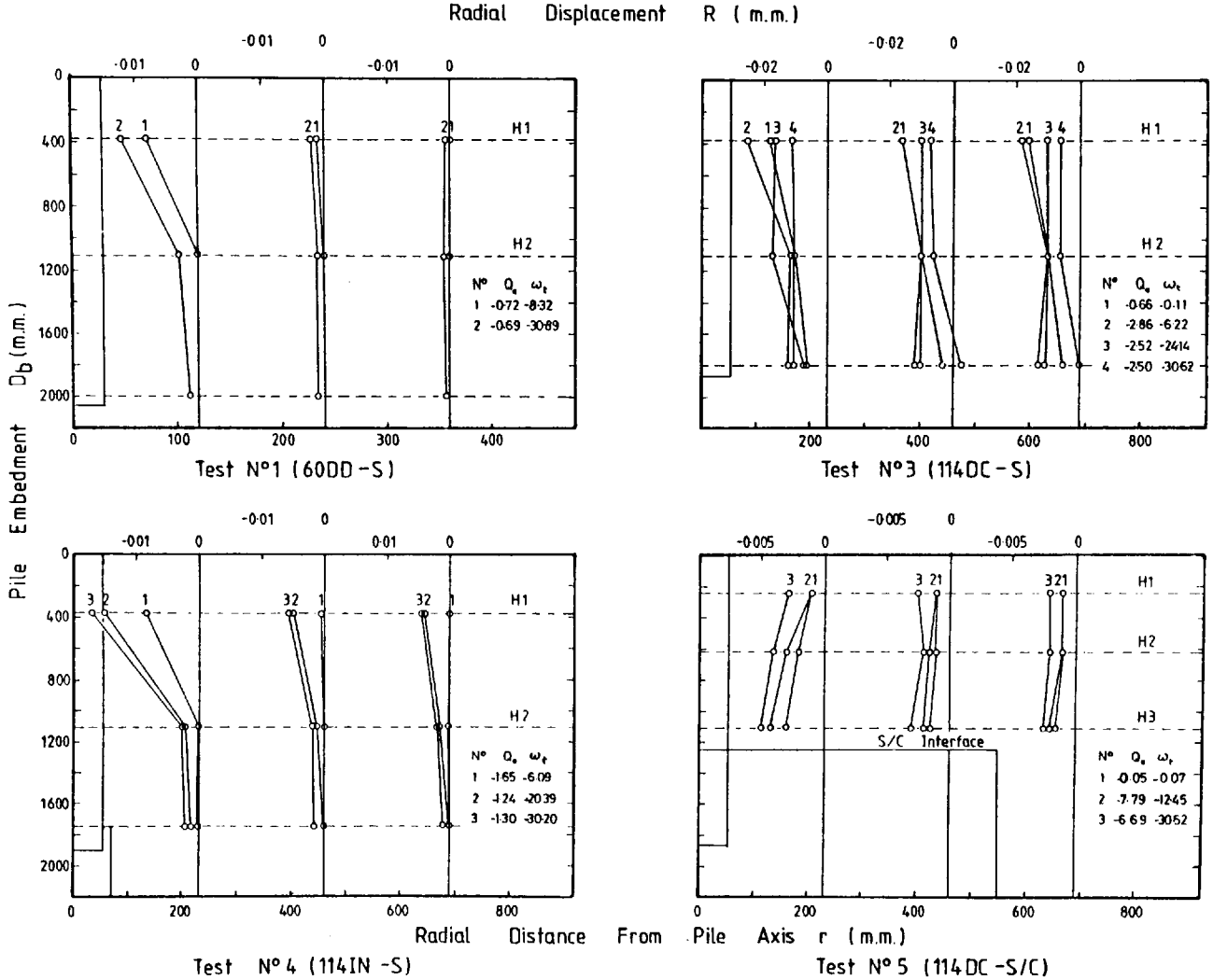

FIGURE N°7.50 DEVELOPMENT OF RADIAL SOIL DISPLACEMENTS DURING THE CONSTANT RATE OF UPLIFT TEST

Plate 7.1 Disturbance Zones Around The Pile Shaft And Pile Base (Test 5 (114DC-S/C))

Plate 7.2 Evidence Of Clay Remoulding Around The Sand Plug Driven Ahead Of The 114mm Diameter Pile Base.

Plate 7.3 The Zone Of Wetted Sand Above The Sand/Clay Interface.

Plate 7.4 Sand Draw Down Into The Clay Layer.

Plate 7.5 Sand/Clay Adhesion To The Pile Shaft Within The Sand Draw Down Region Of The Clay Layer.

Plate 7.6 Sand Plug Driven Into The Clay Layer Ahead Of The Pile Base

APPENDIX 7.1

The development of shaft friction for piles in sand overlying clay

G.O.Rowlands
Reader, The Polytechnic of Wales, United Kingdom

J.Delpak
Principal Lecturer, The Polytechnic of Wales, United Kingdom

J.B.Robinson
Formerly Research Assistant, The Polytechnic of Wales, United Kingdom

SYNOPSIS: The results of driving model piles 60 mm and 114 mm diameter through sand into clay are described. Data is provided on the interaction of the sand and the clay as the piles are driven, the generation of the pore pressure in the clay, the stresses at the interface and the soil displacement. The results show that except in the case of very short piles the contribution of shaft friction and adhesion is similar to that in single layers but the mechanism of load transfer is more complex.

INTRODUCTION

This paper briefly describes some points observed when model segmental steel piles of different dimensions were installed in a clay underlying sand. The soil properties were:

A remoulded silty clay (Mercia Mudstone)
W_l = 39%, I_p = 20 %,
Placement water content = 18%

Uniform Leighton Buzzard sand
C_u = 1.79 C_c = 1.38 Placed dry

The clay was placed at its optimum moisture content in a secondary tank 1.1 m diameter and 1.2 m high located in the base of a concrete tank 3 m diameter and 3 m deep. The larger tank was then filled with dry sand compacted under controlled conditions to a bulk density of 1500 kg/m^3. To minimise moisture migration from the clay a thin layer of sand was placed on the surface of the clay and then sprayed with a waterproof vinyl membrane. This procedure was discontinued in later tests as moisture migration proved to be negligible.

60 mm and 114 mm diameter steel piles were used. The 60 mm diameter pile was instrumented with piezoelectric washers, accelerometers and static axial load cells. It was driven dynamically using a pneumatically controlled hammer system. The 114 mm diameter pile was instrumented with a number of axial core load cells and sensitive boundary orthogonal stress transducers installed in the pile wall to monitor the development of normal (radial) and shear stresses. The pile was driven from the surface at a constant rate of penetration of 10.0 mm per minute. Details of the two systems are respectively given by Lake (1986) and Wersching (1987).

The results of two tests are considered in this paper: Test No 2 where a 60 mm pile was dynamically driven through the sand into the clay and Test No 5 where a 114 mm pile was driven at a constant rate of penetration in increments of approximately 100 mm. Each pile was then subjected to standard constant rate of penetration (CPR) and maintained load (ML) tests. The in-situ density of the sand was monitored during placement and at selected points close to the pile towards the end of the testing programme using the plaster technique developed by Wersching (1983). The movement of the sand around the pile was continuously monitored using an arrangement of electrolytic levels and a system of small plates placed horizontally and vertically and linked to displacement transducers outside the tank.

STRUCTURAL CHANGES IN THE CLAY

The structural changes observed in the clay due to pile installation are illustrated in Figure 1. The clay heaved slightly at the sand/clay interface. This was slightly more pronounced in the case of the dynamically driven pile. Heave extended for a distance of 2.75 B from the pile axis on each case. Surface heave in the sand, on the other hand, extended radially 4.0 B from the pile axis. The sand dragdown zones around the piles extended to depths of 2.5 B and 3.0 B respectively for the 60 mm and the 114 mm diameter piles. The displaced volume of clay was small in both cases due to the relatively short penetration into the clay. It is possible that heave was restricted by the sand overburden as the ratio of the heave to the displaced volume of clay was considerably lower than the values quoted for single layer conditions. The amount of sand dragdown would also tend to reduce this. There was clear evidence of a heavily distorted clay zone approximately 15 - 20 mm wide around both piles. The clay particles were clearly reorientated and all evidence of layering destroyed. It was also found to extend up through the dragdown sand zone and below the sand plug at the base of the pile. There was no evidence of sand in it and the impression is given that the sand plug at the pile tip is an isolated pocket. The sand plugs developed with each pile are illustrated in Figure 1. They appear as hemispherical cones slightly smaller in diameter than the pile shaft and extending 0.6 B below the pile tip. Both plugs were found to be completely saturated with water at the end of the test. This confirms their function as drainage outlets for the dissipation of pore pressure due to pile

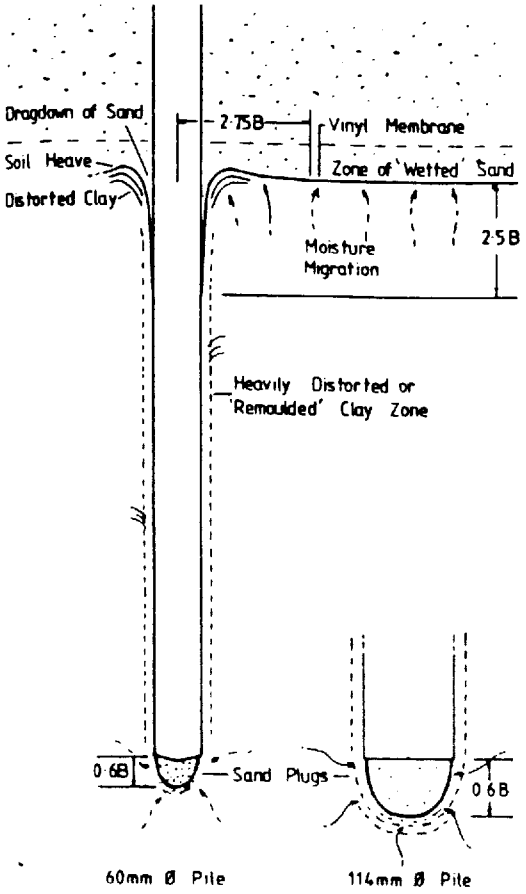

gure 1 Structural Changes in the Clay due to Pile

riving and loading. This was also confirmed y a reduction in moisture in the clay around he plug observed at the end of the test. All hese phenomena are unlikely to have a ignificant effect upon the shaft load arrying capacity except possibly in the case f very short piles. The end bearing esistance of the 114 mm pile in the sand did ot appear to be influenced by the presence of he underlying clay until the pile tip was ithin 250 mm (2.2 B) above it. A significant ecrease in the rate of increase in the value f the bearing capacity factor N below this epth was then observed although the maximum alue occurred at 170 mm (1.5 B) above the lay. The shaft adhesion in the clay was obilised as the pile penetrated beyond the ragdown zone and the value of N c tended to

EVELOPMENT OF PORE PRESSURE

continuous record of the pore pressure in he clay was provided by a series of iezometers installed at three different evels, with the lower level at the level of ile tips. The pattern was essentially similar the two tests apart from the more rapid re pressure build up during pile stallation in the case of the 60 mm pile. he pile was fully driven in 4.5 hours whilst took 8.5 hours to drive the 114 mm diameter ile. In Test 5 an increase in pore pressure due to pile penetration of 200 mm (2 B approximately) into the sand whilst in Test 2 it occurred at a pile penetration of 240 mm (4 B apporximately) into the sand. These observations are consistent with increases in the vertical pressure observed in pressure transducers located close to the pile at the sand/clay interface. Although the pore pressure build up occurred during most of the driving operation through the sand and the clay it appeared to be concentrated in a small area of the clay dirctly beneath the pile. This suggests that in a two layer system the interaction at the interface may restrict the transmission of stresses into the clay except in the region directly beneath the pile. The concentration of pore pressure close to the pile is also consistent with the concept that an expanding cavity develops only in the clay and the sand displaced by the pile is pushed out radially along the clay surface until either the pile or a sand plug ahead of it penetrates the clay.

However, a significant increase in pore water pressure was recorded by the piezometers as the piles penetrated the clay and passed the level of the piezometers. This suggests a high radial pressure gradient from the pile. The pore pressures recorded close to the level of the pile tip were consistently higher than those along the shaft. In the case of the 60 mm pile the maximum pore pressures at a radial distance of 1.5 B were equivalent to 0.36 C_u and 0.27 C_u opposite the base and shaft respectively. The corresponding values were 0.56 C_u and 0.34 C_u respectively for the 114 mm pile.

The maximum piezometer readings recorded during pile installation and subsequent (CRP) and (ML) tsts were plotted against the logarithm of the radial distance from the pile axis in Figure 2. This relationship was found to be consistently linear for the whole embedded length of the piles and is of the form:

$$\Delta u = P\,C_u - R\,C_u \times \ln[2\,r/B]$$

Where P and R define the magnitude of the pore pressure generated.

This relation is similar to the expression prescribed by Steenfelt et all (1979) of the form:

$$\Delta u = 4\,C_u - 2\,C_u \times \ln[2\,r/B]$$

This expression was obtained from a series of tests when a 19 mm diameter pile was jacked into a reconstituted clay.

Figure 2 illustrates that the values of the P and R parameters were of the same order in the driving tests with a higher pore pressure being generated by the 114 mm pile. A similar linear relationship was obtained with the pile loading tests although the values of the parameters P and R and the pore pressures were considerably lower. The values of P and R were also substantially lower than the values given given by Steenfelt et al. This is to be expected due to the low penetration, hence the low L/B ratio, into the clay as well as the additional drainage provided by the sand. In fact the pore expressed as a percentage of individual pile load increment.

An example of pore pressure dissipation rates after installation and loading tests is given in Figure 3. This data was obtained from a piezometer located at a radial distance of

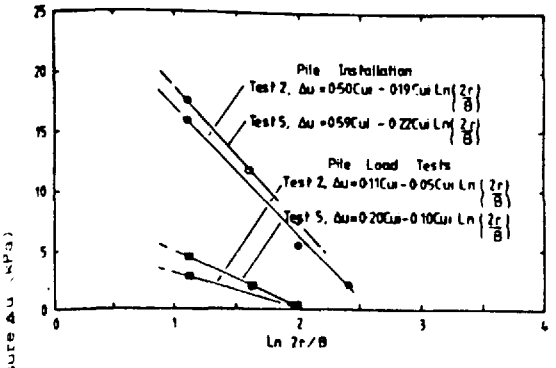

Figure 2. Logarithmic Radial Distribution of Excess Pore Water Pressure Generated within the Clay during Pile Installation and Load Tests

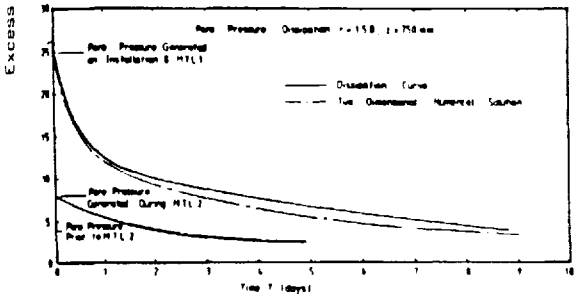

Figure 3 Dissipation of Excess Pore Water Pressure at a depth within the Clay equivalent to the Pile Base Level and at a radial distance r = 1.5 B

5 B from the base of a 60 mm pile
hetrating 750 mm into the clay 85 per cent
re pressure dissipation was achieved in 9
ys after installation and an immediate (ML)
st. A similar test for the 114 mm pile
hieved the same degree of consolidation in
5 days. Possible explanation for the
fferences in dissipation rates are the
fferent sizes of the sand plugs and the pile
meters.
A theoretical prediction of the pore
essure dissipation in the clay has been
rried out using the explicit two dimensional
nite difference method. The solution for a
mm pile assuming the sand/clay interface
d the pile/clay surface to be free draining
undaries is also shown in Figure 3. This
ows good agreement with the actual test
ta.

RESSES AT THE SAND/CLAY INTERFACE

e normal and shear stress transducers
cated radially at selected points in the
dial shear and the vertical effective
resses to be monitored as the piles were
iven and subsequently test loaded. The full
ress path could be evaluated in the case of
st 5 and is described in the following
ction. This was chosen in preference to
st 2 since only the residual stress path
uld be determined in the case of a
namically driven pile. The development of the effective vertical stress in the sand for a pile penetration of about 1000 mm (8.75 B) was consistent with the conventional Boussinesq bulb of pressure. This was approximately 250 mm above the sand/clay interface. But as the pile approached the clay interface and the sand cone penetrated the clay a significant increase in the vertical stress was observed consistent with the heave of the clay. This correlated with the vertical movement recorded in the region.

Similarly during the initial stages of pile penetration a build up of negative radial shear stress was recorded in the shear stress transducers. This is illustrated in Figure 4. This is consistent with the sand flowing radially outwards from the pile and confirmed by the movement of radial displacement plates located 125 mm above the sand/clay interface. As the pile and sand cone approached the clay and negative shear stress increased to a maximum or peak value and then reversed to a to a maximum positive shear and then decreased to a relatively constrant positive value as the pile penetrated further into the clay. This indicates a discontinuity in the lateral movement between the sand and clay (ie greater lateral movement occurring in the clay). A steady state of shear stress was reached with further pile penetration. Before the stress path was plotted it was assumed that the initial stresses at the interface level were $\sigma_{ri} = K_o \sigma_{zi}$, where σ_{zi} was the initial effective overburden stress. The resultant stress path plotted from the changes in these stresses formed failure envelopes with average angles of shearing resistance of 33 degres. This is close to the measured for the sand and it confirms that shear failure was indeed occurring in the sand. Selected points on the stress path profile were plotted to enable the direction of the major principal stress σ_1 in relation to pile embedment D_b to be determined. This is illustrated in Figure 5. The direction of this stress emanated from a point 0.6 B below the pile base ie close to the tip of the sand cone observed at the end of the test (Refer to Figure 1). It is possible that the sand plug would be more sharply pointed as shown in Figure 5 at this stage of the test.

As the radial shear failure was occurring in the reverse direction, when the pile and sand cone approached the clay layer, the major principal stress σ_1 could be determined at this location. A reversal in the direction of σ_1 occurred at this level and appeared to emanate from a point at 1.0 B below the pile base.

It appears from these results that shear failure occurred in the sand to a radial limit of 280 mm from the pile axis. At a radial distance of 480 mm no evidence of shear failure could be detected and the soil beyond this point probably tended towards the "at rest" condition with $\sigma_{ri} = K_o \sigma_{zi}$. Throughout the maintained load tests, the measured changes in effective vertical stress and radial shear stress were small but their values displayed trends consistent with the stress paths observed during pile driving.

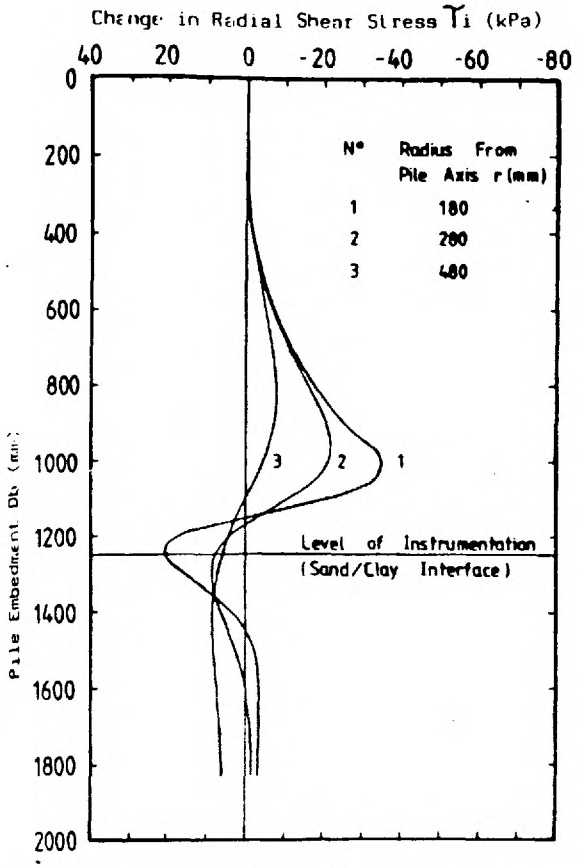

Figure 4 Radial Shear Stress History During Pile Installation.

ERTICAL AND RADIAL DISPLACEMENT OF THE SAND

he development of vertical and radial isplacement of the sand around the pile and t the sand/clay interface was monitored by a ystem of electrolytic levels and metal plates inked to displacement transducers. A typical ertical displacement pattern during pile nstallation for the 114 mm pile is shown in igure 6. This was fairly typical for both iles. In the initial stages of penetration, to a pile embedment depth of approximately 1.0 B, surface heave was evident to a radial distance of 310 mm (2.7 B) from the pile axis. The heave subsided with further penetration and a general downward vertical movement continued as the pile was driven. Within the body of the sand vertical movement increased progressively as the pile base approached the level of the instruments. This rate of movement decreased when the pile base was 2.0 B above the level of instrumentation and heave became apparent as the pile approached a level of 1.0 B. This may well be the onset of local rupture failure referred to by Robinsky and Morrison (1964). The heave extended a radial distance of approximately 1.0 B from the pile axis. It subsided when the pile base penetrated the clay but the sand continued to settle at a steady rate. The vertical movement at the sand/clay interface was generally similar to that detected in the sand. However, as the pile approached and penetrated the interface, the boundary effect

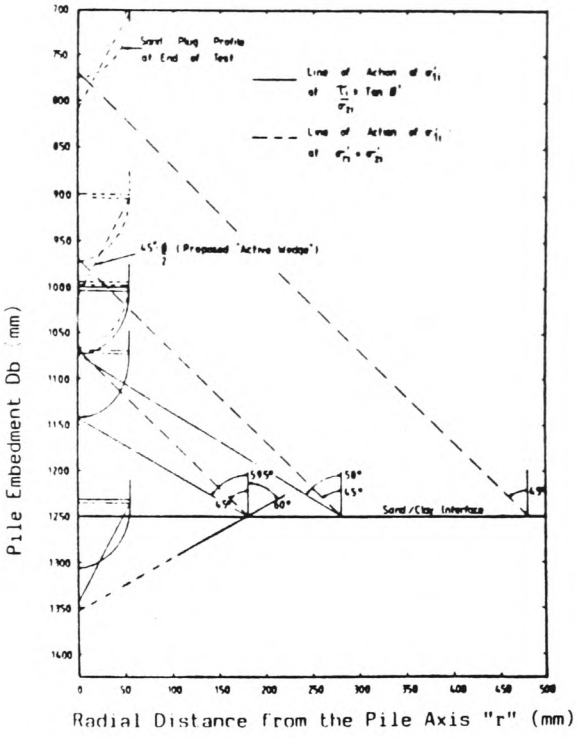

Figure 5 Soil/Pile Geometries associated with the maximum major effective principal stress and the on set of shear failure in a plane at a depth z = 1250 mm

and appreciable heave of the clay had a significant influence on the soil displacement. A resultant compressive strain within the sand was reflected by the development of an effective vertical stress at the interface. As heave subsided with further penetration vertical downward movement resumed as the pile penetrated into the clay.

The radial movement within the sand seemed to be independent of any heave in the clay but was dependant on the size of the pile. A significant feature here again, was that most of the radial movement occurred as the pile base approached the level of the instruments. It peaked when the pile was level with or just below the instruments and then reversed in direction towards the pile with further penetration. This relief in compressive strain was more pronounced in the case of the 60 mm diameter pile.

Figure 7 illustrates the peak radial displacement in the form 2R/B plotted against radial distance in the form 2r/B. The results were obtained from average peak values as the 60 mm and 114 mm diameter piles penetrated the sand. These values are compared with theoretical prediotions of radial movements given by Wersching (1987) in the equation given below.

$$\frac{2R}{B} = C_{\frac{2r}{B}} \times \frac{2r}{B} \quad \ldots\ldots\ldots\ldots (1)$$

where C = compaction factor

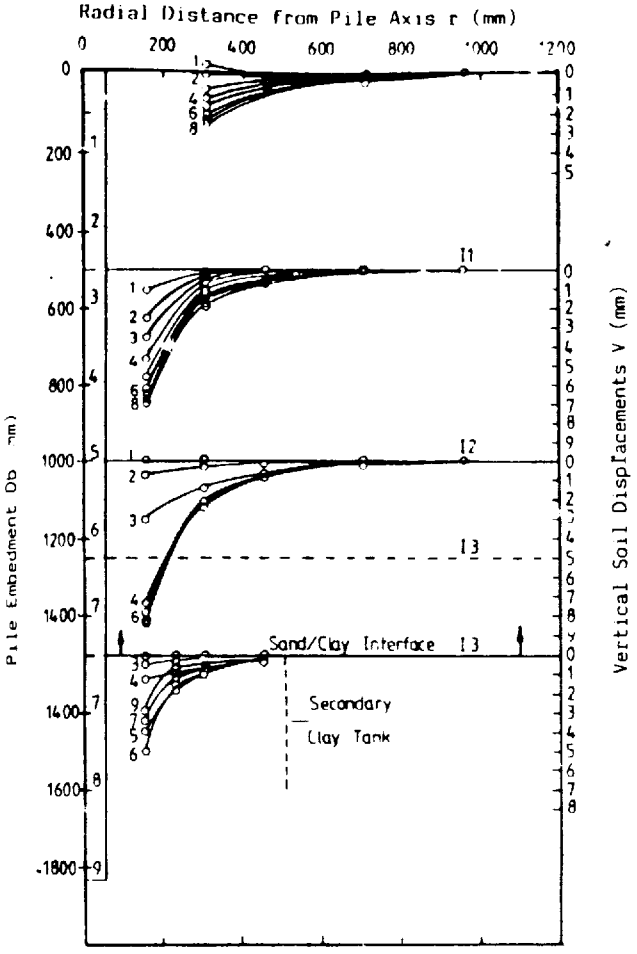

gure 6 Development of Vertical Soil

Displacements During Pile Installation

This is based upon equation (2) given by Randolph et al (1979) for $\epsilon_z = \epsilon_v = 0$ and incorporating an empirical compaction factor (C).

$$\frac{2R}{B} = \left[\left(\frac{2r}{B}\right)^{2} + 1\right]^{1/2} - \frac{2r}{B} \quad \ldots\ldots\ldots(2)$$

Using the average values directly measured during the driving of the 60 mm and the 114 mm piles a compaction factor (C) of 0.88 gives a reasonable curve fit.

REFERENCES

Lake, G.C. (1986). The development of shaft friction and end bearing resistance for dynamically driven model piles, Ph.D.Thesis, C.N.A.A., The Polytechnic of Wales, United Kingdom.

Randolph, M.F., Steenfelt, J.S., and Wroth, C.P., (1979). The effect of pile type on design parameters for driven piles, Proc 7th European Conference, SMFE, 2, 107-114 Brighton.

Robinsky, E.I., and Morrison, C.F., (1964). Sand displacement and compaction around model friction piles, Canadian Geotechnical Journal, (1), 2, 81-93.

Steenfelt, J.S., Randolph, M.F., and Wroth, C.P., (1981). Instrumented model piles jacked into clay, Proc. 10th ICSMFE, 2, 857-864 Stockholm.

Wersching S.N., (1987). The development of shaft friction and end bearing for piles in homogeneous and layered soils, Ph.D. Thesis, C.N.A.A., The Polytechnic of Wales, United Kingdom.

Wersching, S.N., Delpak, R., and Rowlands, G.O. (1983). A method of estimating and in-situ density of dry uniformly graded sand under controlled conditions of placement, Geotechnical Testing Journal, ASTM, (6), 4, 196-200.

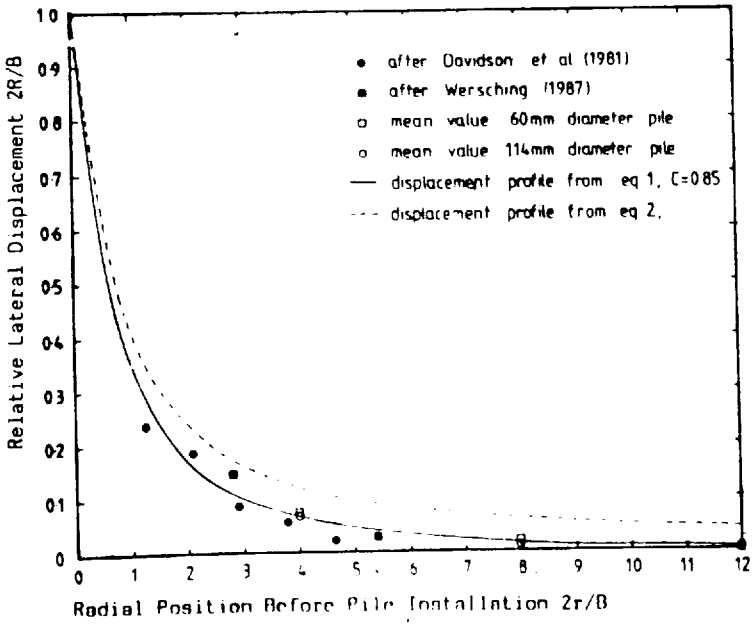

Figure 7 Normalised Radial Displacements In Loose Sand Due to Pile Installation

CHAPTER 8

CONCLUSIONS AND PROPOSALS FOR FUTURE WORK

CHAPTER 8

CONCLUSIONS AND PROPOSALS FOR FUTURE WORK

8.1 Summary of Conclusions.

The main conclusions from this study may be summarized as follows;

i. During pile installation the major principal stress acting at depth within a soil profile, appears to emanate from the face of the active wedge driven ahead of the pile.

ii. The location of the sand/clay interface has a considerable effect on the development of soil displacements and effective vertical stress developed within the overlying sand.

iii. The radial displacement during pile installation is directly related to the pile diamater. Within a sand profile, the peak radial displacement can be predicted using an empirical compaction adjustment factor to theoretically represent radial soil movement.

iv. The local unit shaft friction and radial effective stress is practically constant along the pile shaft in sand for a given pile embedment and increases at a diminishing rate with pile embedment.

v. At full pile embedment and ultimate load the local coefficient of earth pressure K_z, for a driven pile may greatly exceed K_p near the top of the pile and tend to a lower limit of 0.6 near the pile base.

vi. For a placed insitu pile at ultimate load the local coefficient of earth pressure K_z may be less than K_p near

the top of the pile and tend to a K_a near the pile base.

vii. Adjacent to the pile shaft the radial effective stress is the major axial stress.

viii. The development of shaft friction is directly related to displacements within the surrounding sand and on the sand/clay interface.

ix. The influence of the underlying clay layer affects the development of shaft friction to varying limits above and below the sand/clay interface.

x. For shallow pile penetrations into the clay layer the drawdown of sand and sand plug driven ahead of the pile significantly reduces the pore water pressure generated at the soil/pile interface.

xi. The radial distribution of pore water pressure within the clay can be represented be linear logarithmic expression.

xii. The maximum compressive strain due to pile installation in a sand profile radiated from below and around the pile base.

A more detailed account of these conclusions is given in the following sections. They are based on the experimental conditions of the six semi full scale tests. Due account of field conditions should therefore be taken before they may be applied to full scale piles.

8.2 Performance of the Monitoring System and Instrumentation.

In general the monitoring system and instrumentation functioned very satisfactory and generated a substantial quantity of data. At all times in introducing instrumentation into a soil mass the overall aim was to obtain as near as possible a measure of the stresses and

strains that would have existed if the instruments had not been present. It is considered that this was achieved fairly successfully in this investigation.

The following comments are made regarding the performance of the monitoring system and instrumentation.

8.2.1 The Monitoring System

The management control programme developed by Wersching(1987) extended and modified by the author performed satisfactory. The problems of a system failure that did occur during the testing program was overcome. It was decided to continue using the Commodore PET computer system for this work although future development consideration should be given to the use of a more up to-date personal computer system to take advantage of a more reliable and sophisticated data processing facilities.

8.2.2 The Static Load Cells.

The data obtained from the axial core load cells proved in most cases to be disappointing. This was particularly evident in the case of tests with the 60mm diameter pile and the placed insitu tests 4 and 6 carried out on the 114mm diameter pile. The variation in the loads recorded by the load cells along the pile length particularly at low loads rendered it virtually impossible to evaluate the distribution of shaft friction. However a linear polyfit of the data gave a reasonable although not a totally satisfactory evaluation of the shaft friction along the pile shaft.

8.2.3 Boundary Orthogonal Stress Transducers.

The data collected from the B.O.S.T.s was considered to be satisfactory even under low working loads. In some tests the values of the data had reduced below the normal calibration limits of the instruments, but the results still proved to be quite acceptable.

The radial stress component was affected by drift which was also reported by Wersching (1987). However this was overcome by adjusting this stress component in the manner described in section 6.

8.2.4 Displacement Transducers.

The displacement transducers used to measure vertical and horizontal displacements of the soil generally performed very satisfactory. The transducers used to monitor the sand surface movement were less responsive to small soil movement particularly in the case of a reversal in direction. This was probably due to the method used to set up the instrument. However the transducers and method used to monitor lateral soil movement did prove to be more effective and reversals in soil movement were monitored.

8.2.5 Electrolytic Levels.

The use of electrolytic levels again proved to be very successful in the monitoring of displacements within the soil mass in either positive or negative vertical direction. The replacement of the smaller inner inclinometers by the type 0716 proved to be very successful giving better compatibility to the soil displacement profile.

8.2.6 Diaphragm Pressure Transducers.

The D.P.T.s performed satisfactory in the measurement of the change in vertical stress during pile installation and the maintained load tests. Although in the latter the data produced was generally within the calibration limit of the transducers, the trend in the results was consistent throughout the test program.

8.2.7 Interface Shear Stress Transducers.

Following the comments made by Wersching (1987) with regard to the interface shear stress transducers they were installed in both the homogeneous sand and the sand/clay profiles. The data produced by both tests was compatible with the results of the D.P.T.s and were complementary to the shear stresses acting along the pile shaft.

8.3 Pile Installation and Load Test Results.

8.3.1 Pile Installation

8.3.1.1 Homogeneous Sand Profile.

i. The critical depth, D_c , at which q_b and f_s reached limiting values of 1250kPa and 6kPa respectively was 9.6B for test 3. (114mm pile driven at a constant rate of penetration into a sand profile (114DC-S)).

ii. A maximum N_q value of 94 occured within the sand at a value of 500mm (0.45Dc). At full pile embedment it tended to a value of 45.

iii. For shallow pile embedment the values of K_s were greater than K_p but tended to a value of unity for full pile embedment.

8.3.1.2. Sand/Clay Profile.

i. For a pile penetration of 650mm (5.7B) the development of N_q within the sand layer for test 5 (114mm pile driven at a constant rate of penetration into a sand/clay profile (114DC-S/C)) was similar to test 3 (114DC-S). For further pile penetration a divergence in N_q was observed in the tests. At a depth D_b equivalent to the sand/clay interface N_q for test 5 (114DC-S/C) was approximately half that developed during test 3 (114DC-S).

ii. At a D_b value of 1000 mm(8.8B) and 250mm(2.2B) above the sand/clay interface a peak in the Q_b value of 9.6kN was observed. Thereafter it reduced to a minimum value of 6.2kN when the pile base was 0.5B below the sand/clay interface. It then increased to a limiting value of 6.7kN at full pile embedment.

iii. The thickness of sand above the clay layer was not sufficient for the full development of q_b at the critical depth. Thus the value of q_b was influenced by the underlying weaker clay layer.

iv. The underlying clay was also found to influence the development of Q_s. From a pile embedment depth D_b of 1200mm (10.5B) onwards it increased rapidly, giving a corresponding increase in f_s.

v. At full pile embedment the base bearing capacity factor, N_c

tended to a value of 9.

vi. The shaft adhesion factor varied from 0.42 near the sand/clay interface to 0.55 at full pile embedment which is consistent with values expected in the case of a pile driven through a remoulded clay.

8.3.2 Load Tests.

8.3.2.1 Homogeneous Sand Profile.

i. For the driven piles the residual stress within the pile after installation had a significant effect on the distribution of shaft friction and if the residual stress profile was omitted the unit shaft friction increased generally by approximately 2kPa.

ii. For the driven pile the application of a cyclic load equivalent to the Q_{aw} had a negligible effect on its bearing capacity.

iii. The residual stesses set up within the insitu pile tests (114mm pile placed in-situ in sand with and without end bearing for test 4 (114IN-S) and test 6 (114IE-S) respectively) due to sand placement and a constant rate of penetration test were small. The net resultant effect of the shaft friction due to loading was therefore only marginal.

iv. For the insitu pile, test 6 (114IE-S) the application of a cyclic load equivalent to Q_{aw} increased the average unit shaft friction and end bearing by generally 14%.

8.3.2.2 Sand/Clay Profile.

i. The resultant residual stress within the pile due to its installation into a sand/clay profile again had a significant effect on the evaluated distribution of shaft friction along the pile shaft.

ii. If the residual stress was disregarded there was a general increase in the evaluated shaft friction along the pile shaft.

iii. There was a local increase in the unit shaft friction within the region of the sand/clay interface due to the influence of the clay boundary.

iv. With a lapse in time allowing for the dissipation in pore water pressure there was a general increase in the bearing capacity of the pile.

8.4 Boundary Orthogonal Stress Trandsducers.

8.4.1 Pile Installation.

8.4.1.1 Homogeneous Sand profile. (Test 3, 114mm pile driven at a constant rate of penetration.

The test data showed that:-

i. During pile installation f_z tended to a unique function of D_b. Along the pile shaft this function was fairly constant and increased at a reduced rate with pile embedment. Extrapolation of the average friction f_z and D_b values gave a peak f_z value of 8kPa at a pile embedment depth of 2.5m.

ii. The residual values of the local shaft friction, f_z were generally 25% of that recorded during pile installation

iii. The radial stress σ_r' was related to f_z by $1/\tan \delta'$.

iv. The average value of the effective angle of friction between the pile shaft and soil at failure δ', throughout pile installation was 25.7 degrees.

v. The variation in the local coefficient of earth pressure K_z was similar to that obtained by Wersching(1987) i.e;-

(a)Logarithmic plot of K_z with z/B for a given D_b /B was linear with a slope of unity.

(b)K_z integrated between 1 and D_b/B (greater than 1) gave K_s tending to 1.73 for a D_b/B value greater than 10.

8.4.1.2 Layered Soil Profile. Test 5, 114mm Pile driven at a constant rate of penetration into a sand/clay profile.

i. The development of f_z was similar to the sand only profile down to a pile embedment depth of 1050mm (9.2B).

ii. There was a signficant increase in the development of f_z within a distance of 200mm(2B) above the sand/clay interface. This was typically twice the magnitude of that developed in the sand only test, for an equivalent embedment depth.

iii. For pile embedment depths to 650mm(5.7B) the magnitude of residual f_z was similar to the sand only test. Below this depth the residual f_z tended to approximately twice that developed during the sand only test. This is attributed to the greater elastic recovery properties of the underlying clay.

iv. Within the sand the relationship between f_z and σ_r' and the magnitude of δ' were similar to the sand only test.

v. Within the clay the value of δ' was approximately 40 degrees and was a reflection on the high positive residual shear stress at the pile/soil interface.

vi. The relationship $f_z = 1/\tan \delta'$ was generally true within the sand drawdown zone, although the f_z values were higher the relation $f_z = 1/\tan \delta'$ was generally true.

8.4.2 Maintained Load Tests.

8.4.2.1 Homogeneous Sand Profile.

8.4.2.1a Test 3, 114mm Pile driven at a constant rate of penetration into a sand strata (114DC-S).

i. The post compressive residual f_z was negative and fairly linear throughout the depth of the pile. Its value on average was -2kPa. An applied load Q_a of 50% Q_{aw} neutralised f_z over the upper two thirds of the pile shaft.

ii. The development of f_z was reasonably linear with depth to an applied load of 200% Q_{aw}. The greatest rate of increase in f_z was associated with depth.

iii. For an applied load greater than 200% Q_{aw} the distribution in f_z became progressively "D" shaped. The reduction in f_z along the lower section of the pile was associated with the development of "flow and arching" zones around the pile base.

iv. Only marginal increases in the distribution of σ_r' were

evident up to Q_{aw}. Thereafter a steady increase in σ_r' was observed. At an applied load of 150% Q_{aw} the development of σ_r' was proportional to f_z i.e. $f_z/\sigma_r' = \tan \delta'$.

v. The average value of δ during the maintained load test was 26.7 degrees.

vi. At high applied load where there was a reduction in f_z due to the development of flow and arching zone, there was an accompanied reduction σ_r'. These values were still proportional to each other and remained on the δ' line.

vii. The post cyclic load residual f_z increased marginally to on average -2.5kPa.

viii. For each subsequent increment in applied load the value of f_z was marginally greater than that produced from the earlier load test. This was accompanied by an associated increase in the σ_r' values.

ix. At Q_{amax} which was virtually the same for both the maintained load tests, the general value of f_z had increased. An inspection of the load cell results indicated that end bearing had marginally reduced.

x. The increase in shear stress could be as a result of the cyclic load, but is most probably linked to a continued re-application of load. This phenomenon was consistently evident during all the maintained load tests.

xi. For both the load tests at Q_{amax}, K_z varied from a value of 5 (greater than K_p) near the sand surface and 0.65 close to the pile base.

8.4.2.1b Test 4 (114IN-S). 114mm pile, Placed In-Situ with No End Bearing in a Sand Strata

i. The post compressive f_z was positive. The distribution of this stress was fairly linear with depth varying from approximately 0.5kPa near the sand surface to 1.0kPa close to the pile base. This equated to within 97.5% of the pile self weight.

ii. The development of f_z was progressive throughout the load test, the greatest rate of increase was associated with the middle third of the pile shaft.

iii. Up to Q_{amax} there was no apparent reduction in the development of f_z around the "base" of the pile.

iv. The development in σ_r' was similar to that shown during test 3 (114mm pile driven at a constant rate of penetration into a sand strata. At an applied load of 175% Q_{aw}, the development in σ_r' was proportional to f_z. i.e. $f_z/\sigma_r' = \tan \delta'$

v. The average δ' value during pile load testing was approximately 27 degrees.

vi. The post cyclic load residual f_z value reduced marginally.

vii. During the subsequent load test after cyclic loading, the development in f_z was reasonably linear with applied load and depth, but local increases in f_z were evident around the simulated pile base level.

viii. At Q_{amax} for both tests the value of K_z varied from a value of 1.5 for a D_b/B ratio of 2 to K_a close to pile base level.

8.4.2.1 c. Test 6 (114IE-S). 114mm pile, Placed In-Situ with End Bearing in a Sand Strata.

i. The post compressive f_z was negative and fairly linear throughout the depth of the pile. Its value on average was approximately -0.5kPa. An applied load of $0.5Q_{aw}$ generally neutralised f_z to zero.

ii. For applied load of greater than $0.5Q_{aw}$ the distribution of f_z was progressively "D" shaped. The greatest development in f_z being in the middle half of the pile shaft. A reduction in the development of f_z around the base of the pile again being associated with the development of flow and arching zones.

iii. The development in σ_r' was again similar to test 3. At an applied load of 150% Q_{aw} the development in σ_r' became proportional to f_z.

iv. The average value of δ' was 28.18 degrees.

v. As the applied load approached Q_{amax} there was a marginal reduction in the development of f_z along the length of the pile.

vi. The post cyclic load residual f_z values along the pile shaft reduced marginally in value.

vii. The action of the cyclic load increased the capacity of the pile by approximately 15%, probably by the compaction of the sand below the pile base level.

viii. The subsequent application of the applied load gave increased values of f_z when compared to the earlier maintained load test. This was accompanied by an

associated increase in σ'_r .

ix. On average between the two load tests at Qamax, K_z varied from 1.5 near the sand surface to 0.3 near the pile base.

8.4.2.2. Layered Soil Profile. Test 5 (114DC-S/C)

i. The post compressive residual f_z within the sand was marginally greater than test 3 which was due to slightly higher elastic displacement recovery generated by the soil profile.

ii. The residual f_z close to the interface was greater than that within the body of the sand. This was a result of the increased stresses generated within the area of the sand/clay interface.

iii. The development of f_z and σ'_r within the sand layer was similar to test 3, the sand only test.

iv. Within the sand immediately above the sand/clay interface f_z developed more rapidly throughout loading with corresponding increases in the value of σ'_r .

v. The average value of δ' during the maintained load test was 26.7 degrees.

vi. Within the sand drag down zone of the clay layer the residual value of f_z was similar to that exhibited immediately above the sand/clay interface.

vii. Within the body of the clay the residual value of f_z was positive and had an average value of $0.3G_{ui}$.

viii. As the pile was loaded there was a progressive increase in f_z. At Q_{amax} f_z varied from $0.55C_{ui}$ within the sand drag-down zone to $1.0C_{ui}$ near the pile base.

ix. The post compressive residual values of σ_r' varied from $1.8C_{ui}$ to $0.92C_{ui}$ close to the sand/clay interface and pile base respectively.

x. There was a small progressive increase in σ_r' with applied load and at Q_{amax} was typically $1.20C_{ui}$.

xi. After the period of dissipation of pore water pressure, the residual f_z and subsequent behaviour of this stress to further applied loads was similar to that described in test 3.

xii. Over this period the residual f_z within the clay had reduced significantly to approximately $0.3C_{ui}$. Although at Q_{amax} the change in f_z was similar to the previous load test.

xiii. The post cyclic load behaviour of f_z within the sand was similar to that described for test 3.

xiv. There was a significant increase in the distribution of f_z and σ_r' within the sand drag zone of the clay which corresponded to a higher Q_{amax} and higher undrained shear strength of the clay.

8.4.3 Constant Rate of Uplift Tests

8.4.3.1 Homogeneous Sand Profile

8.4.3.1a Test 1 (60DD-S). 60mm Pile, Dynamically Driven into a Sand Strata.

i. A Q_{sf} value of -0.75kN was attained at a ω_t value of -6.52mm

8.4.3.1b Test 3 (114DC-S). 114mm pile, Driven at a Constant Rate of Penetration Into a Sand Strata.

i. A Q_{sf} value of -2.86kN was attained at a pile displacement of -6.22mm

ii. The initial residual f_z condition was fairly linear and uniform along the length of the pile and was on average -2kPa.

iii. At Q_{sf} the relationship between f_z and σ_r' was -tan δ'.

iv. Q_{sf} was reached relatively quickly which gave only marginal fluctuation in the values of f_z and σ_r' .

v. Around the pile base a reduction in f_z was observed for progressive increasing values of ω_t. This was due to the development of flow and arching zones around the void being formed beneath the base.

8.4.3.1c Test 4 (114IN-S). 114mm Pile, Placed In-Situ with No End Bearing in a Sand Strata.

i. The post maintained load test distribution of f_z varied linearily from -0.5kPa to 2.0kPa from top to bottom of the pile.

ii. At Q_{sf} the resultant distribution of f_z varied from -0.5kPa near the pile top to 1.5kPa close to the simulated pile base.

iii. The resultant f_z/σ'_r relationship was proportional to -tan δ'

8.4.3.1d Test 6 (114IE-S). 114mm Pile, Placed In-Situ with End Bearing in a Sand Strata.

i. The post maintained load test distribution of f_z was -0.75kPa near the pile top to -0.1kPa close to the pile base.

ii. A Q_{sf} value of -1.65kN was attained at -6.09mm.

iii. At Q_{sf}, f_z generally reduced by -1kPa.

iv. The development in f_z around the pile base was associated with flow and arching zones forming in and around the void below the pile base, similar to Test 3.

8.4.3.2. Layered Soil Profile

8.4.3.2 Test 5 (114DC-S/C). 114mm Pile, Driven at a Constant Rate of Penetration into a Sand/Clay Stratum.

i. The Compressive residual f_z stress within the sand was -2kPa

ii. Q_{sf} (-7.8kN) was attained at a pile displacement of 12.44mm generally a ω_t value of twice that obtained during a sand only test.

iii. The relationship of f_z/σ'_r was equal to tan δ' within the sand and was maintained throughout the test.

8.5 Sand Density.

i. A zone of increased sand density around the pile shaft extended up to a radial distance of 7B for both types of pile installation.

ii. At radial distances of 2B and 1.4B the volumetric strain was generally 3% for the dynamically driven and constant rate of penetration piles respectively.

iii. For the pile driven at a constant rate of penetration the density variation within the overlying sand in test 5 appeared to be unaffected by the underlying clay. During test 2 with the dynamically driven pile there was a relative increase in the sand density in the overlying sand when compared to the sand only test 1.

8.6 Structural Changes in the Clay layer.

i. At the sand/clay interface soil heave was physically evident in the clay up to a distance of 2.75B from the pile axis.

ii. Sand was dragged down into the clay to limiting distances of 2.5B and 3B for tests 2 and 5 respectively.

iii. A zone of remoulded clay existed around the pile shaft extending a distance of 0.15B - 0.35B from the face of the pile shaft.

iv. A near hemispherical cone of sand was driven ahead of the pile into the clay layer and extended up to 0.6B below the pile base.

8.7 Pore Water Pressure in the Clay.

8.7.1 Pile Installation.

i. Within the radial limits of the piezometers the initial generation and radial distribution of pore water pressure was logarithmic. This relationship was consistent throughout the embedded length of the pile and is as follows,

$$\Delta u = P\ C_{ui} - R\ C_{ui}\ \ln(2r/B)$$

where P and R are values which describe the magnitude of the pore water pressure generated.

ii. Due to the low pile penetrations into the clay and the apparent drainage effects of the sand plug and drag down zone, it is probable that there was an insignificant build-up of pore water pressure at the pile/soil interface.

iii. The pore water pressure dissipation curves for both tests 2 and 5 was reasonably modelled using a two dimensional numerical technique.

8.7.2 Load Test Results.

i. Within the radial limits of the piezometers the generation and radial distribution of pore water pressure during the maintained load tests was consistent with the logarithmic expression derived during pile installation with adjustments made to the P and R values which dictate the magnitude of the pore water pressure.

ii. The pore water pressures generated during the maintained load tests were generally lower by some 20-35% of the values during pile installation.

iii. At the end of cyclic loading a peak value in pore water pressure of 2kPa was recorded at r=1.5B. The generation and radial distribution can again be depicted by the previous expression. The magnitude of these pore pressures had little significant effect on the subsequent load tests.

8.8 Stresses Developed on a Horizontal Plane at depth in a Soil Profile.

8.8.1 Pile Installation.

8.8.1.1 Homogeneous Sand Profile. Test 3, 114mm Pile Driven at a Constant Rate of Penetration into a Sand Strata.

i. The build up and distribution of the effective vertical stresses generated during pile installation were synonymous with the formation of "pressure bulbs"

ii. Towards the end of pile installation σ'_{zi} tended towards a constant limiting value at all radial locations of the instruments and was generally less than the initial effective overburden pressure,

iii. A peak in the radial shear stress τ_i was generally experienced across the level of instrumentaion for a pile embedment of approximatelty 8.5B. As the pile approached and passed through the level of instruments, the change in relative soil displacements altered the direction of the radial shear stress. Towards the end of pile installation τ_i became positive and was complementary to f_z.

iv. The greatest magnitude of σ'_{zi} and τ_i was displayed on the

instrumentation located nearest to the pile axis

v. Towards the end of pile installation σ'_{zi} and τ_i tended towards quasi constant values at the level of instrumentation.

8.8.1.2 Sand/Clay Profile. Test 5, 114mm Pile Driven at a Constant Rate of Penetration.

i. As the pile approached the sand/clay interface the trend and build up in σ'_{zi} was similar to test 3. However as the pile base approached and passed through the level of instruments the soil heave of the clay markedly increased the σ'_{zi} values. Towards the end of pile installation σ'_{zi} was generally slightly less than the initial effective overburden pressure.

ii. The trend in τ_i throughout pile installation was similar to test 3 but the magnitude of the peak and the final stresses towards the end of pile installation were lower.

8.8.2 The State of Two Dimensional Stress Development on the Sand/Clay Interface.

i. During pile installation into the sand/clay profile the direction of the major principal stress acting on the sand/clay interface appeared to emanate from a point 0.6B below the pile base. For the sand only profile it appeared to emanate from a point 1.0B below the pile base.

ii. As the pile base approached the level of instrumentation a reversal in the direction of the principal stresses occurred and appeared to emanate from a point of 1.0B below

the pile base.

iii. A noticeable difference in the generation of the effective vertical stress profiles between the homogeneous sand and the sand/clay profiles was the influence of soil heave in the underlying clay layer.

8.8.3 Maintained Load Test.

8.8.3.1 Homogeneous Sand Profile.

8.8.3.1a Driven Piles. Test 3, 114mm Pile Driven at a Constant Rate of Penetration into a Sand Stratum.

i. Throughout loading, the magnitude of increase in vertical stress was small with peak values being reached at maximum applied loads.

ii. Maximum values in σ'_{zi} were attained near the pile and diminished in magnitude with radial distance from the pile.

iii. Peak values in τ_i were negative indicating outward movement. They were greatest in magnitude close to the pile and diminished with increased radial distance.

8.8.3.1b In-Situ Piles. Test 4 and Test 6, 114mm Piles Placed In-Situ in a Sand Stratum Withand Without End Bearing Respectively.

i. For the insitu pile with end bearing the D.P.T.s were placed at pile base level. There was a general reduction in the σ'_{zi} values recorded during the load test.

ii. The relief in σ'_{zi} was greatest close to the pile and diminished with radial distance from the pile axis. This

adds credence to the development of a flow zone, extensive soil straining around the pile base, due to the incompatibility in soil displacements.

iii. The radial shear stress τ_i demonstrated similar trends in soil movement to the driven piles but were less in magnitude.

8.8.3.2 Layered Soil Profiles.

i. Towards Q_{amax} there was generally an increase in σ'_z typically greater with closer proximity to the pile.

ii. The development in τ_i was similar to the driven piles in sand but were greater in magnitude. This demonstrated the boundary effect of the sand/clay interface.

8.9 Soil Displacements

8.9.1 Pile Installation - Vertical Soil Displacement.

8.9.1.1 Homogeneous Sand Profile. Tests 1 and 3, 60mm and 114mm Piles Driven Dynamically and at a Constant Rate Penetration Respectively, Into a Sand Strata.

The conclusions on observations drawn from the vertical movement of sand due to pile installation were similar to Werscheing (1987) and are as follows,-

i. For test 3 surface soil heave was detected at r=310mm to a pile embedment depth of 210mm, thereafter settlement occured, the rate of which diminished with increased D_b values. No surface heave was detected from the instrumentation during Test 1.

ii. Sub-surface vertical displacement first became evident at a radial distance of r=180mm where the pile base was typically 5-7B away from any one particular level of instruments. With further pile penetration within this region there was a rapid increase in vertical displacement which decreased with radial distance from the pile.

iii. As the pile base approached to within 2.5B of the instrument level there was a marked decline in the vertical movement.

iv. Sub-surface heave was first evident when the pile base was generally 1.0B above the level of instruments. This movement was detected up to 4B from the pile axis for both methods of pile installation and was greatest at the innermost located instruments.

v. As the pile base passed through an influence zone, sub-surface heave subsided, returning to a general downward vertical movement which tended to quasi constant values with remotness from the pile base.

vi. The history of the above vertical soil movement due to a penetrating pile can be defined by six distinct displacement zones.

8.9.1.2 Layered Soil Profile. Tests 2 and 5, 60mm and 114mm Piles Driven Dynamically and at a Constant Rate of Penetration Respectively, Into a Sand/Clay Stratum.

i. Within the sand layer for pile penetration of 1000mm the development of vertical soil movement was similar to that exhibited in the sand only tests.

ii. When the pile base came to within 250mm of the sand/clay interface, the boundary effect of the clay layer became more significant and was reflected in the soil movement monitored at a depth of 1000mm (8.8B).

iii. As the pile base approached and penetrated the sand/clay interface soil heave was detected at this level which restrained the vertical movement within the overlying sand.

iv. Maximum values of soil heave of 1.25mm and 3.0mm were attained at radial distances of 2B and 1.4B for tests 2 and 5 respectively.

v. With further penetration through the interface layer there was a reduction in soil heave which was more significant during test 5.

8.9.2 Pile Installation - Radial Soil Movement.

8.9.2.1 Homogeneous Sand Profile. Test 1 and 3, 60mm and 114mm Piles Respectively Driven Dynamically and at a Constant Rate of Penetration into a Sand Stratum.

i. Radial movement was detected on the innermost instruments when the pile base was generally within 8.0B of a zone within the body of sand.

ii. As the pile base approached this zone the outward lateral movement increased rapidly. This movement reached a maximum when the pile base was generally at the level of the considered zone.

iii. The magnitude and build up of radial movement seemed independent of soil heave but was a function of pile

diameter, tentatively agreeing with expanding cavity theory.

iv. The lateral movement was greatest within the proximity of the pile and decreased with radial distance from the pile axis.

v. When the pile base passed through a level of instruments there was a reversal in lateral movement indicating a release in radial compressive straining. This was more prominent during the dynamic method of pile installation test.

vi. Towards the end of pile installation when the pile base was remote from a considered zone the lateral movement reached a quasi constant value.

vii. The history of the above radial soil movement due to a penetrating pile can be defined by three displacement zones.

viii. The peak radial soil movement within a homogeneous sand can be broadly described by applying a compaction factor to the theoretical radial movement evaluated, assuming $\varepsilon_v = \varepsilon_z = 0$, after Randolph et al (1979)

8.9.2.2 Layered Soil Profile. Test 2 and 5. 60mm and 114mm Piles Respectively Driven Dynamically and at a Constant Rate of Penetration Into a Sand/Clay Strata.

i. The radial soil movement within the sand layer displayed very similar trends to those stated earlier for the homogeneous sand profile.

ii. The instruments near the sand surface demonstrated greater

latitude in movement and achieved a steady state condition for greater pile penetration. This was also prevalent in the sand only tests.

iii. Soil heave at the sand/clay interface had little effect on radial soil movement which was primarily a function of the pile intrusion into the soil profile.

8.9.3 Two Dimension Strain Development Within a Soil Per Unit Pile Penetration.

i. Maximum vertical compressive straining tended to a value of 2B below pile base level.

ii. Maximum vertical extensive straining tended to a value of 1.33B above and at pile base level for the dynamically driven and constant rate of penetration piles respectively.

iii. The ratio of maximum vertical compressive and extensive straining was generally around the order of 2.

iv. Maximum radial compressive straining occured at distances of 1.25B and 2B below the base of the pile for the dynamically driven and constant rate of penetration piles respectively.

v. Further pile penetrations saw a relief in the compressive strain.

vi. The two dimensional strain vectors generally radiate from beneath the pile base. They principally acted within a zone stretching 6B below the pile base and up to a radial distance of 4B from the pile axis, although minor strain development was detected outside these regions. Above pile

base level a steady state in strain development was evident.

8.9.4 Maintained Load Tests

8.9.4.1 Homogeneous Sand Profile.

i. The trend in vertical soil displacement was downward where its magnitude diminished with radial distance from the pile.

ii. For the driven piles in sand the elastic recovery given by the innermost radially located electrolytic levels was in the range of 42-64% of the total displacement at Qamax . The larger recovery was exhibited in the soil surrounding the dynamically driven pile.

iii. For the insitu pile with end bearing elastic recovery was 9% of the total displacement.

iv. The variation in $\log_e(V/Q_a)$ with loge (2r/B) was linear.

v. The radial movement was generally 10 times less than the vertical movement. The trend at low applied loads was an apparent movement inwards towards the pile and at increased loads beyond Q_{aw} the radial movement tended outwards.

8.9.4.2 Sand/Clay Profile.

i. The general magnitude of vertical displacements were greater than comparative values developed during the sand only test.

ii. On release of Q_{amax} the elastic recovery at the sand/clay interface was 85% of the total soil displacement. The soil

displacement recovery within the sand layer was similar to the sand only tests, ranging from 54-62%.

iii. The trend in radial displacements was similar to that exhibited during the sand only test but were generally greater in magnitude.

iv. The vertical displacement profile exhibited during the period of dissipation of pore water pressure was fairly linear with greater displacements with closer proximity to the pile. This illustrates the greater consolidation effects which correlate to the magnitude of the pore water pressure gradient set up within the clay due to pile installation and the subsequent load tests.

8.9.5 Cyclic Loading.

8.9.5.1 Homogeneous Sand Profile.

i. The vertical movement developed during tests 3 and 6 displayed a continuous degredation in the downward direction. A similar trend was experienced during test 4.

ii. The magnitude of this movement after 1600 cycles at the innermost radial located instruments was 11 and 5.5 times greater than the total displacement at pile load failure for tests 3 and 6 respectively.

iii. The magnitude of radial movement was much greater than that generated during the maintained load test.

iv. The sand movement was towards the pile and consistent with the radial movement of sand shown at an equivalent load of Q_{aw} during the maintained load test.

v. Radial movement was more prominent in the upper layers of

the sand and decreased with radial distance from the pile axis.

8.9.5.2 Two Layered Soil System.

i. The boundary effect of the clay layer significantly reduced the development of vertical sand movement. At depths of 500mm and 1000mm into the sand the vertical displacement had reduced by some 80% and 90% of those developed at equivalent depths in the sand only profile. At the sand/clay interface there was little downward vertical movement and towards the end of the cyclic test evidence of soil heave was present at a radial distance of 1.6B.

ii. Radial sand movement was similar to that exhibited in the sand only tests.

8.9.6 Constant Rate of Uplift Test.

8.9.6.1 Homogeneous Sand Profile.

i. For the driven piles a general upward movement was displayed in the vertical soil displacement for loads up to Qsf.

ii. The in-situ pile tests indicated an overall downward trend in the vertical movement throughout the pull out test.

iii. The radial movement was generally towards the pile shaft.

8.9.6.2 Layered Soil Profile.

i. Vertical displacements within the overlying sand were progressively upward throughout the test.

ii. The displacements for test 5 at the sand/clay interface were generally 3 times greater than those generated at an equivalent depth during test 3.

iii. Vertical displacements generated within the overlying sand increased with depth. This resulted in the development of compressive strains and was reflected in the development of σ'_{zi} .

8.10 Proposals for Future Work.

By employing the existing equipment and techniques produced and established at the Polytechnic future research may be undertaken by considering the following proposals:-

i. To establish if possible the nature of the fluctuations in the radial stress acting on the pile, by modifying or otherwise the Boundary Orthogonal Stress Transducer.

ii. Substantiate the function of the variations in local unit shaft friction with pile embedment during pile installation by increasing the driving increment.

iii. Modify the Boundary Orthogonal Stress Transducer so that it can be incorporated into the wall of the 60mm diameter pile.

iv. Make a direct comparative study between the two pile sizes by installing them at a constant rate of penetration.

v. Extending the cyclic loading test to the limits of tensile and compressive failure.

vi. Modify all the axial load cells to increase their reliability and sensitivity.

vii. Introduce piezometers into the wall of the pile, this may

be practically difficult unless a head of water is used within the soil profile.

viii. Introduce more sensitive instrumentation around and below base level in the sand only tests. Incorporating greater number and more sensitive diaphragm pressure transducer.

ix. Because of the tremendous amount of data generated by each experiment each research project's efforts should concentrate on just one of the two soil profiles.

x. A natural progression for future research work is pile interaction within a pile group.

xi. Change the sand to obtain a variation in sand density to establish a range of ϕ' and δ' relationships.

BIBLIOGRAPHY

BIBLIOGRAPHY

ACER Y.B., DURGUNOGLU H.T. & TUMAY M.T. (1982). Interface Properties of Sand Journal of the Geotechnical Engineering Division, ASCE, Vol 108, No.GT4, pp 684-694.

AIRHART T.P., COYLE H.M., HIRSCH T.J. & BUCHANAN S.J. (1969). Pile-Soil System Response in a Cohesive Soil . Performance of Deep Foundations. ASTM STP 444. pp 264-294.

APPENDINO M. & PODESTA E. (1979). Driven Piles: Measurement and Interpretation Procedures. Design Parameters in Geot . Engineering. B.S.G. London Vol.3, pp 9-14.

BALIGH M.M. (1986a). Undrained Deep Penetration, I:Shear Stresses . Geotechnique, Vol.36, No.4, pp 471-485.

BALIGH M.M. (1986b). Undrained Deep Penetration, II:Pore Pressures . Geotechnique, Vol.36, No.4, pp 487-501.

BENNETT D.H. & GISBOURN R. (1971). Stress Strain Behaviour of Soils , Proceedings of the Roscoe Memorial Symposium, Cambridge University, pp 459-466.

BEREZANTZEV V.G., KHRISTOFORAV V.S & GOLUBKOV V.N. (1961). Load Bearing Capacity and Deformation of Piled Foundations Proceedings of the 5th International Conference of Soil Mechanics and Foundation Engineering, Vol 2 pp 11-15.

BERGDAHL U & WENNERSTRAND J. (1976). Bearing Capacity of Driven Piles in Loose Sand . Proceedings of the 6th European Conf on Soil Mechanics and Foundation Engineering , Wien, Vol.2.1, pp 355-360.

BISHOP A.W. & HENKEL D.J. (1972). The Measurement of Soil Properties in the Triaxial Test . Edward Arnold Pub, London.

BJERRUM L., BRINCH HANSEN J., & SEVALDSON R. (1958). Geotechnical Investigations for a Quay Structure in Horten. N.G.I., Pub No.28, pp 1-17.

BJERRUM L., & JOHANNESSON I.J. (1960). Pore Pressures Resulting from Driving Piles in Soft Clay . Conf. on Pore Pressure & Soil Suction, Australia, pp 14-17.

BRIAUD J-L. & FELIO G.Y. (1986). Cyclic Axial Loads on Piles . Analysis of Existing Data. Canadian Geot. Journal, Vol 23, pp 362-371.

BRITISH STANDARDS INSTITUTION (1972), Code of Practice for Foundations , CP2004 The British Standards Institution.

BRITISH STANDARDS INSTITUTION (1975), Methods of Testing Soils for Engineering Purposes , B.S.1377, The British Standards Institution.

BRINCH HANSEN J. (1968). A Theory for Skin Friction in Piles , The Danish Goetechnical Institute, Bulletin No 25, Copenhagen.

BROMS B.B. (1966) Methods of Calculating the Ultimate Bearing Capacity of Piles Sols SOils, Vol.5, pp 21-32.

BROMS B.B. & SILBERMAN J.O. (1964). Skin Friction Resistance for Piles in Cohesionless Soils . Sols Soils No.10. pp 33-43.

BROWN S. F. (1973) Measurement of Insitu Stress and Strain in Soils , Symposium on Field Instrumentation in Goetechnical Engineering , London, Part 1, pp 38-52.

BROWN S.F., ANDERSEN H.K., & McELVANEY J. (1977). The Effect of Drainage on Cyclic Loading of Clay . Proc 9th Int Conf on Soil Mech & Foundation Engineering, Tokyo, Vol.2, pp 195-200.

BUTTERFIELD R. & ANDRAWES K.Z. (1972). On the Angle of Friction Between Sand and Plane Surfaces , Journal of Terramechanics Vol.8, No.4, pp 15-23.

BUTTERFIELD R. & BANNERJEE P.K. (1970). The Effect of Pore Pressure on the Ultimate Bearing Capacity of Driven Piles , Proceedings of the 2nd South East Asian Conference on Soil Engineering , Bangkok, pp 385-394.

BUTTERFIELD R. & GHOSH N. (1977). The Response of Singles Piles in Clay to Axial Load . 9 Int Conferance of Soil Mech & Foundations, Tokyo, Vol.1, pp 451-457.

BUTTERFIELD R. & JOHNSTON I.W. (1973). The Stress Acting on a Continuously Penetrating Pile , Proceedings of the 8th Int Conf on Soil Mechanics and Foundation Engineering, Vol.2.1, pp 39-42.

CARR R.W. & HANNA T.H. (1971). Sand Movement Measurements Near Anchor Plates . Proc of A.S.C.E. Journal of Soil Mech and Foundation Engineering. SM5. Vol.97, pp 833-840.

CARTER J.P., RANDOLPH M.F. & WROTH C.P. (1978). Stress and Pore Pressure Changes in Clay During and After the Expansion of a Cylindrical Cavity . CUED/C-SOILS/TR51.

CHAUDHURI K.P.R. & SYMONS M.V. (1983). Uplift Resistance of Model Single Piles , Proc Conf in Geotechnical Practise in Offshore Engineering, A.S.C.E., Austin, Texas, pp 335-355.

CHANDLER J.P. & MARTINS C.P. (1982). An Experimental Study of Skin Friction Around Piles in Clay . Geotechnique, Vol.32, No.2, pp 119-132.

CLARK J.I. & MEYERHOF G.G. (1972). The Behaviour of Piles Driven in Clay. Part 1. An Investigation of Soil Stress and Pore Water Pressure as Related to Soil Properties . Canadian Geotechnical Journal, Vol.9, pp 351-373.

CLARK J.I. & MEYERHOF G.G. (I973). "The Behaviour of Piles Driven in Clay , Part 2. Investigation of the Bearing Capacity Using Total and Effective Stress Parameters". Canadian Geotechnical Journal, Vol.10, pp 86-102.

CLEMENTS S.P. & BRUMUND W.F. (1975). "Large Scale Model Test of a Drilled Pier i Sand", Journal of the Geotechnical Engineering Division, A.S.C.E, Vol.101, No.GT6, pp 537-550.

CHAN S.F. & HANNA T.H. (1979). "The Loading Behaviour of Initially Bent Large Scale Laboratory Piles in Sand. Canadian Geotechnical Journal, Vol.16, pp 43-58.

COOKE R.W. & PRICE G. (1973a) "Horizontal Inclinometers for the Measurement of Vertical Displacement in the Soil Around Experimental Foundations". Proceedings of the Symposium on Field Instrumentation in Geotechnical Engineering, London, pp 112-125.

COOKE R.W. (1985). "Research on Piled Foundations - Historical Review and Future Needs". I.C.E. Informal Discussion, London.

COOKE R.W. (1979). "Influence of Residual Installation Forces on the Stress Transfer and Settlement Under Working Loads of Jacked and Bored Piles in Cohesive Soils." A.S.T.M. pp 231-249.

COOKE R.W. (1978). "The Design of Piled Foundation Developments in Soil Mechanics", ed. by C.R. SCOTT. Applied Science Publishers.

COOKE R.W. & PRICE G. (1973). "Strains & Displacement Around Friction Piles." B.R.E. Publication CP 2873. & 8th Conference of Soil Mechanics & Foundation Engineering. Moscow, Vol.2, No.1, pp 53-60.

COOKE R.W. & PRICE G. & TARR K. (1979) "Jacked Piles in London Clay, A Study of load Transfer and Settlement Under Working Conditions." Geotechnique Vol.11, No.1 pp 1-13.

COOKE R.W. & WHITAKER T. (1961). " Experiments in Model Piles With Enlarged Bases". Goetechnique, Vol.11, No.1, ppl-13.

COYLE H.M. & CASTELLO R.R.(1979). "A New Look at Bearing Capacity Factors for Piles." 11th Annual Offshore Technology Conference, Houston, Texas. Vol.1, pp 427-431.

COYLE H.M. & CASTELLO R.R. (1981). "New Design Correlations for Piles in Sand." Journal of the Geotechnical Engineering Division, A.S.C.E., Vol.107, No.GT7, pp 965-986.

COYLE H.M. & SULAINMAN I.H. (1987). "Skin Friction on Steel Piles in Sand." Journal of S.M. & F.E. Division, A.S.C.E., Vol.93, No.SM6, pp 261-278.

D'APPOLONIA D.J. & LAMBE T.W. (1971). "Performance of Four Foundations on End Bearing Piles". J.S.M.F.D, A.S.C.E. Vol.89, SM6, pp 55-77.

DAVIDSON J.L., MORTENSEN R.A. & BARREIRO D (1981). "Deformation in Sand Around a Cone Penetrometer Tip", 10th International Conf. On Soil Mechanics and Foundation Engineering, Stockholm, Vol.2, pp 467-470.

DE BEER E.E. (1971). "Methodes de Deduction de la Capacite Portante d'un Pieu a Partir des Resultants des Essais de Penetration". Annales des Travaux Publics des Belqique. Vol.72, No's.4-6. pp1-142.

DELPAK R., HAGUE W.F., LAKE G.C., PESHKAM V., ROWLANDS G.O. " Mathematical Modelling of the Load Bearing Characteristics of a Dynamically Driven Pile."

DESAI C.S. (1974). "Numerical Design Analysis for Piles in Sand." Journal of the Geotechnical Eng. Div. Vol.1, No GT6. June. pp 613-635.

ESRIG M.E. & KIRBY R.C. (1979a) "Advances in General Effective Stress Method for the Prediction of Axial Capacity for Driven Piles in Clay", 11th Annual Offshore Technology Conference, Houston, Texas, Vol.1, pp437-443

ESRIG M.E. & KIRBY R.C. (1979b). "Soil Capacity for supporting Deep Foundation Members in Clay", Behaviour of Deep Foundations, ASTM STP620, American Society For Testing Materials, pp26-63.

FEDA J. (1963). "Skin Friction in Piles Due to Dilatancy", Proceedings of the Budapest Soil Mechanics Conference, pp 243-252.

FEDA J. (1976). "Skin Friction of Piles", Proceedings of the 6th European Conference of Soil Mechanics and Foundation Engineering, Wien, Vol.2.1, pp 423-361.

FRANCESCON M. (1982). "Model Pile Test in Clay" Stresses and Displacements due to Installation and Axial Loading", Ph.D. Thesis, Cambridge University, Cambridge.

FREDLUND D.G. (1973) "Volume Change Behaviour Of Unsaturated Soil". Ph.D Thesis, University Alberta, Canada.

GEDDES J.D. (1966). "Stresses in Foundation Soils Due to Vertical Subsurface Loading", Geotechnique, Vol.16, No.3, pp 231-255.

GEDDES J.D. (1969). "Boussinesq Based Approximation to the Vertical Stresses Caused by Pile-Type Subsurface Loading", Geotechnique, Vol.19, No.4, pp 509-514.

GREGERSEN O.S., AAS G., & DIBIAGIO E. (1973). " Load Tests on Friction Piles in Loose Sand." Proc. 8th International Conf. Soil Mechanics. Vol.2.1. pp 109-117.

GOBLE G.G., RAUSHE F. & LIKINS G.E. (1980). "The Analysis of Pile Driving". A State Of The Art. Int. Seminar in the Application of Stress Wave Theory on Piles, Stockholm, pp 131-161.

GHAZZALY O.I & HOBOU H.A. (1975). "Pore Pressure and Strains After Repeated Loading of Saturated Clay". Discussion. Canadian Geot. Journal. Vol.12, pp 265-268.

GARBRECHT D. (1978). "Application of the Wave Equation Analysis to Friction Piles in Sand. Discussion." Canadian Geot.Journal. Vol.15, pp 301-311.

HANNA T.H. (1967). "The Measurement of Pore Pressure Adjacent to a Driven Pile", Canadian Geotechnical Journal, Vol.4, No.3, pp313.

HANNA T.H. (1969). "The Mechanism of Load Mobilization in Friction Piles", Journal of Materials, JMLSA, Vol.4, No.4 pp 924-937.

HANNA T.H. & TAN R.H.S. (1971). "The Load Movement Behaviour of Long Piles", Journal of Materials, JMLSA, Vol.6, No.3, pp 532-554.

HANNA T.H. & TAN R.H.S. (1973). "The Load Behaviour of Long Piles Under Compressive Loads in Sand", Canadian Geotechnical Journal, Vol.10, No.3, pp 311-340.

HEAD K. H. (1986). "Manual of Soil Laboratory Testing, Volume 3, Effective Stress Tests". Pentech Press, London.

HEINS W.L. & DELEEUW E.H. (1977). "Large Scale Cyclic Loading Tests". 9th Int. Conf. of Soil Mechanics and Foundation Engineering. Tokyo, pp 541-554.

HIGHT D.W. (1985). "A Simple Piezometer for the Routine Measurement of Pore pressure in Triaxial Tests on Saturated Soils".

HILL R. (1949). "General Features of Plastic Elastic Problems as Exemplified by Some Particular Solutions", Journal of Applied Mechanics, pp 295-300.

HOLLOWAY D.M. & CLOUGH G.W & VESIC A.S. (1978). "The Effects of Residual Driving Stresses on Pile Performance under Axial Load." 10th Offshore Tech. Conf. OTC3306 Huston, Texas.

HOLMQUIST D.V. & MATLOCK H. (1976)."Resistance- Displacement Relationships for Axial Loaded Piles in Soft Clay." Offshore Tech. Conf. Dallas, Texas. OTC2474.

HOLTZ R.D. & BOMAN P. (1974). "A New Technique for Reduction of Excess Pore Pressure During Pile Driving", Canadian Geotechnical Journal, Vol.11, No.3, pp 423-430.

HUGHES A.F.L & TOWNSEND D.L. (1966). "Probe for Measurement of Pore Water Pressure in Varved Clays", Canadian Geotechnical Journal, Vol.3, Part 1, pp 46-50.

HUNTER A.H. & DAVISSON M.T. (1969). "Measurement of Pile Load Transfer", Preformance of Deep Foundations, ASTM, SPT.444, pp 106-117.

HYDE A.F.L. & WARD S.J. (1985). "A Pore Pressure and Stability Model for a Silty Clay Under Repeated Loading " Geotechnique Vol.35, No.2, pp 113-125.

KAY W.F. (1980). "The Development of Shaft Friction in Semi Full Scale Piles Passing Through Granular Soils." Ph.D. Thesis, Polytechnic Of Wales.

KERISEL J. (1961). "Deep Foundations in Sand: Variation in Ultimate Bearing Capacity with Soil Density, Depth, Diameter and Speed", Proceedings of the 5th Int. Conf. on Soil Mechanics and Foundation Engineering, Vol.2, pp 73-83.

KERISEL J. (1964). "Deep Foundations - Basic Experimental Facts", Proceedings on the Conference on Deep Foundations, Mexico City, Vol.1, pp 5-44.

KIRBY R.C. & ESRIG M.I. (1979). "Further Development of a Effective Stress Method for Pridiction of Axial Capacity for Driven Piles in Clay", Conference on Recent Developments in the Design and Constitution of Piles, The Institute of Civil Engineers, London.

KISHIDA H. (1964). "Stress Distribution by Model Piles in Sand", Soil and Foundation, Vol.5, No.1, pp 1-23.

KISHIDA H. (1967). "Ultimate Bearing Capacity of Piles Driven Into Loose Sands". Soils & Foundations, Vol.7, No.3 pp 20-29.

KOIZUMI Y. (1971). "Field Tests on Piles in Sand", BCP Committee, Soils And Foundations, Vol.11, No.2, pp 29-49.

KOIZUMI Y. & ITO K. (1967). "Field Tests With Regard to Pile Driving and Bearing Capacity of Piled Foundations." Soils and Foundations No.3, pp30

KRAFT L.M. FOCHT J.A. & AMERANSINGHE S.F, (1981). "Friction Capacity of Piles Driven into Clay." A.S.C.E. G.T.1.

LADANYI B. (1963). "Expansion of a Cavity in a Saturated Clay Medium", Journal of S.M. & F.E., Vol.89, SM4, pp127-161.

LAKE G.C. (1986). "The Development of Shaft Friction and End Bearing Resistance for Dynamically Driven Models". Ph.D Thesis, Polytechnic of Wales.

LAGONI P.(1982). "Skin Friction on Piles", 3rd Int Conf on Behaviour of Offshore Structures, pp 221-240.

LAMBE T.W & HORN H.M. (1965). "The Influence on an Adjacent Building of Pile Driving For The M.I.T. Material Center." Proc. 6th Int. Conf. S.M.&F.E., Vol.2. pp280.

LAMBE T.W & WHITMAN R.V (1979). "Soil Mechanics", S.I. Version. John Wiley & Sons, London.

LEE K.L. & BOLTON SEED H. (1967). "Cyclic Stress Conditions Causing Liquefaction of Sand", Journal of S.M. & F.E., ASCE, Part SM1, pp 47-70.

LEVINSON M. & WILSON N.E. (1975). "A Rheological Model for Soil Structure Interaction Under Cyclic Loading." Canadian Geo. J. Vol.12, No.2, pp 262-264.

LO K.Y. & STERMAC A.G. (1964). "Some Pile Load Tests in Stiff Clay". Canadian Geot. Journal. Vol.1, No.2.

LO K.Y. and STERMAC A.G. (1965). "Induced Pore Pressures During Pile Driving Operations". Proc. 6th Conf. S.M.&F.E., Vol.2. pp285

MANSUR C.I. &. KAUFMAN R.I. (1956)."Pile Tests, Low-Sill Structure, Old River, Louisiana", Journal of S.M. & F.E., Vol.123, pp 435-466.

MARTINS J.P. (1983). "Shaft Resistance of Axially Loaded Piles in Clay", Ph.D THesis, Imperial College, London.

MARTINS J.P. & POTTS D.M. (1982), "A Numerical Study of Skin Friction Around Driven Piles." 3rd Int. Conf. on Behaviour of Off-shore Structures, Aug. 2-5. Massachusetts. U.S.A.

MASSARSCH K.R., BROMS B.B. & SANDQUIST Q. (1975). "Pore Pressure Determination With Multiple Piezometers." A.S.C.E. Conf. on In-situ Measurements of Soil Properties.

MASSARSCH K.R. & BROMS B.B. (1977). "Fracturing of Soil Caused by Pile Driving in Clay". Proc. of 9th Int. Conf S.M.&F.E. Vol.1, pp 197-200

MASSARSCH K.R. (1976). "Soil Movement Caused by Pile Driving in Clay". Royal Int. of Tech. Sweden. Report No.6.

MAZURKIEWICK B.K. (1968). "The Danish Goetechnical Institute, Bulletin, Copenhagen.

MEYERHOF G.G. (1951). "The Ultimate Bearing Capacity of Foundations", Geotechnique, Vol.2, No.4, pp 301-332.

MEYERHOF G.G. (1956). "Penetration Tests and Bearing Capacity of Cohesionless Soils", Journal of S.M. & F.E., A.S.C.E., No.SM1, pp 1-19.

MEYERHOF G.G. (1959). "Compaction of Sands and Bearing Capacity of Piles", Journal of S.M. & F.E., A.S.C.E, Vol.85, No.SM6, pp 1-29.

MEYERHOF G.G. (1963). "Some Recent Research on the Bearing Capacity of Foundations", Canadian Geotechnical Journal, Vol.1, No.1, pp 16-26.

MEYERHOF G.G. (1976). "Bearing Capacity and Settlement of Pile Foundations", Journal of the Geotechnical Engineering Division, Vol.102, No.GT3, pp 195-228.

MEYERHOF G.G. & SASTRY V.V.R.N. (1978a). "Bearing Capacity of Piles in Layered Soils: Part 1 Clay Overlying Sand", Canadian Geotechnical Journal, Vol.15, No.2, pp 171-182.

MEYERHOF G.G. $ SASTRY V.V.R.N. (1978b). "Bearing Capacity of Piles in Layered Soils: Part 2 Sand overlying Clay", Canadian Geotechnical Journal, Vol.15, No.2, pp 183-189.

MEYERHOF G.G. & VALSANGKAR A.J. (1977). " Bearing Capacity of Piles in Layered Soils", 9th Int. Conf. on S.M. & F.E., Japan, Vol.1, PP 645-650.

MOGAMI T. & KISHIDA H. (1961) "Some Pile Problems", 5th Int. Conf. on S.M. & F.E., Vol.2, pp 111-115.

MOHAN D., JAIN G.S. & KUMAR V. (1963). "Load-Bearing Capacity of Piles", Geotechnique, Vol.13, pp 76-86.

NISHIDA Y. (1963). "Pore Pressures in Clay Induced By Pile Friction", Proceedings of 2nd Pan American Conference, S.M. & F.C., Vol.2, pp 225-233.

NORLAND R.L. (1963). "Bearing Capacity of Piles in Cohesionless Soils", Journal of S.M & F.E., ASCE, No.SM3, pp 1-35.

NOVAK M. (1974). "Dynamic Stiffness and Damping in Piles." Can. Geo. J. Vol.II. No.4. pp 574-598.

NOVAK M. & GRIGG R.F. (1976). " Dynamic Experiments With Small Pile Foundations." Can. Geot. J. Vol.13, No.4, pp 372-385.

NOVAK M. & El SHARNOUBY B.(1983). "Stiffness Constants of Single Piles." J. of Geot. Eng. Division, A.S.C.E., Vol.109, No.7.

ORRJE O. & BROMS B.B. (1967). "Effects of Pile Driving on Soil Properties", J.S.M.F.D. ASCE Vol.93, SM5, pp 59-73.

PALMER A.C. (1972). "Undrained Plane Strain Expansion of a Cylinderical Cavity in Clay: A Simple Interpretation of the Pressuremeter Test", Geotechnique, Vol.22, No.3, pp 451-457.

PARRY R.H.G. & SWAIN C.W. (1977a) "Effective Stress Methods of Calculating Skin Friction of Driven Piles in Soft Clay". Ground Engineering, Vol.10, No.3, pp 24-26.

PARRY R.H.G. & SWAIN C.W. (1977b) "A Study of Skin Friction on Piles in Stiff Clay". Vol.10, No.8, pp 33-37.

PENMAN A.D.M. (1961). "A Study of the Response Time of Various Types of Piezometers". Proc. Conf. on Pore Pressures and Suction in Soils, pp53-58.

PERREN F.J. (1978). "A Case History Of Piling in the Glacial Material of South Wales", M.Phil. Thesis, Polytechnic of Wales.

POTTS D.M. & MARTINS J.P. (1982). "The Shaft Resistance of Axially Loaded Piles in Clay", Geotechnique, Vol.32, No.4, pp 369-386.

POTYONDY J.G. (1961). "Skin Friction Between Various Soils and Construction Materials", Geotechnique, Vol.11, No.4, pp 339-353.

POULOS H.G. & DAVIS E.H. (1980). "Pile Foundation Analysis and Design", John Willey & Sons Ltd. New York.

PUECH A.A. (1982). "Basic Data for the Design of Tension Piles in Silty Soils". Proc. 3rd Int. Conf. on the Behaviour of Offshore Structures, Aug. 2-5, Massachusetts, U.S.A., pp 141-157.

PREMCHITT J. & BRAND E.W. (1981). "Pore Pressure Equalization of Piezometers in Compressible Soils". Geotechnique, Vol.31, No.1, pp 105-123.

PRICE G. " A Survey of Work on the Behaviour of Piled Foundations Under Vertical and Horizontal Loading Carried out by the Geotechnical Division, B.R.E.", B.R.E. Publication.

PRICE G. & WARDLE I.F. "Recent Developments In Pile/Soil Instrumentation System." B.R.E. Publication.

RANDOLPH M.F. & WROTH C.P. (1979). "An Analytical Solution for the Consolidtion Around a Driven Pile", Int. Journal for Numerical and Analytical Methods in Geomechanics, Vol.3, pp 217-229.

RANDOLPH M.F. & WROTH C.P. (1982). "Application of the Failure State in Undrained Simple Shear to the Shaft Capacity of Driven Piles". Geotechnique, Vol.31, No.1, pp 143-157.

RANDOLPH M.F. CARTER J.P. & WROTH C.P. (1979). "Driven Piles in Clay - The Effects of Installation and Subsequent Consolidation", Geotechnique, Vol.29, No.4, pp 361-393.

RANDOLPH M.F. STEENFELT J.S. & WROTH C.P. (1979). "The Effect of Pile Type on Design Parameters for Driven Piles." Design Parameters in Geo. Eng. B.G.S., London., Vol.2, pp 102-114.

RAUSCHE F. & GOBLE G.G. (1977). "Performance of Pile Driving Hammers." Journal of the Construction Division. Proceeding of the A.S.C.E. Vol.2, pp 201-217.

REESE L.C. & COX W.R. (1976). "Pullout Tests of Piles in Sand", 8th Annual Offshore Technology Conference, Houston, Texas, Vol. 1, pp 527-538.

REESE L.C. & SEED H.B. (1955). Pressure Distribution Along Friction Piles", Proceedings of the ASTM, Vol.55, pp 1156-1182.

REMPE D.M. & DAVISSON M.T. (1977). "Performance of Diesel Pile Hammers. "9th Int. Conf., Tokyo, Vol.2, pp 347-354.

RIGDEN W.J., PETTITT J.J., St JOHN H.D. & POSKITT T.J. (1979). "Developments in Offshore Structures", Proc. of the 2nd Int. Conf. on the Behaviour of Offshore Structures, London, Paper 67.

RIGDEN W.J. & POSKITT T.J. (1979). "Wave Equation in Piling", Piling Group Discussion.

ROBINSKY E.I. & MORRISON C.F. (1964). "Sand Displacement and Compaction Around Model Friction Piles", Canadian Geotechnical Journal, Vol.1, No.2, pp 81-93.

ROBINSKY E.I. SAGAR W.L. & MORRISON C.F. (1964). "Effect of Shape And Volume on the Capacity of Model Piles in Sand", Canadian Geotechnical Journal, Vol.1, No.4, pp 731-754.

ROSCOE K.H., AUTHUR J.R.F. & JAMES R.G. (1963). "The Development of Strains in Soils by an X-Ray Method". Civil Engineering and Public earks Review, Vol.58, No.685, pp 1009-1012.

ROWLANDS G.O., DELPAK R. & ROBINSON R.B. (1989) "The Development of Shaft Friction for Piles in Sand Overlying Clay". To be Published at the 12th Int. Conf. on S.M.&F.E., Rio de Janeiro.

ROY M., BLANCHET R., TAVENAS F. & La ROCHELLE P. (1981). "Behaviour of a Sensitive Clay During Pile Driving.", Canadian Geotechnical Journal, Vol.18, pp 67-85.

ROY M., TREMBLAY M., TAVENAS F. & La ROCHELLE P. (1982). "Development of Pore Pressure in Quasi Static Penetration Tests in Sensitive Clay. "Canadian GeotechnicalJournal, Vol.19, No.1, pp 124-138.

SEED H.B. & REESE L.C. (1955). "The Action of Soft Clay Along Friction Piles", Transactions, ASCE, Vol.122, pp 731-754.

SHURI F.S., DRISCOLL D.D. & GARNER S.J. (1985). "Controlled Displacement - Rate Insitu Shear Tests with Pore Pressure Measurement". Can. Geo. Jnl. Vol.22, pp 136-142.

SKEMPTON A.W. (1951). "The Bearing Capacity of Clays", Proceedings of the Building Research Congress, London, Vol.1, pp 180-189.

SMITH E.A.L. (1955). "Impact & Longitudinal Wave Transmission", Trans American Soc. Mech. Eng. pp 163-173.

SMITH E.A.L. (1960). "Pile Driving Analysis by the Wave Equation." J. of the Soil Mech. & Found. Div., pp 35-61.

SODERBERG L.O. (1962). "Consolidation Theory Applied To Foundation Pile Time Effects". Geot. Vol.12, pp 112.

STEENFELT J.S., RANDOLPH M.F. & WROTH C.P. (1981). "Instrumented Model Piles Jacked into Clay". Int Conf on S.M.&F.E., Stockholm, Vol.2.

TAN Y.G. (1983). "Load Testing of Piled Foundations". Ph.D. Thesis. U.W.I.S.T., Cardiff, South Wales.

TAVENAS F.A. (1971). "Load Tests on Friction Piles in Sand", Canadian Geotechnical Journal, Vol.8, pp 7-22.

TAVENAS F.A. & AUDIBERT J.M.E. (1977). "Application of the Wave Equation Analysis to Friction Piles in Sand."Canadian Geo. J. Vol,14, Part 34.

TEJCHMAN A. (1971). "Skin Friction on a Model Pile in Sand", The Danish Geotechnical Institute, Bulletin No 29, Copenhagen.

THORBURN S. (1976). "The Static Penetration Test and the Ultimate Resistance of Driven Piles in Fine Grained Non Cohesive Soils", The Structural Engineer, Vol.54, pp 205-211.

TOMLINSON M.J. (1970). "Adhesion of Piles in Stiff Clay", Construction Industry Research and Information Association, Research Report 26, November, pp 1-47.

TOMLINSON M.J. (1971). "Some Effects of Pile Driving on Skin Friction", Conference on Behaviour of Piles, Institute of Civil Engineers, London, pp 107-114.

TOMLINSON M.J. (1981). "Pile Design and Construction Practice", Viewpoint Publication.

TOUMA F.T. & REESE L.C. (1974). "Behaviour of Bored Piles in Sand", Journal of Geotechnical Engineering Division, ASCE, Vol.100, No.GT7, pp 749-761.

TUMAY M.T. ACAR Y.B. & CEKIRGE M.E. (1985). "Flow Fields Around Cones in Steady Penetration", A.S.C.E., Vol.3, No.2.

VESIC A.S. (1963). "Bearing Capacity of Deep Foundation in Sand". National Acadamy of Science, National Research Council, Highway Research Record 39, pp 112-153.

VESIC A.S. (1964). "Investigation of Bearing Capacity of Piles in Sand", Proceedings of North American Conference on Deep Foundations, Mexico City, Vol.1, pp 197-224.

VESIC A.S. (1965). "Ultimate Loads and Settlements of Deep Foundations in Sand", Proceedings of a Symposium on Bearing Capacity and Settlement of Foundations, Duke University, Durham, N.C., pp 53-68.

VESIC A.S. (1967). "A Study of Bearing Capacity of Deep Foundations", Final Rrport Project B189, School Of Civil Engineering, Georgia Institute of Technology, Atlanta.

VESIC A.S. (1969a). "Load Transfer, Lateral Loads and Group Action of Deep Foundations. "Performance of Deep Foundations, A.S.T.M., S.T.P.444, pp 5-14.

VESIC A.S. (1969b). "Discussion: Proceedings of 7th Int. Conf. on S.M. & F.E., Vol.3, pp 242-244.

VESIC A.S. (1970). "Tests on Instrumented Piles, Ogeechee River Site", Journal of the Soil Mechanics and Foundations Division, ASCE, Vol.96, No.SM2, pp 561-585.

VESIC A.S. (1972). "Expansion of Cavities in Infinite Soil Mass ." Proceedings A.S.C.E. SM3.

VESIC A.S. (1977). "Design of Pile Foundations", Synthesis of the Highway Practice No.42, National Co-operative Highway Research Programme, Transport Research Board, National Research Council, Washington D.C., pp 68.

WELTMAN A.J. (1980). Pile Load Testing Procedures", C.I.R.I.A. Report PG7.

WELTMAN A.J. & HEALY P.R. (1978). Piling in Boulder Clay and Other Glacial Tills", C.I.R.I.A. Report PG5

WERSCHING S.N. (1987). "The Development of Shaft Friction and End Bearing of Piles in Homogeneous and Layered Soils", Ph.D Thesis, Polytechnic Of Wales.

WERSCHING S.N., DELPAK R. & ROWLANDS G.O. (1983). "A Method of Estimating the Insitu Density of Dry, Uniformally Graded Sand Under Controlled Condition of Placement", Geotechnical Testing Journal, ASTM, Vol.6, No.4, pp 196-200.

WHITAKER T. (1970). " The Design of Piled Foundations", Oxford, Pergamon Publication.

WHITAKER T. & COOKE R.W. (1961). "A New Approach to Pile Testing", 5th Int. Conf. on S.M. & F.E., Paris, Vol.2, pp 171-176.

WILSON N.E. & ELGOMARY M.M. (1974). "Consolidation of Soils Under Cyclic Loading." Canadian Geo. J. Vol.11, No.3, pp 420-423.

WILSON N.E. & GREENWOOD J.R. (1974). "Pore Pressures and Strains After Repeated Loading of Saturated Clays ." Canadian Geo. J. Vol.11, No.2, pp 269-277.

YOSHIMI Y. & KISHIDA T. (1981). "Friction Between Sand and Metal Surfaces", 10th International Conference on Soil Mechanics and Foundation Engineering, Stockholm , Vol.1, pp 831-834.